

**EVOLUTION AND FUNCTIONAL MORPHOLOGY
OF PTYCHOIDY IN PTYCTIMA (ACARI, ORIBATIDA)**

Dissertation

der Mathematisch-Naturwissenschaftlichen Fakultät
der Eberhard-Karls Universität Tübingen
zur Erlangung des Grades eines

**Doktors der Naturwissenschaften
(Dr. rer. nat.)**

vorgelegt von

Herrn Dipl.-Biol. Sebastian Schmelzle
aus Pforzheim

Tübingen
2015

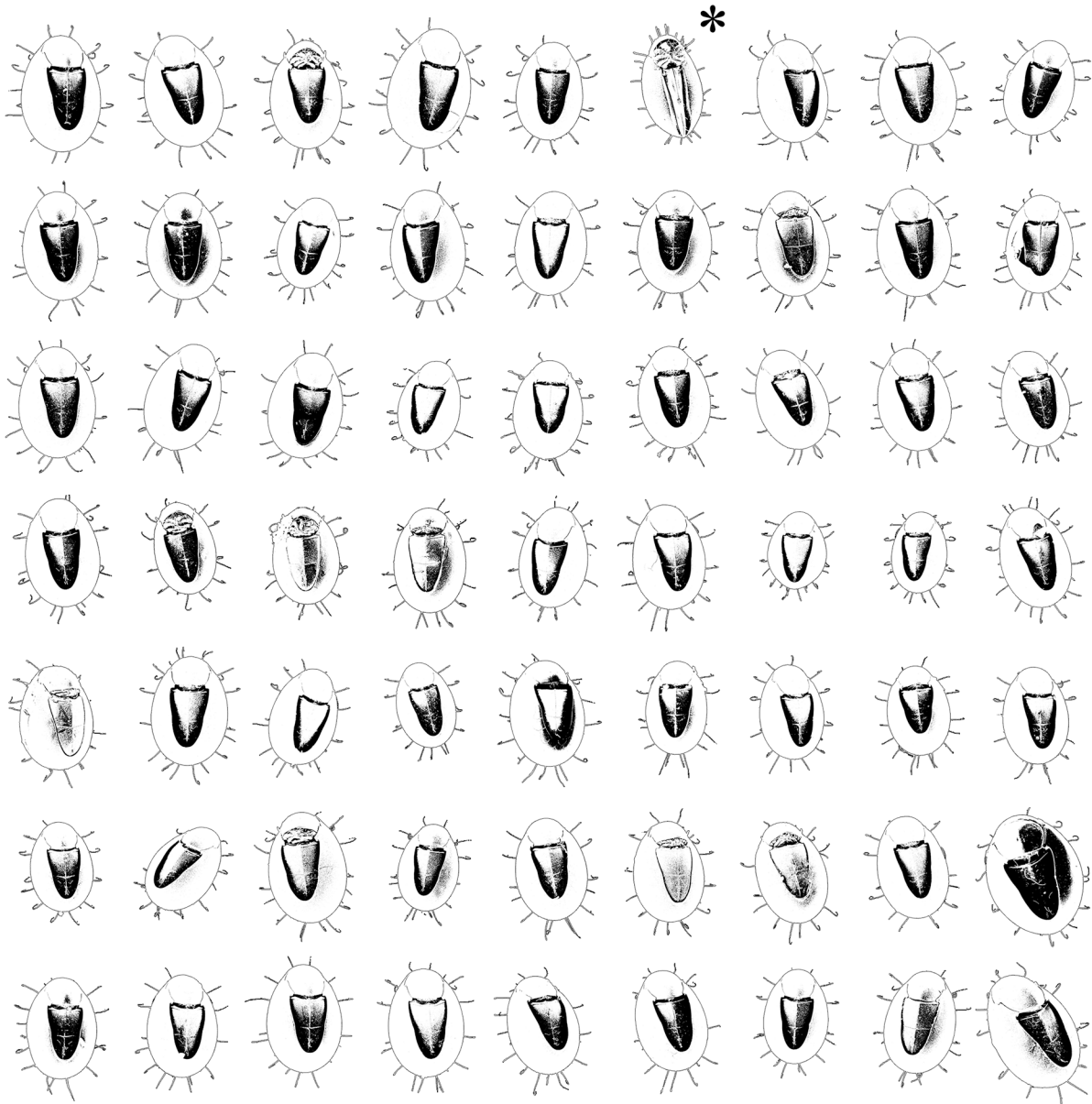
Gedruckt mit Genehmigung der Mathematisch-Naturwissenschaftlichen Fakultät der
Eberhard Karls Universität Tübingen.

Tag der mündlichen Qualifikation: 19.06.2015

Dekan: Prof. Dr. Wolfgang Rosenstiel

1. Berichterstatter: PD Dr. Michael Heethoff

2. Berichterstatter: Prof. Dr. Oliver Betz



*,'Share our similarities,
celebrate our differences.'

— M. SCOTT PECK

CURRICULUM VITAE

SEBASTIAN SCHMELZLE

Date of birth	27.03.1982
Place of birth	Pforzheim
Nationality	Deutsch

EDUCATION

2009 – 2015	PhD: ‘Evolution and functional morphology of Ptychoidea of Ptyctima (Acari, Oribatida)’
2008	Diploma in Biology, grade: 1.7
2007 – 2008	Diploma thesis: ‘Evolution und Funktion von Ptychoidie bei verschiedenen Hornmilben (Acari, Oribatida)’, grade: 1.0
2003 – 2007	‘Graduate’ (Hauptstudium) of biology with major Zoology and minors animal physiology, and experimental physics
2001 – 2003	‘Undergraduate’ (Grundstudium) of Biology at the ‘Eberhard Karls University’, Tübingen
1992 – 2001	Johannes-Kepler-Gymnasium, Weil der Stadt; finishing with ‘Abitur’, grade: 2.7

WORK

2013 - now	Research assistant for PD Dr. Michael Heethoff, Technical University, Darmstadt: Project ‘ASTOR’
2013	Teaching assistance at the Technical University, Darmstadt: soil ecology
2012 - 2013	Technical assistance at the professorship <i>Evolutionary Biology of Invertebrates</i> , Eberhard Karls University, Tübingen
2009	Research assistant for Prof. Dr. Sven Gemballa, Eberhard Karls University, Tübingen: project ‘Darwin 2.0’
2011 – 2012	Field work at the Eberhard Karls University, Tübingen: tagging of Alpine newts <i>Ichthyosaura alpestris</i>
2008 – 2009	Research assistant for Dr. Daniel Bumbarger, Max-Plank-Institute, Tübingen: work on <i>Pristionchus pacificus</i>
2007	Research assistant for PD Dr. Michael Heethoff, Eberhard Karls University, Tübingen: work on <i>Archeogozetes longisetosus</i>
2005 - 2011	Research assistant for Prof. Dr. Oliver Betz, Eberhard Karls University, Tübingen: work on staphylinid beetles
2005 – 2014	Research periods at the ESRF, Grenoble, and the ANKA, KIT, Karlsruhe: Synchrotron X-ray microtomography
2002 – 2013	Teaching assistance at the Eberhard Karls University, Tübingen: basic and advanced courses in zoology; 2D and 3D image editing; soil ecology; phylogeny; bionics; zoological field trips

PUBLICATIONS

- 2015 **Schmelzle, S.**, R. A. Norton, M. Heethoff. Mechanics of the ptychoid defense mechanism in *Ptyctima* (Acari, Oribatida): one problem, two solutions. – *Zoologischer Anzeiger - A Journal of Comparative Zoology* 254, 27–40. doi:10.1016/j.jcz.2014.09.002
- 2012 **Schmelzle, S.**, R. A. Norton, M. Heethoff. A morphological comparison of two closely related ptychoid oribatid mite species: *Phthiracarus longulus* and *P. globosus* (Acari: Oribatida: Phthiracaroidea). – *Soil Organisms* 84 (2): 431 – 443.
- 2011 Alberti, G., M. Heethoff, R. A. Norton, **S. Schmelzle**, A. Seniczak, S. Seniczak. Fine structure of the gnathosoma of *Archezogetes longisetosus* [corrected] AOKI (Acari: Oribatida, Trhypochthoniidae). – *Journal of Morphology* 272 (9): 1025 – 1079.
- 2010 **Schmelzle, S.**, L. Helfen, R. A. Norton & M. Heethoff. The ptychoid defensive mechanism in *Phthiracarus longulus* (Acari, Oribatida, Phthiracaroidea): Exoskeletal and muscular elements. – *Soil Organisms* 82 (2): 253 – 273.
- 2009 **Schmelzle, S.**, L. Helfen, R. A. Norton & M. Heethoff. The ptychoid defensive mechanism in Euphthiracaroidea (Acari: Oribatida): A comparison of muscular elements with functional considerations. – *Arthropod Structure and Development* 38 (6): 461 – 472. doi:10.1016/j.asd.2009.07.001.
- 2008 **Schmelzle, S.**, L. Helfen, R. A. Norton & M. Heethoff. The ptychoid defensive mechanism in Euphthiracaroidea (Acari: Oribatida): A comparison of exoskeletal elements. – *Soil Organisms* 80 (2): 227 – 241.

LIST OF PUBLICATIONS USED IN THIS DISSERTATION

Publication 1

Schmelzle, S., Helfen, L., Norton, R.A., Heethoff, M. (2008). The ptychoid defensive mechanism in Euphthiracaroida (Acari: Oribatida): A comparison of exoskeletal elements. *Soil Organisms* 80 (2), 227–241.

Publication 2

Schmelzle, S., Helfen, L., Norton, R.A., Heethoff, M. (2009). The ptychoid defensive mechanism in Euphthiracaroida (Acari: Oribatida): A comparison of muscular elements with functional considerations. *Arthropod Structure and Development* 38 (6), 461–472. DOI: 10.1016/j.asd.2009.07.001

Publication 3

Schmelzle, S., Helfen, L., Norton, R.A., Heethoff, M. (2010). The ptychoid defensive mechanism in *Phthiracarus longulus* (Acari: Oribatida): Exoskeletal and muscular elements. *Soil Organisms* 82 (2), 253–273.

Publication 4

Schmelzle, S., Norton, R.A., Heethoff, M. (2012). A morphological comparison of two closely related ptychoid oribatid mite species: *Phthiracarus longulus* and *P. globosus* (Acari: Oribatida: Phthiracaroida). *Soil Organisms* 84 (2), 431–443.

Publication 5

Schmelzle, S., Norton, R.A., Heethoff, M. (2015). Mechanics of the ptychoid defense mechanism in *Ptyctima* (Acari, Oribatida): one problem, two solutions. *Zoologischer Anzeiger – A Journal of Comparative Zoology* 254, 27–40. DOI: 10.1016/j.jcz.2014.09.002

ABSTRACT

Oribatida (Acari, Arachnida) are diverse and abundant in temperate forest litter. As particle feeding saprophages or mycophages, their food is of relatively low quality, which supposedly results in slow movement, prolonged generation time and reduced reproductive potential. Hence, oribatid mites developed a number of different defensive mechanisms. The most complex mechanical defensive mechanism is ptychoidy, where the animals can retract their legs and mouthparts into a secondary cavity in the idiosoma and encapsulate by deflecting the prodorsum. In this state the animals do not exhibit soft membrane but only—through biomineralization—hardened, thick cuticle, and are therefore well protected against many predators. Certain prerequisites have to be met for the evolution of ptychoidy: the coxisternum must be free from solid exoskeletal connections, i.e. embedded in soft membrane; the cuticle of the opisthosoma has to be hardened; the coxisternum must be foldable; and a system able to accommodate huge volume changes is needed.

Despite this complexity, ptychoidy evolved three times independently, once in the Ptyctima and twice in the Enarthronota (Mesoplophoridae and Protoplophoridae). We used synchrotron X-ray microtomography (SR μ CT), scanning electron microscopy and high-speed videography to investigate the morphological and functional characteristics of ptychoidy in both superfamilies of the Ptyctima (Euphthiracaroida and Phthiracaroida).

At first glance Euphthiracaroida and

Phthiracaroida considerably differ in the arrangement of the ventral plates. Phthiracaroida possess fused anal and adanal (anal valves) as well as fused genital and agenital plates (genital valves). The genital and anal valves are separated from each other and are embedded in soft membrane (anogenital membrane).

Euphthiracaroida possess either completely fused holoventral plates (complete fusion of anal and genital valves) or retain only a suture between anal and genital valves. In both cases the ventral plates are elongated and surrounded by the plicature plates, a sclerotization of the surrounding membrane.

The musculature associated with the ventral plates differs accordingly. In Euphthiracaroida the notogaster lateral compressor connects the notogaster and the junction between the ventral and plicature plates on the complete length and combined with the ventral plate adductor and ventral plate compressor bridges the ventral plates in the area of the preanal apodeme. A simultaneous contraction of these muscles leads to a transmission of forces via the preanal apodeme onto the notogaster resulting in a lateral compression. In Phthiracaroida on the other hand the notogaster lateral compressor is restricted to the last third of the ventral plates, inserting on the anogenital membrane. A contraction of the notogaster lateral compressor—along with the postanal muscle—leads to a retraction of the temporarily unified ventral plates into the idiosoma.

Other differences concern for example the

manubrium (present in Euphthiracaroidea, absent in Phthiracaroidea), and the sensillus ridge allowing for an un-pinched stowage of the sensillus in encapsulated state (absent in Euphthiracaroidea, present in Phthiracaroidea). The coxisternal protractor, which is able to act as retractor as well as protractor of the legs, could only be found in the investigated species of Phthiracaroidea, but in none of the species of Euphthiracaroidea.

In conclusion, the mode of pressure build-up associated with ptychoidy is functionally different in the two groups of Ptyctima, but morphologically based on the same characters. Molecular data and for example the location of the taenidiophore also suggest a common origin. A comparison to a potential sister group of Ptyctima, the Colohmannioidea, indicates that the mode of pressure build-up of Euphthiracaroidea is ancestral (based on the elongated state of the ventral plates and the associated musculature). This is also affirmed by molecular studies showing that the Phthiracaroidea are a derived group originating from euphthiracaroid ancestors. Further investigations regarding ptychoidy

should include the two remaining—unexamined—ptyctima groups, Synichotritiidae (Euphthiracaroidea) and Steganacaridae (Phthiracaroidea), and the two groups that have evolved ptychoidy independently within the Enarthronota, Mesoplophoridae and Protoplophoridae. Especially the two enarthronote groups are of particular interest since they developed ptychoidy on a different phylogenetic basis. External observation of the Mesoplophoridae for example leads to the assumption that their mode of pressure build-up might be similar to that of the Phthiracaroidea. However, anal and genital valves of Mesoplophoridae are embedded in a single ventral plate of partially notogastral origin. In Protoplophoridae the anal and genital valves are not observable externally in encapsulated state. They are covered by cuticular plates that were converted from static notogastral plates into moveable and retractable plates that potentially function as system for the build-up of pressure.

These observations support the assumption of a convergent evolution of ptychoidy in the three groups.

ZUSAMMENFASSUNG

Hornmilben (Oribatida) sind in der Laubstreu gemäßigter Wälder arten- und zahlreich vertreten. Sie sind detritivor oder fungivor und verzehren diese Nahrung in Form von festen Partikeln. Diese relativ niederwertige Nahrung soll zu einer langsamen Bewegungsweise, einer verlängerten Generationsdauer und einer verminderten Reproduktionsrate führen. Deshalb haben Hornmilben zahlreiche verschiedene und sehr effektive Mechanismen zum Schutz vor Prädation entwickelt.

Der wohl komplexeste mechanische Defensivmechanismus ist die Ptychoidie, welche es den Tieren erlaubt ihre Beine und das Gnathosoma in einen sekundären Hohlraum im Idiosoma einzuziehen und mit dem Prodorsum zu verschließen. In diesem eingekapselten Zustand präsentieren die Tiere nach außen hin nur noch feste, durch Sklerotisierung und Biomineralisierung gehärtete, Kutikula und keine weichhäutigen Membranen mehr. Dadurch erlangen sie einen effektiven Schutz vor zahlreichen Fressfeinden. Für die Evolution der Ptychoidie müssen bestimmte Vorbedingungen erfüllt sein: das Coxisternum muss frei beweglich sein, darf also mit keiner anderen kutikulären Struktur fest verbunden sein; die Kutikula des Notogaster muss gehärtet sein; das Coxisternum muss zusammenklappbar sein; und es muss ein System geben, welches die mit der Ptychoidie assoziierte Volumenänderung kompensieren kann.

Trotz dieser Komplexität ist die Ptychoidie vermutlich dreifach unabhängig entstanden:

einmal bei den Ptyctima und zweimal innerhalb der Enarthronota (bei den Mesoplophoridae und Protoplophoridae).

Zur Untersuchung der morphologischen und funktionellen Merkmale der Ptychoidie in den beiden Überfamilien der Ptyctima (Euphthiracaroida und Phthiracaroida), verwendeten wir Synchrotron-Röntgen-Mikrocomputertomographie (SR μ CT), Rasterelektronenmikroskopie und Hochgeschwindigkeitsaufnahmen.

Schon auf den ersten Blick unterscheiden sich Euphthiracaroida und Phthiracaroida in der Ausprägung der Ventralplatten-Morphologie. Die Phthiracaroida besitzen verschmolzene Anal- und Adanalplatten (Analklappen) sowie verschmolzene Genital- und Agenitalplatten (Genitalklappen). Die Anal- und Genitalklappen sind dabei voneinander abgegrenzt und sind in einer umlaufenden weichhäutigen Membran eingebettet (Anogenitalmembran).

Die Euphthiracaroida besitzen entweder Holoventralplatten (vollständig verschmolzene Anal- und Genitalklappen) oder behalten nur eine feine Naht zwischen den beiden Klappen. In beiden Fällen sind die Platten stark verlängert und sind umrahmt von den Holoventralfalten, die eine Sklerotisierung der Anogenitalmembran darstellen.

Die mit den Ventralplatten assoziierte Muskulatur unterscheidet sich dementsprechend ebenfalls. Der Lateralkompressor des Notogaster (*nlc*) verbindet bei den Euphthiracaroida über die gesamte Länge den Notogaster mit der

Gelenkstelle zwischen den (Holo-) Ventralplatten und Holoventralfalten. Die Gruppe bestehend aus *nlc*, Ventralplattenkompressor (*vpc*) und Ventralplattenadduktor (*vpa*) überspannt dabei auf Höhe des präanal Apodems wie eine Brücke die ventralen Platten. Die simultane Kontraktion dieser Muskeln bewirkt eine Übertragung der Kräfte via des präanal Apodems auf den Notogaster und führt somit zu einer lateralen Kompression desselben. Bei den Phthiracaroida hat der *nlc* seinen Ursprung zwar ebenfalls am Notogaster, jedoch nur im letzten Drittel des Körpers und inseriert, anders als bei den Euphthiracaroida, auf der Anogenitalmembran. Die Kontraktion des *nlc* führt hier aber in Kombination mit der Kontraktion des postanal Muskels (*poam*) zu einem Einziehen der Ventralplatten in das Idiosoma.

Weitere Unterschiede betreffen beispielsweise das Manubrium (nur bei den Euphthiracaroida vorhanden) und eine Nut, die ein Einklemmen des Sensillus' zwischen Notogaster und Prodorsum im eingekapselten Zustand der Tiere verhindert (in dieser Ausprägung nur bei den Phthiracaroida vorhanden). Der Protraktor des Coxisternum (*csp*) kommt nach dem bisherigen Stand unserer Forschung nur bei den Phthiracaroida vor. Er ist in der Lage sowohl als Pro- wie auch als Retraktor der Beine zu fungieren.

Das Druck-Kompensationssystem für die Volumenänderung unterscheidet sich funktionell deutlich zwischen den zwei Gruppen, obwohl zum großen Teil dieselben morphologischen Strukturen involviert sind. Molekulare Untersuchungen und zum Beispiel die Position der Taenidiophore sprechen

ebenfalls für einen gemeinsamen Ursprung der beiden Überfamilien. Durch den Vergleich mit einer potentiellen Außengruppe der Ptyctima, den Collohmannioidea, kann angenommen werden, dass die laterale Kompression wie sie bei den Euphthiracaroida zu finden ist den ursprünglichen Zustand darstellt (basierend zum Beispiel auf der in die Länge gezogenen Form der Ventralplatten und der damit assoziierten Muskulatur). Dies wird auch durch molekulare Studien belegt, die zeigen, dass die Phthiracaroida eine abgeleitete Gruppe darstellen die ihren Ursprung in den Euphthiracaroida haben.

Weitere Forschungsvorhaben zur Ptychoidie sollten den Fokus auf die zwei verbleibenden (bisher nicht untersuchten) Gruppen der Ptyctima, Synichotritiidae und Steganacaridae, sowie die zwei Gruppen, die den Defensivmechanismus Ptychoidie innerhalb der Enarthronota entwickelt haben (Mesoplophoridae und Protoplophoridae), richten.

Die beiden Gruppen der Enarthronota sind dabei von besonderem Interesse, da sie die Ptychoidie auf einer gänzlich anderen phylogenetischen Basis evolviert haben. Schon eine äußerliche Betrachtung der Mesoplophoridae lässt den Schluss zu, dass der Druckaufbau ähnlich wie bei den Phthiracaroida funktioniert. Allerdings sind hier die Anal- und Genitalklappen anders als bei den Phthiracaroida in eine unpaare ventrale Platte eingebettet, die zum Teil aus Platten des Notogaster aufgebaut ist. Bei den Protoplophoridae sind die Ventralplatten (Anal- und Genitalklappen) durch eine äußerliche Betrachtung eingekapselter Tiere nicht

auszumachen. Sie sind durch ehemals statische Platten des Notogaster verdeckt, die zu beweglichen und einziehbaren Strukturen umgewandelt worden sind und

jetzt potentiell dem Druckaufbau dienen.

Diese äußerliche Betrachtung festigt die Annahme konvergenter Evolution der Ptychoidie bei den drei Gruppen.

TABLE OF CONTENTS

INTRODUCTION	1
Acari	1
Oribatida	2
Defense mechanisms	2
Ptychoidy	3
Ptyctima	4
Goal of this thesis	5
MATERIAL AND METHODS	6
SYNOPSISSES	7
Publication 1	7
Publication 2	7
Publication 3	8
Publication 4	10
Publication 5	11
CONCLUSION	13
OUTLOOK	14
Ptychoidy in Ptyctima	14
Ptychoidy in Enarthronota	14
<i>Mesoplophoridae</i>	16
<i>Protoplophoridae</i>	16

Evolution of ptychoidy	17
<i>Ontogenesis</i>	17
<i>Phylogeny</i>	17
<i>Sphaerochthonius</i>	18
<i>Palaeosomata</i>	19
New methods for structural research	21
<i>Wet scans</i>	21
<i>ASTOR</i>	21
Tables	24
<i>Table 1</i>	24
<i>Table 2</i>	24
<i>Table 3</i>	25
REFERENCES	26
PUBLICATIONS.	29
Publication 1	31
Publication 2	49
Publication 3	63
Publication 4	87
Publication 5	103
ACKNOWLEDGEMENTS	119

INTRODUCTION

Acari

The Oribatida belong to the Acari (Fig. 1), an arachnid group with a small body size (about 100–1500 μm) that is, according to newer phylogenetic studies, likely diphyletic (split into the two groups Acariformes and Parasitiformes; Giribet et al. 2002, Shultz 2007, Regier et al. 2010, Dabert et al. 2010, Sharma et al. 2014). Grandjean (1969a) classified the Acari into three groups: the Opilioacarida, Anactinotrichida and Actinotrichida, but Evans et al. (1961), van der Hammen (1972, 1977, 1989), and Krantz (1978) placed the Opilioacarida within the Parasitiformes (= Anactinotrichida), leaving the Acari with only two main groups. Based on sperm morphology, Alberti (2006) also is of the opinion that only two main groups exist within the Acari (*cf.* Alberti 1980a,b, 1984): (i) Parasitiformes

(=Anactinotrichida) including Opilioacarida, Holothyrida, Ixodida, Gamasida, and (ii) Acariformes (= Actinotrichida) including Actinedida, Oribatida, and Acaridida. Besides sperm morphology especially the eponymous “absence (Anactinotrichida) or presence (Actinotrichida) of birefringence of setal structures ... under polarized light” (Alberti 2006) differentiates the two groups.

Regarding the phylogenetic relationship of those two groups within the Arachnida, Dabert et al. (2010) stated that the Solifugae are well supported as sister group to the Actinotrichida, whereas the Pseudoscorpionida turned out to be the sister group of the Anactinotrichida, but with less support. Giribet et al. (2002) found the same relationship of Pseudoscorpionida with—in this case—Opilioacarida and Parasitiformes.

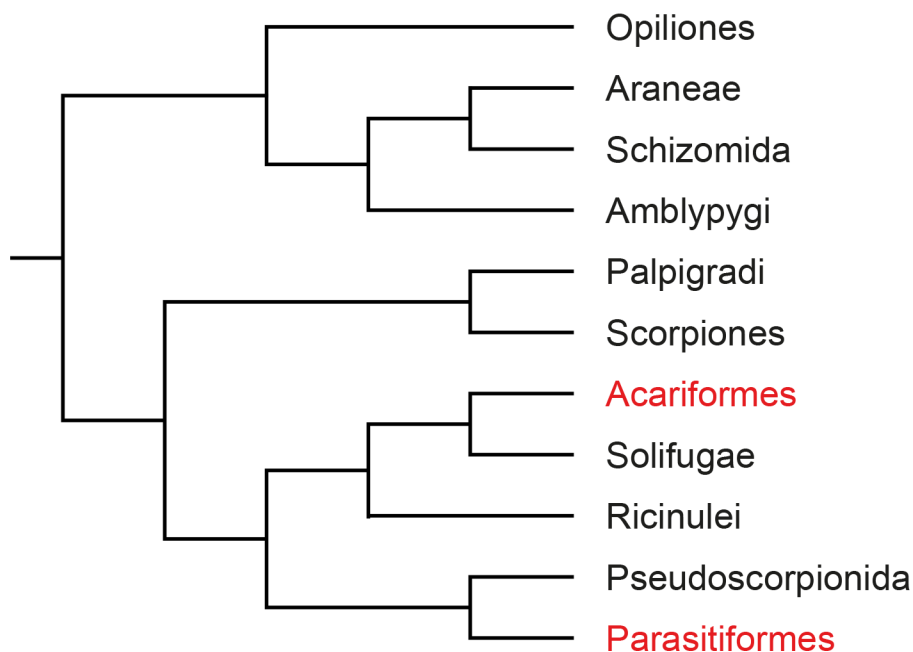


Fig. 1. Phylogenetic tree based on molecular data showing the position of the likely diphyletic Acari (Acariformes and Parasitiformes; in red) within the Arachnida (after Dabert et al. 2010).

Oribatida

With about 10,000 described species and estimations of up to 100,000 species (Travé et al. 1996, Schatz 2002, Subías 2004), Oribatida are diverse and abundant in temperate forest litter (going up as high as 400.000 individuals per m² making them a possible valuable resource for predators; Heethoff et al. 2009), tropical forests, lichens, moss (hence the common name 'moss mites'), decaying wood, tree bark, and also inhabit fresh and salt water, e.g. intertidal zones, and natural springs (*cf.* Evans 1992, Weigmann 2006; Krantz & Walter 2009 and citations therein). They are an important part of the soil decomposer system and were probably among the first land colonizers directly following the first terrestrial plants (Silurian/Devonian; Schaefer et al. 2010). They nourish on particles of dead or dying plant matter (as either external or internal saprophages), or even on fungi (mycophagy) decomposing the very same plant matter (Norton 2007). Hence, as secondary particle feeders that evolved out of a more or less purely fluid-feeding phylogenetic relationship (the Arachnida; Walter & Proctor 1998, Heethoff & Norton 2009b) coupled with low quality food (Norton 2007, Heethoff & Norton 2009a, b), they are burdened with constraints like a comparatively slow movement, a prolonged generation time and a low reproductive potential (Norton 1994, Sanders & Norton 2004, Heethoff et al. 2007). To cope with these constraints and the consequential constant risk of predation (also due to their high abundance), and to ultimately achieve reproduction requiring a long adult life, the animals developed several complex defensive strategies.

Defensive mechanisms

Defensive mechanisms in Oribatida are very common and diverse. They can be of a chemical, mechanical and behavioral nature. Chemical defensive strategies are based on secretions of the opisthonotal glands (also known as oil glands, Michael 1884). The secretions can include alarm pheromones, and predator repellents as well as antimicrobial agents (Kuwahara et al. 1975; Shimano et al. 2002, Raspotnig 2006, Saporito et al. 2007, Heethoff et al. 2011).

Behavioral strategies include for example thanatosis (playing dead), finding sheltered gaps or even habitation in places predators can't reach, e.g. for oviposition or habitation inside leaf veins during the juvenile life phase, respectively (Hansen 1999; see also Chapter 'Outlook - Evolution of the ptychoid defensive mechanism', p. 21).

Mechanical defense for example includes heavy sclerotization, or even biomineralization of the cuticle (calcium carbonate, calcium oxalate or calcium phosphate; Norton & Behan-Pelletier 1991a,b). Protective setae can be either permanently erected to build a safe space around the animal (Norton 2007) or can be actively erected (Michael 1888), which is believed to be the "first morphological adaptation for predator defense in oribatid mites" (Norton 2001). They can either be erected in independent rows, as a whole (Enarthronota, *cf.* Norton 2001), or individually (Palaeosomata, Norton 2007). Some mites possess flattened and hardened armor plate like setae, others adhere debris to their cuticle to create armor (Norton 2007). Pedofossae (grooves on the body for the safe stowage of

legs) and tecta protecting the joints are very common and diverse (Schmid 1988, Norton 2007). The latter can in some cases also be moveable to completely hide the legs (so called pteromorphs; Norton 2007). But the most complex mechanical defensive mechanism is ptychoidy.

Ptychoidy (*cf.* Tables 1–3)

Ptychoidy enables the animals to retract the legs and gnathosoma into a secondary body cavity in the idiosoma and by deflecting the prodorsum they can encapsulate themselves. This is always combined with a hardening of the exoskeleton through mineralization (Norton & Behan-Pelletier 1991a,b), and can in some groups also be combined with secretions of the opisthonotal glands (*e.g.* *Oribotritia berlesei*, Raspotnig et al. 2008), presumably functioning as chemical defense (*e.g.* own observations of *Euphthiracarus cribrarius* BERLESE when confronted with the predatory staphylinid beetle *Stenus* sp.). As morphological addition in some groups—resulting in an altered flight behavior—an escape jump can be present (Wauthy et al. 1998).

For the complete encapsulation of the animals several exoskeletal and muscular features are necessary. Grandjean (1969b) stated three prerequisites found in the direct ancestors to enable ptychoidy and Norton (2001) added a fourth: (i) the coxisternum must be embedded in a soft membrane and free from solid exoskeletal connections, (ii) the cuticle of the opisthosoma (hysterosoma) has to be hardened, (iii) the coxisternum itself must be foldable and (iv) there must be a system that can accommodate the huge volume changes

associated with ptychoidy (Sanders & Norton 2004, Grandjean 1969b). Since Acari lack most antagonistic musculature (*cf.* Evans 1992, Krantz & Walter 2009), functions like the flexing of the legs are facilitated by specialized systems through the build-up of hemocoel pressure, becoming especially important in ptychoidy. Exceptions from this lack of antagonistic musculature can be found for example in the claws and the chelicerae where both, flexors and extensors of the moveable elements, are present (Heethoff & Koerner 2007).

Another externally visual characteristic in the sister groups of ptychoid taxa is, that the prodorsum is also hardened and separated by the notogaster through soft membrane or at least distinct cuticular folds that could have evolved into pliable membrane (sejugal furrow/articulation, *cf.* Norton 2001, Sanders & Norton 2004, Norton & Sidorchuk 2014).

Ptychoidy probably evolved three times independently (Fig. 2), one time each in the Ptyctima and in the two enarthronote groups Protoplophoridae and Mesoplophoridae (groups that are separated for about 380 million years; Shear et al. 1984, Norton et al. 1988; trace evidence for the Ptyctima and body fossils of Protoplophoridae both date back to the Carboniferous: Labandeira et al. 1997 and Subías & Arillo 2002, respectively). Although their phylogenetic relationship changes depending on what phylogeny is considered, the three ptychoid groups are always clearly separated (Maraun et al. 2004, Pächl et al. 2012), strongly supporting a convergent evolution of this complex defensive mechanism. Out of the three groups, the first study

regarding morphology and function of ptychoidy was done on the Ptyctima (Sanders & Norton 2004). They have a worldwide distribution and are abundant in soil collected in Germany (see for example Niedbała 2012); therefore obtaining samples of numerous ptyctime species is fairly easy, especially in contrast to the Mesoplophoridae and even more the Protoplophoridae (cf. Niedbała 2004, Subías 2004, Niedbała 2012).

Ptyctima

The completely ptychoid Ptyctima consist of two superfamilies, the Euphthiracaroidea and the Phthiracaroidea. Whilst the Phthiracaroidea

only comprise of Phthiracaridae, the Euphthiracaroidea consists of three families: Euphthiracaridae, Oribotritiidae and Synichotritiidae (cf. Norton & Lions 1992, Lions & Norton 1999). The former sister family of the Phthiracaridae, the Steganacaridae, has been widely dismissed (e.g. Balogh & Mahunka 1983, Mahunka 1990, Subías 2004) and its species have been allocated to the Phthiracaridae. Sanders & Norton (2004) did the first detailed study of the ptychoid defensive mechanism studying the exoskeletal, muscular and functional characteristics of a member of Euphthiracaridae,

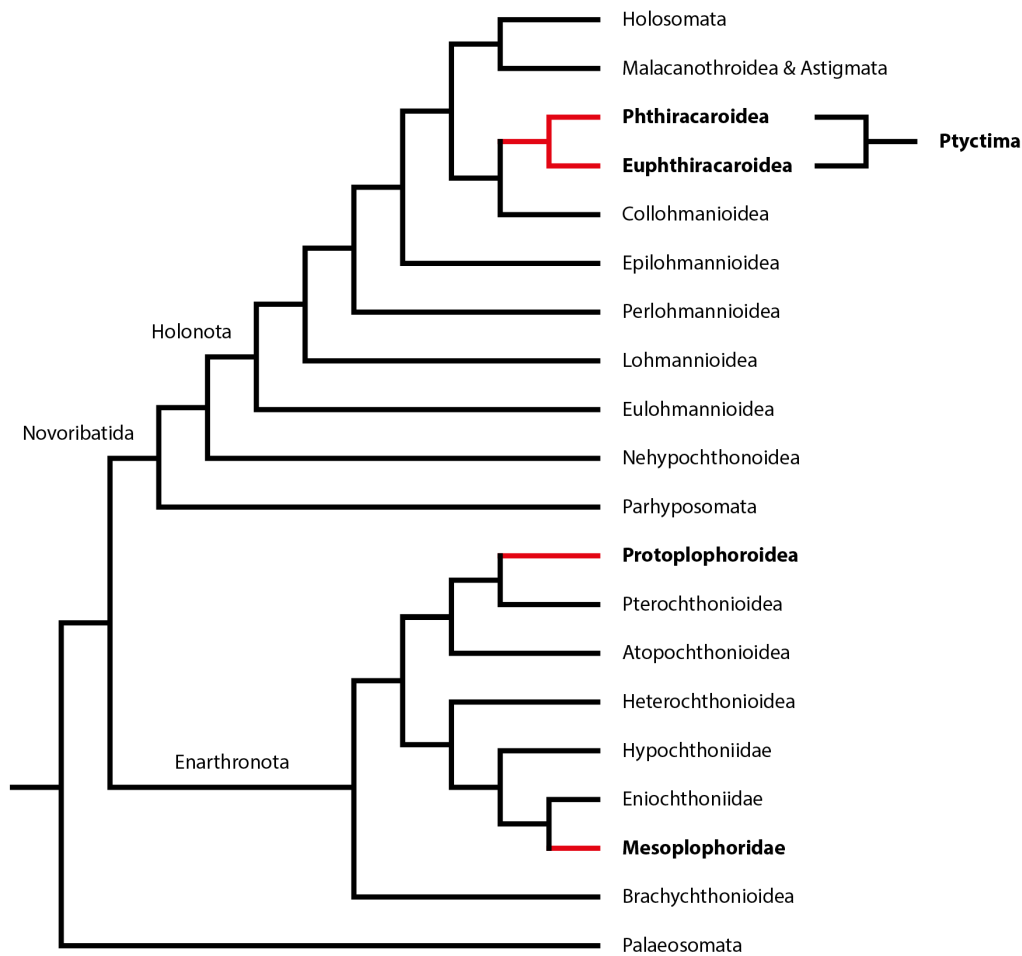


Fig. 2. Phylogenetic tree based on molecular data showing the position of ptychoidy (red branches) within the Oribatida (after Maraun et al. 2008).

Euphthiracarus cooki NORTON, SANDERS, & MINOR (Euphthiracaridae, Euphthiracaroida), in great detail.

Goal of this thesis

The goal of this study is to gain further knowledge about the morphology and function of ptychoidy in the Ptyctima. For that purpose we posed several questions:

- 1) Are the characteristics of ptychoidy consistent within the Euphthiracaroida, within the Phthiracaroida, and ultimately within the Ptyctima?
- 2) Do Euphthiracaroida and Phthiracaroida differ from each other regarding ptychoidy-related characteristics?
- 3) In comparison to members of their sister group (Collohmannioidea), which superfamily within the Ptyctima most likely resembles the ancestral state?

The study of Sanders & Norton (2004) regarding ptychoidy was done on one species

of the Euphthiracaridae (*Euphthiracarus cooki*), but to answer the questions above, it is necessary to gain knowledge on a broad basis, *i.e.* to study more groups within Euphthiracaroida and Phthiracaroida. Therefore we first investigated two more species of Euphthiracaroida from two more genera belonging to two families. We compared the exoskeletal (Schmelzle et al. 2008) and muscular characteristics (Schmelzle et al. 2009, including some functional aspects) of *Acrotritia ardua* KOCH (Euphthiracaridae) and *Oribotritia banksi* OUDEMANS (Oribotritiidae). In the next step we investigated a species of Phthiracaroida (with its single family Phthiracaridae; *Phthiracarus longulus* KOCH, Schmelzle et al. 2010) and afterwards another species from the same genus to see if there are noticeable differences between closely related species (*Phthiracarus globosus* KOCH, Schmelzle et al. 2012). To truly understand the functional aspects of ptychoidy, we studied the morphological characteristics regarding ptychoidy and on this basis compiled our knowledge regarding the functional morphology (Schmelzle et al. 2015).

MATERIAL AND METHODS

To facilitate our studies on exoskeletal and muscular elements involved in ptychoidy in their natural position, we used non-invasive synchrotron X-ray microtomography (SR μ CT). With this technique it is possible to gain virtual serial sections without the destruction of the specimen (like for example histological sectioning) and associated artifacts (for a detailed description of the method see Betz et al. 2007, Heethoff & Cloetens 2008, Heethoff et al. 2008, Heethoff & Norton 2009a). We then used voxel rendering (VGStudio MAX 1.2.1, Volume Graphics, Heidelberg, Germany) and segmentation (creation of 3D models; amira™ 4.0.1 and Amira 5.6.0, FEI SAS, France.) as

well as scanning electron microscopy for visualization. Furthermore, we used high-speed videography to capture the dynamic of en- and ecptychosis (*cf.* Table 1). A combination of both methods, SR μ CT and high-speed videography, allows for an animation of the generated 3D models and thus the *in silico* calculation of relative force vectors, which additionally gives us an insight into the dynamic of the musculature. For a Glossary of Terms (procedural and morphologic) related to ptychoidy and a list containing muscle names and abbreviations as well as their origin and insertion see Tables 1–3, p. 24-25.

SYNOPSIS

Publication 1: The ptychoid defensive mechanism in Euphthiracaroida (Acari, Oribatida): A comparison of exoskeletal elements

[2008; Schmelzle, S., Helfen, L., Norton, R.A., Heethoff, M.; Soil Organisms 80 (2), 227–241]

Sanders & Norton (2004) studied the functional morphology of the ptychoid defense mechanism for one species of Euphthiracaroida. Their study on *Euphthiracarus cooki* was done in great detail and reveals the exoskeletal and muscular characteristics responsible for the ability to encapsulate as well as the temporal dynamic underlying the whole process (e.g. the 'lazy hinge' mechanism). However, the superfamily Euphthiracaroida comprises three families: Euphthiracaridae, Oribotritiidae and Synichotritiidae. To fully understand the ptychoid defense mechanism in Euphthiracaroida, we studied the exoskeletal characteristics of ptychoidy in two species, *Rhysotritia ardua* (= *Acrotritia ardua*; Euphthiracaridae) and *Oribotritia banksi* (Oribotritiidae) by means of synchrotron x-ray microtomography (SR μ CT) and compared our results to those of *Euphthiracarus cooki*. We were able to show that although the families are closely related they show distinct differences. In contrast to *R. ardua* and *E. cooki*, *O. banksi* lacks interlocking triangles, the terminal fissure, the sagittal apodeme, the scale receptacle, and retains the articulation between ventral plates (in contrast to a complete fusion, called holoventral plates). Furthermore, its manubrium

is—compared to the other two—relatively small. On the other hand, *R. ardua* and *O. banksi* share the location of the sensillus (beneath in contrast to above the bothridial scale), lack of the tooth as prolongation of the lateral anterior tectum (as found in *E. cooki*), and the presence of two (instead of three) carinae lateral on the prodorsum. As unique feature, the postanal apodeme of *R. ardua* is much smaller than the preanal apodeme, whereas in *E. cooki* and *O. banksi* both are of nearly the same size.

In conclusion, functional constraints related to ptychoidy lead to similar exoskeletal characteristics in all three species, but the closer relationship of *R. ardua* and *E. cooki* (both belonging to the family Euphthiracaridae) leads to distinct differences from *O. banksi* (belonging to the Oribotritiidae). Similarities between *O. banksi* and *R. ardua* clearly differing from *E. cooki* are of a rather cosmetic nature.

Publication 2: The ptychoid defensive mechanism in Euphthiracaroida (Acari: Oribatida): A comparison of muscular elements with functional considerations

[2009; Schmelzle, S., Helfen, L., Norton, R.A., Heethoff, M.; Arthropod Structure and Development 38 (6), 461–472, DOI: 10.1016/j.asd.2009.07.001]

Sanders & Norton (2004) studied ptychoidy in *E. cooki* (Euphthiracaridae) including the musculature, whereas Schmelzle et al. (2008) only studied the exoskeletal characteristics

related to ptychoidy in *Acrotritia ardua* (= *Rhysotritia ardua*; Euphthiracaridae) and *Oribotritia banksi* (Oribotritiidae). There are four muscle systems actively involved in ptychoidy: (i) dorsoventral muscles of the prosoma (*DVP*), (ii) endosternal division of the prosoma (*EDP*), (iii) longitudinal division of the prosoma (*LDP*), and (iv) opisthosomal compressor system (*OCS*). Differences between the muscular characteristics of the three species (*R. ardua*, *O. banksi* and for comparison *E. cooki*) can be of a quantitative (e.g. number of muscle fibers) as well as of a qualitative nature (e.g. the presence or absence of muscles).

Dorsoventral muscles of the prosoma (*DVP*) - The coxisternal retractor (*csr*) has 12 muscle fibers in *E. cooki*, 17 in *R. ardua*, and 80 in *O. banksi*. The body size of the studied species greatly differs (300, 900, and 1800 μm , respectively). Hence there could be a correlation between body size and number of muscle fibers.

Endosternal division of the prosoma (*EDP*) - The area of insertion of the anterior dorsal endosternal muscle (*ade*) is comparatively small in *O. banksi*. This could be due to the smaller manubrium simply not allowing for a broad insertion, as it is the case in *E. cooki* and *R. ardua*.

Longitudinal division of the prosoma (*LDP*) - The origin of the inferior prodorsal retractor (*ipr*) is more posterior in *E. cooki* and *R. ardua* than in *O. banksi*. It consists of 13 muscle fibers in *E. cooki*, 28 - 32 in *R. ardua* and 90 - 100, strongly resembling the proportions found for the coxisternal retractor and thus also indicating a possible correlation of body size and number of muscle fibers.

The insertion of the prodorsum lateral adjustor (*pla*) on the manubrium of *O. banksi* is like the insertion of the anterior dorsal endosternal muscle comparatively small and its origin is dorsal in contrast to dorsolateral (as it is the case for *R. ardua* and *E. cooki*).

Opisthosomal compressor system (*OCS*) - Sanders & Norton (2004) named the muscles of the *OCS* according to the conditions they found in *E. cooki*. This is unfortunate since structures used in the naming of some muscles are not present in all of the euphthiracarid groups, more precisely the holovenral plates. Unfortunately, *O. banksi* lacks these completely fused ventral plates and hence the muscle names would be misleading. Thus we suggested a renaming from holovenral adductor (*hva*) and holovenral compressor (*hvc*) to ventral plate adductor (*vpa*) and ventral plate compressor (*vpc*), respectively, using ventral plates as simple term for the entirety of anal, adanal, genital, agenital, and plicature plates.

In contrast to *E. cooki* and *R. ardua*, *O. banksi* lacks the ventral plate adductor, and the notogaster lateral compressor (*nlc*) inserts not directly but via tendons on the medial edge of the ventral plates.

For the analysis of relative force vectors, the prodorsum lateral adjustor was ideal because its insertion on the manubrium is fairly stable, but its point of origin differs between the species. The analysis revealed more differences between the species in addition to the purely morphologic observation.

The lateral force vector of *O. banksi* is comparatively small. Its dynamic is two times higher in *R. ardua* and possibly also in *E. cooki* judging by the origin and insertion of its

prodorsum lateral adjustor. This discrepancy can possibly be explained by the lack of a scale receptacle within the tectonotal notch in *O. banksi*: the bothridial scale comes to rest on the tectonotal notch in *O. banksi* and does not need to be anchored within the scale receptacle. Therefore the need for a muscle being able to correct a lateral misalignment of the prodorsum does not exist. The posterior force vector of the prodorsum lateral adjustor on the other hand is very high in *O. banksi*, possibly providing for a stabilizing connection of bothridial scale and tectonotal notch. The presence of the scale receptacle in *R. ardua* leads to a drop of the posterior force vector of the prodorsum lateral adjustor by a factor of 8.

Due to the presence of holovertral plates, and the more complex connection of prodorsum and notogaster, the Euphthiracaridae supposedly are more derived than the Oribotritiidae. The development of the prodorsum lateral adjustor thereby follows the evolution of the scale receptacle.

Publication 3: The ptychoid defensive mechanism in Phthiracarus longulus (Acari, Oribatida, Phthiracaridae): Exoskeletal and muscular elements

[2010; Schmelzle, S., Helfen, L., Norton, R.A., Heethoff, M.; Soil Organisms 82 (2), 253–273]

The Ptyctima comprises the two sister groups Euphthiracaroida and Phthiracaroida. So far the ptychoid defensive mechanism had only been studied for species of Euphthiracaroida (Sanders & Norton, 2004; Schmelzle et al. 2008, 2009).

The Phthiracaroida comprise only one family,

the Phthiracaridae. The former sister family, Steganacaridae, had been disregarded (e.g. Balogh & Mahunka 1983, Mahunka 1990, Subías 2004).

Phthiracarus longulus differs from previously investigated species of Euphthiracaroida in some exoskeletal key features of ptychoidy. The most obvious difference is the complete separation of anal and genital valves (fusion of anal with adanal and genital with agenital plates, respectively) that are embedded in soft membrane (in contrast to plicature plates in Euphthiracaroida). The state of the anterior lock (left-fitting or right-fitting lock at the anterior margin of the anal valves) is equally distributed ($n=67$, LR $\chi^2 = 2.54$, $p = 0.11$) and indicates intraspecific variation rather than a taxonomic character (van der Hammen, 1989). *P. longulus* lacks a terminal fissure, but like *E. cooki* has a tooth (prolongation of the lateral anterior tectum) that in this case internally articulates with the ventral plates. The notogastral gap housing the ventral plates has a broad marginal tectum. At its posterior end there is a distinct indentation present, which has a counterpart on the posterior end of the anal valves (lock and key principle). Like *E. cooki* and *R. ardua*, *P. longulus* has a scale receptacle within the tectonotal notch, but in contrast to any of the euphthiracaroid species also has a pronounced sensillus ridge for the safe, un-pinched deposition of the sensillus in encapsulated state. Similar as in *O. banksi*, the manubrium is short, but more delicate than in any of the euphthiracaroid species.

Dorsoventral muscles of the prosoma (DVP) - The coxisternal retractor of *P. longulus* has 20–30 muscle fibers, but a body size of only 540

µm. Having more muscle fibers than *R. ardua* and at the same time being smaller contradicts a correlation of body size and the number of muscle fibers found in Euphthiracaroida for at least the entirety of Ptyctima.

The coxisternal protractor (*csp*) originates lateral on the notogaster and inserts on the sejugal apodeme. It has not been described for the Euphthiracaroida and seems to be a unique feature of the Phthiracaroida. Unique is also its assumed functional morphology, because (i) it acts as protractor for the legs (and therefore as antagonist) and (ii) during ptychosis changes its function from protractor to retractor and back.

Endosternal division of the prosoma (*EDP*) - In contrast to Euphthiracaroida the anterior dorsal endosternal muscle of *P. globosus* is longer, but due to the small manubrium has a small insertion area like *O. banksi*.

Longitudinal division of the prosoma (*LDP*) - The inferior prodorsal retractor of *P. longulus* again fits the body size / number of muscle fiber correlation found in Euphthiracaroida: *E. cooki* has 13 muscle fibers and a body size of 300 µm, *P. longulus* 20–25 muscle fibers and a body size of 540 µm, *R. ardua* has 28–32 muscle fibers and a body size of 900 µm, and *O. banksi* has 90–100 muscle fibers and a body size of 1800 µm.

Opisthosomal compressor system (*OCS*) - The different organization of ventral plates leads to different muscle morphology as well. *E.g.* the notogaster lateral compressor inserts on the soft anogenital membrane as opposed to the medial ridge of the ventral plates. It consists of 2 portions, an anterior and a posterior one, although the anterior one is hardly

distinguishable from the genital papilla retractors. Also, considering the different morphology of the ventral plates, the ventral plate adductor and ventral plate compressor probably play no role in ptychosis.

Phthiracaroid species clearly differ from euphthiracaroid species in features relating to functional aspects of ptychoidy, but overall they have the same set of systems enabling ptychoidy and the common origin of both groups is still strongly supported (*e.g.* by the location of the taenidiophore).

Publication 4: A morphological comparison of two closely related ptychoid oribatid mite species: Phthiracarus longulus and P. globosus (Acari: Oribatida: Phthiracaroida)

[2012; Schmelzle, S., Norton, R.A., Heethoff, M.; Soil Organisms 84 (2), 431–443]

In this study, we investigated the exoskeletal and muscular characters related to ptychoidy in *Phthiracarus globosus* and compared our results to the closely related *Phthiracarus longulus*. Although they are closely related they show subtle differences mainly concerning 'soft characters' though: in comparison to *P. longulus*, the body of *P. globosus* is more spherical, the sensillus groove more prominent, the bothridial scale more angular, the notogastral cuticle thicker, the sagittal apodeme and the indentation at the posterior end of the marginal tectum more pronounced.

Although stated differently before (Schmelzle et al., 2010), Phthiracaroida do not possess a real manubrium in the sense of a hard, posterolateral prolongation of the prodorsum, but rather a manubrial sclerite within the

articulating membrane (surrounding the prodorsum) located at the same area the manubrium would be and acting as a functional manubrium.

The differences between the two closely related species concerning 'soft characters' also continue regarding muscle morphology: all of the differences are found only in the quantity of muscle bands and muscle fibers. Again contradicting the body size / muscle fiber correlation, the inferior prodorsal retractor of *P. globosus* (body size 495 μm) has 35–40 muscle fibers, the anterior dorsal endosternal muscle has 5–6, and the superior prodorsal retractor (*spr*) has 8 muscle fibers in total (4 muscle bands with 2 muscle fibers each) whereas the inferior prodorsal retractor of *P. longulus* (body size 540 μm) has 20–25 muscle fibers, the anterior dorsal endosternal muscle 2 muscle fibers, and the superior prodorsal retractor 2–4 muscle fibers. Thus, the number of muscle fibers of the instanced muscles of *P. globosus* is two to three times higher than the number of homologous muscles in *P. longulus*. We suspect, that the correlation to body size actually concerns muscle volume instead of the number of muscle fibers. The notogaster lateral compressor in *P. globosus* only consists of the posterior portion described in Schmelzle et al. (2010) leading us to believe that the anterior portion in both species are actually muscle fibers of the genital papilla retractors (as already suspected). The coxisternal protractor newly described for *P. longulus* (Schmelzle et al., 2010) is also present in *P. globosus* and is of similar shape making it a probable synapomorphy for the Phthiracaridae and possibly also the Phthiracaroidae.

The study of *P. globosus* and the comparison to the closely related *P. longulus* shows that the informative signals on a large phylogenetic scale are in the presence or absence of whole characters whereas informative signals on a small phylogenetic scale are mostly in the quality and quantity of characters.

Publication 5: Mechanics of the ptychoid defense mechanism in Ptyctima (Acari, Oribatida): one problem, two solutions

[2015; Schmelzle, S., Norton, R.A., Heethoff, M.; Zoologischer Anzeiger - A Journal of Comparative Zoology 254, 27–40; DOI: 10.1016/j.jcz.2014.09.002]

Oribatida lack most antagonistic musculature (cf. Evans 1992, Krantz & Walter 2009). Exceptions are for example the extensors of the chelicerae and the claws. During ptychosis the animals have to accommodate huge volume changes and hemolymph movement. Norton (2001) noted this as fourth precondition enabling the evolution of ptychoidy and Sanders & Norton (2004) already suspected two different modes of pressure build-up within the Ptyctima; one associated with each of the superfamilies Euphthiracaroidae and Phthiracaroidae. To elucidate these different functions we studied one species of each superfamily: *Acrotritia ardua* (= *Rhysotritia ardua*, Euphthiracaroidae) and *Phthiracarus longulus* (Phthiracaroidae).

High-speed recordings revealed a narrowing of the notogastral gap housing the ventral plates (holoventral and plicature plates) and a lateral compression of the notogaster during eptychosis in *A. ardua*. No such observation

could be made for the Phthiracaroida. Instead, during ecptychosis the ventral plates (anal and genital valves) functionally combined into one big ventral plate get retracted into the idiosoma. As suspected before, the Euphthiracaroida seem to use lateral compression as mode for the build-up of pressure whereas the Phthiracaroida use a piston-like technique by retracting the single ventral plate. Based on the study of Sanders & Norton (2004), the muscle system responsible for the compression of the notogaster is the opisthosomal compressor system (OCS) comprising three different muscles (terminology according to Schmelzle et al., 2009): the ventral plate adductor (*vpa*), ventral plate compressor (*vpc*) and the notogaster lateral compressor (*nlc*). The combined contraction of those muscles leads to a transmission of force via the preanal apodeme (acting as a kingpost) onto the notogaster, thereby narrowing the notogastral gap and compressing the notogaster laterally. Phthiracaroida possess the same muscle system, although developed differently. The notogaster lateral compressor is restricted to the last third of the animal and inserts on the soft anogenital membrane surrounding the single ventral plate. A contraction of the notogaster lateral compressor then leads to a retraction of the ventral plate. And so does the postanal muscle (*poam*) based on its position and orientation (originating terminal on the notogaster and inserting on the postanal apodeme which gets retracted as well in the process of ecptychosis). A calculation of its dynamic revealed a possible contraction of 40% of its original length (length in encapsulated state), whereas the dynamic of the postanal

muscle in *A. ardua* is basically zero (just being able to act as stabilizing element for the ventral plates). This would make the postanal muscle an integral part of the opisthosomal compressor system. The ventral plate adductor and ventral plate compressor on the other hand seem to play no role in this process except possibly holding the ventral plates together.

Calculations of volume changes during ptychosis revealed a possible volume change of about 2–3.5 % for both groups and although seemingly low, this amount seems to be sufficient. How the animals deal with defecation and oviposition is still not yet clear. The total amount of 'disposables' adds up to about 18% of the body volume of the animals, exceeding the calculated volume change by lateral compression as well as the intake of the ventral plates by a factor of six. A fluxional system where the animals strictly control uptake and disposal to maintain a more or less constant volume and therefore pressure level seems to be most likely.

Since Phthiracaroida probably evolved within the Euphthiracaroida (Pachl et al., 2012), lateral compression seems to be the ancestral mode of operation. This hypothesis is supported by comparison with the suspected sister group of the Ptyctima, the Collohmannioidea, which also uses lateral compression (Norton 2006) instead of—by Acari often used (e.g. *Archezogetes longisetosus*)—dorsoventral compression.

CONCLUSIONS

Out of the four families of Ptyctima, ptychoidy has now been well studied in three: Euphthiracaridae, Oribotritiidae, and Phthiracaridae.

Differences regarding ptychoidy can even be found in closely related species (e.g. within a genus, cf. *Phthiracarus*), although the differences on such a small phylogenetic scale are mostly 'soft characters', i.e. qualitative and quantitative differences in the state of characters: for example the number of muscle fibers of the *csr*, and the depth of the tectonotal notch. On a larger phylogenetic scale (e.g. between families, cf. Euphthiracaridae and Oribotritiidae) the informative signals are mostly differences in the presence or absence of whole characters ('hard characters'), although 'soft character' differences of course are still present: for example the presence of holoventral plates in Euphthiracaridae, but not in Oribotritiidae and again the number of muscle fibers of the *csr*. On superfamily level those differences can even add up to differences on key functional characters regarding ptychoidy, like the build-up of hemocoel pressure facilitated by lateral compression in Euphthiracaroida on the one hand, and by retraction of the (functionally unified) single ventral plate into the idiosoma in Phthiracaroida on the other hand. Another example is the *csp* that can act as a protractor for the legs. So far it is exclusively found in

phthiracaroid species and might be a synapomorphy for the Phthiracaroida.

In the beginning we posed some questions and now we can address them:

1) Are the characteristics of ptychoidy consistent within the Euphthiracaroida, within the Phthiracaroida, and ultimately within the Ptyctima?

The characteristics of ptychoidy are mostly consistent within the Euphthiracaroida, within the Phthiracaroida, and—with exceptions—also within the Ptyctima.

2) Do Euphthiracaroida and Phthiracaroida differ from each other in regard to ptychoidy-related characteristics?

*The most substantial difference between Euphthiracaroida and Phthiracaroida is the system responsible for the build-up of pressure and the absence or presence of the coxisternal protractor (*csp*), respectively.*

3) In comparison to members of their sister group (Collohmannioidea), which superfamily within the Ptyctima most likely resembles the ancestral state?

Based on the similar morphology of the ventral plates and the associated system for the build-up of pressure, the Euphthiracaroida likely represent the ancestral state.

OUTLOOK

Despite the insights gained through this thesis, the knowledge of the ptychoid defensive mechanism is still far from complete:

What is the state of ptychoidy in the remaining unexamined ptyctime groups Synichotritiidae (and Steganacaridae)?

How is the ptychoid defensive mechanism realized in the two groups of Enarthronota, Mesoplophoridae and Protoplophoridae?

And what are the morphological and functional differences to the Ptyctima? For example, what principles is their system of pressure build-up based on?

How did ptychoidy evolve, *i.e.* what can we learn from the ontogenesis and from direct non-ptychoid sister groups and in turn what inference can be drawn on possible pre-adaptations in the ground plan of the Oribatida?

Are there new techniques better suited to gain these insights?

In the following I will shortly address each of these points:

Ptychoidy in Ptyctima

To actually confirm the synapomorphy of the *csp* more ptyctime species have to be studied, including species of the-in regard to ptychoidy- so far unexamined Synichotritiidae (Euphthiracaroida) as well as phthiracaroid species of other genera (*e.g.*

Hoplophthiracarus) and especially the genus *Steganacarus* (Phthiracaroida; Fig. 3), which once constituted the family Steganacaridae until it has been disregarded and its entire species have been attributed to the Phthiracaridae (Balogh & Mahunka 1983, Mahunka 1990, Subías 2004). Niedbała (1992, 1994), however, does not acknowledge this re-classification.

Another factor is, that *Steganacarus* in contrast to *Phthiracarus* seems to better withstand an attack of the predatory staphylinid beetle *Euconnus pubicollis* MÜLLER AND KUNZE (Jaloszynski & Olszanowski 2013). The question just is, why?

What morphological or functional characteristics distinguish *Steganacarus* from *Phthiracarus* giving it a better protection against this beetle (*cf.* Fig. 3)?

Ptychoidy in Enarthronota

As stated before, ptychoidy probably evolved three times independently, once in the Ptyctima and twice within the Enarthronota (one time each in the Mesoplophoridae and Protoplophoridae). So far the ptychoid defensive mechanism has been well studied for the Ptyctima (Sanders & Norton, 2004; Schmelzle et al. 2008, 2009, 2010, 2012, 2015), but no studies have been done for any of the ptychoid enarthronote species. The Enarthronota are defined by a notogaster comprised of several cuticular plates and serial transverse scissures that can be modified in various ways up to the point where they

become articulations (Grandjean 1947, see also Grandjean 1969b), which becomes especially important in ptychoidy.

The question remains: How is the ptychoid defensive mechanism realized in the two enarthronote groups and how does it differ from

the ptyctime state? Based on our findings and the findings of Sanders & Norton (2004), especially regarding the functional morphology (Schmelzle et al. 2009, 2010, 2015), we can try to elucidate these questions.

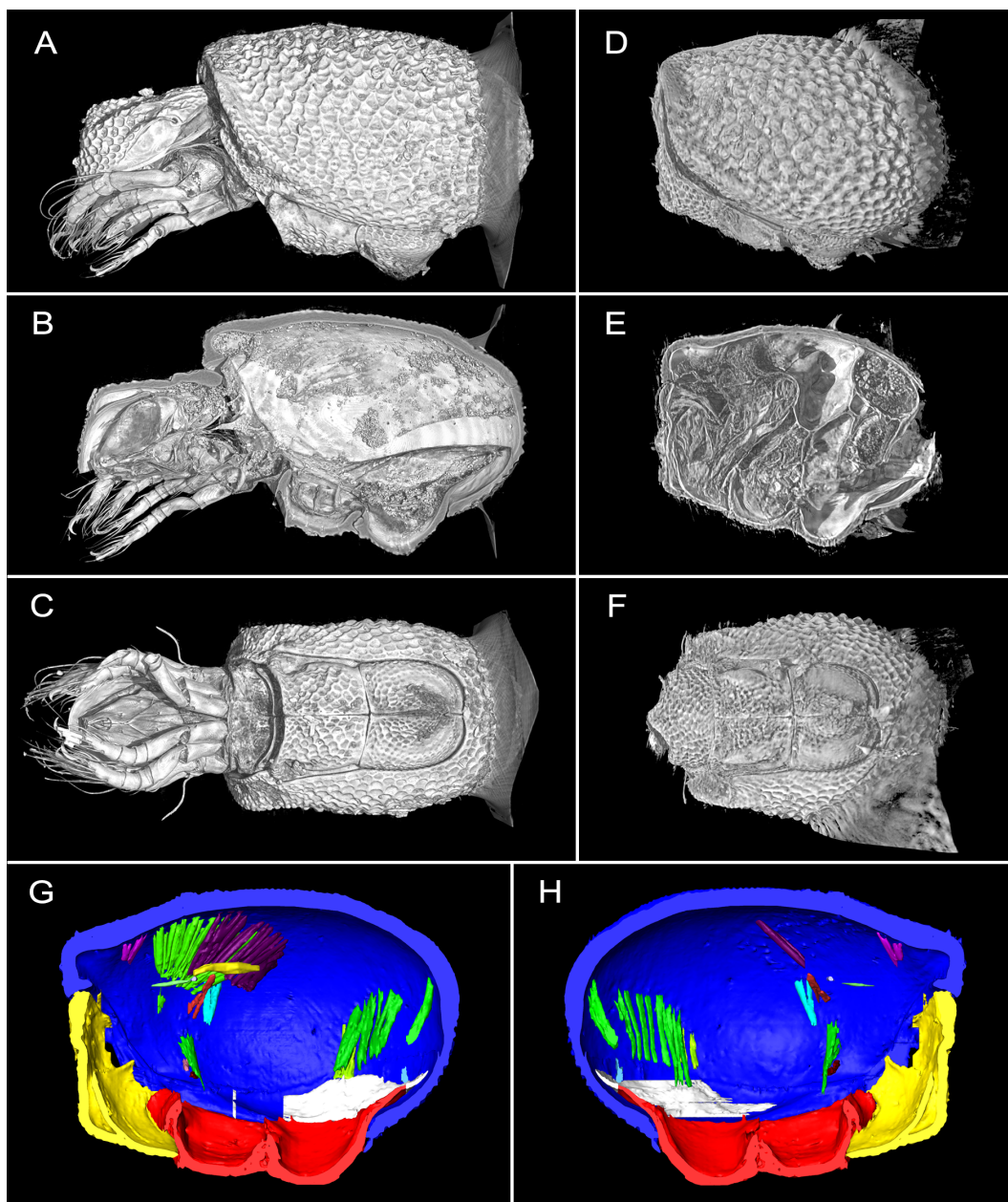


Fig. 3. Voxel renderings of two specimens of *Steganacarus carinatus* KOCH in extended (A, B, C) and encapsulated (D, E, F) state, and sagittal sections of a 3D model showing right (G) and left (H) half. A, D. Lateral view. B, E. Lateral view of a virtual sagittal section. C, F. Ventral view. G, H. Lateral view of a virtual sagittal section of 3D model showing musculature involved in ptychoidy (incomplete). Notogaster in blue, prodorsum in yellow, ventral plates in red.

Mesoplophoridae – In *Mesoplophoridae* the anal and genital valves are embedded within a single ventral plate that takes up nearly the whole ventral side of the species. This plate is a secession of parts of the notogaster (*cf.* Norton 2001). Anal and genital valves can be either spatially separated by a ventral plate bridge (in the genus *Mesoplophora*, Fig. 4) or in direct contact with each other (in the genus *Archoplophora*). The single ventral plate and the overall body form suggest a mode of pressure build-up similar to the Phthiracaroida: the retraction of the single ventral plate into the notogaster.

Protoplophoridae – Externally, the ventral plates of the *Protoplophoridae* are not or only partly visible in the encapsulated animals (*e.g.* in *Prototritia major* JACOT and *P. n. sp.*, respectively; own observations of both; *cf.* Fig 6). The notogaster is divided into three parts: 1) the pronotaspis, functionally corresponding the whole notogaster of the Ptyctima and as static element, 2) the unpaired pygidium and 3) the paired pleuraspis (Fig. 5). The set-up of the pygidium and the pleuraspis together with the ventral plates functionally corresponds to the dynamic elements: to the single ventral plate encompassing the anal and genital venter of

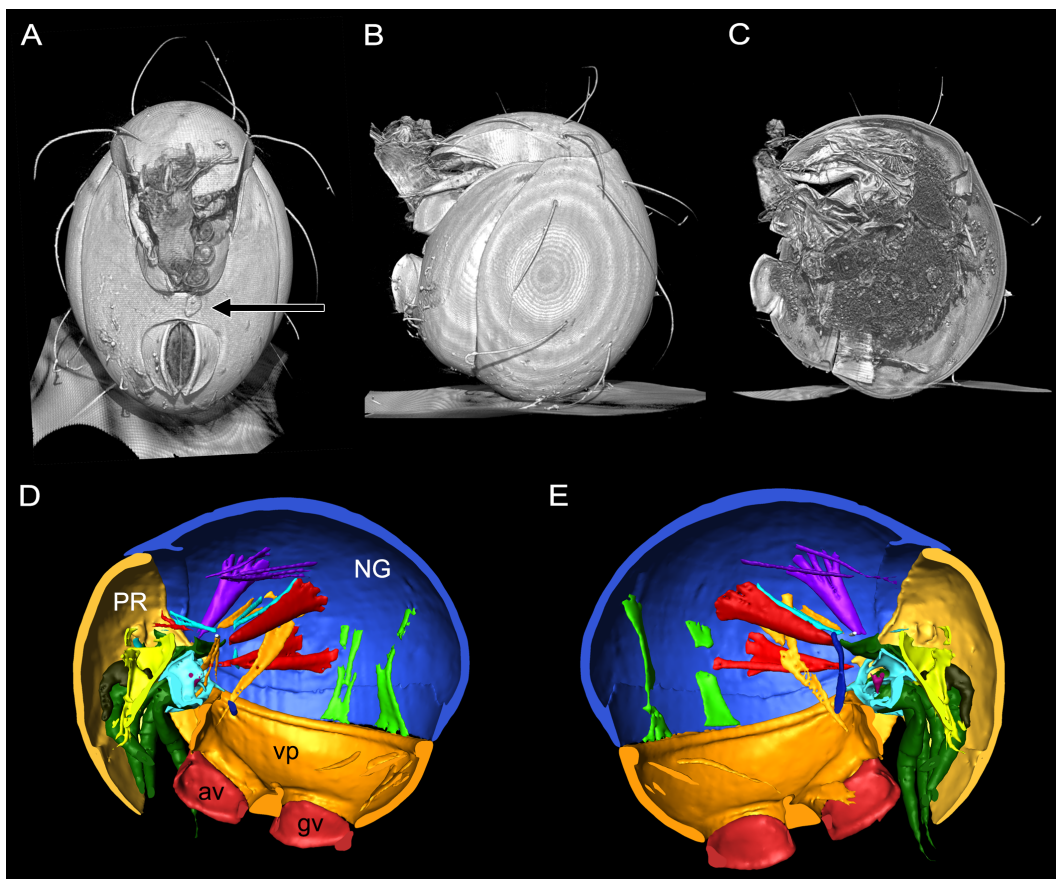


Fig. 4. Voxel renderings of *Mesoplophora cubana* CALUGAR AND VASILIU in nearly encapsulated state (A – C), and sagittal sections of 3D model showing right (D) and left (E) half. A. Ventral view. B. Lateral view showing left half of animal. C. Lateral view of a virtual sagittal section. D, E. Lateral view of virtual sagittal section of 3D model showing musculature involved in ptychoidy (incomplete). av, anal venter (in red); gv, genital venter (in red); NG, notogaster (in blue); PR, prodorsum (in yellow); vp, single ventral plate (in orange). Arrow indicates the separation of genital and anal valves.

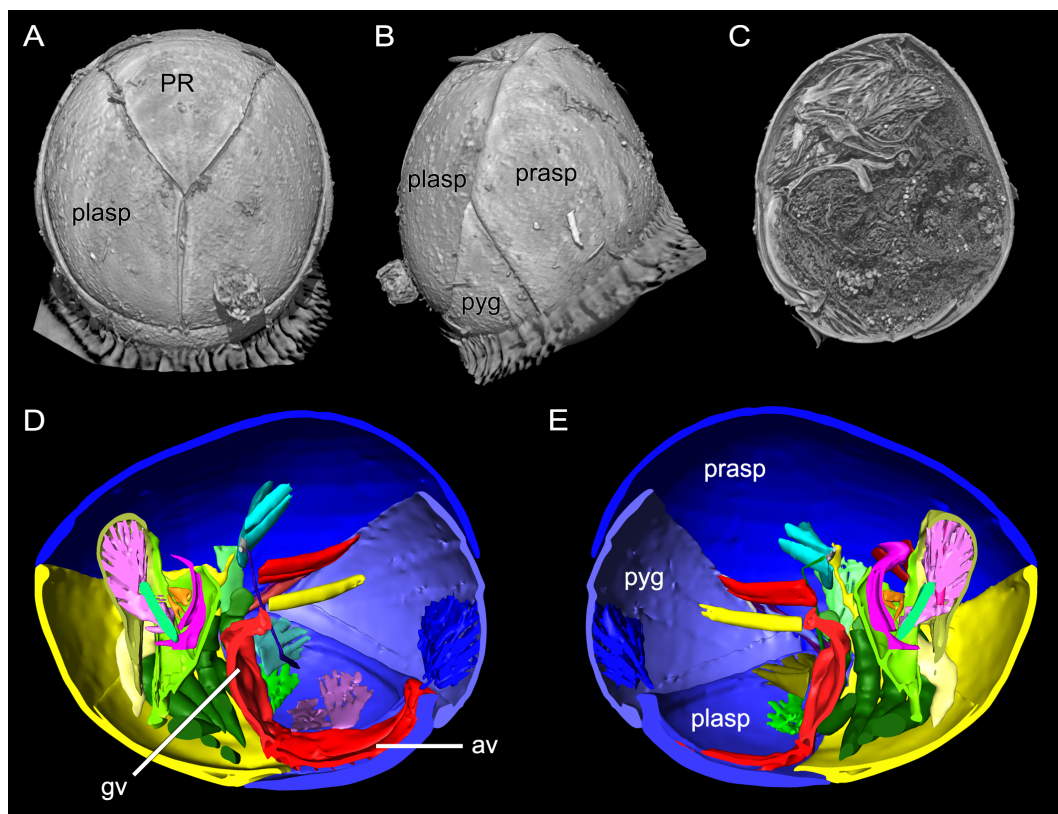


Fig. 5. Voxel renderings of *Prototritia major* JACOT in encapsulated state (A – C), and sagittal sections of 3D model showing right (D) and left (E) half. A. Ventral view. B. Lateral view showing left half of animal. C. Lateral view of a virtual sagittal section. D, E. Lateral view of a virtual sagittal section of 3D model showing musculature involved in ptychoidy (incomplete). Note the position of the ventral plates (in red) inside the encapsulated animal and dorsal to the pleuraspis. av, anal venter (in red); gv, genital venter (in red); PR, prodorsum (in yellow). Notogastral parts (in shades of blue): plasp, pleuraspis; prasp, pronotaspis; pyg, pygidium.

Mesoplophoroidea and the functionally unified ventral plates (anal and genital venter combined) of Phthiracaridae. During ptychosis this set-up gets retracted into the idiosoma as well, though the mode of operation is different: first the paired pleuraspis plates get pulled to the side gliding on a rail built by the pygidium in the process exposing the ventral plates up to a point where the membrane between pleuraspis and ventral plates is maximally strained. The setup including the pygidium then gets retracted into the idiosoma.

Evolution of ptychoidy

Ontogenesis – Another important aspect of the ptychoid defensive mechanism is its distribution over the ontogenetic stages: juveniles of the Ptyctima are not ptychoid whereas enarthronote juveniles are (Fig. 6; cf. Weigmann 2006). This is presumably linked to their way of life: burrowed in leaf veins (Hansen 1999, also adults of *A. ardua*) vs. free-living in soil, respectively. Studying the ontogenetic stages could provide new insights into the evolution of ptychoidy in these groups.

Phylogeny – The study of sister groups to each ptychoid group allows for the distinction of phylogenetic and functional traits of ptychoidy. For example, the newly described *Collohmannia johnstoni* NORTON AND SIDORCHUK (Norton & Sidorchuk 2014; Fig. 7), regarded as a member of the Ptyctima sister group, already shows exoskeletal characteristics that resemble the euphthiracaroid pattern (e.g. the elongated state of the anal and genital valves; white arrows in Fig. 7A,C). Further outgroups include

Eniochthonius minutissimus BERLESE for the Mesoplophoridae (Fig. 8A-D) and species of the genus *Sphaerochthonius* for the Protoplophoridae (Fig. 8E-H).

Sphaerochthonius (Sphaerochthoniidae) – The genus *Sphaerochthonius* is not only interesting because of its phylogenetic position as a member of the sister group of Protoplophoridae, but also because it shows some sort of gradient behavior to ptychoidy: the animals are able to fold up their legs (white

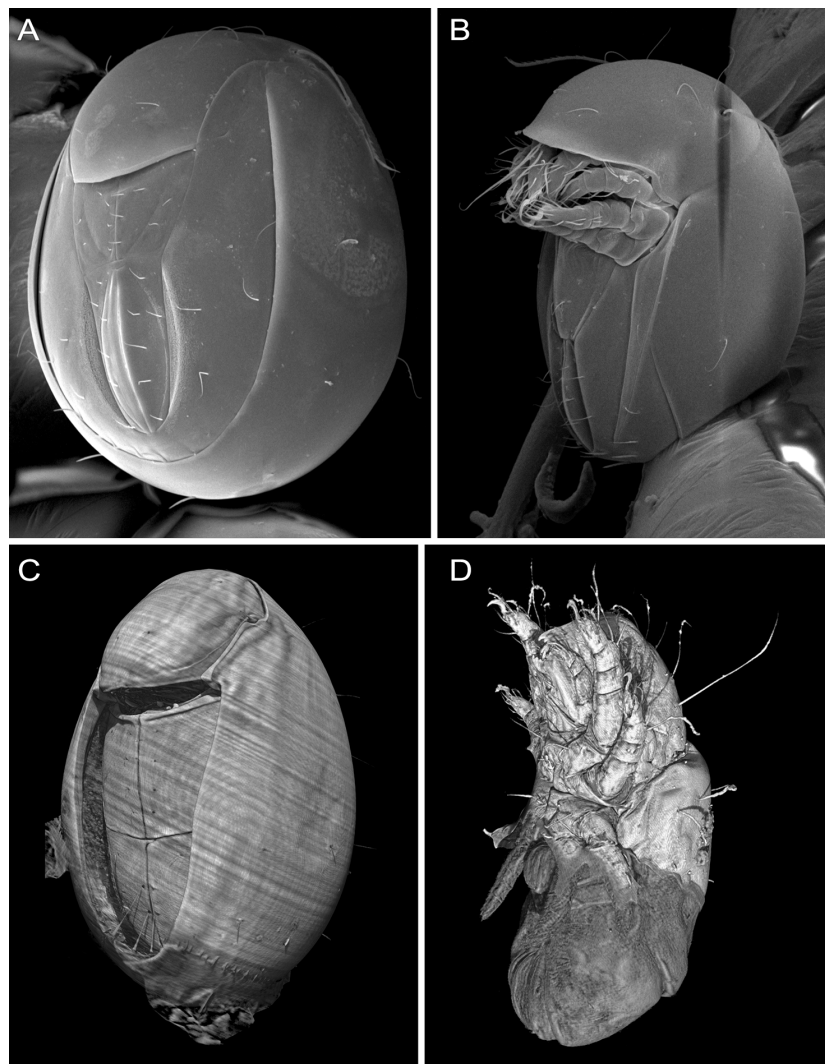


Fig. 6. Scanning electron micrographs showing ventrolateral views of *Archoplophora rostralis* WILLMANN in adult (A) and juvenile stage (B) and voxel renderings of *Phthiracarus longulus* in adult (C) and non-ptychoid juvenile stage (D).

arrows in Fig. 8G,H), pull them towards their body and subsequently fold down the prodorsum a little bit giving the whole animal a more compact body form, though not [yet] able to encapsulate themselves (Fig. 8G,H). This behavior indicates, that most exoskeletal and muscular characteristics regarding ptychoidy in Protoplophoridae should already be present in *Sphaerochthonius*.

Palaeosomata – The inference on pre-adaptations to ptychoidy can only be resolved by studying and comparing the basal oribatid out-group *Palaeosomata* (cf. Fig. 2). *Palaeosomata* still have a low degree of cuticular hardening (Norton 2001), supposedly resembling the ground plan of the Oribatida. Therefore they are perfect to study the hypothesized pre-adaptations to ptychoidy.

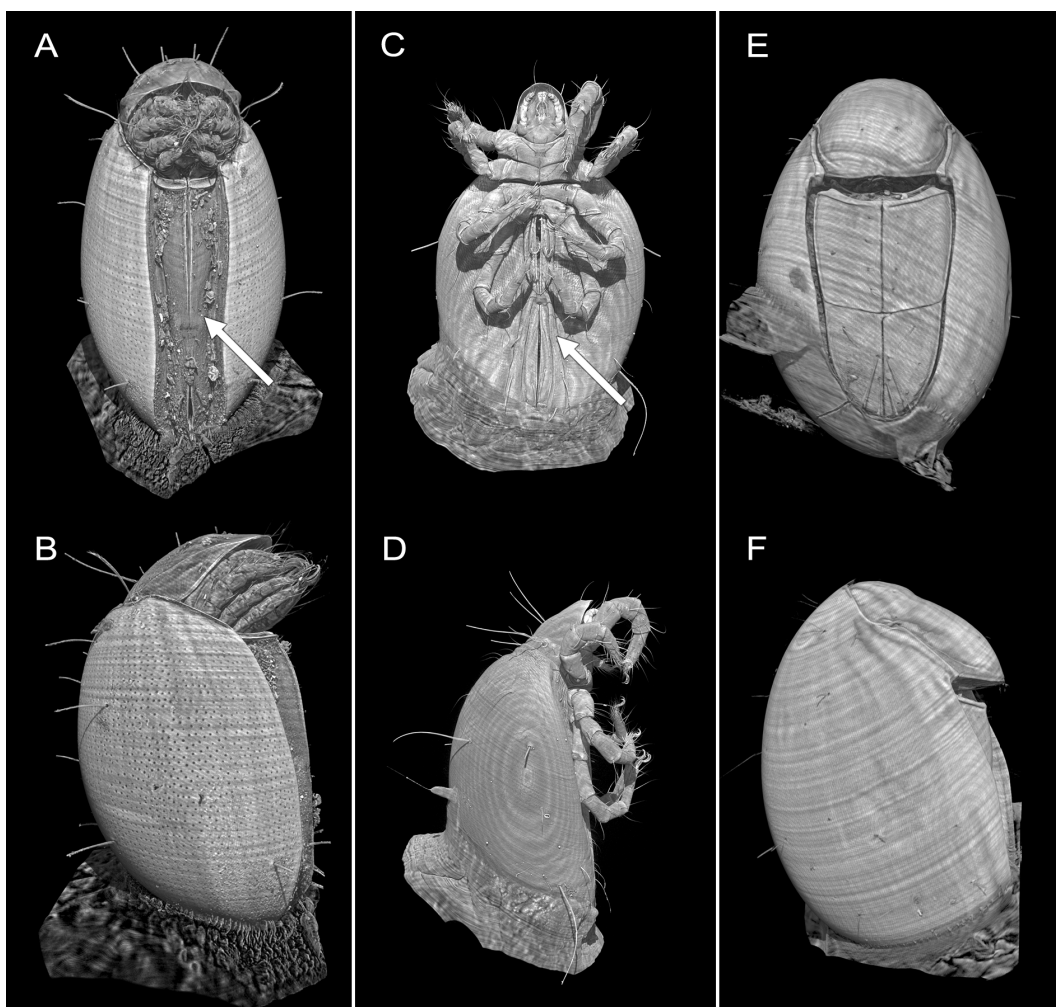


Fig. 7. Voxel renderings showing the two ptyctime groups and their sister group Collohmanniidae. A, B. *Acrotritia ardua* (Euphthiracaroida). C, D. *Collohmanna johnstoni* (cf. Norton & Sidorchuk 2014). E, F. *Phthiracarus longulus* (Phthiracaroida). Upper images show ventral view; lower images lateral view. Arrows indicate the elongated state of the ventral plates in Euphthiracaridae and Collohmanniidae.

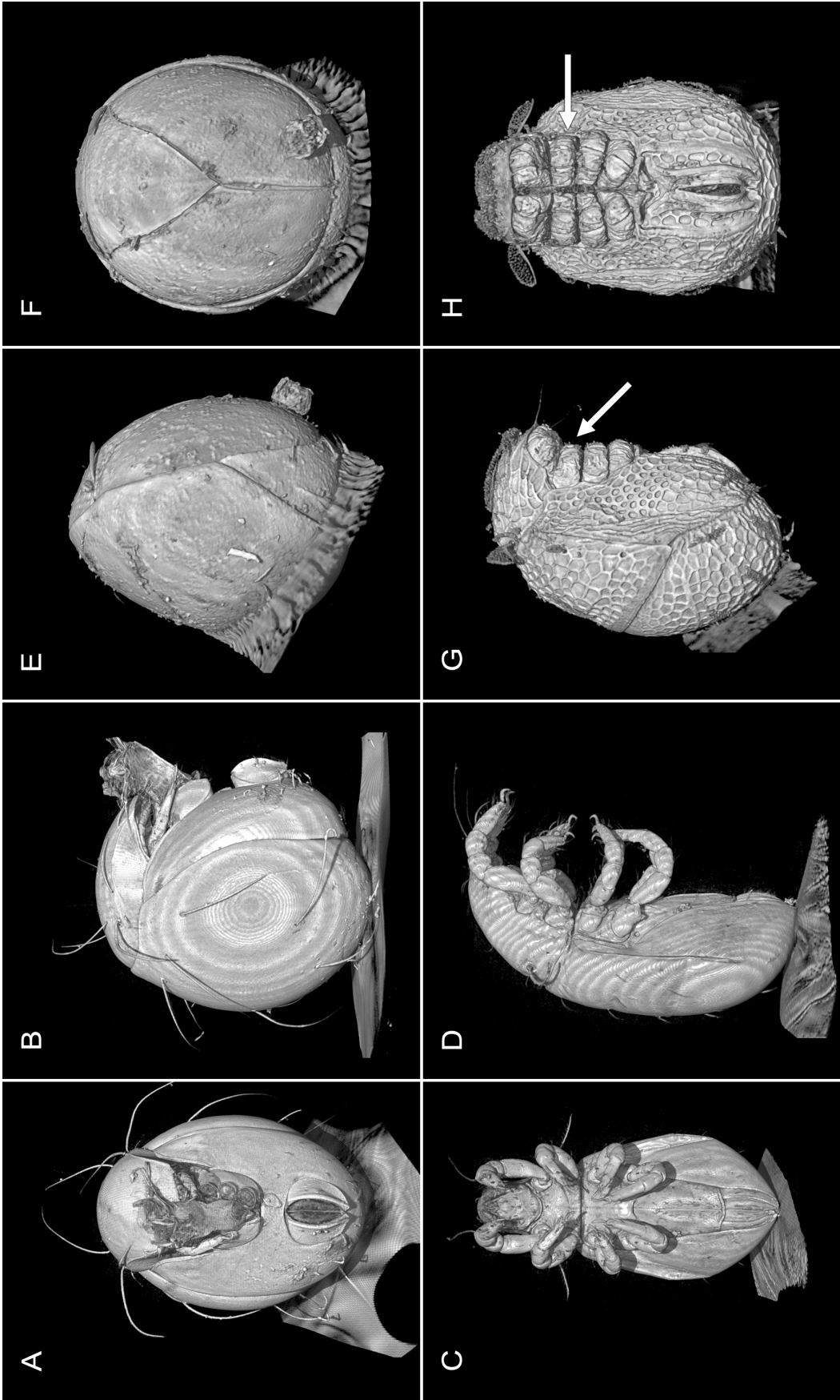


Fig. 8. Voxel renderings showing the two enarthronote groups and their respective sister groups in ventral (A, C, F, H) and lateral view (B, D, E, G). A, B. *Mesoplophora cubana* (Mesoplophoridae). C, D. *Eniochthonius minutissimus* (Eniochthoniidae). E, F. *Prototrertia major* (Protoplophoridae). G, H. *Sphaerochthonius* sp. (Sphaerochthoniidae; white arrows indicate the folded up legs).

New methods for structural research

Wet scans – Using ultra-fast tomography, the time for a complete SR μ CT scan of a sample is greatly reduced (within seconds) and thus samples can now also be scanned within a liquid (100% EtOH) without complete evaporation of the liquid that would occur during a long-time scan (15–45 minutes). This eliminates artifacts originating from the drying of the animals (critical point drying with liquid carbon dioxide) like shrinking of tissues and the associated tearing of e.g. muscle fibers (cf. Fig. 9). The clarity of the scans is greatly enhanced especially when combined with a contrasting agent (e.g. 1% iodine solution). For example, muscle fibers within a muscle bundle can be clearly separated from each other since agglutination of the former is no longer a problem. Furthermore, artifacts coming from the fixing of the animals on the sample holder (instant adhesive collar; Fig. 9; cf. Fig. 3 - 8) are hereby eliminated. The container holding the sample can be easily removed from the virtual image stack without affecting specimen data.

ASTOR – After already using high-speed radiography (cf. Fig. 10), the next step would be time-resolved computer tomography (4D SR μ CT or cine-tomography; cf. dos Santos Rolo et al. 2014) of small animals like mites enabling the observation of—for example—muscle contractions in 3D/4D. A project funded by the BMBF (Bundesministerium für Bildung und Forschung, Germany) dealing with this issue is currently ongoing: **Arthropod Structure revealed by ultra-fast Tomography and Online Reconstruction** (ASTOR - project number 05K13VTA). First achieved goals include high-throughput tomography and high-speed radiography of living animals, which—in contrast to conventional high-speed videography—also exposes dynamic processes within the animal, e.g. the movement of the gut and the positioning of the legs during entychosis (Fig. 10).

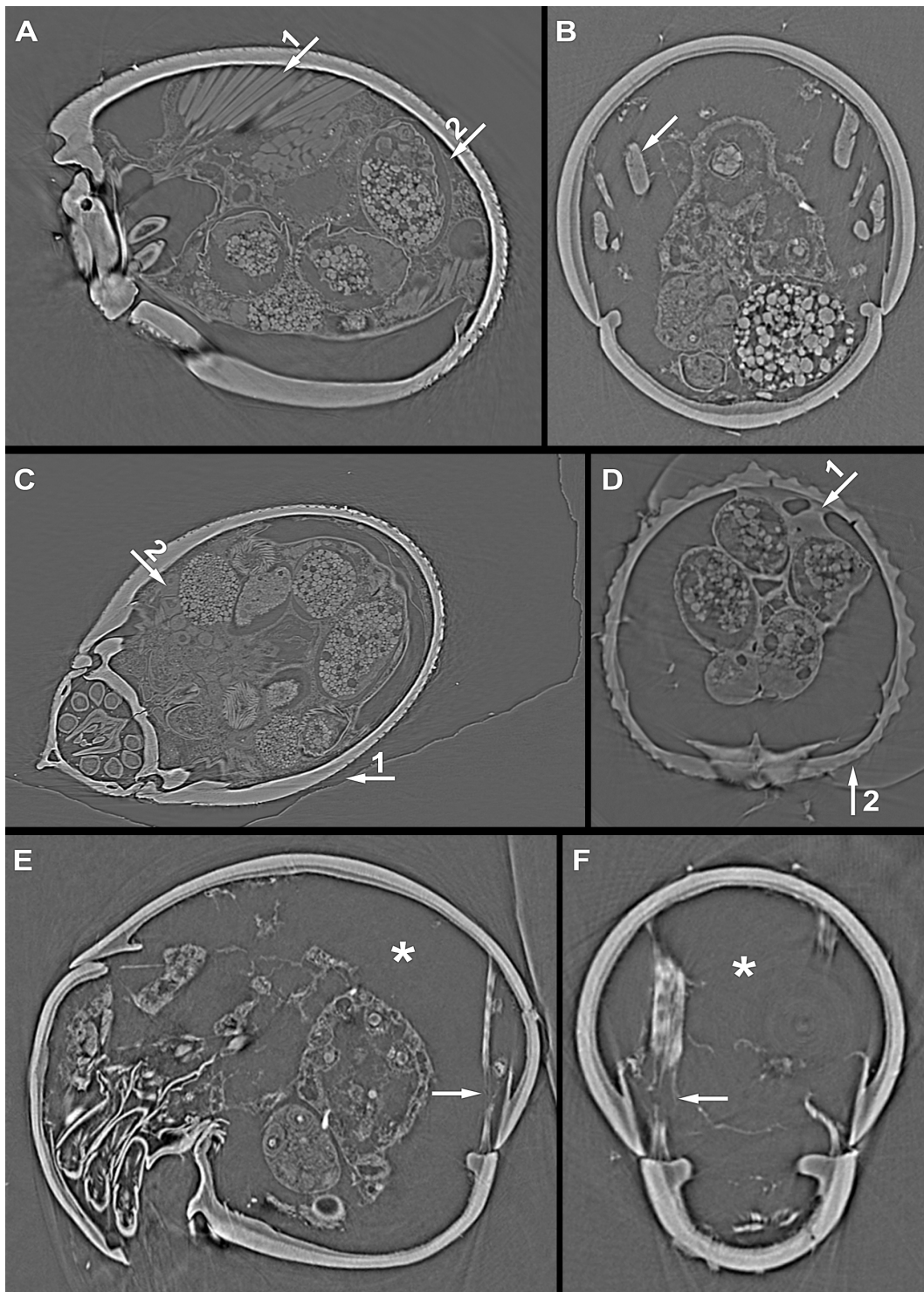


Fig. 9. Comparison of 'raw' data of wet and dry scans showing multiple related artifacts. A. Wet scan of *Steganacarus magnus* NICOLET. Arrow 1 points to clearly separated muscle fibers. Arrow 2 points to tissue still directly in contact with cuticle. B. Dry scan of *Mesoplophora cubana*. Arrow indicates muscle bundle with indissoluble muscle fibers due to agglutination during drying. C. Wet scan of *Steganacarus magnus*. Arrow 1 points to gap between specimen and sample holder. Arrow 2 points to well preserved cells. D. Dry scan of *Steganacarus carinatus*. Arrow 1 points to instant adhesive that entered the dried specimen. Arrow 2 points to instant adhesive directly touching the specimen. E, F. Dry scan with *Mesoplophora cubana*. Arrows point to tearing of muscle fibers. Asterisks indicate the empty space left behind by shrinkage of the tissue.

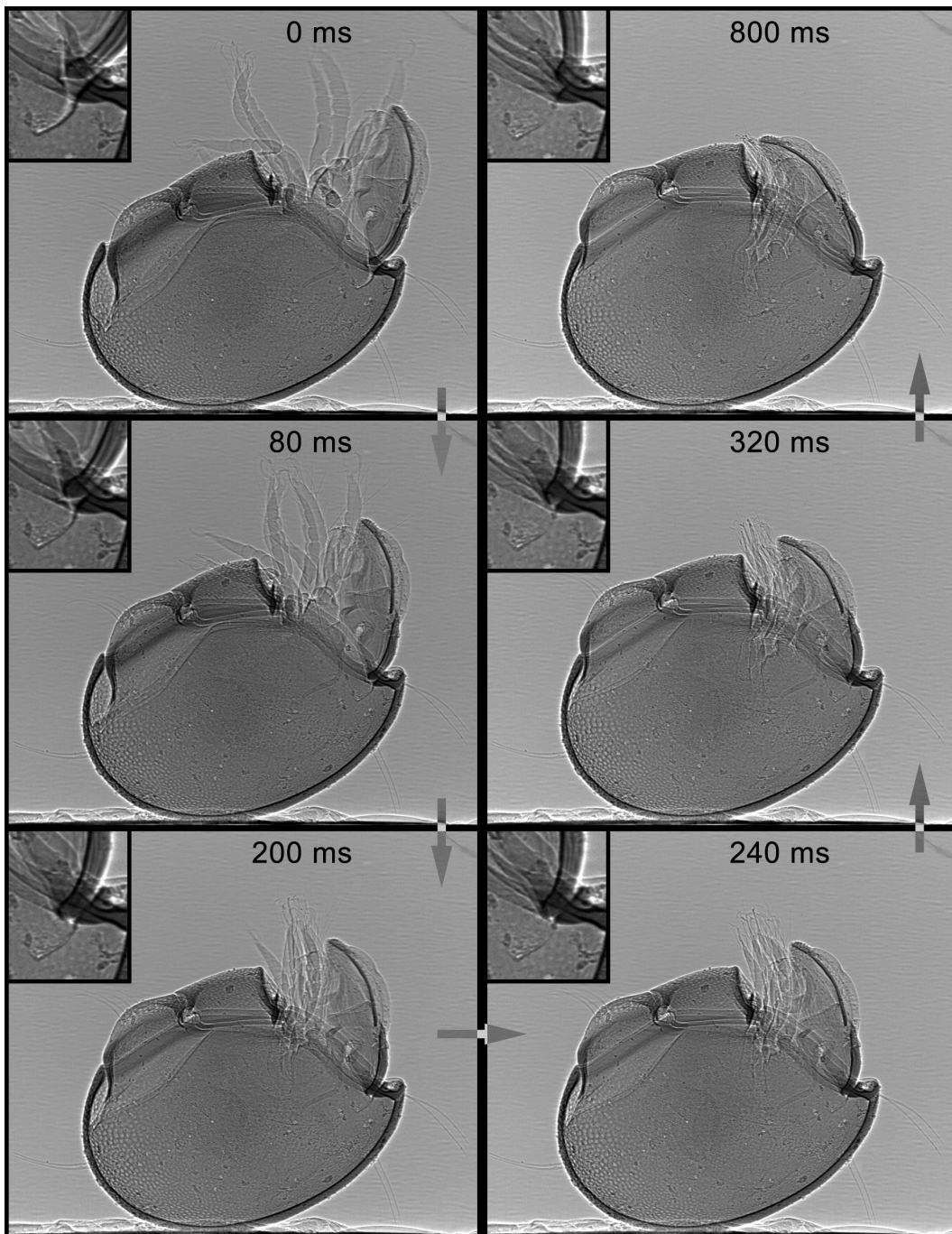


Fig. 10. Still images of Synchrotron radiography showing the entptychosis of *Steganacarus magnus* (recorded at 250 frames per second). Ventral plates, coxisternum and internal organs are well visible through the cuticle of the notogaster.

Table 1. Glossary of procedural terms (after Schmelzle et al. 2015).

Term	Definition
Ptychoidy	The mechanism/body form/ability to encapsulate
Ptychosis	The process of changing between states/the process 'enabled' by the ptychoid body form
Emptychosis	The process of encapsulation
Ecptychosis	The process of extension/re-opening
Extended	The state of being extended/open. 'Active' mode of operation, <i>i.e.</i> walking, feeding, etc.
Encapsulated	The state of being encapsulated/closed. 'Inactive' mode of operation

Table 2. Glossary of morphological terms (modified after Schmelzle et al. 2009).

Structure	Description
coxisternum	ventral assemblage of epimeres
endosternum	transverse ligament dorsal to coxisternum
epimere	coxal elements of walking leg segment
epiprosoma	acron and cheliceral and pedipalpal segments
gnathosoma	anterior body region (containing the segments that bear mouthparts (chelicerae) and pedipalps)
holoventral plates	fused genital, agenital, anal, and anal plates
idiosoma	posterior body region (containing the segments that bear legs, ventral plates, etc.)
inferior retractor process	ridge in the lateral margin of prodorsum
manubrium	handle-like postero-lateral process of prodorsum
notogaster	dorso-lateral cuticular shield of opisthosoma
plicature plates	sclerotized plates connecting notogaster and holoventral plates
prodorsum	dorsal shield of epiprosoma
sagittal apodeme	unpaired medial apodeme of prodorsum
subcapitulum	fusion of sternite and pedipalpal coxae
taenidiophore	condyle on each side of the subcapitulum

Table 3. List of muscle names and corresponding abbreviations (modified after Schmelzle et al. 2012).

Muscle	Abbr.	Origin	Insertion
Dorsoventral muscles of the Prosoma			
DVP			
coxisternal retractors	<i>csr</i>	notogaster, dorsal	apodeme 2 of the epimeres, apodemal shelves 3 and 4
coxisternal protractors	<i>csp</i>	notogaster, lateral	sejugal apodeme
Endosternal Division of the Prosoma			
EDP			
anterior dorsal endosternal muscles	<i>ade</i>	manubrium	endosternum
Longitudinal Division of the Prosoma			
LDP			
inferior prodorsal retractors	<i>ipr</i>	notogaster, dorsolateral	inferior retractor process, intercalary wall induration
prodorsum lateral adjustors	<i>pla</i>	notogaster, dorsolateral	manubrium
superior prodorsal retractors	<i>spr</i>	notogaster, dorsal	basis of manubrium
Opisthosomal Compressor System			
OCS			
notogaster lateral compressors	<i>nlc</i>	notogaster, ventral curvature	anogenital membrane
postanal muscles	<i>poam</i>	terminal at posterior end of notogaster	postanal apodeme
ventral plate adductors	<i>vpa</i>	preanal apodeme	genital valve
ventral plate compressors	<i>vpc</i>	preanal apodeme	lateral edge of genital valve

REFERENCES

- Alberti, G. (1980a). Zur Feinstruktur der Spermien und Spermioctogenese der Milben (Acari). I. Anactinotrichida. Zoologische Jahrbücher. Abteilung für Anatomie und Ontogenie der Tiere 104, 77–138.
- Alberti, G. (1980b). Zur Feinstruktur der Spermien und Spermioctogenese der Milben (Acari). II. Actinotrichida. Zoologische Jahrbücher. Abteilung für Anatomie und Ontogenie der Tiere 104, 144–203.
- Alberti, G. (1984). The contribution of comparative spermatology to problems of acarina systematics. In: Griffiths, D.A., Bowman, C.E. (Eds), Acarology VI, Vol. 1. Ellis Horwood Publ., Chichester, UK: pp. 479–490.
- Alberti, G. (2005). On some fundamental characteristics in acarine morphology. Atti della Accademia Nazionale Italiana di Entomologia Rendiconti 53, 315–360.
- Balogh, J., Mahunka, S. (1983). Primitive Oribatid mites of the Palaearctic region. In: Balogh, J., Mahunka, S. (Eds), The Soil Mites of the World. Akadémiai Kiadó, Budapest: 372 pp.
- Betz, O., Wegst, U., Weide, D., Heethoff, M., Helfen, L., Lee, W.-K., Cloetens, P. (2007). Imaging applications of synchrotron X-ray phase-contrast microtomography in biological morphology and biomaterials science. I. General aspects of the technique and its advantages in the analysis of millimeter-sized arthropod structure. Journal of Microscopy 227 (1), 51–71.
- Dabert, M., Witalinski, W., Kazmierski, A., Olszanowski, Z., Dabert, J. (2010). Molecular phylogeny of acariform mites (Acari, Arachnida): Strong conflict between phylogenetic signal and long-branch attraction artifacts. Molecular Phylogenetics and Evolution 56, 222–241.
- dos Santos Rolo, T., Ershov, A., van de Kamp, T., Baumbach, T. (2014). In vivo X-ray cine-tomography for tracking morphological dynamics. Proceedings of the National Academy of Sciences of the United States of America 111, 3921–3926. doi:10.1073/pnas.1308650111
- Evans, G.O. (1992). Principles of Acarology. CAB International Publishing, Wallingford, UK, 576 pp.
- Evans, G.O., Sheals, J.G., Macfarlane, D. (1961). The terrestrial Acari of the British Isles. Vol. 1. British Museum (Natural History), London: 219 pp.
- Giribet, G., Edgecombe, G.D., Wheeler, W.C., Babbitt, C. (2002). Phylogeny and Systematic position of Opiliones: a combined analysis of chelicerate relationships using morphological and molecular data. Cladistics 18, 5–70.
- Grandjean, F. (1969a). Stases. Actinopilinae. Rappel de ma classification des Acariens en 3 groupes majeurs. Terminologie en soma. Acarologia 11, 796–827.
- Grandjean, F. (1969b). Considerations sur le classement des oribates: leur division en 6 groupes majeurs. Acarologia 11, 127–153.
- Hansen, R.A. (1999). Red oak litter promotes a microarthropod functional group that accelerates its decomposition. Plant and Soil 209, 37–45.
- Heethoff, M., Koerner, L. (2007). Small but powerful - The oribatid mite *Archegozetes longisetosus* Aoki (Acari, Oribatida) produces disproportionately high forces. Journal of Experimental Biology 210, 3036–3042.
- Heethoff, M., Cloetens, P. (2008). A comparison of synchrotron X-ray phase contrast tomography and holotomography for non-invasive investigations of the internal anatomy of mites. Soil Organisms 80, 205–215.
- Heethoff, M., Norton, R.A. (2009a). A new use of synchrotron X-ray microtomography (SR- μ CT): three-dimensional biomechanical modeling of chelicerate mouthparts and calculation of theoretical bite forces. Invertebrate Biology 128, 332–339.
- Heethoff, M., Norton, R.A. (2009b). Role of musculature during defecation in a particle-feeding arachnid, *Archegozetes longisetosus* (Acari, Oribatida). Journal of Morphology 270, 1–13.
- Heethoff, M., Laumann, M., Bergmann, P. (2007). Adding to the reproductive biology of the parthenogenetic oribatid mite *Archegozetes longisetosus* (Acari, Oribatida, Trhypochthoniidae). Turkish Journal of Zoology 31, 151–159.
- Heethoff, M., Koerner, L., Norton, R.A., Raspotnig, G. (2011). Tasty but protected - first evidence of chemical defense in oribatid mites. Journal of Chemical Ecology 37, 1037–1043.
- Heethoff, M., Norton, R.A., Scheu, S., Maraun, M. (2009). Parthenogenesis in oribatid mites (Acari, Oribatida): evolution without sex. In: Schön, J., Martens, K., van Dijk, P. (Eds), Lost sex. Springer, Dordrecht: pp. 241–257.
- Jaloszynski, P., Olszanowski, Z. (2013). Specialized feeding of *Euconnus pubicollis* (Coleoptera: Staphylinidae: Scydmaeninae) on oribatid mites: Prey preferences and hunting behavior. European Journal of Entomology 110 (2), 339–353.
- Krantz, G.W. (1978). A Manual of Acarology. 2nd ed. Oregon State University Book Stores, Corvallis, USA: 509 pp.
- Krantz, G.W., Walter, D.E. (2009). A Manual of Acarology. 3rd ed. Texas Tech University Press, Lubbock, USA: 807 pp.
- Kuwahara, Y., Ishii, S., Fukami, H. (1975). Neryl formate: alarm pheromone of the cheese mite, *Tyrophagus putrescentiae* (Schrank) (Acarina, Acaridae). Experientia 31, 1115–1116.
- Labandeira, C.C., Phillips, T.L., Norton, R.A. (1997). Oribatid Mites and the Decomposition of Plant Tissues in Paleozoic Coal-Swamp Forests. Palaios V. 12, 319–353.

- Lions, J.-C., Norton, R.A. (1998). North American Synichotritiidae (Acari: Oribatida). 2. *Synichotritia spinulosa* and *S. caroli*. *Acarologia* 39, 265–284.
- Mahunka, S. (1990). Notes and remarks on Oribatid taxa (Acari), I. *Annales Historico-Naturales Musei Nationalis Hungarici* 82, 191–215.
- Maraun, M., Heethoff, M., Schneider, K., Scheu, S., Weigmann, G., Cianciolo, J., Thomas, R.H., Norton, R.A. (2004). Molecular phylogeny of oribatid mites (Oribatida, Acari): evidence for multiple radiations of parthenogenetic lineages. *Experimental and Applied Acarology* 33: 183–201.
- Michael, A.D. (1884). *British Oribatidae*, Vol. I. The Ray Society, London.
- Michael, A.D. (1888). *British Oribatidae*, Vol. 2. The Ray Society, London.
- Niedbala, W. (1992). Phthiracaroida (Acari, Oribatida) systematic studies. Polish Scientific Publishers, Warszawa: 612 pp.
- Niedbala, W. (1994). Supplement to the classification of Phthiracaroida, with redescriptions and descriptions of some species (Acari, Oribatida, Euptyctima). *Genus*, 5(1-2), 1–152.
- Niedbala, W. (2004). Protoplophoridae (Acari, Oribatida) of the World. *Annales Zoologici* 54(4), 807–834.
- Niedbala, W. (2012). Ptyctimous mites (Acari: Oribatida) of the Palaearctic Region –Distribution. *Fauna Mundi* 5, 3–348
- Norton, R.A. (1994). Evolutionary aspects of oribatid mite life histories and consequences for the origin of the Astigmata. In: Houck, M. (Ed), *Mites. Ecological and evolutionary analyses of life-history patterns*. Chapman and Hall, New York: pp. 99–135.
- Norton, R.A. (2001). Systematic relationships of Nothrolahmanniidae, and the evolutionary plasticity of body form in Enarthronota (Acari: Oribatida). In: Halliday, R. B., Walter, D.E., Proctor, H.C., Norton, R.A., Colloff, M.J. (Eds), *Acarology: Proceedings of the 10th International Congress*. CSIRO Publishing, Melbourne: pp. 58–75.
- Norton, R.A. (2006). First record of *Collohmanna* (*C. schusteri* n. sp.) and *Hermannia* (*H. sellnicki* n. sp.) from Baltic amber, with notes on Sellnick's genera of fossil oribatid mites (Acari: Oribatida). *Acarologia* 46, 111–125.
- Norton, R.A. (2007). Holistic acarology and ultimate causes - examples from oribatid mites. In: Morales-Malacara, J.B., Behan-Pelletier, V. M., Ueckermann, E., Pérez, T.M., Estrada-Nenegas, E.G., Badii, M. (Eds), *Acarology XI: Proceedings of the International Congress*. Sociedad Latinoamericana de Acarología, Universidad Nacional Autónoma México, México: pp. 3–20.
- Norton, R.A., Behan-Pelletier, V.M. (1991a). Calcium carbonate and calcium oxalate as hardening agents in oribatid mites (Acari: Oribatida). *Canadian Journal of Zoology* 69, 1504–1511.
- Norton, R.A., Behan-Pelletier, V.M. (1991b). Epicuticular calcification in *Phyllozetes* (Acari: Oribatida). In: Dusbábek, F., Bukva, V. (Eds), *Modern Acarology Vol. 2*. SPB Academic Publishing bv, The Hague; Academia, Prague: pp. 323–324.
- Norton, R.A., Lions, J.-C. (1992). North American Synichotritiidae (Acari: Oribatida). 1. *Apotritia walkeri* n. g., n. sp., from California. *Acarologia* 33, 285–301.
- Norton, R.A., Sidorchuk, E.A. (2014). *Collohmanna johnstoni* n. sp. (Acari, Oribatida) from West Virginia (U.S.A.), including description of ontogeny, setal variation, notes on biology and systematics of Collohmanniidae. *Acarologia* 54(3), 271–334.
- Norton, R.A., Bonamo, P.M., Grierson, J.D., Shear, W.A. (1988). Oribatid mite fossils from a terrestrial Devonian deposit near Gilboa, New York. *Journal of Paleontology* 62, 259–269.
- Pachl, P., Domes, K., Schulz, G., Norton, R.A., Scheu, S., Schaefer, I., Maraun, M. (2012). Convergent evolution of defense mechanisms in oribatid mites (Acari, Oribatida) shows no “ghosts of predation past”. *Molecular Phylogenetics and Evolution* 65, 412–420.
- Rasputnig, G. (2006). Chemical alarm and defence in the oribatid mite *Collohmanna gigantea* (Acari:Oribatida). *Experimental and Applied Acarology* 39, 177–194.
- Rasputnig, G., Kaiser, R., Stabentheiner, E., Leis, H.-J. (2008). Chrysolmelidial in the opisthonotal glands of the oribatid mite, *Oribotritia berleseii*. *Journal of Chemical Ecology* 34, 1081–1088.
- Regier, J.C., Shultz, J.W., Zwick, A., Hussey, A., Ball, B., Wetzer, R., Martin, J.W., Cunningham, C.W. (2010). Arthropod relationships revealed by phylogenomic analysis of nuclear protein-coding sequences. *Nature* 463, 1079–1083.
- Sanders, F.H., Norton, R.A. (2004). Anatomy and function of the ptychoid defensive mechanism in the mite *Euphthiracarus cooki* (Acari: Oribatida). *Journal of Morphology* 259, 119–154.
- Saporito, R. A., M. A. Donnelly, R. A. Norton, H. M. Garraffo, T. F. Spande, Daly, J. W. (2007). Oribatid mites as a major dietary source for alkaloids in poison frogs. *Proceedings of the National Academy of Sciences* 104, 8885–8890.
- Schaefer, I., Norton, R.A., Scheu, S., Maraun, M. (2010). Arthropod colonization of land – Linking molecules and fossils in oribatid mites (Acari, Oribatida). *Molecular Phylogenetics and Evolution* 57, 113–121.
- Schatz, H. (2002). Die Oribatidenliteratur und die beschriebenen Oribatidenarten (1758 - 2001) – Eine Analyse. *Abhandlungen und Berichte des Naturkundemuseums Görlitz* 74 (1), 37–45.
- Schmelzle, S., Helfen, L., Norton, R.A., Heethoff, M. (2008). The ptychoid defensive mechanism in Euphthiracaroida (Acari: Oribatida): A comparison of exoskeletal elements. *Soil Organisms* 80 (2), 227–241.

- Schmelzle, S., Helfen, L., Norton, R.A., Heethoff, M. (2009). The ptychoid defensive mechanism in Euphthiracaroida (Acari: Oribatida): A comparison of muscular elements with functional considerations. *Arthropod Structure and Development* 38 (6), 461–472. doi:10.1016/j.asd.2009.07.001
- Schmelzle, S., Helfen, L., Norton, R.A., Heethoff, M. (2010). The ptychoid defensive mechanism in *Phthiracarus longulus* (Acari: Oribatida): Exoskeletal and muscular elements. *Soil Organisms* 82 (2), 253–273.
- Schmelzle, S., Norton, R.A., Heethoff, M. (2012). A morphological comparison of two closely related ptychoid oribatid mite species: *Phthiracarus longulus* and *P. globosus* (Acari: Oribatida: Phthiracaroida). *Soil Organisms* 84 (2), 431–443.
- Schmelzle, S., Norton, R.A., Heethoff, M. (2015). Mechanics of the ptychoid defense mechanism in Ptyctima (Acari, Oribatida): one problem, two solutions. *Zoologischer Anzeiger - A Journal of Comparative Zoology* 254, 27–40. doi:10.1016/j.jcz.2014.09.002
- Schmid, R. (1988). Morphological Adaptations in a Predator-Prey-System: Scydmaenidae and Armoured Mites. *Zoologische Jahrbücher - Abteilung für Systematik, Ökologie und Geographie der Tiere* 115, 207–228.
- Sharma, P.P., Kaluziak, S.T., Pérez-Porro, A.R., González, V.L., Hormiga, G., Wheeler, W.C., Giribet, G. (2014). Phylogenomic interrogation of Arachnida reveals systemic conflicts in phylogenetic signal. *Molecular Biology and Evolution* 31: 2963–2984.
- Shear, W.A., Bonamo, M., Grierson, J.D., Rolfe, W.D.I., Smith, E.L., Norton, R.A. (1984). Early land animals in North America: evidence from Devonian age arthropods from Gilboa, New York. *Science* 224, 492–494.
- Shimano, S., T. Sakata, Y. Mizutani, Y. Kuwahara, Aoki, J. I. (2002). Geranial: The alarm pheromone in the nymphal stage of the oribatid mite, *Nothrus palustris*. *Journal of Chemical Ecology* 28: 1831–1837.
- Shultz, J.W. (2007). A phylogenetic analysis of the arachnid orders based on morphological characters. *Zoological Journal of the Linnean Society* 150: 221–265.
- Subías, L.S. (2004). Listado sistemático, sinonímico y biogeográfico de los Ácaros Oribátidos (Acariformes, Oribatida) del mundo (1748-2002). *Graellsia* 60: 3–305.
- Subías, L.S., Arillo, A. (2002). Oribatid mite fossils from the Upper Devonian of South Mountain, New York and the Lower Carboniferous of County Antrim, Northern Ireland (Acariformes, Oribatida). *Estudios del Museo de Ciencias Naturales de Alava* 17, 93–106.
- Travé, J., André, H.M., Taberly, G., Bernini, F. (1996). Les Acariens Oribates. In: Editions AGAR and SIALF, Belgium: 110 p.
- van der Hammen, L. (1972). A revised classification of the mites (Arachnidea, Acarida) with diagnoses, a key and notes on phylogeny. *Zoologische Mededelingen (Leiden)* 47: 273–292.
- van der Hammen, L. (1977). A new classification of Chelicerata. *Zoologische Mededelingen (Leiden)* 5: 307–319.
- van der Hammen, L. (1989). An Introduction to Comparative Arachnology. SPB Publishing bv, The Hague: 576 pp.
- Walter, D.E., Proctor, H.C. (1998). Feeding behaviour and phylogeny: Observations on early derivative Acari. *Experimental and Applied Acarology* 22, 51–60.
- Wauthy, G., Leponce, M., Banaï, N., Sylin, G., Lions, J.-C. (1998). The backward jump of a box moss mite. *Proceedings of the Royal Society B – Biological Sciences* 265, 2235–2242.
- Weigmann, G. (2006). Hornmilben (Oribatida). *Goecke & Evers, Kelttern*: 520 p.

PUBLICATIONS

Publication 1	The ptychoid defensive mechanism in Euphthiracaroida (Acari: Oribatida): A comparison of exoskeletal elements.	pp. 31–47
Publication 2	The ptychoid defensive mechanism in Euphthiracaroida (Acari: Oribatida): A comparison of muscular elements with functional considerations.	pp. 49–62
Publication 3	The ptychoid defensive mechanism in <i>Phthiracarus longulus</i> (Acari: Oribatida): Exoskeletal and muscular elements.	pp. 63–85
Publication 4	A morphological comparison of two closely related ptychoid oribatid mite species: <i>Phthiracarus longulus</i> and <i>P. globosus</i> (Acari: Oribatida: Phthiracaroida).	pp. 87–101
Publication 5	Mechanics of the ptychoid defense mechanism in Ptyctima (Acari, Oribatida): one problem, two solutions.	pp. 103–118

Publication 1

**The ptychoid defensive mechanism in Euphthiracaroida (Acari: Oribatida):
A comparison of exoskeletal elements.**

Schmelzle, S., Helfen, L., Norton, R.A., Heethoff, M.

Published in Soil Organisms 80 (2), pp. 227–241.

Submitted	Accepted	Published
13 December 2007	6 June 2008	2008

Authors' contribution:

- Schmelzle, Sebastian: Specimen preparation, data acquisition, data processing, data analysis, image processing, manuscript writing and preparation
- Helfen, Lukas: Data acquisition and support during, partial review of manuscript
- Norton, Roy A.: Initial concept, specimen collection and fixation, general support and discussion, revision of manuscript
- Heethoff, Michael: Initial concept, supervision, data acquisition, general support and discussion, revision of manuscript

Methods used:

- Synchrotron X-ray microtomography (SR μ CT)
- Scanning Electron Microscopy (SEM)

The ptychoid defensive mechanism in Euphthiracaroidea (Acari: Oribatida): A comparison of exoskeletal elements

Sebastian Schmelzle^{1*}, Lukas Helfen², Roy A. Norton³ & Michael Heethoff¹

¹ Universität Tübingen, Zoologisches Institut, Abteilung Evolutionsbiologie der Invertebraten, Auf der Morgenstelle 28E, 72076 Tübingen, Germany; e-mail: sebastianschmelzle@gmail.com

² Institute for Synchrotron Radiation, ANKA, Forschungszentrum Karlsruhe, 76021 Karlsruhe, Germany

³ State University of New York, College of Environmental Science and Forestry, 1 Forestry Drive, Syracuse NY 13210, USA

* Corresponding author

Abstract

Ptychoidity is a mechanical defensive mechanism of some groups of oribatid mites, in which the legs and coxisternum can be completely retracted into the idiosoma and the prodorsum acts as a seal to the encapsulated animal. Here, we use two microscopical techniques, scanning electron microscopy and synchrotron X-ray microtomography, to compare exoskeletal features of two species of ptychoid oribatid mites. *Oribotritia banksi* and *Rhysotritia ardua* both belong to the superfamily Euphthiracaroidea and are analysed here in direct comparison to *Euphthiracarus cooki*, for which the functional morphology has already been described. *Rhysotritia ardua* and *E. cooki* – both members of Euphthiracaridae – are similar in most skeletal features that relate to ptychoidity, but differ in the size of their postanal apodemes. *Oribotritia banksi* – a member of Oribotritiidae – differs from the former two in some well-known features, including the retention of articulations between components of the ventral plates (compared to fused, holovalental plates in Euphthiracaridae), and the absence of interlocking triangles that are associated with the pre- and postanal apodemes in Euphthiracaridae. Our study uncovered two internal skeletal differences in the prodorsum that relate to muscle attachment surfaces: compared to *E. cooki* and *R. ardua*, *O. banksi* lacks the sagittal apodeme and has a distinctly smaller manubrium, but only the latter functions in ptychoidity.

Keywords: Synchrotron-X-Ray-Microtomography, *Euphthiracarus cooki*, *Rhysotritia ardua*, *Oribotritia banksi*

Zusammenfassung

Ptychoidity ist ein bei einigen Gruppen der Oribatida verbreiteter mechanischer Defensivmechanismus, bei dem die Beine und das Coxisternum komplett in das Idiosoma eingezogen werden können und das Prodorsum dann als Verschlusskappe des eingekapselten Tieres fungiert. Wir verwenden hier zwei verschiedene mikroskopische Techniken, Rasterelektronenmikroskopie und Synchrotron-Röntgen-Mikrotomographie, um die exoskeletalen Anpassungen zweier Gattungen ptychoider Oribatida zu vergleichen. *Oribotritia banksi* und *Rhysotritia ardua* gehören beide zu der Gruppe der Euphthiracaroidea und werden im direkten Vergleich mit *Euphthiracarus cooki*, bei dem die funktionelle Morphologie schon beschrieben ist, untersucht. *Rhysotritia ardua* und *E. cooki* – beide zur Familie der

Euphthiracaridae gehörend – besitzen in den meisten skeletalen Merkmalen die in Verbindung mit Ptychoidie stehen große Ähnlichkeit, weichen aber in der Größe des postanalen Apodems voneinander ab. *Oribotritia banksi* – zur Familie der Oribotritiidae gehörend – unterscheidet sich von den beiden in einigen Merkmalen: zwischen den Komponenten der ventralen Platten befinden sich Gelenke, welche bei den verschmolzenen holozentralen Platten der Euphthiracaridae fehlen; weiterhin fehlen den Euphthiracaridae die den prä- und postanal Apodemen zugehörigen Verbindungsdreiecke. Unsere Untersuchung deckt zwei interne skeletale Unterschiede im Prodorsum auf, die sich auf Muskelansatzstellen beziehen: im Vergleich zu *E. cooki* und *R. ardua* fehlt *O. banksi* das sagittale Apodem und diese Art besitzt ein deutlich kleineres Manubrium, wobei nur letzteres bei der Ptychoidie eine Rolle spielt.

1. Introduction

Oribatid mites are a speciose group of mainly soil-dwelling microarthropods. About 9000 – 10 000 species have been described, but estimates of true diversity range from 50 000 – 100 000 (Travé et al. 1996, Schatz 2002, Subías 2004). Oribatid mites have an unusual feeding behaviour among the Chelicerata: they consume particulate instead of fluid food. The lower quality of the resources and a lower digestive efficiency result in slow growth, a relatively long generation time and low reproductive potential, which requires a long adult life-span (Norton 1994). Hence, another characteristic of the Oribatida is their diverse strategies and adaptations for predator defence. Some relate to chemical defences associated with opisthotal oil glands, which produce a variety of hydrocarbons, terpenes, aromatic compounds and alkaloids that are demonstrated or thought to relate to alarm pheromones, antimicrobial activity or predator repulsion (e.g. Shimano et al. 2002, Raspotnig 2006, Saporito et al. 2007). Mechanical defences include modified body setae, which can variously result in a hedgehog-like appearance or scale-like covering of the body. Cuticular hardening by sclerotisation or mineralisation is widespread. The latter can involve deposition of calcium carbonate, calcium phosphate or calcium oxalate (Norton & Behan-Pelletier 1991; Alberti et al. 2001). If the cuticle is hardened, protection of soft articulations can be achieved through the formation of overhanging tecta (Grandjean 1934).

A special defensive strategy is seen in the ptychoid body form, which involves several exoskeletal adaptations. The walking legs and the coxisternum can be completely retracted into the idiosoma, after which the prodorsum seals the secondary cavity to create an encapsulated state, in which the animals are firmly closed and appear seed-like (Figs 1B, D). In the active extended state, they look and move much like mites with a dichoid body form (Figs 1A, C). As a defensive behaviour, a few species exhibit a combination of ptychoidy with an escape jump (Wauthy et al. 1998). The ptychoid body form presumably has evolved at least three times (Sanders & Norton 2004). Two families of the Enarthronota, Protoplophoridae and Mesoplophoridae, have developed ptychoidy independently (Grandjean 1969, Norton 1984, Norton 2001). All other ptychoid families are members of Ptyctima (Mixonomata), including the two superfamilies Phthiracaroidae and Euphthiracaroidae (Grandjean 1954, Grandjean 1967, Balogh & Balogh 1992).

With such convergence on a similar set of adaptations, there is a strong possibility that mechanical problems were solved in different ways, but to demonstrate this requires good

knowledge of each group. Here, we present a comparative study of the exoskeletal features associated with ptychoidy in two species of Euphthiracaroida, *Oribotritia banksi* Oudemans and *Rhysotritia ardua* Koch, and compare the results with the morphology of *Euphthiracarus cooki* (Sanders & Norton 2004). General features of these mites were described by Märkel & Meyer (1959; see Mahunka 1990 and Haumann 1991 for discussions of their systematics and evolution). Since exoskeletal adaptations to ptychoidy are found in different parts of the body, we examine five distinct regions: the prodorsum, the opisthosomal venter, the notogaster, the podosoma and the subcapitulum.

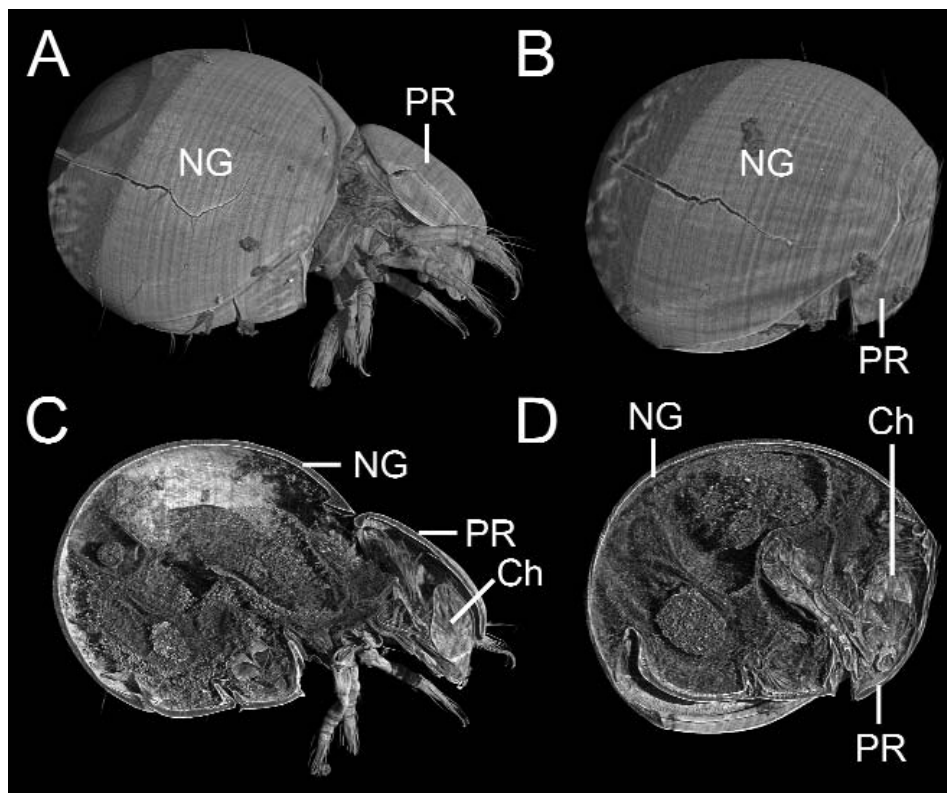


Fig. 1 Renditions of synchrotron-X-ray-microtomography data of *Phthiracarus globulosus* in extended (A, C) and encapsulated state (B, D). A: Extended animal showing a nearly dichoid body form. B: Encapsulated animal showing a seed-like appearance. C: Virtual sagittal section showing the positions of the legs and the organs in extended state. D: Same, but in encapsulated state. Ch: chelicera; NG: notogaster; PR: prodorsum.

1.1. Prodorsum

The prodorsum acts as an operculum-like seal for the encapsulated animal. Thus, there are adaptations that provide suitable origins or insertions for the musculature that is responsible for entpychosis (the enclosing of the animal) and ecptychosis (the opening of the animal). Additionally there are adaptations that help fit the prodorsum perfectly onto the opisthosoma. The distal part of the prodorsum is the solid rostral limb that merges with the rostraphragma (Grandjean 1939 called it the ‘cloison rostral’) which, in turn, merges with the tegulum, the soft cuticular frame around the chelicerae (Sanders & Norton 2004). Attachment points for musculature include the manubrium, a process at the posterior laterovenral edge of the prodorsum; the inferior retractor process at the lateral interior wall; and the sagittal apodeme, which is located medially on the posterior wall of the prodorsum. Two types of structures interact with nearby body regions to ensure that the prodorsum aligns properly during entpychosis. One is the bothridial scale, a process located laterodorsally near the bothridial seta, or sensillus. The other includes two or three lateral, longitudinal carinae. The dorsal and sometimes middle carinae originate at the bothridial scale, while the ventral carina, near the prodorsal border, originates in the nuchal region. All end near the rostral notch, a gentle depression of the ventral outline of the prodorsum.

1.2. Opisthosomal venter

The opisthosomal venter consists of a number of elongated paired plates that comprise: the plicature plates (sclerotised ventral plicature band of Grandjean 1933, 1967); the fused aggenital and adanal plates; and genital and anal plates that may be independent (in Oribotritiidae) or may be fused with each other and with the former to form a holovenral plate (in Euphthiracaridae; Norton et al. 2003). The holovenral plate occurs only in Euphthiracaridae. At the anterior (podosomal) edge, these plates turn vertically to form the phragma, with the pair connected through the phragmatal bridge; since they lack muscle attachments, these structures are considered solely structural, adding transverse stability to the venter (Sanders & Norton 2004). Anteriorly, the ventral plates can form a carina, which accommodates to the rostrum and thereby helps in completely sealing the encapsulated animal. In Euphthiracaridae, between the genital (about at the middle of the holovenral plates) and anal atrium (at the posterior end of the holovenral plates) an inward facing sclerotised structure, the prominence of the preanal apodeme, connects the two holovenral plates together. At its ventral margin is the anterior interlocking triangle, which is formed by interdigitating corrugations of the opposing plates. At the posterior end of the anal atrium, a similar postanal apodeme and interlocking triangle may be present.

1.3. Notogaster

The notogaster is heavily mineralised and therefore very rigid. For building up hemocoel pressure, the notogaster can be flexed inward so that its opening at the ventral end lessens. This is accomplished by a series of muscles that span the folds of the venter, which when contracted decreases the angle between the plates, thereby flexing the notogaster. This increases the hemocoel pressure for the ecptychosis, the opening of the enclosed animal (Sanders & Norton 2004). The notogastral fissure at the posterior end of the notogaster ensures that – even at that especially firm location – a certain level of flexure is possible.

Anterior adaptations allow the prodorsum to fit perfectly onto the notogaster at entychosis. The notogastral collar at the anterior border of the notogaster is divided into two parts, the pronotal tectum and the lateral anterior tectum. In the encapsulated state the lateral anterior tectum fits perfectly to the dorsal carina of the prodorsum and the pronotal tectum covers the articulation between notogaster and prodorsum. Between the pronotal tectum and the lateral anterior tectum is an emargination, the tectonotal notch. This notch comprises the scale receptacle that anchors the bothridial scale of the prodorsum when encapsulation is complete, and is supposed to add precision to the movement during entychosis (Walker 1965).

1.4. Podosoma

The podosoma is very soft, except for the epimeres, with three different lines or furrows. The abjugal line marks the anterior boundary of the podosoma to the epiprosoma (consisting of prodorsum, chelicerae and subcapitulum) and the disjugal line marks the posterior boundary of the podosoma and the idiosoma. The podosoma itself is divided by the sejugal line, which runs between the leg bearing segments two and three, separating the proterosoma and hysterosoma. The soft podosoma with its different articulating lines is one of the adaptations that enable entychosis. The articulation between subcapitulum and epimeres 1 is V-shaped, the circumcapitular furrow. The articulation between epimeres 2 and 3 comprises the ventrosejugal furrow. Epimeres 1 are the largest and are undivided, but other epimeres are subdivided by a soft median furrow of different widths (Sanders & Norton 2004). In the centre of the coxisternum (all epimeres, collectively) is a large area of membrane, the coxisternal umbilicus. It functions as a reservoir that holds enough membrane for the folding and reorienting of the epimeres during entychosis (Sanders & Norton 2004).

1.5. Subcapitulum

At least in *Euphthiracarus cooki*, the subcapitular adaptations for ptychoidy include a prominent capitular apodeme and equally prominent projection of the mentum, as well as the fusion of the taenidiophore part of supracoxal sclerite 1 to the subcapitulum. In most oribatid mites, the capitular apodeme protrudes into the interior as a narrow sclerotised shelf. In Ptyctima, the capitular apodeme can instead be a large triangular, flat process. The capitular apodeme is reinforced at its margins by a lemniscus (Sanders & Norton 2004). Normally in oribatid mites, the taenidiophore projects from the expanded dorsal border of supracoxal sclerite 1 and acts as a dicondylic articulation between the subcapitulum and the podosoma.

2. Materials and methods

2.1. Specimens

Living specimens of *Oribotritia banksi* were collected by R. A. Norton from forest litter in the Otter Creek Wilderness, West Virginia, USA, in May 2005 and extracted the following year after prolonged storage. Specimens of *Rhysotritia ardua* were collected by R. A. Norton in Lafayette, New York, USA, in November 2006 and extracted immediately.

2.2. Sample preparation

Live specimens were killed and fixed in 1 % glutaraldehyde for 60 hours and then stored in 70 % ethanol for shipping. Afterwards the specimens were dehydrated stepwise in an increasing ethanol series of 70 %, 80 %, 90 %, 95 %, and 100 %, with each step being repeated three times for 10 minutes. The samples were stored overnight in fresh 100 % ethanol and then critical-point dried in CO₂ (CPD 020, Balzers).

2.3. Imaging techniques

2.3.1. Scanning electron microscopy

Dried specimens were sputter-coated with a 20-nm thick layer of a gold-palladium mixture. Micrographs were taken on a Cambridge Stereoscan 250 Mk2 scanning electron microscope at 20 keV.

2.3.2. Synchrotron-X-Ray-Microtomography

Dried specimens were super-glued to the tip of a plastic pin (1.2 cm long; 3.0 mm in diameter) and mounted onto a goniometer head. Microtomography scans were carried out at the European Synchrotron Radiation Facility (ESRF) in Grenoble at beamline ID19 (experiment SC-2127). For each scan, a multitude (typically 1500) of x-ray radiographs (with a resolution of up to 2048 x 2048 pixels) with an effective pixel size of 0.7 µm were acquired at an x-ray energy of 20.5 keV and an object-detector distance of 20 mm, making use of the coherence properties of the incident x-ray beam to obtain edge-enhancing phase contrast. For further information on the technique, see Betz et al. (2007). The tomographic voxel-data were visualised with VGStudio MAX (Volume Graphics, Heidelberg, Germany) and segmented in amira™ (Mercury Computer Systems Inc., Chelmsford, Massachusetts).

3. Results

3.1. Prodorsum

The inner texture of the prodorsum itself is uniform in *Rhysotritia ardua* (Fig. 2B), but rough-textured in *Oribotritia banksi* (Fig. 2A). In *R. ardua* the differentiation between the solid, distal rostral limb (rl) and the rostrum (rp) at point y and between the rostrum and the tegulum (teg) at point x (Fig. 3B) is distinct. In contrast, at least the sum-along-ray picture (a virtual x-ray rendering of the 3D data) of the prodorsum of *O. banksi* (Fig. 3A) shows no clear differentiation, although it is visible in the original synchrotron micrographs. The manubrium differs between the species. In *O. banksi* it is a short stump (Fig. 3C, mn), with a broad and very robust base. In *R. ardua*, it is longer, with the base being relatively smaller (Fig. 3D, mn). The inferior retractor process appears similar in both species, though it is slightly shallower in *O. banksi* (Fig. 3E, irp). The sagittal apodeme in *R. ardua* is well developed (Fig. 3F, sa), but in *O. banksi* there is no evidence of it at all. The bothridial scale of *O. banksi* (Figs 4C, E; bs) is slightly more rounded with a small distal dent, compared to the relatively square one of *R. ardua* (Figs 4D, F; bs). The sensillus of the two species is very different: in *O. banksi* it tapers distally (Fig. 4E, ss), while it splits into many small branches in *R. ardua* (Fig. 4F, ss). In both species, the bothridium is ventral to the bothridial

scale, so that at emptychosis it is squashed into the articulation (Figs 2A – D). Around the internal part of the bothridium is a system of chambers. Laterally on the prodorsum there are two carinae – dorsal and ventral – in both animals (Figs 5A, B; Figs 3C, D). They end near the rostral notch, which is more distinct in *R. ardua* (Fig. 5A, rn) than in *O. banksi* (Fig. 3B).

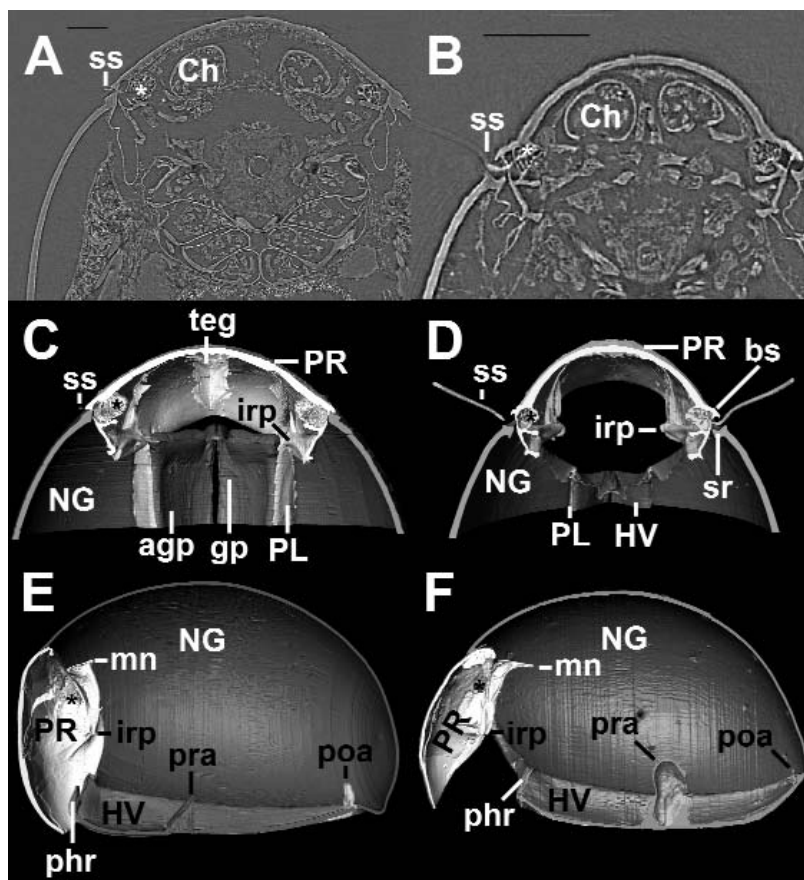


Fig. 2 Virtual transverse sections of synchrotron-X-ray-microtomography data (A, B) and virtual sections of synchrotron-X-ray-microtomography data of 3-D models (C, D dorsal view; E, F lateral view). A: *O. banksi*. Detail in the region of the bothridium. A: *R. ardua*, same. C: *O. banksi*, same as in A. D: *R. ardua*, same. E: *O. banksi*, prominence of preanal and postanal apodeme are clearly shown, also the manubrium. The aggenital and genital plate are not distinguishable on this picture; therefore they are combined as the genital region (gr). The adanal and anal plate are not distinguishable on this picture; therefore they are combined as the anal region (ar). F: *R. ardua*, same. The three-dimensional modelling (segmentation) of the tegulum on C – F is not completed. agp: aggenital plate; ar: anal region; bs: bothridial scale; Ch: chelicera; gp: genital plate; gr: genital region; HV: holoventral plates; irp: inferior retractor process; mn: manubrium; NG: notogaster; phr: phragma of holoventral plate; PL: plicature plates; poa: postanal apodeme; PR: prodorsum; pra: prominence of preanal apodeme; ss: sensillus; teg: tegulum. Asterisk indicates bothridium.

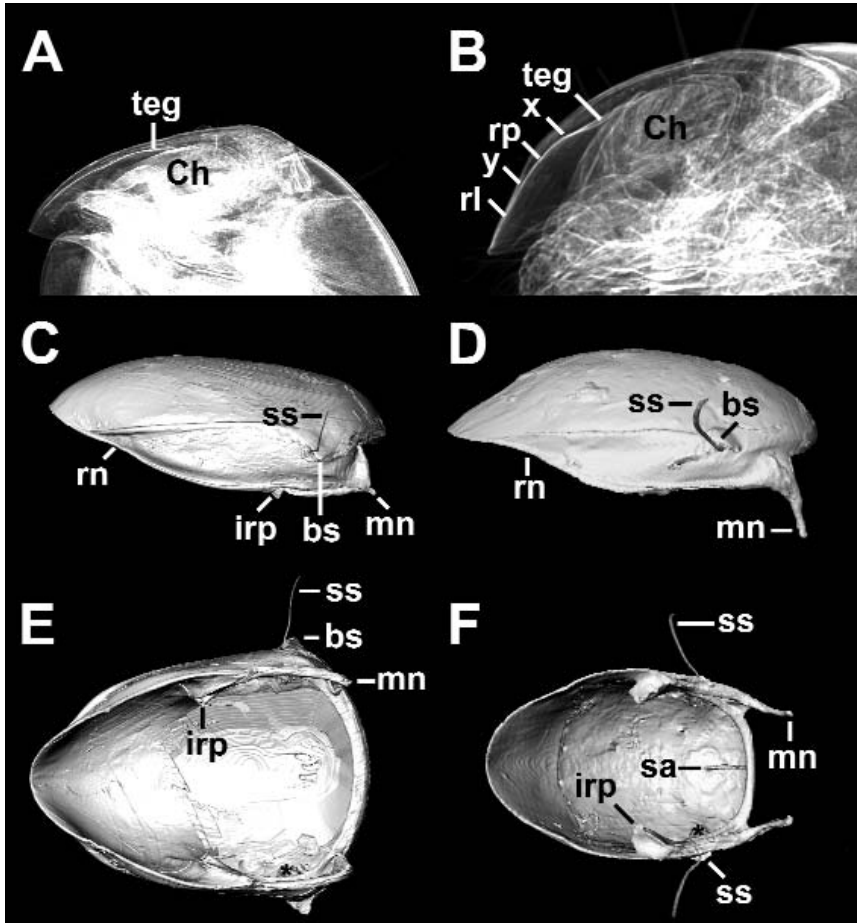


Fig. 3 Lateral view of renderings of the prodorsum with synchrotron-X-ray-microtomography data. a, b; Sum along ray (a rendering option in 'VGStudio Max': a virtual x-ray projection of the 3D data), and 3D models (C, D lateral view; E, F posterior view). A: *O. banksi*. X-ray-like image to illustrate the structure of the prodorsum. B: *R. ardua*, same as in A. C: *O. banksi*, lateral view of prodorsum with short manubrium. D: *R. ardua*, lateral view of prodorsum with long manubrium. E: *O. banksi*. F: *R. ardua*, same as in E. The tegulum in E and F is not shown. bs: bothridial scale; Ch: chelicerae; irp: inferior retractor process; mn: manubrium; PR: prodorsum; rl: rostral limb; rn: rostral notch; rp: rostraphragma; sa: sagittal apodeme; ss: sensillus; teg: tegulum; x, y: proximal and distal limits of rostraphragma. Asterisk indicates bothridium.

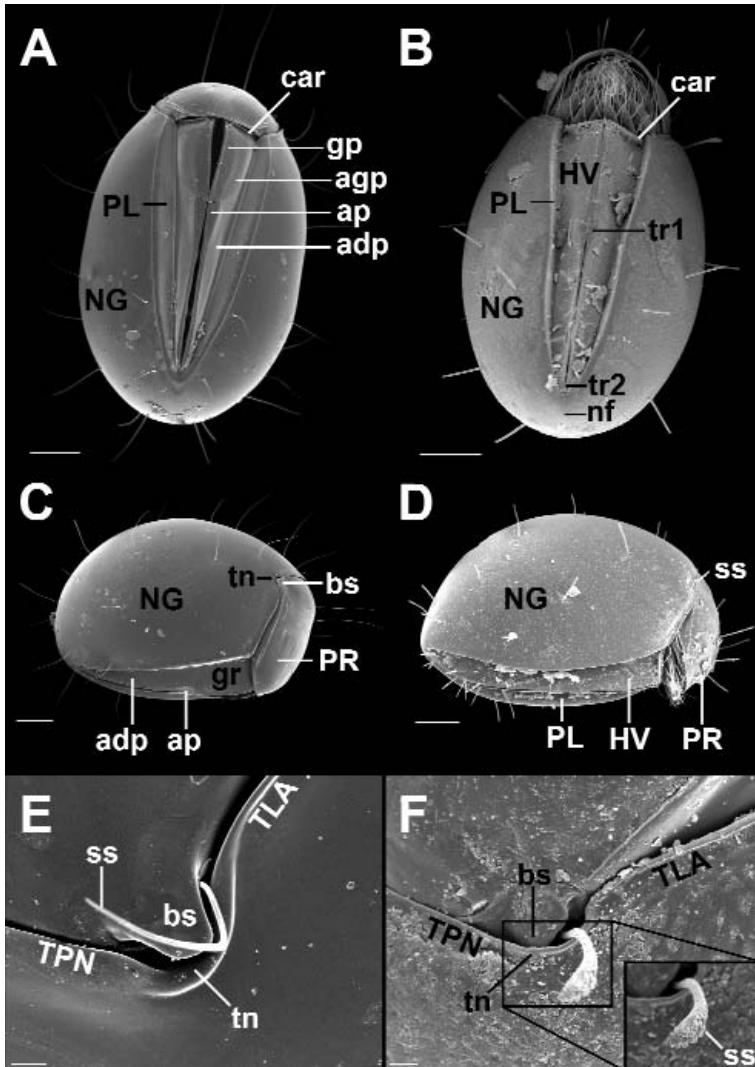


Fig. 4 Scanning electron micrographs. A: *Oribotritia banksi* in nearly encapsulated state, ventral view (scale bar: 200 μm). B: *Rhysotrititia ardua* in partly encapsulated state, ventral view (scale bar: 100 μm). C: *O. banksi* in nearly encapsulated state, lateral view. The aggenital and genital plate are not distinguishable in this picture; therefore they are combined as the genital region (gr) (scale bar: 200 μm). D: *R. ardua* in partly encapsulated state, lateral view (scale bar: 100 μm). E: Detail of the bothridial scale, the sensillus and the tectonotal notch of *O. banksi* (scale bar: 20 μm). F: Same as in E, but from *R. ardua* (scale bar: 10 μm). The frame shows the same area, but with focus on the tip of the sensillus. adp: adanal plate; agp: aggenital plate; ap: anal plate; bs: bothridial scale; car: carina; gp: genital plate; gr: genital region; HV: holoventral plates; nf: notogastral fissure; NG: notogaster; PL: plicature plates; PR: prodorsum; ss: sensillus; TLA: lateral anterior tectum; tn: tectonotal notch; TPN: pronotal tectum; tr1: interlocking triangle one; tr2: interlocking triangle two.

3.2. Opisthosomal venter

The plicature plates run paramedian from the anterior margin of the notogaster and fade out to posterior in both species. Those of *R. ardua* (Fig. 4B, PL) are rather narrow, relative to those of *O. banksi* (Fig. 4A, PL). The holovenal plates of *R. ardua* are nearly constant in width except close to the posterior margin (Figs 6F, 4B; HV), whereas the homologous collective plates of *O. banksi* narrow continually, from anterior to posterior (Figs 2E, 4A; HV). Additionally, the holovenal plates, present in *R. ardua*, do not exist in *O. banksi* where the adanal and anal plates as well as the aggenital and genital plates are not fused (Figs 4A, 7A, C). There is no distinct difference between the carina, phragma or phragmatal bridge in *O. banksi* and *R. ardua* (Figs 7A, B; 5C, D). The postanal apodeme in *R. ardua* is extremely small, whilst the prominence of the preanal apodeme is relatively large (Fig. 2F, poa, pra). By contrast, in *O. banksi*, the size of these two apodemes is quite similar (Fig. 2E, poa, pra). The interlocking triangle 1 of *R. ardua* has six interdigitating corrugations (Fig. 6B, tr1), while that of interlocking triangle 2 has four (Fig. 6D, tr2). As in all members of Oribotritiidae, there is no interlocking triangle associated with either apodeme in *O. banksi* (Fig. 6C). Instead, it looks like an overhang of the anterior plate, directed posteriorly.

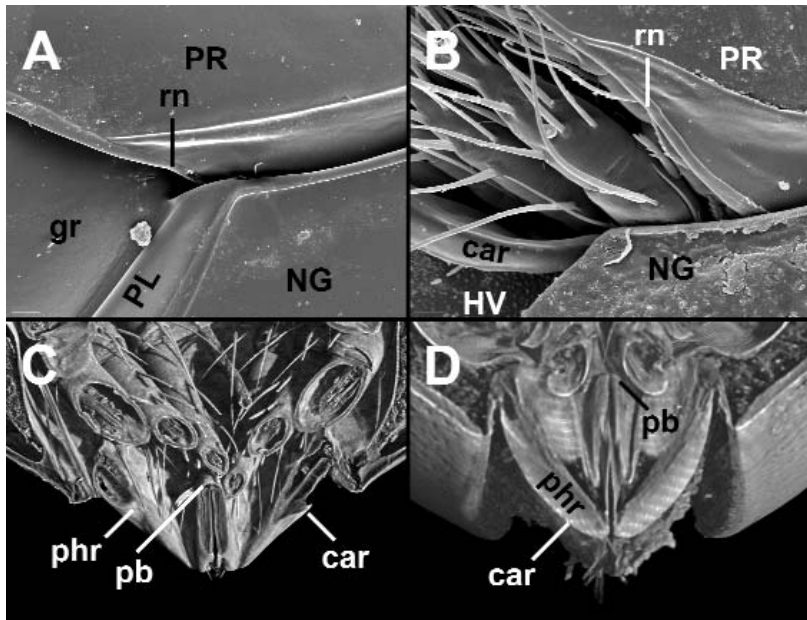


Fig. 5 Scanning electron micrographs, lateral view (A, B) and renderings of transversal sections with synchrotron-X-ray-microtomography data (C, D), frontal view. A: *O. banksi*. Detail of the rostral notch region. The aggenital and genital plate are not distinguishable in this picture; therefore they are combined as the genital region (gr). (scale bar: 20 μ m). B: Same, but from *R. ardua*. (scale bar: 10 μ m). C: *O. banksi*. Detail of the anterior region of the ventral plates. Visible is also the connecting phragmatal bridge. D: *R. ardua*, same as in C. car: carina; gr: genital region; HV: holovenal plates; NG: notogaster; pb: phragmatal bridge; phr: phragma of ventral plate; PL: plicature plate; rn: rostral notch.

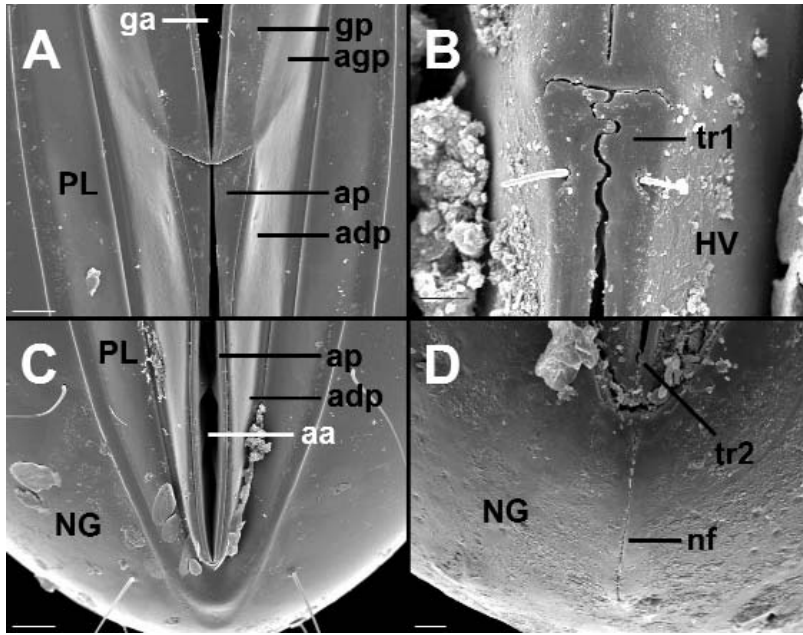


Fig. 6 Scanning electron micrographs, ventral view. A: *O. banksi*. Detail of the region of the interlocking triangle 1 (scale bar: 50 μm). B: *R. ardua*. Detail of the region of the interlocking triangle 1 (scale bar: 10 μm). C: *O. banksi*. Detail of the region of the interlocking triangle 2 (scale bar: 50 μm). D: *R. ardua*. Detail of the region of the interlocking triangle 2 and the notogastral fissure (scale bar: 50 μm). aa: anal atrium; adp: adanal plate; agp: aggenital plate; ap: anal plate; ga: genital atrium; gp: genital plate; HV: holoventral plates; nf: notogastral fissure; NG: notogaster; PL: plicature plates; tr1: interlocking triangle one; tr2: interlocking triangle two.

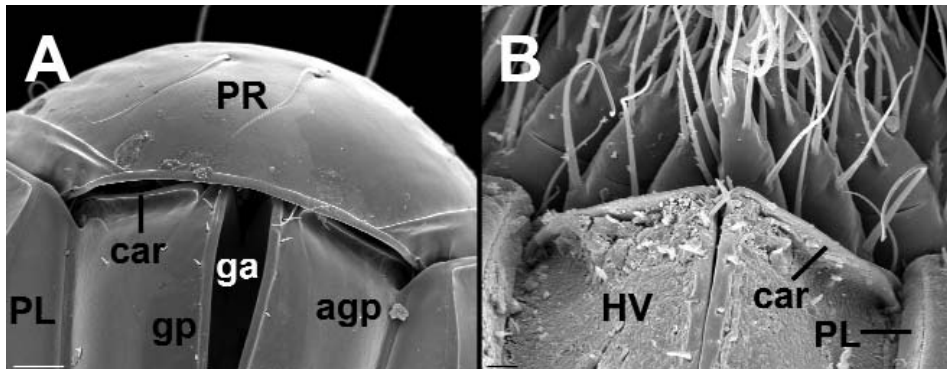


Fig. 7 Scanning electron micrographs. Specimens in nearly encapsulated state, ventral view. The carina is located at the anterior margin of the ventral plates. A: *O. banksi* (scale bar: 50 μm). B: *R. ardua* (scale bar: 10 μm). car: carina; ga: genital atrium; HV: holoventral plates; NG: notogaster; PL: plicature plates; PR: Prodorsum.

3.3. Notogaster

Oribotritia banksi lacks a terminal notogastral fissure (Fig. 6C), but it is present in *R. ardua* (Fig. 6D, nf). The pronotal tectum and the lateral anterior tectum are similar in both species (Figs 4E, F; TPN, TLA). The margin of the tectonotal notch of *R. ardua* is a nearly round, continuous half circle (Fig. 4F; tn), while in *O. banksi* it has a lateral elevation (Figs 4C, E; tn). In *R. ardua*, the scale receptacle is visible as a furrow on the anterior margin of the notogaster (Fig. 2D; sr), but there is no obvious receptacle in *O. banksi* (Fig. 2C).

3.4. Podosoma

There is no noticeable difference in the podosoma of *O. banksi* and *R. ardua*. Both species feature the circumcapitular furrow, ventrosejugal furrow, the median furrow and the coxisternal umbilicus.

3.5. Subcapitulum

The capitular apodeme and its lemniscus are nearly identical in *O. banksi* and *R. ardua*. The location of the taenidiophore has not yet been discovered.

4. Discussion

Grandjean (1969) suggested three exoskeletal characteristics that were necessary prior to the evolution of ptychoidy in any oribatid mite group, and Norton (2001) suggested a fourth. First, the coxisternum must be surrounded only by flexible integument with no direct connection to hard cuticular elements. Second, except for articulations, the opisthosomal cuticle must be hardened. Third, the coxisternum must be articulated and therefore deformable. Fourth, some aspect of structure must be able to accommodate the large internal volume changes associated with leg retraction and extension, and be able to inflate a pliable podosoma hydraulically with sufficient pressure to support ambulatory activity. These traits are present in *Oribotritia banksi* and *Rhysotritia ardua*, but these species differ in some details, which are compared below with those of *Euphthiracarus cooki*, as described by Sanders & Norton (2004).

4.1. Prodorsum

The inner texture of the prodorsum is uniform in both *E. cooki* and *R. ardua* but rough-textured in *O. banksi*. The proximal and distal borders of the rostrrophragma are distinct in *R. ardua* and *E. cooki*, but not in *O. banksi*. The manubrium is elongated in *E. cooki* and *R. ardua*, but that of *O. banksi* is merely a short stump. The inferior retractor process is similar in all three species. The sagittal apodeme is well developed in *R. ardua* and *E. cooki*, but absent in *O. banksi*. The bothridial scale of *O. banksi* and *E. cooki* is slightly rounder than in *R. ardua*. Only the latter species has a small indentation at its distal margin, which could be a resting place for the sensillus during entpychosis. The sensillus differs in all three species: split into many small branches in *R. ardua*, broadened in *E. cooki*, and tapered in *O. banksi*. In both *O. banksi* and *R. ardua*, the bothridial scale is located dorsally to the sensillus. However, it is located ventrally to it in *E. cooki*, so that it remains free of the articulation at entpychosis. Around the internal part of the bothridium is a system of chambers in all species.

Grandjean (1967) described them as internalised cuticular chambers, which in Euphthiracaridae have short tracheae that are probably respiratory structures.

Lateral on the prodorsum there are two carinae in both *O. banksi* and *R. ardua*, but three carinae (dorsal, medial and ventral) in *E. cooki*. The rostral notch of *E. cooki* is far more distinct than in *R. ardua* or in *O. banksi* (Fig. 3B).

4.2. Opisthosomal venter

Rhysotritia ardua and *E. cooki* are very similar in having holovenral plates that taper very little along their length, whereas in *O. banksi*, the various ventral plates are not fused and collectively they gradually taper posteriorly. The former two species share interlocking triangles at the bases of the preanal and postanal apodemes – which are absent from *O. banksi* – although the posterior triangle in *R. ardua* is less conspicuous than that of *E. cooki*. Various authors have mistakenly considered the posterior triangle to be absent from members of *Rhysotritia* and used this as a diagnostic trait (e.g. Märkel & Meyer 1959, Balogh & Balogh 1991). The posterior apodeme in *R. ardua* is also much smaller in vertical dimension than the anterior one, whereas in both *E. cooki* and *O. banksi* the two apodemes are similar in size (Fig. 2E, poa, pra). The anterior carina is similar in all the species.

4.3. Notogaster

At its ventral end, the lateral anterior tectum of *E. cooki* is prolonged into a tooth, but both *R. ardua* and *O. banksi* lack this tooth. Both *R. ardua* and *E. cooki* have the terminal notogastral fissure, but *O. banksi* lacks it. The pronotal tectum and the lateral anterior tectum are similar in all three species. In *O. banksi* and *E. cooki* the tectonotal notch has a lateral elevation, but the margin of the notch in *R. ardua* is a continuous half circle. In both *R. ardua* and *E. cooki* the scale receptacle is present as a furrow on the anterior margin of the notogaster, but a receptacle is not distinctly developed in *O. banksi*.

4.4. Podosoma and subcapitulum

The podosoma of *O. banksi* and *R. ardua* is essentially indistinguishable from that of *E. cooki*. Both the capitular apodeme and its lemniscus are identical in all three species.

4.5 Conclusions

Ptychoidy is a complex mechanical defensive mechanism with a number of functional constraints for internal and external morphological features. For most exoskeletal characters, *R. ardua* and *E. cooki* are similar, as would be expected for confamilial species (Euphthiracaridae). We showed that *Oribotritia banksi*, a member of Oribotritiidae, differs from them in a number of exoskeletal characters. The internal functional morphology of ptychoidy, especially the arrangements of musculature and their attachment sites, remains to be compared for the three species. Further studies of ptychoidy in other families of the Ptyctima, as well as in groups of the Protoplophoridae and Mesoplophoridae, in combination with comparisons to non-ptychoid closely related outgroups, will help to differentiate between functional and phylogenetic constraints of ptychoidy.

5. Acknowledgements

We thank Karl-Heinz Hellmer for taking the SEM-micrographs. We thank Paavo Bergmann, Michael Laumann and Peter Cloetens for their help on the project SC-2127 at the ESRF in Grenoble. We thank the European Synchrotron Radiation Facility for the beam time.

6. References

- Alberti, G., R. A. Norton & J. Kasbohm (2001): Fine structure and mineralisation of cuticle in Enarthronota and Lohmannioidea (Acari: Oribatida). – In: Halliday, R. B., D. E. Walter, H. C. Proctor, R. A. Norton & M. J. Colloff (eds): *Acarology: Proceedings of the 10th International Congress*. – CSIRO Publishing, Melbourne: 230 – 241
- Balogh, J. & P. Balogh (1992): *The oribatid mites genera of the world, Vol. 1*. – Hungarian National Museum Press, Budapest: 263 pp.
- Betz, O., U. Wegst, D. Weide, M. Heethoff, L. Helfen, W.-K. Lee & P. Cloetens (2007): Imaging applications of synchrotron x-ray micro-tomography in biological morphology and biomaterial science. I. General aspects of the technique and its advantages in the analysis of arthropod structure. – *Journal of Microscopy* **22**: 51 – 71
- Grandjean, F. (1933): Structure de la region ventrale chez quelque Ptyctimina (Oribates). – *Bulletin du Muséum national d'Histoire naturelle (2e ser)* **5(A)**: 309 – 315
- Grandjean, F. (1934): Observations sur les Oribates (6e série). – *Bulletin du Muséum national d'Histoire naturelle* **6**: 353 – 360
- Grandjean, F. (1939): Observations sur les Oribates (11e série). – *Bulletin du Muséum national d'Histoire naturelle* **11**: 110 – 117
- Grandjean, F. (1954): Essai de classification des oribates. – *Bulletin de la Société Zoologique de France* **78**: 421 – 446
- Grandjean, F. (1967): Nouvelles observations sur les oribates (5e serie). – *Acarologia* **9**: 242 – 272
- Grandjean, F. (1969): Considerations sur le classement des oribates leur division en 6 groupes majeurs. – *Acarologia* **11**: 127 – 153
- Haumann, G. (1991): *Zur Phylogenie primitiver Oribatiden, Acari: Oribatida*. – dbv Verlag für die Technische Universität Graz, Graz: 237 pp.
- Mahunka, S. (1990): A survey of the superfamily Euphthiracaroida Jacot, 1930 (Acari: Oribatida). – *Folia Entomology Hungary* **51**: 37 – 80
- Märkel, K. & I. Meyer (1959): Zur Systematik der deutschen Euphthiracarini (Acari, Oribatei). – *Zoologischer Anzeiger* **163**: 327 – 342
- Norton, R. A. (1984): Monophyletic groups in the Enarthronota (Sarcoptiformes). – In: Griffiths, D. A. & C. E. Bowman (eds): *Acarology VI, vol. I*. – Ellis Horwood, Chichester: 233 – 240
- Norton, R. A. (1994): Evolutionary aspects of oribatid mite life histories and consequences for the origin of the Astigmata. – In: Houck, M. (ed.): *Mites. Ecological and evolutionary analyses of life-history patterns*. – Chapman and Hall, New York: 99 – 135
- Norton, R. A. (2001): Systematic relationships of Nothrolhmanniidae, and the evolutionary plasticity of body form in Enarthronota (Acari: Oribatida). – In: Halliday, R. B., D. E. Walter, H. C. Proctor, R. A. Norton & M. J. Colloff (eds): *Acarology: Proceedings of the 10th International Congress*. – CSIRO Publishing, Melbourne: 58 – 75
- Norton, R. A. & V. Behan-Pelletier (1991): Calcium carbonate and calcium oxalate as cuticular hardening agents in oribatid mites (Acari: Oribatida). – *Canadian Journal of Zoology* **69**: 1504 – 1511

- Norton, R. A., F. H. Sanders & M. A. Minor (2003): *Euphthiracarus cooki* n. sp., a new oribatid mite (Acari: Oribatida) from Michigan and New York. – In: Smith, I. M. (ed.): An Acarological Tribute to David R. Cook – from Yankee Springs to Wheeny Creek. – Indira Publishing House, West Bloomfield: 201 – 210
- Rasputnig, G. (2006): Chemical alarm and defence in the oribatid mite *Collohmanna gigantea* (Acari: Oribatida). – *Experimental and Applied Acarology* **39**: 177 – 194
- Sanders, F. H. & R. A. Norton (2004): Anatomy and function of the ptychoid defensive mechanism in the mite *Euphthiracarus cooki* (Acari: Oribatida). – *Journal of Morphology* **259**: 119 – 154
- Saporito, R. A., M. A. Donnelly, R. A. Norton, H. M. Garraffo, T. F. Spande & J. W. Daly (2007): Oribatid mites as a major dietary source for alkaloids in poison frogs. – *Proceedings of the National Academy of Sciences* **104**: 8885 – 8890
- Schatz, H. (2002): Die Oribatidenliteratur und die beschriebenen Oribatidenarten (1758–2001) – eine Analyse. – *Abhandlungen und Berichte des Naturkundemuseums Görlitz* **74**: 37 – 45
- Shimano, S., T. Sakata, Y. Mizutani, Y. Kuwahara & J.-I. Aoki (2002): Geranial: The alarm pheromone in the nymphal stage of the oribatid mite, *Nothrus palustris*. – *Journal of Chemical Ecology* **28**: 1831 – 1837
- Subias, L. S. (2004): Listado sistemático, sinonímico y biogeográfico de los Ácaros Oribátidos (Acarifomes, Oribatida) del mundo (1748-2002). – *Graellsia* **60**: 3 – 305
- Travé, J., H.M. André, G. Taberly & F. Bernini (1996): Les Acariens Oribates. – In: Éditions AGAR and SIALF, Belgium
- Walker, N. A. (1965): Euphthiracaridae of California Sequoia litter, with a reclassification of the families and genera of the world. – *Fort Hayes Studies, Science Series* **3**: 1 – 155
- Wauthy, G., M. Leponce, N. Banaï, G. Sylin & J.-C. Lions (1998): The backward jump of a box moss mite. – *Proceedings of the Royal Society B* **265**: 2235 – 2242

Publication 2

**The ptychoid defensive mechanism in Euphthiracaroida (Acari: Oribatida):
A comparison of muscular elements with functional considerations.**

Schmelzle, S., Helfen, L., Norton, R.A., Heethoff, M.

Published in Arthropod Structure and Development 38 (6), pp. 461–472.

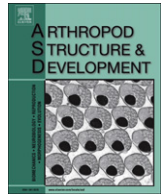
Submitted	Accepted	Published
2 April 2009	6 July 2009	2009

Authors' contribution:

- Schmelzle, Sebastian: Specimen preparation, data acquisition, data processing, data analysis, image processing, manuscript writing and preparation
- Helfen, Lukas: Data acquisition and support during, partial review of manuscript
- Norton, Roy A.: Specimen collection and fixation, general support and discussion, revision of manuscript
- Heethoff, Michael: Supervision, data acquisition, general support and discussion, revision of manuscript

Methods used:

- Synchrotron X-ray microtomography (SR μ CT)
- Scanning Electron Microscopy (SEM)



The ptychoid defensive mechanism in Euphthiracaroida (Acari: Oribatida): A comparison of muscular elements with functional considerations

Sebastian Schmelzle^{a,*}, Lukas Helfen^b, Roy A. Norton^c, Michael Heethoff^a

^a Universität Tübingen, Institut für Evolution und Ökologie, Abteilung Evolutionsbiologie der Invertebraten, Auf der Morgenstelle 28E, D-72076 Tübingen, Germany

^b Institute for Synchrotron Radiation, ANKA, Forschungszentrum Karlsruhe, D-76021 Karlsruhe, Germany

^c State University of New York, College of Environmental Science and Forestry, 1 Forestry Drive, Syracuse NY 13210, USA

ARTICLE INFO

Article history:

Received 2 April 2009

Accepted 6 July 2009

Keywords:

Synchrotron X-ray microtomography

Rhysotritia ardua

Oribotritia banksi

Ptychoidy

Functional morphology

ABSTRACT

Ptychoidy is a mechanical predator defence in some groups of Oribatida (Acari), where the animals can retract their legs into the idiosoma and encapsulate. This mechanism is enabled by a number of morphological adaptations. We used the non-invasive technique of synchrotron X-ray microtomography to compare muscular elements involved in ptychoidy of two species from the Euphthiracaroida (*Oribotritia banksi* and *Rhysotritia ardua*) which differ in a number of cuticular elements involved in ptychoidy. We hypothesize that a strong functional correlation exists between these cuticular structures and their corresponding musculature. We found a number of distinct differences concerning quantitative and qualitative muscle morphology. For testing the functional impact of different muscle configurations we simulated two conditions *in silico* (encapsulated / opened) and analysed the spatial relative force vectors of the prodorsum lateral adjustor muscles (*pla*) which are responsible for retraction and adjustment of the prodorsum during encapsulation. We show that the functional morphology of these muscles strongly differs between the two species and that this can be explained by the structure of corresponding cuticular elements. Furthermore, the dynamics of *pla*, as measured by the extent of contraction during encapsulation, is more than two times higher in *R. ardua* than in *O. banksi*.

© 2009 Elsevier Ltd. All rights reserved.

1. Introduction

Oribatid mites (Acari, Oribatida) are a group of mainly soil-dwelling microarthropods, which in contrast to most other Chelicerata feed on particulate rather than fluid food (Heethoff and Norton, 2009). The constraints of low diet quality (usually dead plant parts or saprophagous fungi) and a low digestive efficiency lead to life history traits that are often mistaken for results of K-selection, including slow growth, a relatively long generation time and a low reproductive potential with an elongated adult life span (Norton, 1994; Sanders and Norton, 2004). In this context, two different approaches to defence from antagonists have evolved – chemical and mechanical. Chemical predator defence is one role – perhaps the ancestral role – for secretions of the opisthotal oil glands, which most oribatid mites possess. Oil glands produce a variety of hydrocarbons, terpenes, aromatic compounds and alkaloids that function in predator repulsion, antimicrobial activity

and as alarm pheromones (Shimano et al., 2002; Rasputnig, 2006; Saporito et al., 2007). Mechanical predator defence is achieved in various ways, for example through prolongation of the body setae to form a hedgehog-like appearance. Overhanging cuticular tecta conceal articulations (Grandjean, 1934) and indentations of the notogaster provide room for safely containing the legs. A mechanical hardening of the notogaster, whether through sclerotization or through mineralization with calcium carbonate, calcium phosphate and calcium oxalate, is also common (Norton and Behan-Pelletier, 1991; Alberti et al., 2001).

Another mechanical approach to predator defence in oribatid mites is called ptychoidy – a special body form in which all legs and the coxisternum can be completely retracted into a temporary cavity in the idiosoma to achieve a seed-like appearance (Fig. 1); in this state, all soft integument is hidden and therefore not available for a possible attack. This body form can also be combined with an escape jump (Wauthy et al., 1998). The ptychoid defensive mechanism has probably evolved three times independently (Sanders and Norton, 2004) – in two families of the Enarthronota (Protoplophoridae and Mesoplophoridae; Grandjean, 1969; Norton, 1984, 2001) and once in the Mixonomata

* Corresponding author. Tel.: +49 7071/2976953; fax: +49 7071/294631.

E-mail address: sebastianschmelzle@gmail.com (S. Schmelzle).

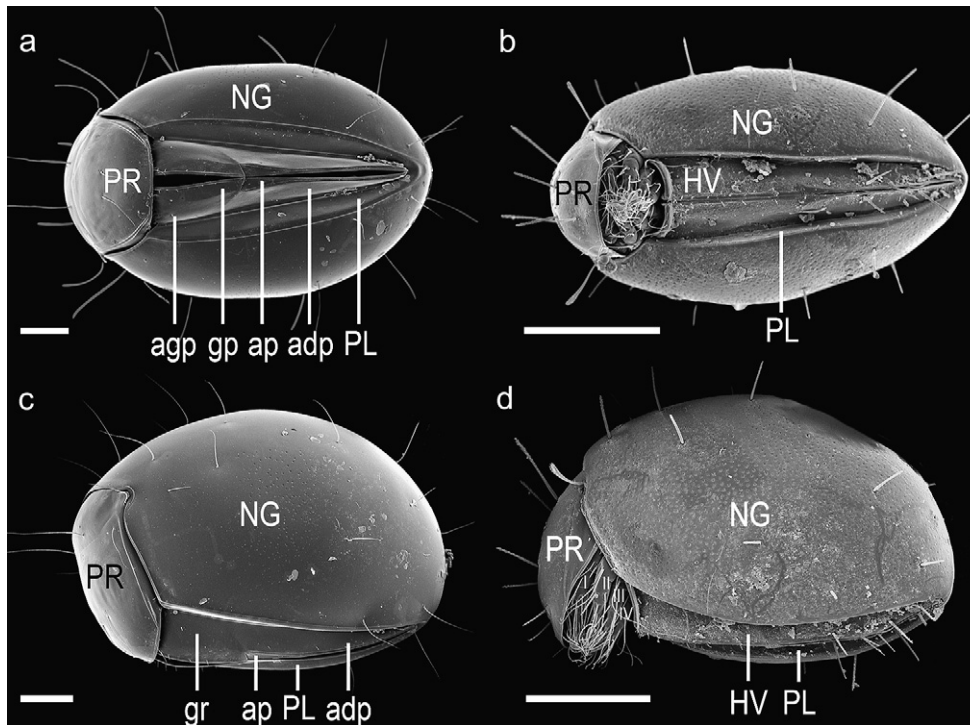


Fig. 1. Scanning electron micrographs of two ptychoid mite species, *Oribotritia banksi* and *Rhysotritia ardua*. Overview (anterior: left). (a) *O. banksi* in encapsulated state, ventral view. (b) *R. ardua* in partly encapsulated state, ventral view. (c) *O. banksi* in encapsulated state, lateral view. (d) *R. ardua* in partly encapsulated state, lateral view. Scale bars = 200 μ m. (adp, adanal plate; agp, aggenital plate; ap, anal plate; gp, genital plate; gr, genital region; HV, holoventral plates; NG, notogaster; PL, plicature plates; PR, prodorsum.)

(the monophylum Ptyctima containing the superfamilies Phthiracaroida and Euphthiracaroida; Grandjean, 1954, 1967; Balogh and Balogh, 1992). The ptychoid body form requires numerous exoskeletal and muscular adaptations (see Table 1 for a glossary of terms). Descriptions of exoskeletal elements for three species of euphthiracaroid mites are available: *Euphthiracarus cooki* Norton et al., 2003 (Sanders and Norton, 2004) and *Oribotritia banksi* (Oudemans, 1916, Fig. 1a,c) and *Rhysotritia ardua* (Koch, 1841, Fig. 1b,d, in Schmelzle et al., 2008).

Entptychosis (the process of retraction and encapsulation) and ecptychosis (the process of opening) are enabled by several muscular elements and the cuticular plates or apodemes on which they insert. The most important muscle insertions on the prodorsum are on the inferior retractor process, the exobothridial field, the sagittal apodeme and the manubrium (Sanders and Norton, 2004; Schmelzle et al., 2008). Muscles associated with the opisthosomal venter insert on the plicature plates and the various paired plates (anal and adanal, genital and aggenital) or their fused analogue, the holoventral plates (Figs. 1 and 2). Additional insertions are on the preanal and postanal apodemes, located anterior and posterior to the anal opening, respectively (Sanders and Norton, 2004; Schmelzle et al., 2008). Muscle insertions on the notogaster are simple, as this plate lacks specialized exoskeletal structures on the inner surface. The podosoma consists of a soft, pliable podosomal membrane and the coxisternum. The podosomal membrane itself also functions as a muscle insertion area, however, also without specialized cuticular regions. The coxisternum, consisting of the four epimeres, also bears places for muscle insertions – the apodemes and apodemal shelves. Some muscles that insert on the trochanters of the walking legs are secondarily involved in the process of ptychoidy (Sanders and Norton, 2004). The subcapitulum bears muscle insertions on the taenidiophore, the mentum of the subcapitulum and the anchoral process of the subcapitulum apodeme. Another crucial structure for ptychoid-

related muscle insertions is the endosternum, a transversely positioned 'ligament' that offers a loosely suspended and moveable, 'customizable' endoskeletal element within the podosoma (Sanders and Norton, 2004).

The muscles associated with ptychoidy in euphthiracaroid oribatid mites were first studied by Yastrebstov (1991) and Akimov and Yastrebstov (1991), but Sanders and Norton (2004) provided a more detailed analysis. According to the latter authors, these

Table 1
Glossary of terms.

Structure	Description
Coxisternum	Ventral assemblage of epimeres
Ecptychosis	Process of opening
Endosternum	Transverse ligament dorsal to coxisternum
Entptychosis	Process of encapsulation
Epimere	Coxal elements of walking leg segment
Epiprosoma	Acron and cheliceral and pedipalpal segments
Exobothridial field	Internal posterior field of the prodorsum
Holoventral plates	Fused genital, aggenital, anal and adanal plates
Inferior retractor process	Internal ridge / apophysis in the lateral margin of prodorsum
Manubrium	Handle-like posterolateral process of prodorsum
Mentum of the subcapitulum	Sternite of the pedipalpal segment
Notogaster	Dorsolateral cuticular shield of opisthosoma
Opisthosomal venter	Sum of ventral plates (aggenital, genital, adanal, anal or their homologues) in opisthosoma
Plicature plates	Sclerotized plates connecting notogaster and holoventral plates or their homologues
Podosoma	Leg-bearing segments
Prodorsum	Dorsal shield of epiprosoma
Ptychoidy	Special body form enabling encapsulation
Sagittal apodeme	Unpaired medial apodeme of prodorsum
Subcapitulum	Fusion of sternite and pedipalpal coxae
Taenidiophore	Condyle on each side of the subcapitulum

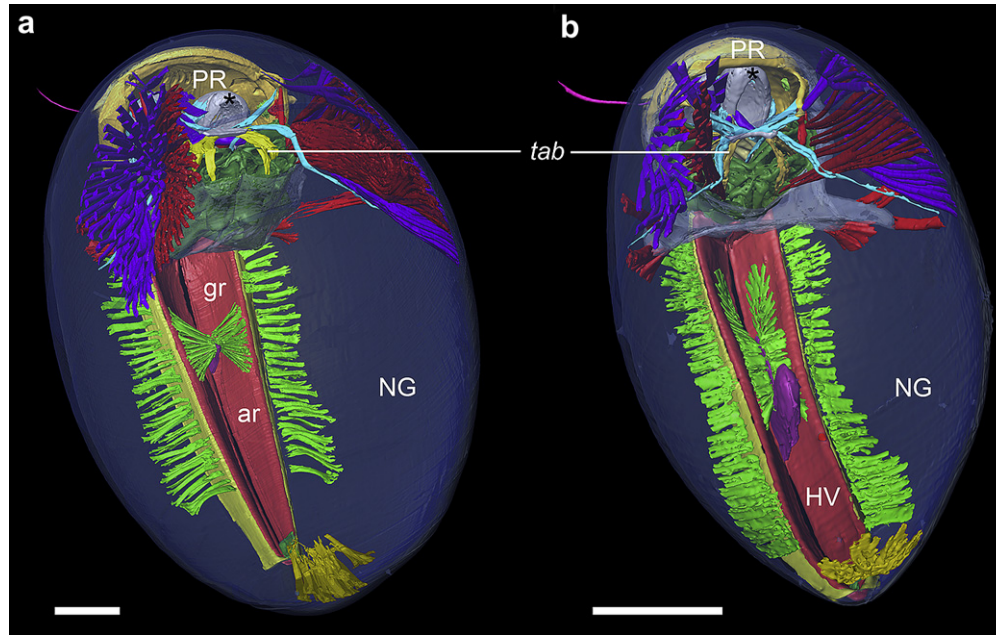


Fig. 2. Posterodorsal view of segmented synchrotron X-ray microtomography data of *Oribotritia banksi* and *Rhysotritia ardua* with transparent notogaster (blue). All relevant muscles for ptychoidy are shown. Red, dorsoventral muscles of the prosoma (DVP); turquoise, endosternal division of the prosoma (EDP); purple, longitudinal division of the prosoma (LDP); green, opisthosomal compressor system (OCS); yellow, additional muscles. (a) 3D model of *O. banksi*. (b) 3D model of *R. ardua*. Scale bars = 200 μ m. (ar, anal region; gr, genital region; HV, holoventral plates; NG, notogaster; PR, prodorsum; tab, trochanteral abductor. Asterisk indicates insertion of cheliceral retractors (*chr*).

muscles (all paired) can be grouped into four systems (Fig. 2, Table 2): (i) the dorsoventral muscle division of the prosoma (DVP; in red); (ii) the endosternal division of the prosoma (EDP; in turquoise); (iii) the longitudinal muscle division of the prosoma (LDP; in purple); and (iv) the opisthosomal compressor system (OCS; in green).

The DVP consists of the coxisternal retractors (*csr*), the inferior podosomal membrane adjusters (*ima*), the prodorsal dorsoventral

muscle (*pdv*) and the superior podosomal membrane adjusters (*sma*). This system is responsible for the retraction of the coxi-sternum, the podosomal membrane and the proper positioning of the latter in the temporary chamber.

The EDP consists of the muscles associated with the endosternum, namely the anterior dorsal endosternal muscles (*ade*), the posterior dorsal endosternal muscles (*pde*), the subcapitulum endosternal retractors (*ser*) and the taenidiophore endosternal

Table 2

Abbreviations, origin and insertion of the muscular elements.

Muscle	Abbreviation	Origin	Insertion
Dorsoventral muscles of the prosoma	DVP		
Coxisternal retractors	<i>csr</i>	Notogaster, dorsal	Apodeme 2 of the epimeres, apodemal shelves 3 and 4
Inferior podosomal membrane adjusters	<i>ima</i>	Anterior half of notogaster, ventrolateral	Podosomal membrane
Prodorsal dorsoventral muscles 1	<i>pdv1</i>	Exobothridial field	Lateral margin of apodemes 1
Prodorsal dorsoventral muscles 2	<i>pdv2</i>	Exobothridial field	Lateral margin of apodemes 2
Prodorsal dorsoventral muscles 3	<i>pdv3</i>	Manubrium	Sejugal apodeme
Superior podosomal membrane adjusters	<i>sma</i>	Notogaster, lateral	Podosomal membrane
Endosternal division of the prosoma	EDP		
Anterior dorsal endosternal muscle	<i>ade</i>	Manubrium	Endosternum
Posterior dorsal endosternal muscles	<i>pde</i>	Notogaster, dorsolateral	Endosternum
Subcapitulum endosternal retractors	<i>ser</i>	Endosternum	Mentum of subcapitulum
Taenidiophore endosternal retractors	<i>ter</i>	Endosternum	Taenidiophore
Longitudinal division of the prosoma	LDP		
Inferior prodorsal retractors	<i>ipr</i>	Notogaster, dorsolateral	Inferior retractor process, intercalary wall induration
Prodorsum lateral adjusters	<i>pla</i>	Notogaster, dorsolateral	Manubrium
Subcapitular retractors	<i>scr</i>	Apodeme 1, 2 of the epimeres 1	Anchoral process of subcapitular apodeme
Superior prodorsal retractors	<i>spr</i>	Notogaster, dorsal	Basis of manubrium
Opisthosomal compressor system	OCS		
Holoventral adductors	<i>hva</i>	Preanal apodeme	Lateral edge in genital region of holoventral plates
Ventral plate adductors	<i>vpa</i>	Preanal apodeme	Lateral edge in genital region of ventral plates
Holoventral compressors	<i>hvc</i>	Preanal apodeme	Lateral edge in genital region of holoventral plates
Ventral plate compressors	<i>vpc</i>	Preanal apodeme	Lateral edge in genital region of ventral plates
Notogaster lateral compressors	<i>nlc</i>	Notogaster, ventral	Medial edge of ventral plates
Cheliceral retractors	<i>chr</i>	Posterior wall of prodorsum, sagittal apodeme	Posterior surface of basal cheliceral segment
Postanal muscles (=holoventral levators)	<i>poam</i>	Terminal at posterior end of notogaster	Postanal apodeme
Trochanteral abductor	<i>tab</i>	Endosternum	Leg trochanter

retractors (*ter*). This supplementary system is responsible for the retraction and positioning of the subcapitulum, the coxisternum and the prodorsum.

The LDP consists of the inferior prodorsal retractors (*ipr*), the prodorsum lateral adjustors (*pla*), the subcapitular retractors (*scr*) and the superior prodorsal retractors (*spr*). These muscles are important for the movement of the cheliceral and pedipalpal segments and the acron (epiprosoma).

Muscles of the OCS are grouped because of their functional role in ptychoidy. These muscles build up the hemocoel pressure needed for both emptychosis and ecptychosis, and the upkeep of the active state. The system consists of the holoventral adductors (*hva*), the holoventral compressors (*hvc*) and the notogaster lateral compressors (*nlc*).

Other muscles (Fig. 2; in yellow), which are only indirectly involved in ptychoidy by withdrawing extremities, are the trochanteral abductors (*tab*), originating on the endosternum and inserting on the leg trochanter, and the cheliceral retractors (*chr*), originating on the sagittal apodeme and exobothridial field and inserting directly on the chelicerae. The postanal muscles (*poam*, Heethoff and Norton, 2009; also known as holoventral levators, Sanders and Norton, 2004) originate on the posterior end of the notogaster and insert on the postanal apodeme. The latter muscles presumably act solely as a system to withstand hemocoel pressure in that area (Sanders and Norton, 2004).

Here, we present a comparative study of the muscular elements associated with ptychoidy in *Oribotritia banksi* and *Rhysotritia ardua*, which represent two families of Euphthiracaroida (Oribotritiidae and Euphthiracaridae, respectively). We compare our results with those of Akimov and Yastrebtsov (1991) and Yastrebtsov (1991) on the same or similar species, and of Norton and Sanders (2004) on *Euphthiracarus cooki*. Qualitative differences are analyzed and discussed with respect to their functional implications (relative spatial force transmission).

Data were obtained at the European Synchrotron Radiation facility (ESRF) in Grenoble by means of synchrotron X-ray microtomography (Betz et al., 2007). This non-invasive method allows studying internal structures in their natural state with a pixel resolution of 0.7 μm . In contrast to thin sectioning, the resulting voxel dataset is already perfectly aligned and there are no sectioning artefacts (for details see Betz et al., 2007; Heethoff and Cloetens, 2008).

2. Methods

2.1. Specimens

Adults of *Oribotritia banksi* (size about 1800 μm) were collected from rhododendron leaf litter in a mixed forest at the Otter Creek Wilderness, Randolph Co., WV, USA. Adults of *Rhysotritia ardua* (= *Acrotitria ardua*; size about 900 μm) were collected from litter of Norway spruce (*Picea abies*) in Lafayette, Onondaga Co., NY, USA.

2.2. Sample preparation

Specimens were killed and fixed in 1% glutaraldehyde for 60 h and stored in 70% ethanol. For the final preparation, specimens were dehydrated in an increasing ethanol series with steps of 70, 80, 90, 95 and 100%, with three changes at each step and 10 min at each change. After storage in fresh 100% ethanol they were critically point dried in CO_2 (CPD 020, Balzers).

2.3. Scanning electron microscopy (SEM)

Critical-point dried specimens were glued onto a T-section-like metal foil sitting on a stub and then sputtered with a 20 nm thick

layer of a gold–palladium mixture. Micrographs were taken on a Cambridge Stereoscan 250 Mk2 scanning electron microscope with a beam energy of 20 keV.

2.4. Synchrotron X-ray microtomography

Critical-point dried animals were fixed by the notogaster to the tip of a plastic pin (1.2 cm long; 3.0 mm diameter) using instant adhesive. Radiographs were taken at the European Synchrotron Radiation Facility (ESRF) in Grenoble at beamline ID19 with a beam energy of 20.5 keV and at a sample–detector distance of 20 mm. A cooled 14-bit CCD-camera with a resolution of 2048 \times 2048 pixels and an effective pixel size of 0.7 μm per pixel was used (a detailed description of the method is given in Betz et al., 2007 and Heethoff and Cloetens, 2008).

The data were visualized with the program VGStudio MAX 1.2.1 (Volume Graphics, Heidelberg, Germany) and three-dimensional modeling of muscles and cuticular elements were conducted with amira™ 4.0.1 (Mercury Computer Systems Inc., Chelmsford, MA). Counting of muscle fibers was conducted with the original phase contrast microtomography data and, where not possible, by the number of split ends in the resulting 3D model. Different portions of muscles (cf Fig. 4d, *ima*) are called muscle bands and subdivisions of muscle bands are called muscle fibers (Sanders and Norton, 2004).

2.5. Functional analyses

An encapsulated and opened condition was simulated *in silico* for both species in amira™ through rotation and translation of the prosomal surface. The coordinates (x, y, z) of muscle origin and insertion of the prodorsum lateral adjustor were measured for both situations. The length, spatial organization and relative spatial force vectors of *pla* were calculated in a Cartesian coordinate system (Fig. 3), where the X-axis corresponded to the medial–lateral axis, the Y-axis corresponded to the anterior–posterior axis and the Z-axis corresponded to the ventral–dorsal axis. Angles were calculated based on Pythagoras' theorem and relative force vectors,

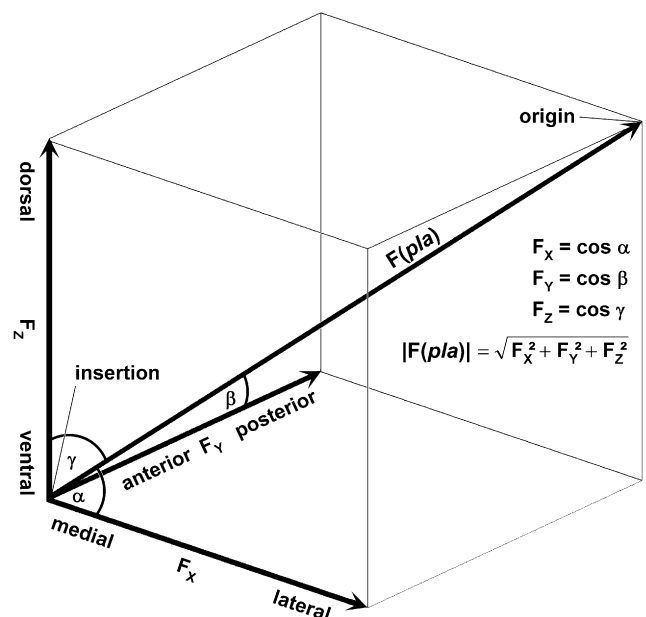


Fig. 3. Diagram showing the three-dimensional calculation of force composition in lateral, posterior and dorsal components. (*pla*, prodorsum lateral adjustors.)

based on corresponding angles, were calculated using the formulas given in Fig. 3.

3. Results

3.1. Dorsoventral muscles of the prosoma (DVP)

Each coxisternal retractor of *Oribotritia banksi* (Fig. 4a) consists of 80 muscle fibers. Its origin is dorsal on the notogaster and the insertion is on apodeme 2 of the epimeres and apodemal shelves 3 and 4 (Table 2). *Rhysotritia ardua* differs only in the number of muscle fibers, 17 in each muscle (Fig. 4b). For both species, the origin of the inferior podosomal membrane adjuster (Fig. 4c,d) is ventrolateral on the anterior half of the notogaster and the insertion is on the podosomal membrane. Both species have two muscle bands, but bands of *O. banksi* (Fig. 4c) have about 10 fibers while those of *R. ardua* have nine fibers each (Fig. 4d). The superior podosomal membrane adjuster originates laterally on the notogaster and also inserts on the podosomal membrane. The muscles have a similar general appearance, but in *O. banksi* each muscle has a single band with about nine fibers (Fig. 4c) while in *R. ardua* (Fig. 4d) it consists of two muscle bands with 1–3 fibers each. In contrast to *R. ardua*, the *sma* of *O. banksi* is connected with the podosomal membrane through tendons. The prodorsal dorsoventral muscle (Fig. 4e,f) is divided into three pairs of muscles – *pdv1*, *pdv2* and *pdv3*. The largest of the three muscles, *pdv3*, originates on the manubrium and inserts at the sejugal apodeme, but *pdv1* and *pdv2* originate on the exobothridial field and insert on the lateral margin of apodemes 1 and 2, respectively. The number of muscle fibers for *pdv1* (two) and *pdv2* (one) is equal in *O. banksi* (Fig. 4e) and *R. ardua* (Fig. 4f); presumably the same is true for *pdv3*, which has at least two muscle fibers, but this was not proven.

3.2. Endosternal division of the prosoma (EDP)

The anterior dorsal endosternal muscle (Fig. 5a,b) originates on the manubrium and inserts on the endosternum. In both *O. banksi* (Fig. 5a) and *R. ardua* (Fig. 5b) it consists of two muscle bands. The origin on the manubrium is broader in *R. ardua* than in *O. banksi*, probably due to the relatively longer manubrium. The posterior dorsal endosternal muscle (Fig. 5a,b) consists of two muscle fibers each. They are long and thin and insert on the endosternum. The origin in *R. ardua* (Fig. 5b) is dorsolateral on the notogaster at about half its length, whilst in *O. banksi* (Fig. 5c,d) the origin is more anterior, at about one-third the length of the notogaster. The subcapitulum endosternal retractor and the taenidiophore endosternal retractor are similar in *O. banksi* (Fig. 5c) and *R. ardua* (Fig. 5d). Both muscles have their origin on the endosternum and have two fibers each. Respectively, they insert on the mentum of the subcapitulum and, via tendons, on the tip of the taenidiophore.

3.3. Longitudinal division of the prosoma (LDP)

The inferior prodorsal retractors each consist of 90–100 muscle fibers in *O. banksi* (Fig. 6a) and 28–32 fibers in *R. ardua* (Fig. 6b). They insert by tendons on the inferior retractor process and the intercalary wall induration of the prodorsum. The origin is dorso-lateral on the notogaster, far more posterior in *O. banksi* than in *R. ardua*. The prodorsum lateral adjuster (Fig. 6c,d) originates in *R. ardua* on the notogaster at about the same level where the ventral plates begin, but more posteriorly in *O. banksi* (at about the level the anal plates begin). The origin on the notogaster is dorsolateral in *R. ardua*, but only dorsal in *O. banksi*. The insertion is on the manubrium and consists of two muscle bands with two fibers each in *O. banksi* (Fig. 6c) and up to five fibers each in *R. ardua* (Fig. 6d).

The insertion is directly on the manubrium in *R. ardua*, but the fibers merge and insert via a single tendon in *O. banksi*. The functional consequences of the different orientation of *pla* and their role in ecptychosis and entptychosis will be discussed below. The subcapitular retractor (Fig. 7a,b) connects the coxisternum and the subcapitulum. The four muscle fibers originate as two muscle bands, one band each on the first and second apodemes; these merge on their way anteriorly, and insert as a single muscle band on the anchoral process of the subcapitular apodeme. There appears to be no difference between the *scr* of *O. banksi* (Fig. 7a) and *R. ardua* (Fig. 7b). The superior prodorsal retractor (Fig. 7c,d) each consists of four muscle fibers with its origin located dorsally on the notogaster and its insertion on the basis of the manubrium. Again, there appears to be no difference between *O. banksi* (Fig. 7c) and *R. ardua* (Fig. 7d).

3.4. Opisthosomal compressor system (OCS)

The antero-medial components of this system originate on the preanal apodeme (Fig. 8). *Oribotritia banksi* (Fig. 8a) has only one paired muscle originating on the preanal apodeme and inserting on the lateral edge of the ventral plates (*vpc*; see Section 4), with 25 muscle fibers. *Rhysotritia ardua* has two such paired muscles. The holovertral adductor runs diagonally to its insertion in the genital region of the holovertral plates (Fig. 8b); each consists of about 40, partly very flat and short, muscle fibers. The holovertral compressor each consists of 10–20 muscle fibers, running to its insertion on the lateral edge of the holovertral plates (Fig. 8b).

The notogaster lateral compressor consists of a paired series of transverse muscle fibers running nearly the whole length of the opisthosomal venter (Fig. 8). It originates on the ventral curvature of the notogaster and inserts on the lateral edge of the ventral plates (i.e., on the holovertral plates in *R. ardua* and on the adanal and aggenital plates in *O. banksi*). In *O. banksi* (Fig. 8a) there are 30–34 thin muscle bands with 2–6 fibers each, but the muscles do not extend as far posteriorly as in *R. ardua* (Fig. 8b), which has only 25 slightly broader muscle bands with 3–6 fibers each.

3.5. Additional muscles

The cheliceral retractors and the trochanteral abductors are well developed in both species (Fig. 2). The origin of the *chr* in *R. ardua* is on the sagittal apodeme and the exobothridial field (the posterior wall of the prodorsum), but in *O. banksi* – which lacks this apodeme – all muscle bands insert directly on the posterior wall of the prodorsum. The insertion is directly on the posterior surface of the basal cheliceral segment. The *tab* originates on the endosternum and inserts on the inner surface of the leg trochanters.

The postanal muscle (or holovertral levator; Fig. 8) each consists of eight muscle bands with 4–5 fibers in *O. banksi* (Fig. 8a), while in *R. ardua* it consists of two muscle bands with approximately 10–20 fibers (Fig. 8b). In both species the *poam* originates on the posterior end of the notogaster and inserts on the postanal apodeme, directly in *R. ardua* but through tendons in *O. banksi*.

4. Discussion

4.1. Dorsoventral muscles of the prosoma (DVP)

The coxisternal retractor of *R. ardua* and *O. banksi* (Fig. 4a,b) do not differ from those of *E. cooki* (Sanders and Norton, 2004) in their origin and insertion, but do differ in the number of muscle fibers (12 in *E. cooki* vs. 17 and 80 muscle fibers in *R. ardua* and *O. banksi*, respectively). The number of fibers correlates roughly with the size of the species: *E. cooki* is only 300 µm long, hence

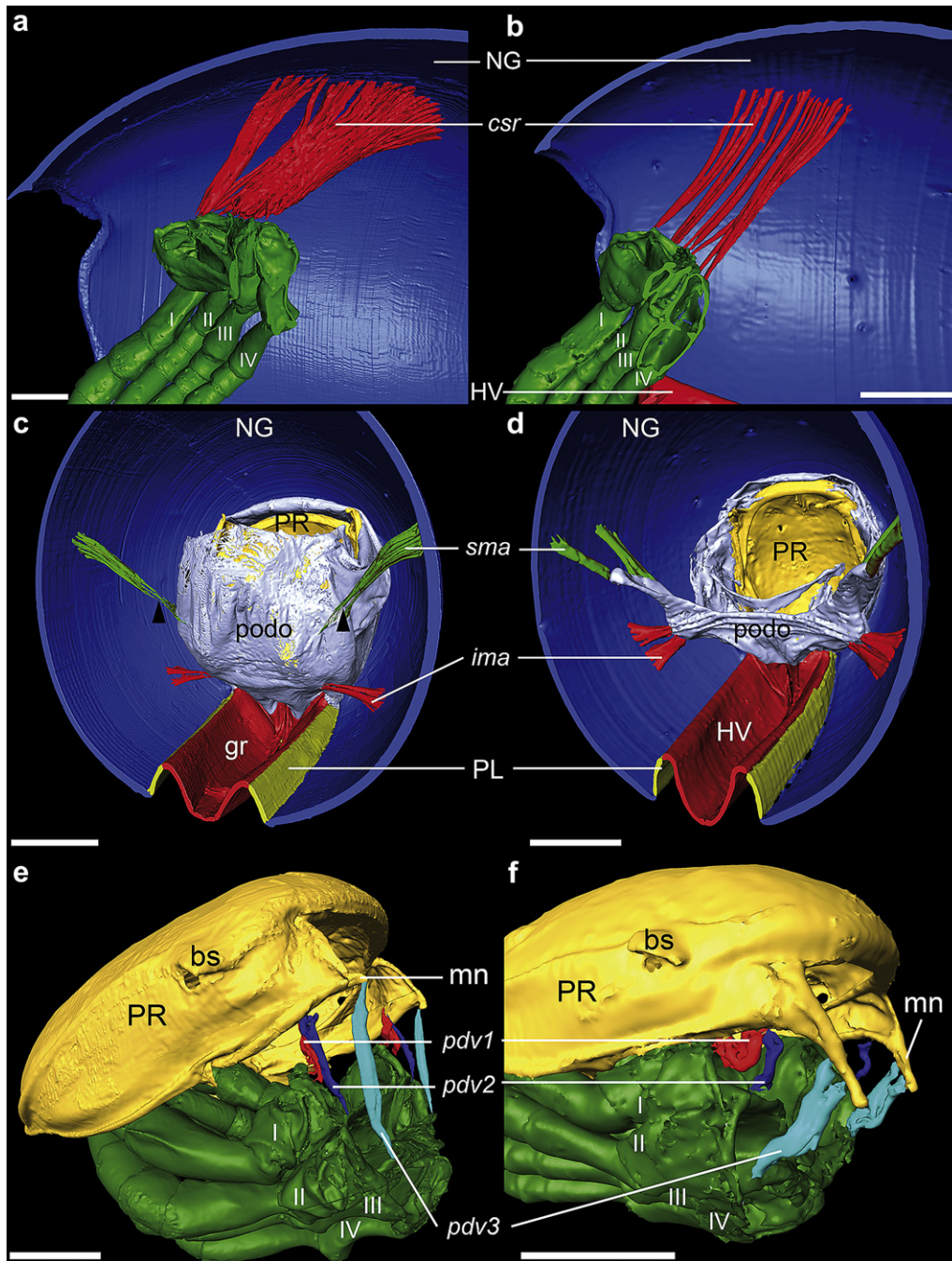


Fig. 4. DVP. Renderings of segmented synchrotron X-ray microtomography data of *Oribotritia banksi* and *Rhysotritia ardua*. Coxisternal retractors (*csr*) (lateral view of renderings of a virtual sagittal section): (a) 3D model of *O. banksi* (anterior: left). Scale bar = 100 μ m. (b) 3D model of *R. ardua* (anterior: left). Scale bar = 100 μ m. Inferior podosomal membrane adjusters (*ima*) and superior podosomal membrane adjusters (*sma*) (posterior view of segmentations of a virtual cross-section): (c) 3D model of *O. banksi*. Scale bar = 200 μ m. (d) 3D model of *R. ardua*. Scale bar = 100 μ m. Prodorsal dorsoventral muscles (*pdv*) (lateral view of renderings of the legs and prodorsum): (e) 3D model of *O. banksi* (anterior: left). Scale bar = 100 μ m. (f) 3D model of *R. ardua* (anterior: left). Scale bar = 100 μ m. (I, II, III, IV, walking legs; bs, bothridial scale; *csr*, coxisternal retractors; gr, genital region; HV, holoventral plates; *ima*, inferior podosomal membrane adjusters; mn, manubrium; NG, notogaster; *pdv*, prodorsal dorsoventral muscle; PL, plicature plates; podo, podosomal membrane; PR, prodorsum; *sma*, superior podosomal membrane adjusters; tn, tectonotal notch. Arrowheads indicate tendons.)

small compared to *R. ardua* (900 μ m) and *O. banksi* (1800 μ m). This correlation probably relates to the need for higher force to move the heavier coxisternum and legs in larger species, which presumably requires a higher number of muscle fibers. Yastrebtsov (1991) and Akimov and Yastrebtsov (1991) named these muscles 'retractors of the walking legs' (abbreviated '*rst*' and alternatively '*rep*'). In Table 3 of Akimov and Yastrebtsov (1991) this muscle is accidentally abbreviated as '*rpe*'. In this work the *csr*

is stated to insert on apodeme 1 of the epimeres of *R. ardua*. This contrasts with our results as we found that these muscles insert on apodeme 2 of the epimeres – as was also shown for *E. cooki* (Sanders and Norton, 2004). Also, there is no evidence for crossing of the muscle fibers of apodeme (1 and) 2 with the ones of apodeme 3 and 4 (as shown by Yastrebtsov, 1991 and Akimov and Yastrebtsov, 1991) and the number of muscle fibers drawn for *R. ardua* (four; Akimov and Yastrebtsov, 1991, Fig. 5:2) and

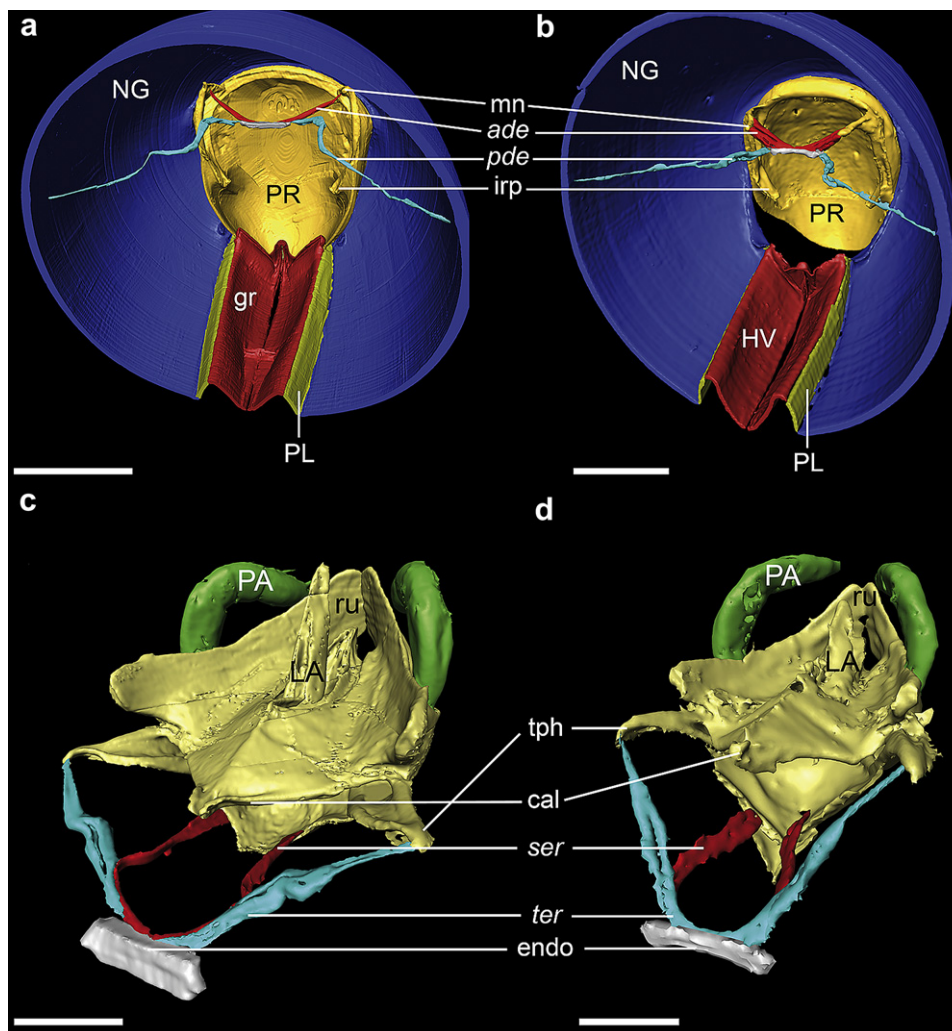


Fig. 5. EDP. Segmentations of synchrotron X-ray microtomography data of *Oribotritia banksi* and *Rhysotritia ardua*. Anterior dorsal endosternal muscle (*ade*) and posterior dorsal endosternal muscle (*pde*) (posterior view of renderings of a virtual cross-section): (a) 3D model of *O. banksi*. Scale bar = 300 μ m. (b) 3D model of *R. ardua*. Scale bar = 100 μ m. Subcapitulum endosternal retractors (*ser*) and taeniophore endosternal retractors (*ter*) (posterior view of segmentations of subcapitulum and endosternum): (c) 3D model of *O. banksi* (anterior: right). Scale bar = 100 μ m. (d) 3D model of *R. ardua* (anterior: right). Scale bar = 50 μ m. (*ade*, anterior dorsal endosternal muscles; *cal*, lemniscus of capitular apodeme; *endo*, endosternum; *gr*, genital region; *HV*, holoventral plates; *irp*, inferior retractor process; *LA*, labrum; *mn*, manubrium; *NG*, notogaster; *PA*, pedipalpus; *pde*, posterior dorsal endosternal muscles; *PL*, plicature plates; *PR*, prodorsum; *ru*, rutella; *ser*, subcapitulum endosternal retractors; *ter*, taeniophore endosternal retractors; *tph*, taeniophore.)

Oribotritia sp. (eight; Yastrebtsov, 1991, Fig. 2.3) are not congruent with our results either. The inferior podosomal membrane adjuster (Fig. 4c,d) concurs in all three species. The number of muscle bands (two) and fibers (nine and 10) is nearly congruent in *R. ardua* and *O. banksi*. It is not exactly known for *E. cooki* (Sanders and Norton, 2004). The superior podosomal membrane adjuster (Fig. 4c,d) comprises one muscle band with 3–4 fibers in *E. cooki* and nine fibers in *O. banksi*. In *R. ardua* we found two muscle bands with 1–3 fibers each. The prodorsal dorsoventral muscle (Fig. 4e,f) consists of three portions (*pdv1*, *pdv2*, *pdv3*) and the origin and insertion do not differ among the three species. The *ima*, *sma* and *pdv* do not appear in the work of Yastrebtsov (1991) or Akimov and Yastrebtsov (1991) and therefore cannot be compared.

4.2. Endosternal division of the prosoma (EDP)

The anterior dorsal endosternal muscle (Fig. 5a,b) inserts broadly on the manubrium of *E. cooki* and *R. ardua*, but only in a small region in *O. banksi*, probably due to its rather short

manubrium. The posterior dorsal endosternal muscle (Fig. 5) is quite similar in all three species, except that the origin on the notogaster is a bit more anterior in *O. banksi*. The taeniophore endosternal retractor (Fig. 5c,d) each consists of one muscle fiber in *E. cooki* and two muscle fibers in *R. ardua* and *O. banksi*. In all three species, this muscle inserts through tendons on the taeniophore.

In Akimov and Yastrebtsov (1991) all three mentioned endosternal muscles are called ‘suspenders of the endosternite’ (‘ses’). In their Table 3, the origins of these muscles are stated to be the dorsal (for *ade*) and dorsolateral (*pde*) surface of the hysterosoma, but the origin of the *ade* is on the manubrium, not the notogaster. The location of the insertion and origin of our *ter* in Table 3 of their publication is inverted and the insertion is not located on the hysterosoma (rather notogaster), but the taeniophore. The *ser* is termed ‘flexor of the gnathosoma’ (‘f_{gn}’) or ‘dilator of the gnathosoma’ (‘d_{gn}’). Their list (Chapter 2.1) and all their figures only show the *dgn*, whereas their Table 3 only lists the *f_{gn}*. The insertion for the *ser* is the endosternum, which is correctly listed in their Table 3, but is incorrectly drawn in their Fig. 3 (which shows the posterior prodorsum as insertion).

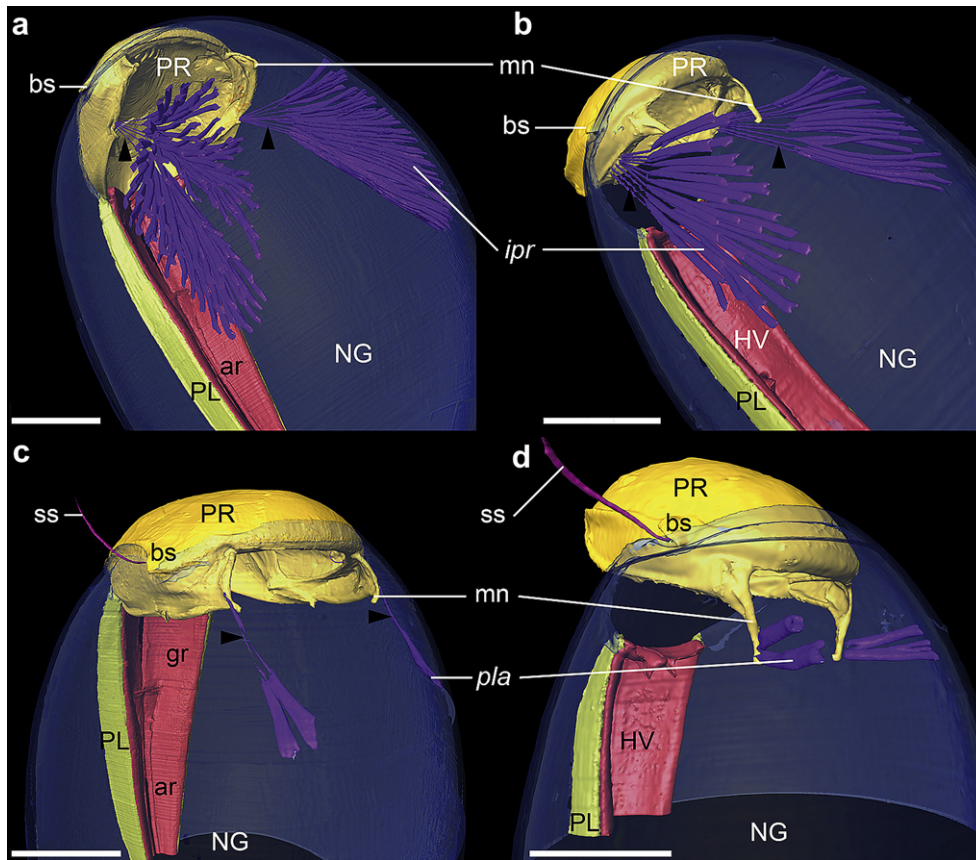


Fig. 6. LDP. Posterolateral view of segmentations based on synchrotron X-ray microtomography data of *Oribotritia banksi* and *Rhysotritia ardua* with transparent notogaster. Inferior prodorsal retractors (*ipr*): (a) 3D model of *O. banksi*. Scale bar = 200 μ m. (b) 3D model of *R. ardua*. Scale bar = 100 μ m. Prodorsum lateral adjustors (*pla*): (c) 3D model of *O. banksi*. Scale bar = 200 μ m. (d) 3D model of *R. ardua*. Scale bar = 100 μ m. (ar, anal region; bs, bothridial scale; gr, genital region; HV, holoventral plates; *ipr*, inferior prodorsal retractors; mn, manubrium; NG, notogaster; PL, plicature plates; *pla*, prodorsum lateral adjustors; PR, prodorsum; ss, sensillus. Arrowheads indicate tendons.)

4.3. Longitudinal division of the prosoma (LDP)

The insertion of the inferior prodorsal retractors (Fig. 6a,b) is identical in all investigated species. The origin, however, is located more posteriorly in *E. cooki* and *R. ardua* (about two-thirds of the length of the notogaster) than in *O. banksi* (about one-third). But, as for the *csr* (Fig. 4a,b), the number of muscle fibers differs strongly: *E. cooki* has 13, *R. ardua* 28–32 and *O. banksi* 90–100 fibers. As for the *csr*, this probably can be explained by the different absolute size of the respective structures (in this case, the prodorsum). The different types of insertion of the prodorsum lateral adjustor (broadly on the manubrium of *E. cooki* and *R. ardua* (Fig. 6d), and through a single tendon in *O. banksi* (Fig. 6c) resemble those of the *ade*. The different origin (dorsolateral in *R. ardua* and *E. cooki*, dorsal in *O. banksi*) suggests a different function of this muscle in Euphthiracaridae and Oribotritiidae, as will be discussed below. The origin of the subcapitular retractor is located on apodemes 1 and 2 in *R. ardua* and *O. banksi*, but only on apodeme 1 in *E. cooki*. For this muscle Yastrebtsov (1991) and Akimov and Yastrebtsov (1991) seem to use two terms more or less interchangeably: 'levator of the gnathosoma' ('*lgn*') and 'extensor of the gnathosoma' ('*egn*'). In their figures, the origin of this muscle also varies. In Fig. 1 of Akimov and Yastrebtsov (1991) the partly drawn muscle is directed posteriorly, whilst in their Fig. 3 the origin is located on the posterior part of the prodorsum. The list in their Chapter 2.1 only contains the 'levator of the gnathosoma' ('*lgn*'), and their Table 3 only the 'extensor of the gnathosoma' ('*egn*'). Also the insertions listed are confusing. For the *scr* (Fig. 7a,b) they named the origin as

the 'lateral surface of the sejugal fissures, in the back of the cheliceral retractors' and the insertion as the 'posterior lateral surface of the epistoma'.

The superior prodorsal retractor (Fig. 7c,d) each consists of three (*E. cooki*) or four (*R. ardua* and *O. banksi*) muscle fibers. The *spr* are named 'extensors of the camerostome' ('*eks*'; for *Oribotritia* sp.) in Yastrebtsov (1991) and 'muscles of the camerostome' ('*mca*'; for *R. ardua*) in Akimov and Yastrebtsov (1991). They probably used the term camerostome to indicate the prodorsum; in fact, 'camerostome' denotes the secondary cavity formed around the chelicerae by the rostral limb and the subcapitulum (van der Hammen, 1980). The *spr* inserts on the manubrium, hence the term camerostome is misapplied by Akimov and Yastrebtsov. Except for the *scr*, the insertions of the muscles of the LDP (*ipr*, *pla*, *spr*) are located more posteriorly in *E. cooki* and *O. banksi* than in *R. ardua*.

4.4. Opisthosomal compressor system (OCS)

As mentioned above, *O. banksi* has only one muscle pair originating on the preanal apodeme, compared to two pairs (*hva*, *hvc*) in Euphthiracaridae (Fig. 8a, cf Fig. 8b). According to its origin and insertion, this muscle is probably the homologue of the holoventral compressor – despite its star-shaped orientation in contrast to the more or less direct lateral orientation in *R. ardua*. Since plates in the genital and anal regions of *O. banksi* are not fused to form holo-ventral plates, we propose to call this muscle the ventral plate compressor (*vpc*).

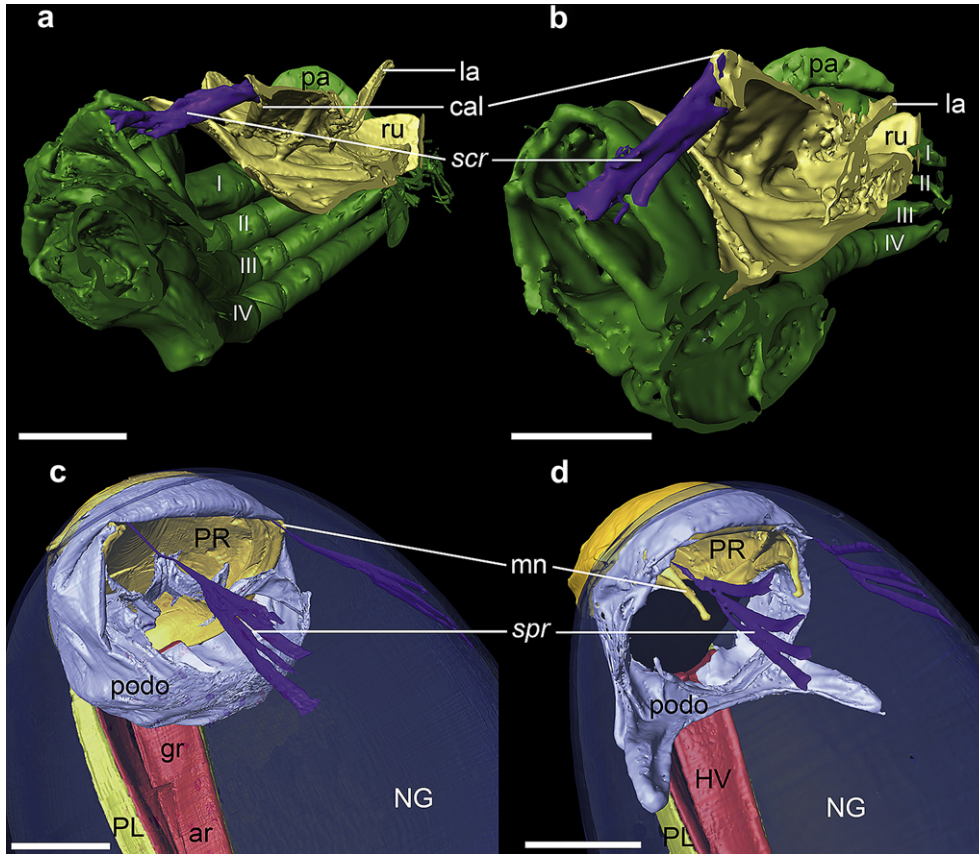


Fig. 7. LDP. Segmentations of synchrotron X-ray microtomography data of *Oribotritia banksi* and *Rhysotritia ardua*. Subcapitular retractors (*scr*) (posterior view of renderings of sagittal section of subcapitulum and legs): (a) 3D model of *O. banksi* (anterior: right). Scale bar = 100 μ m. (b) 3D model of *R. ardua* (anterior: right). Scale bar = 50 μ m. Superior prodorsal retractors (*spr*) (posterolateral view of renderings with transparent notogaster): (c) 3D model of *O. banksi*. Scale bar = 200 μ m. (d) 3D model of *R. ardua*. Scale bar = 100 μ m. (I, II, III, IV, walking legs; ar, anal region; cal, lemniscus of capitular apodeme; gr, genital region; HV, holoverntal plates; mn, manubrium; NG, notogaster; la, labrum; pa, pedipalpus; PL, plicature plates; podo, podosomal membrane; PR, prodorsum; ru, rutella; *scr*, subcapitular retractors; *spr*, superior prodorsal retractors.)

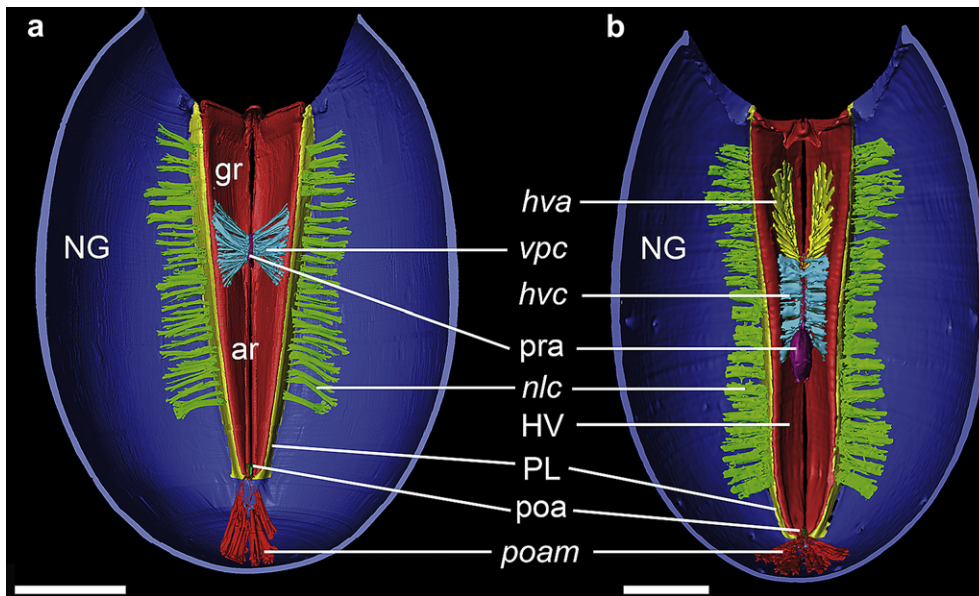


Fig. 8. OCS and postanal muscles (*poam*) of *Oribotritia banksi* and *Rhysotritia ardua*. Dorsal view of segmentations of a virtual horizontal section based on synchrotron X-ray microtomography data. (a) 3D model of *O. banksi*. Scale bar = 300 μ m. (b) 3D model of *R. ardua*. Scale bar = 100 μ m. (ar, anal region; gr, genital region; HV, holoverntal plates; *hva*, holoverntal adductors; *hvc*, holoverntal compressors; NG, notogaster; *nlc*, notogaster lateral compressors; PL, plicature plates; *poa*, postanal apodeme; *poam*, postanal muscles; *pra*, prominence of preanal apodeme; *vpc*, ventral plate compressors.)

Table 3
Measurements of the prodorsum lateral adjusters (*pla*).

		<i>Oribotritia banksi</i>	<i>Rhysotritia ardua</i>
Encapsulated	Length (μm)	247	54
	$F_X = \cos \alpha$ (lateral)	0.06	0.53
	$F_Y = \cos \beta$ (posterior)	0.81	0.67
	$F_Z = \cos \gamma$ (dorsal)	0.59	0.54
Extended	Length (μm)	300	144
	$F_X = \cos \alpha$ (lateral)	0.04	0.22
	$F_Y = \cos \beta$ (posterior)	0.48	0.08
	$F_Z = \cos \gamma$ (dorsal)	0.88	0.97

In our studies, the *hvc* consists of 10–20 (*R. ardua*; Fig. 8b) and the *vpc* of 25 (*O. banksi*; Fig. 8a) muscle fibers. *Euphthiracarus cooki* has five muscle bands with an unknown number of fibers. In *O. banksi* the muscle fibers are more or less arranged star-like around the preanal apodeme, whilst in the other two species they are directed more or less straight laterally. Yastrebtsov (1991) and Akimov and Yastrebtsov (1991) called them ‘internal dilators of the anal valves’ (*‘dan2’*) and ‘internal dilators of the genital valves’ (*‘dge1’*). Considering their function, taking part in the buildup of the hemocoel pressure, these names are rather confusing, as was recently discussed by Heethoff and Norton (2009).

The holovertral adductor exists in *E. cooki* (with 25 or more flat, broad muscle fibers) and *R. ardua* (with 40 muscle fibers; Fig. 8b). Their homologue in *Oribotritia* we propose to call the ventral plate adductor (*vpa*; Table 2); this pair exists in the unidentified *Oribotritia* sp. studied by Yastrebtsov (1991; his Fig. 2), but not in *O. banksi*. For both *Oribotritia* sp. and *R. ardua*, Yastrebtsov (1991) and Akimov and Yastrebtsov (1991) call them the ‘constrictors of the genital valve’ or ‘genital plate constrictors’ (*‘cge’*) and depict the origin as the ‘anterior edge of the anal valve’ and the insertion as the ‘lateral edge of the genital valve leaflets’. At least for *R. ardua*, their stated origin is incorrect: it is the preanal apodeme.

Each notogaster lateral compressor consists of 30–40 muscle bands with 2–6 muscle fibers each in *O. banksi* (Fig. 8a), 25 muscle bands with 3–6 fibers each in *R. ardua* (Fig. 8b) and 21 muscle bands in *E. cooki*. In contrast to *R. ardua* and *E. cooki*, the muscle bands of *O. banksi* insert through tendons on the medial margin of the plicature plates. Yastrebtsov (1991) and Akimov and Yastrebtsov (1991) termed them the ‘external dilators of the anal valves’ (*‘dan1’*) and the ‘external dilators of the genital valves’ (*‘dge2’*).

According to Sanders and Norton (2004) the OCS builds up hemocoel pressure, particularly important during ecptychosis. However, it was shown for non-ptychoid mites that these muscles can also act in closing the anal valves (Heethoff and Norton, 2009). By a system of three different muscles originating and inserting on the ventral plates and the preanal apodeme, the force of the contracting muscles is transferred onto the notogaster which leads to its lateral compression. This compression increases hemocoel pressure.

4.5. Additional muscles

The cheliceral retractors of all three species are quite similar. These muscles originate partly on the sagittal apodeme in *E. cooki* and *R. ardua*, but on the exobothridial field in *O. banksi*. This can be explained by the lack of a sagittal apodeme in *O. banksi* (Schmelzle et al., 2008). According to Akimov and Yastrebtsov (1991; their Fig. 1 and Table 3) the *chr* of *R. ardua* originate on the medial and lateral wall of the ‘camerostome’. A sagittal apodeme is not mentioned.

The trochanteral abductors of all three species are similar. They were called ‘remotors of the trochanter’ (*‘rpe1’*) by Akimov and Yastrebtsov (1991); in some of their figures (e.g. Fig. 5:2) this

abbreviation is also used for the ‘retractors of the walking legs’ (it should have been ‘*rep*’). Also, Yastrebtsov (1991) stated that these muscles do not exist in *Oribotritia* sp., which is probably wrong; they are present in *O. banksi* and they seem necessary for leg movement.

The postanal muscle (Fig. 8) is called ‘constrictors of the anal valve’ in Yastrebtsov (1991) and Akimov and Yastrebtsov (1991). The origin is said to be the ‘anterior edge of the anal shield’ (it is normally the posterior end of the notogaster) and the insertion is said to be the ‘anterior transversal sclerites of the anal valve’ (it is normally the postanal apodeme). We construe this to be a simple mistake in their list, as did Heethoff and Norton (2009). On Fig. 2:3 of Yastrebtsov (1991) the origin of these muscles in *Oribotritia* sp. is located dorsally on the notogaster, but we found the pair to originate terminally on the notogaster of *O. banksi*, and insert through tendons on the postanal apodeme.

4.6. Functional analyses of *pla*

The variable origin of the prodorsum lateral adjuster (dorsolateral in *R. ardua* but dorsal in *O. banksi*) and the fact that this muscle originates and inserts on stable cuticular rather than membranous structures (notogaster and manubrium), which can be well simulated *in silico* in both the extended and encapsulated state, make it a valuable system for functional analyses. By simulating the correlation of origin and insertion in the extended and encapsulated state, the spatial relative force vectors of this muscle can be calculated. For *R. ardua*, there are two muscle bands, therefore two points for origin and insertion, but the bands operate in parallel. Hence, the midpoints define the virtual origin and insertion of the resulting muscle and were used for subsequent analysis. The *pla* of *Oribotritia banksi* has two points of origin, but just a single insertion point by tendon on the manubrium. We calculated the midpoint on the notogaster to define the virtual origin of the resulting muscle. In this manner we identified a set of coordinates (x, y, z) for origin and insertion of *pla* for both species in the two states (extended, encapsulated; Fig. 9). Using the formulas given in Fig. 3, we calculated the length of *pla* and the relative force vectors (F_X, F_Y, F_Z) in lateral, posterior and dorsal directions (Table 3, Fig. 10). During ecptychosis, the *pla* shortens by a factor of 1.2 (from 300 μm to 247 μm) in *O. banksi* and a factor of 2.6 (from 144 to 54 μm) in *R. ardua*. Not only is *pla* twice as dynamic in *R. ardua* as in *O. banksi*, but the relative distribution of force vectors strongly differs between the two species.

4.6.1. Lateral force vector

In *R. ardua*, the lateral component of the *pla* force vector in the encapsulated state is 0.53, which is almost nine times more than in *O. banksi* (0.06). When extended, the *pla* has a lateral force component of 0.22 and 0.04 for *R. ardua* and *O. banksi*, respectively. Furthermore, the *pla* has a (small) inward orientation in *O. banksi* and not an outward one, as in *R. ardua*. In *E. cooki*, the lateral component of *pla* is responsible for correcting lateral misalignments of the prodorsum with respect to the lateral notogastral tecta (Sanders and Norton, 2004). Since the *pla* of *R. ardua* has a high relative lateral force vector, we assume a similar function in this species. However, in *O. banksi* there is almost no lateral force component, so a function related to lateral corrections of misalignments seems virtually impossible. During en- and ecptychosis, the prodorsum rotates around a transverse pseudo-articulation, which results from a temporary connection of the bothridial scale (prodorsum, Figs. 4e,f, and 6c,d) and the tectonotal notch (notogaster, Fig. 4a,b). This connection is stabilized by a scale receptacle in *R. ardua* and *E. cooki*, but not in *O. banksi* (Sanders and Norton, 2004; Schmelzle et al., 2008). The lateral component of the

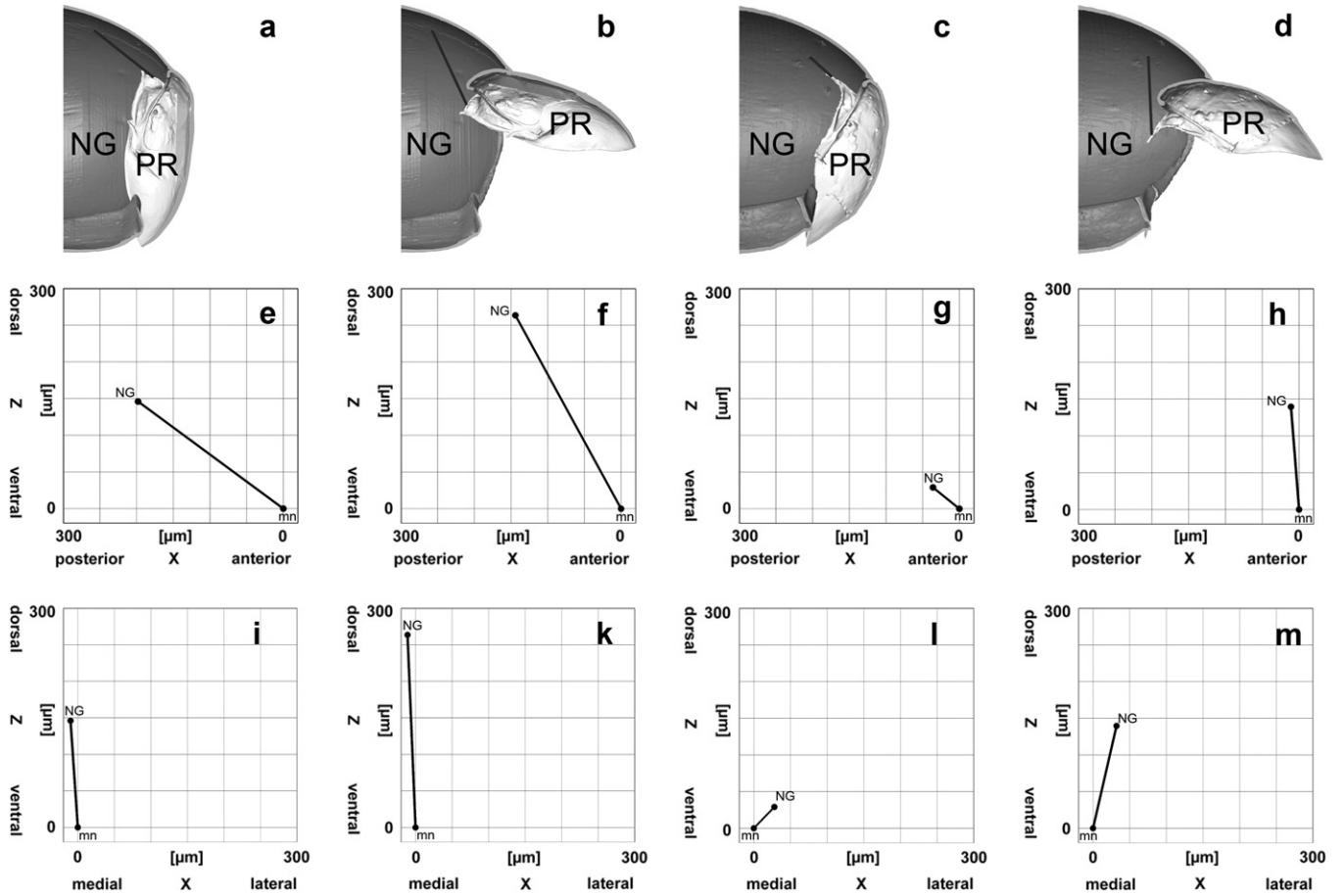


Fig. 9. Virtual sagittal sections and force vectors through simulated encapsulated and extended states of *Rhysotritia ardua* and *Oribotritia banksi*. The black line indicates the course of the resulting virtual prodorsum lateral adjustor (*pla*) from its origin on the notogaster to its insertion on the manubrium of prodorsum. (a) *O. banksi*, encapsulated. (b) *O. banksi*, extended. (c) *R. ardua*, encapsulated. (d) *R. ardua*, extended. Sagittal projections of the orientation of *pla*. (e) *O. banksi*, encapsulated. (f) *O. banksi*, extended. (g) *R. ardua*, encapsulated. (h) *R. ardua*, extended. Cross-sectional projections of the orientation of *pla*. (i) *O. banksi*, encapsulated. (k) *O. banksi*, extended. (l) *R. ardua*, encapsulated. (m) *R. ardua*, extended. (mn, manubrium; NG, notogaster; *pla*, prodorsum lateral adjustors, PR, prodorsum.)

pla presumably plays an additional role in adjusting the bothridial scale into the scale receptacle during entpychosis in *R. ardua*, which is not necessary in *O. banksi*. In the latter species, the connection of the bothridial scale and the tectonotal notch is realized by a broad

and deep cuticular furrow, and the bothridial scale encompasses the tectonotal notch on the outer surface to attain a stable attachment (Schmelzle et al., 2008). This seems to supersede a muscular lateral adjustment of the prodorsum, but requires a larger posterior and dorsal force vector to maintain the connection. Furthermore, in the active extended state, the lateral stabilization of the prodorsum by the scale receptacle is lost in *R. ardua*, while the bothridial scale still encompasses the tectonotal notch in *O. banksi*. Hence, necessary lateral stabilization must be established by muscular activity in *R. ardua*. This might explain the more than five times higher lateral force component in *R. ardua*, compared with *O. banksi*, in the extended state.

4.6.2. Posterior force vector

The posterior component of the *pla* force vector in the encapsulated state is 0.67 and 0.81 for *R. ardua* and *O. banksi*, respectively, and changes to 0.08 for *R. ardua* and 0.48 in *O. banksi* after ecptychosis. The posterior component of *pla* is mainly responsible for the retraction of the prodorsum during entpychosis. However, since *O. banksi* lacks a lateral force component in the *pla*, the tight connection of the bothridial scale and the tectonotal notch also has to be maintained by posterior (and dorsal) force transmission in the active state. This explains why the posterior force component remains relatively high in the extended state of *O. banksi*, but drops tremendously, by a factor of eight, in *R. ardua*.

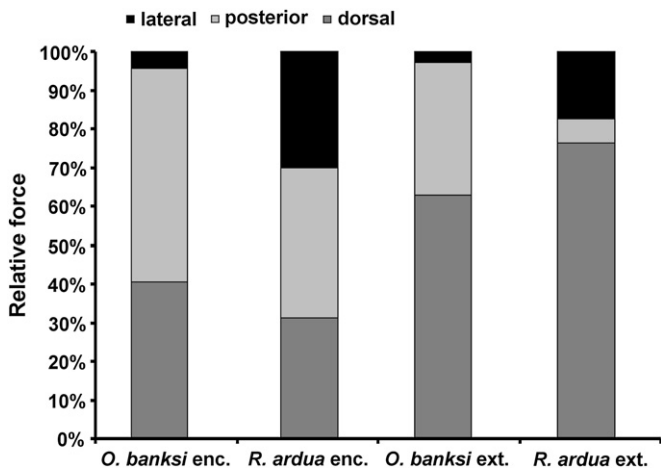


Fig. 10. Relative force components of the prodorsum lateral adjustor (*pla*) of *R. ardua* and *O. banksi* in lateral, posterior and dorsal direction. (enc., encapsulated state; ext., extended state).

4.6.3. Dorsal force vector

With respective values of 0.54 and 0.59, *R. ardua* and *O. banksi* have almost identical force components in the dorsal direction after entptychosis. In the extended state, the dorsal force component of *pla* is 0.97 in *R. ardua* and 0.88 in *O. banksi*.

The functional role of the dorsal component lies in the deflection of the prodorsum during entptychosis. This is obviously the main function in both species.

The existence of holovertral rather than separated ventral plates suggests a more derived phylogenetic position of Euphthiracaridae, compared to Oribotritiidae (Haumann, 1991; Sanders and Norton, 2004; Weigmann, 2006). This is also supported by the more complex connection of the prodorsum and the notogaster via a scale receptacle in the Euphthiracaridae. Hence, we propose that the plesiomorphic condition of the *pla* more or less resembles that of *O. banksi* and presumably lacks a lateral force vector. The general evolution and function of the *pla* seems to be connected to the evolution of the prodorsal–notogastral connection. This system seems to be well suited to differentiate between functional and phylogenetic constraints of ptychoidy in other groups of Ptyctima, as well as in the enarthronote families Mesoplophoridae and Protoplophoridae.

Acknowledgements

We thank Karl-Heinz Hellmer for the critical-point drying and taking the SEM micrographs. We thank Paavo Bergmann, Michael Laumann and Peter Cloetens for their help on the user experiment SC-2127 at the ESRF in Grenoble. We thank the European Synchrotron Radiation Facility for the beam time attributed.

References

- Akimov, I.A., Yastrebtsov, A.V., 1991. Skeletal–muscular system of oribatid mites (Acariformes: Oribatida). *Zoologische Jahrbücher für Anatomie und Ontogenie der Tiere* 121, 359–379.
- Alberti, G., Norton, R.A., Kasbohm, J., 2001. Fine structure and mineralisation of cuticle in Enarthronota and Lohmannioidea (Acari: Oribatida), in: Halliday, R.B., Walter, D.E., Proctor, H.C., Norton, R.A., Colloff, M.J. (Eds.), *Acarology: Proceedings of the 10th International Congress*. CSIRO Publishing, Melbourne, pp. 230–241.
- Balogh, J., Balogh, P., 1992. *The Oribatid Mites Genera of the World*, Vol. 1. Hungarian National Museum Press, Budapest.
- Betz, O., Wegst, U., Weide, D., Heethoff, M., Helfen, L., Lee, W.K., Cloetens, P., 2007. Imaging applications of synchrotron x-ray micro-tomography in biological morphology and biomaterial science. I. General aspects of the technique and its advantages in the analysis of arthropod structure. *Journal of Microscopy* 22, 51–71.
- Grandjean, F., 1934. Observations sur les Oribates (6e série). *Bulletin du Muséum National d'Histoire Naturelle* 6, 353–360.
- Grandjean, F., 1954. Essai de classification des oribates. *Bulletin de la Société Zoologique de France* 78, 421–446.
- Grandjean, F., 1967. Nouvelles observations sur les oribates (5e série). *Acarologia* 9, 242–272.
- Grandjean, F., 1969. Considérations sur le classement des oribates leur division en 6 groupes majeurs. *Acarologia* 11, 127–153.
- Haumann, G., 1991. Zur Phylogenie primitiver Oribatiden, Acari: Oribatida. dbv Verlag für die Technische Universität Graz, Graz.
- Heethoff, M., Cloetens, P., 2008. A comparison of synchrotron X-ray phase contrast tomography and holotomography for non-invasive investigations of the internal anatomy of mites. *Soil Organisms* 80, 205–215.
- Heethoff, M., Norton, R.A., 2009. Role of musculature during defecation in a particle-feeding arachnid, *Archegozetes longisetosus* (Acari, Oribatida). *Journal of Morphology* 270, 1–13.
- Norton, R.A., 1984. Monophyletic groups in the Enarthronota (Sarcoptiformes). In: Griffiths, D.A., Bowman, C.E. (Eds.), *Acarology VI*, vol. 1. Ellis Horwood, Chichester, pp. 233–240.
- Norton, R.A., 1994. Evolutionary aspects of oribatid mite life histories and consequences for the origin of the Astigmata. In: Houck, M. (Ed.), *Mites. Ecological and Evolutionary Analyses of Life-History Patterns*. Chapman and Hall, New York, pp. 99–135.
- Norton, R.A., 2001. Systematic relationships of Nothrolahmanniidae, and the evolutionary plasticity of body form in Enarthronota (Acari: Oribatida), in: Halliday, R.B., Walter, D.E., Proctor, H.C., Norton, R.A., Colloff, M.J. (Eds.), *Arcaology: Proceedings of the 10th International Congress*. CSIRO Publishing, Melbourne, pp. 58–75.
- Norton, R.A., Behan-Pelletier, V., 1991. Calcium carbonate and calcium oxalate as cuticular hardening agents in oribatid mites (Acari: Oribatida). *Canadian Journal of Zoology* 69, 1504–1511.
- Raspotnig, G., 2006. Chemical alarm and defence in the oribatid mite *Collohmanna gigantea* (Acari: Oribatida). *Experimental & Applied Acarology* 39, 177–194.
- Sanders, F.H., Norton, R.A., 2004. Anatomy and function of the ptychoid defensive mechanism in the mite *Euphthiracarus cooki* (Acari: Oribatida). *Journal of Morphology* 259, 119–154.
- Saporito, R.A., Donnelly, M.A., Norton, R.A., Garraffo, H.M., Spande, T.F., Daly, J.W., 2007. Oribatid mites as a major dietary source for alkaloids in poison frogs. *Proceedings of the National Academy of Sciences of the USA* 104, 8885–8890.
- Schmelzle, S., Helfen, L., Norton, R.A., Heethoff, M., 2008. The ptychoid defensive mechanism in Euphthiracaroida (Acari: Oribatida): a comparison of exoskeletal elements. *Soil Organisms* 80 (2), 227–241.
- Shimano, S., Sakata, T., Mizutani, Y., Kuwahara, Y., Aoki, J.I., 2002. Geranial: the alarm pheromone in the nymphal stage of the oribatid mite, *Nothrus palustris*. *Journal of Chemical Ecology* 28, 1831–1837.
- van der Hammen, L., 1980. *Glossary of Acarological Terminology*, Volume 1. Junk BV Publishers, The Hague.
- Wauthy, G., Leponce, M., Banaï, N., Sylin, G., Lions, J.C., 1998. The backward jump of a box moss mite. *Proceedings of the Royal Society – Biological Sciences* 265, 2235–2242.
- Weigmann, G., 2006. Hornmilben (Oribatida). Goecke & Evers, Keltern.
- Yastrebtsov, A.V., 1991. Peculiarities of the muscular system and skeletal parts of the oribatid mite *Oribotritia* sp. (Oribatida, Ptyctima). *Revue d'Entomologie de l'URSS* 70, 495–499 (in Russian).

Publication 3

**The ptychoid defensive mechanism in *Phthiracarus longulus* (Acari: Oribatida):
Exoskeletal and muscular elements.**

Schmelzle, S., Helfen, L., Norton, R.A., Heethoff, M.

Published in Soil Organisms 82 (2), pp. 253–273.

Submitted
18 December 2009

Accepted
12 April 2010

Published
2010

Authors' contribution:

- Schmelzle, Sebastian: Specimen preparation, data acquisition, data processing, data analysis, image processing, manuscript writing and preparation
- Helfen, Lukas: Data acquisition and support during, partial review of manuscript
- Norton, Roy A.: Specimen collection and fixation, general support and discussion, revision of manuscript
- Heethoff, Michael: Supervision, data acquisition, general support and discussion, revision of manuscript

Methods used:

- Synchrotron X-ray microtomography (SR μ CT)
- Scanning Electron Microscopy (SEM)

The ptychoid defensive mechanism in *Phthiracarus longulus* (Acari, Oribatida, Phthiracaroida): Exoskeletal and muscular elements

Sebastian Schmelzle^{1*}, Lukas Helfen², Roy A. Norton³ & Michael Heethoff¹

¹ Universität Tübingen, Institut für Evolution und Ökologie, Abteilung für Evolutionsbiologie der Invertebraten, Auf der Morgenstelle 28E, 72076 Tübingen, Germany

² Institut für Synchrotronstrahlung (ISS/ANKA), Karlsruher Institut für Technologie (KIT), Hermann-von-Helmholtz- Platz 1, 76344 Eggenstein-Leopoldshafen, Germany

³ State University of New York, College of Environmental Science and Forestry, 1 Forestry Drive, Syracuse, NY, 13210, USA

* Corresponding author (schmelzle@oribatida.com, Tel. 07071/2976953, Fax 07071/294634)

Abstract

The most complex defensive mechanism in oribatid mites is ptychoity, a special body form allowing the animals to retract their legs and coxisternum into a secondary cavity in the idiosoma and to seal it off with the prodorsum. Many exoskeletal and muscular adaptations are required to enable the functionality of this mechanism, e.g. a soft and pliable podosoma. Its membranous part not only gives the coxisternum the ability to move independently from the rest of the hardened cuticular elements, but also builds up the ‘walls’ of the secondary cavity. Here, using scanning electron microscopy and synchrotron microtomography we present the first detailed study on ptychoity in a phthiracaroid mite, *Phthiracarus longulus*, and compare it to the Euphthiracaroida. Morphological differences regarding ptychoity between these groups are already noticeable from the outside: the ventral plates of *P. longulus* are embedded into the soft anogenital membrane, whereas euphthiracaroid mites connect the ventral plates to the notogaster through the hardened plicature plates. Internally, we discovered a not yet described coxisternal protractor muscle, which presumably assists haemolymph pressure during the deployment of the coxisternum during eptychosis.

Keywords: Synchrotron X-ray microtomography, *Phthiracarus longulus*, ptychoity, Phthiracaridae, box mite, convergent evolution, predator defence

1. Introduction

Particle feeding, the general mode of food ingestion in oribatid mites, is rare among the mostly fluid-feeding chelicerates (Heethoff & Norton 2009). The low digestive efficiency resulting from feeding on dead plant parts or saprophagous fungi leads to certain constraints: slow growth, relatively long generation time and low reproductive potential with an elongated adult life span (Norton 1994, Sanders & Norton 2004, Heethoff et al. 2007). These characteristics necessitate effective predator defence mechanisms, which evolved in various ways among oribatid mites. In general, there are two physically different strategies: chemical

defence through secretion of predator-repelling substances from the opisthonotal oil glands (e.g. Shimano et al. 2002, Raspotnig 2006, Saporito et al. 2007), and several mechanical defence mechanisms (e.g. prolongation of the body setae to form a hedgehog-like appearance, overhanging cuticular tecta concealing articulations; Grandjean 1934). Often these defensive mechanisms are combined with a mechanical hardening of exposed cuticle (Norton & Behan-Pelletier 1991, Alberti et al. 2001).

The most complex mechanical defensive mechanism in oribatid mites is ptychoidy, where the legs and the coxisternum can completely be withdrawn into a temporary cavity into the idiosoma (Sanders & Norton 2004, Schmelzle et al. 2008, 2009). In the encapsulated state the animals – commonly known as ‘box mites’ – then exhibit no soft membrane for a possible attack by predators (Figs. 1A, 2A, B). Rarely, this defensive mechanism can additionally be combined with an escape jump (Wauthy et al. 1998). Ptychoidy has probably evolved three times independently (Sanders & Norton 2004): in the Mixonomata (the monophylum Ptyctima containing the superfamilies Phthiracaroida and Euphthiracaroida; Grandjean 1954, Grandjean 1967, Balogh & Balogh 1992) and in two unrelated families of Enarthronota, Mesoplophoridae and Protoplophoridae (Grandjean 1969, Norton 1984). The special body form needs certain requirements, which accompany several exoskeletal and muscular adaptations: (i) the coxisternum must be isolated from all other hardened cuticle by a soft, pliable integument (ii) the opisthosomal cuticle must be hardened (iii) the coxisternum must be articulated and deformable and (iv) there must be a system that can manage the large internal volume changes.

Exoskeletal elements involved in ptychoidy can be divided into 5 groups. The *prodorsum* (*PR*) acts as an operculum-like seal for the encapsulated animal (Sanders & Norton 2004) and it bears several structures for insertion of muscles that are directly involved in ptychoidy, for instance the *manubrium* (*mn*) and the *inferior retractor process* (*irp*; Fig. 3; Schmelzle et al. 2008, 2009). The *opisthosomal venter* is the exoskeletal group that shows by far the most structural variation among the various ptychoid families and genera, and it is often used for identification. Only in Phthiracaroida, which is the focus of this paper, is the basic structure fixed. It always consists of two pairs of large plates: the genital valves (Wauthy 1984), consisting of the fused genital and aggenital plates, and the anal valves, consisting of the fused anal and adanal plates (Figs. 1A, 2A, B). Movements of the opisthosomal venter relative to the notogaster (see below), which are connected through a broad articulating membrane, the anogenital membrane (Wauthy 1984), are responsible for changes in haemocoel pressure that are required for ptychoidy. The *notogaster* – dorsal plate of the opisthosoma – is ovate to nearly spherical and hardened through mineralisation with calcium carbonate or calcium oxalate (Figs. 1A, 2A, B; Norton & Behan-Pelletier 1991, Alberti et al. 2001). For smaller predators (e.g. parasitiform mites) it presumably is an impenetrable and indestructible barrier. The *podosoma*, or leg-bearing region, comprises a supportive coxisternum, itself composed of four pairs of hardened epimeral plates (Sanders & Norton 2004), and a voluminous, pliable membranous part. The membranous part is one of the main adaptations to ptychoidy; it enables retraction of the legs into a secondary cavity built up by the membrane itself (Grandjean 1967). The *subcapitulum* – venter of the gnathosoma – has adaptations for ptychoidy that include a prominent capitular apodeme and an equally prominent projection of the mentum, as well as a fusion with the taenidiophore part of supracoxal sclerite 1 (Fig. 6A; Märkel 1964, Walker 1965, Sanders & Norton 2004).

Tab. 1 Abbreviations, origin and insertion of the muscular elements associated with ptychoidy in *Phthiracarus longulus*.

Muscle	Abbreviation	Origin	Insertion
Dorsoventral muscles of the Prosoma			
<i>DVP</i>			
coxisternal retractors	<i>csr</i>	notogaster, dorsal	apodeme 2 of the epimeres, apodemal shelves 3 and 4
coxisternal protractors	<i>csp</i>	notogaster, lateral	sejugal apodeme
inferior podosomal membrane adjustors	<i>ima</i>	anterior half of notogaster, ventrolateral	podosomal membrane
prodorsal dorsoventral muscles 1	<i>pdv1</i>	exobothridial field	lateral margin of apodemes 1
prodorsal dorsoventral muscles 2	<i>pdv2</i>	exobothridial field	lateral margin of apodemes 2
prodorsal dorsoventral muscles 3	<i>pdv3</i>	manubrium	sejugal apodeme
superior podosomal membrane adjustors	<i>sma</i>	notogaster, lateral	podosomal membrane
Endosternal Division of the Prosoma			
<i>EDP</i>			
anterior dorsal endosternal muscles	<i>ade</i>	manubrium	endosternum
posterior dorsal endosternal muscles	<i>pde</i>	notogaster, dorsolateral	endosternum
subcapitulum endosternal retractors	<i>ser</i>	endosternum	mentum of subcapitulum
taenidiphore endosternal retractors	<i>ter</i>	endosternum	taenidiphore
Longitudinal Division of the Prosoma			
<i>LDP</i>			
inferior prodorsal retractors	<i>ipr</i>	notogaster, dorsolateral	inferior retractor process, intercalary wall induration
prodorsum lateral adjustors	<i>pla</i>	notogaster, dorsolateral	manubrium
subcapitular retractors	<i>scr</i>	apodeme 1, 2 of the epimeres 1	anchoral process of subcapitular apodeme
superior prodorsal retractors	<i>spr</i>	notogaster, dorsal	basis of manubrium
Opisthosomal Compressor System			
<i>OCS</i>			
ventral plate adductors	<i>vpa</i>	preanal apodeme	genital valve
ventral plate compressors	<i>vpc</i>	preanal apodeme	lateral edge of genital valve
notogaster lateral compressors	<i>nlc</i>	notogaster, ventral curvature	anogential membrane
cheliceral retractors	<i>chr</i>	posterior wall of prodorsum, sagittal apodeme	posterior surface of basal cheliceral segment
postanal muscles (= holovertral levators)	<i>poam</i>	terminal at posterior end of notogaster	postanal apodeme
trochanteral abductor	<i>tab</i>	endosternum	leg trochanter

Muscles that are directly involved in ptychoidity are grouped into four systems (Sanders & Norton 2004; Schmelzle et al. 2009; Tab. 1). Muscles not directly involved in ptychoidity (but nonetheless supporting the ptychoid process) are grouped together as 'additional muscles'. Those are the cheliceral retractor (*chr*), the trochanteral abductor (*tab*) and the postanal muscle (*poam*). These systems play different general roles in ptychoidity. (i) The *dorsoventral muscles of the prosoma* (DVP; Figs 4, 5) are responsible for retracting, protracting and correctly aligning the legs and the podosomal membrane in the idiosoma. (ii) The *endosternal division of the prosoma* (EDP; Fig. 6) comprises the muscles associated with the endosternum. Its main function is the retraction and correct alignment of the prodorsum in relation to the coxisternum and the subcapitulum. (iii) The *longitudinal division of the prosoma* (LDP; Fig. 7) is mainly responsible for retraction of the cheliceral and pedipalpal segments and the acron (epiprosoma) and for maintaining the encapsulated state. (iv) The function of the *opisthosomal compressor system* (OCS, Fig. 8) in ptychoidity is the build-up of sufficient haemocoel pressure for re-extension of the encapsulated animal. It is also responsible for building up pressure needed during the active state (extension of the legs, etc.).

The opisthosomal compressor system comprises three muscles according to Sanders and Norton (2004). The classification and nomenclature of the muscles involved is based on the morphology (associated muscle origin and insertion) of the euphthiracaroid mite *Euphthiracarus cooki* Norton et al. 2003.

To date, all detailed functional studies of ptychoidity are related to members of Euphthiracaroida (Akimov & Yastrebtsov 1991, Sanders & Norton 2004, Schmelzle et al. 2008, 2009, Yastrebtsov 1991) or cover only parts of the characteristics relevant to ptychoidity (e.g. the ano-genital system of *Phthiracarus nitens* in: Wauthy 1984). Here, we used the non-invasive technique of synchrotron X-ray microtomography to describe the morphology of exoskeletal and muscular elements in the phthiracaroid mite *Phthiracarus longulus* (C.L. Koch, 1841) (Phthiracaridae).

2. Materials and methods

Specimens

Phthiracarus longulus is a holarctic species of the family Phthiracaridae that has many synonyms (Niedbała 2008), of which the one most used in North American literature is *P. setosellus* (Jacot). It is common and abundant in temperate forest litter, where the non-ptychoid juvenile stages burrow within decaying woody substrates. Adults for our studies (mean total length about 540 µm) were collected from accumulated decaying needles and cone scales of introduced Norway spruce (*Picea abies*) in LaFayette, Onondaga Co., NY, USA.

Sample preparation

Specimens were killed and fixed in 1 % glutaraldehyde for 60 h and stored in 70 % ethanol. For the final preparation, specimens were dehydrated in an increasing ethanol series with steps of 70, 80, 90, 95 and 100 %, with three changes at each step and 10 min at each change. After storage in fresh 100 % ethanol they were critical-point dried in CO₂ (CPD 020, Balzers).

Scanning electron microscopy

Critical-point dried specimens were glued onto a T-section-like metal foil on a stub and then sputtered with a 20 nm thick layer of a gold-palladium mixture. Micrographs were taken on a Cambridge Stereoscan 250 Mk2 scanning electron microscope at 20 keV.

Synchrotron X-ray microtomography

Critical-point dried animals were fixed by the notogaster to the tip of a plastic pin (1.2 cm long; 3.0 mm diameter) using instant adhesive. For each specimen, typically 1500 radiographs under different projection angles were taken at the European Synchrotron Radiation Facility (ESRF) in Grenoble using beamline ID19 with a beam energy of 20.5 keV and using a sample-detector distance of 20 mm. A cooled 14-bit CCD-camera with a resolution of 2048 x 2048 pixels and an effective pixel size of 0.3 µm per pixel was used (a detailed description of the method is given in Betz et al. 2007, Heethoff & Cloetens 2008, Heethoff et al. 2008).

The data were visualised with the program VGStudio MAX 1.2.1 (Volume Graphics, Heidelberg, Germany) and three-dimensional modeling of muscles and cuticular elements was conducted with amira™ 4.0.1 (Mercury Computer Systems Inc., Chelmsford, MA). Muscle fibres were counted using the original phase contrast microtomography data or, if that was not possible, by the number of split ends in the resulting 3D model. Different portions of muscles are called muscle bands and subdivisions of muscle bands are called muscle fibres (Sanders & Norton 2004).

Terminology

Since phthiracaroid mites differ from euphthiracaroid mites in some morphological characteristics, some of the muscle names would in this case be misleading. For reasons of simplicity and comparability we will address the muscles of the opisthosomal compressor system according to Schmelzle et al. (2009) throughout the manuscript. We will address the issue of the muscles (origin, insertion and the therefore resulting name) in detail in the discussion (cf. Tab. 2).

Tab. 2 Comparison of muscle names of the Opisthosomal Compressor System (OCS) used in the literature.

Schmelzle et al. (2009)	Hoebel-Mävers (1967, in German) ¹	Sanders & Norton (2004)	Heethoff & Norton (2009) ²	origin	insertion in Euphthiracaroida	insertion in Phthiracaroida
ventral plate adductor (<i>vpa</i>)	<i>G.MU.</i>	holoventral adductor (<i>hva</i>)	muscles of the genital plate (<i>gm</i>)	preanal apodeme	genital region of the ventral plates	genital valve
ventral plate compressor (<i>vpc</i>)	<i>PR.A.MU.</i> ('Praeanale Spannmuskeln')	holoventral compressor (<i>hvc</i>)	preanal muscles (<i>pram</i>)	preanal apodeme	lateral edge of the genital plates	lateral edge of the genital valve
notogaster lateral compressor (<i>nlc</i>)	<i>NOT.MU.</i> ('Notogastrale Depressor-Muskelbänder')	notogaster lateral compressor (<i>nlc</i>)	outer anal muscles (<i>oam</i>)	ventral curvature of the notogaster	lateral edge of the ventral plates	anogenital membrane

¹ On the non-ptychoid mite *Nothrus palustris* KOCH.

² On the non-ptychoid mite *Archezogetes longisetosus* AOKI.

3. Results

3.1 Exoskeletal elements

Prodorsum

The interior surface of the prodorsum (*PR*) is uniformly textured (Figs. 2B, 3) and is differentiated into the solid, distal rostral limb (*rl*; Fig. 3B), the rosthrophragma and the tegulum (not shown). The inferior retractor process (*irp*), located at about mid-length of the prodorsum on the ventrolateral inner border, is broad, robust and long and is angled anteromedially at about 45° (Figs. 2B, 3). The manubrium (*mn*) at the posterolateral end of the prodorsum is rather short and slim (Figs. 2B, 3A, B). The sagittal apodeme (*sa*) is located medially on the posterior wall of the prodorsum and shows a triangular cross section (Figs. 2, 3B, D). The rounded bothridial scale (*bs*) overhanging the bothridium and base of the sensillus (*ss*) laterally on the prodorsum (Fig. 3A, D) is, in the encapsulated state, firmly anchored in the corresponding scale receptacle (*sr*) resting in the tectonotal notch (*tn*) on the anterior margin of the notogaster (Figs 3D, 4A). The short, medially thickened sensillus (= bothridial seta; *ss*) originates in the cup-like bothridium positioned below the bothridial scale (*bs*) and, in the encapsulated state, partly lies in a notogastral indentation – therefore pointing ventrally (Figs 1B, 3C). The bothridium is internally surrounded by a system of chambers (Figs 2B, 3C,D). A longitudinal carina (*car*) is present on each side of the prodorsum (Figs. 3A, 5). The carina originates at the bothridial scale and proceeds to the anterior tip of the prodorsum, where it gradually effaces. There is no evidence of a rostral notch (Fig. 3A).

Opisthosomal venter

The venter consists of two pairs of large compound plates, the genital (fused genital and a genital plates) and anal (fused anal and adanal plates) valves (*gv* and *av*, respectively), which are smooth and lack indication of the fusion between components. Collectively, the valves are broad, narrowing only slightly posteriorly, with the anal valves being rounded posteriorly (Fig. 1A; *av*). The valves are embedded in the pliable anogenital membrane that connects them with the notogaster (Figs. 2, 8; *mem*). The preanal apodeme (Fig. 2; *pra*) extends across the whole width of the ventral plates, whereas the postanal apodeme (*poa*) is relatively narrow and confined to the posterior end of the anal valves (Fig. 2; *av*). Each pair of valves is also connected transversely: the genital valves (*gv*) are integrally connected to each other anteriorly by the phragmatal bridge (Fig. 3C, D; *pbr*), whereas the anal valves (*av*) are only functionally connected at two locking points. The latter include the left-fitting or right-fitting anterior anal lock, consisting of two corresponding, interdigitating apophyses on each side (partly visible on the surface; Figs. 1A, D, 2B), and the posterior anal lock, consisting of 2–3 small corresponding lobes on each side (Fig. 2B). Among the 67 examined specimens, 40 individuals showed the right-fitting and 27 the left-fitting state. Hence the state of the anterior lock is uniformly distributed (LR $\chi^2 = 2.5385$, d.f. = 1, $P = 0.1111$). Each genital valve has a distinct transverse carina in the anterior region (Figs 1C, 2B; *car*) and a special notch at each anterolateral corner that enables some sort of articulation with a corresponding tooth of the notogaster (Fig. 1A, C).

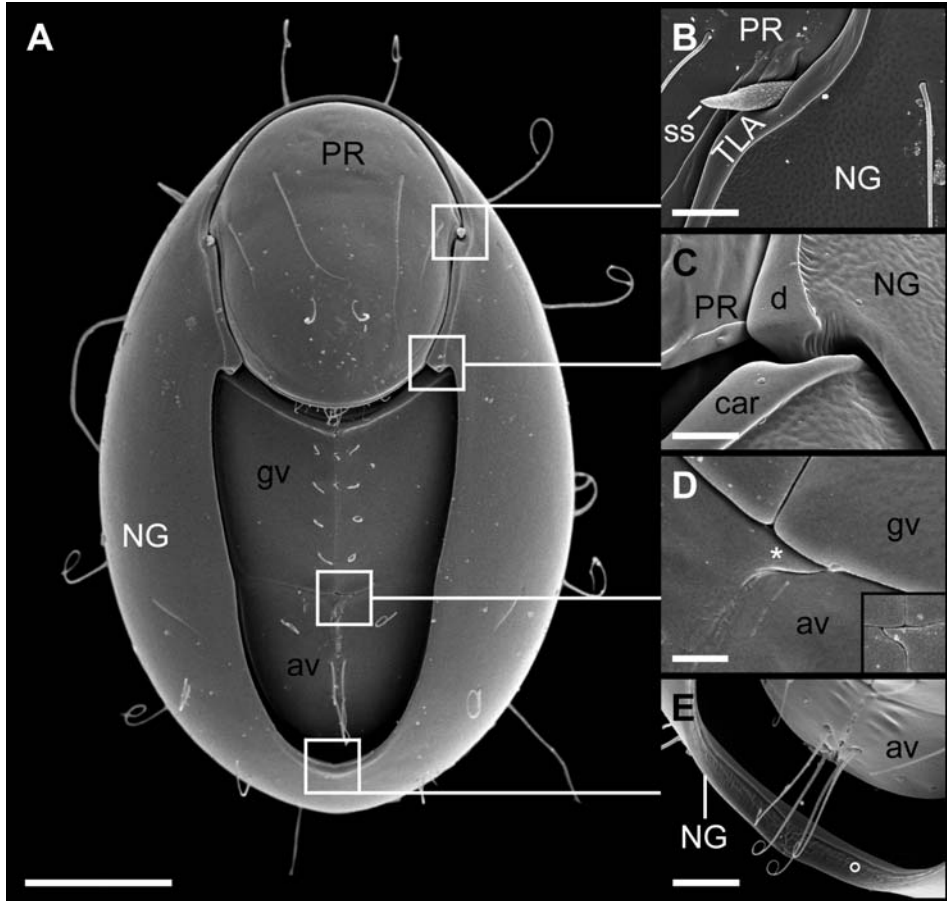


Fig. 1 *Phthiracarus longulus*. Scanning electron micrographs of 3 specimens (specimen 1: A, B, E; specimen 2: C; specimen 3: D). A: Ventral overview of encapsulated specimen (the withdrawn position of the ventral plates and the curled ends of notogastral setae are considered fixation artifacts; scale bar: 200 μ m); B: Detail of the bothridial scale, the sensillus and the tectonotal notch (scale bar: 20 μ m); C: Detail of the articulation of ventral plates and notogaster (scale bar: 10 μ m); D: Detail of the right-fitting (bottom right corner) and left-fitting state of the anterior anal lock (scale bar: 20 μ m); E: Detail of the simple U-shaped ventral margin of the notogaster (scale bar: 20 μ m). av: anal valve; car: carina; d: tooth; gv: genital valve; NG: notogaster; PR: prodorsum; TLA: lateral anterior tectum. Asterisk (*) indicates the left-fitting state of the anterior lock of the anal plates and degree ($^{\circ}$) indicates the U-shaped plain lateral margin of the notogaster.

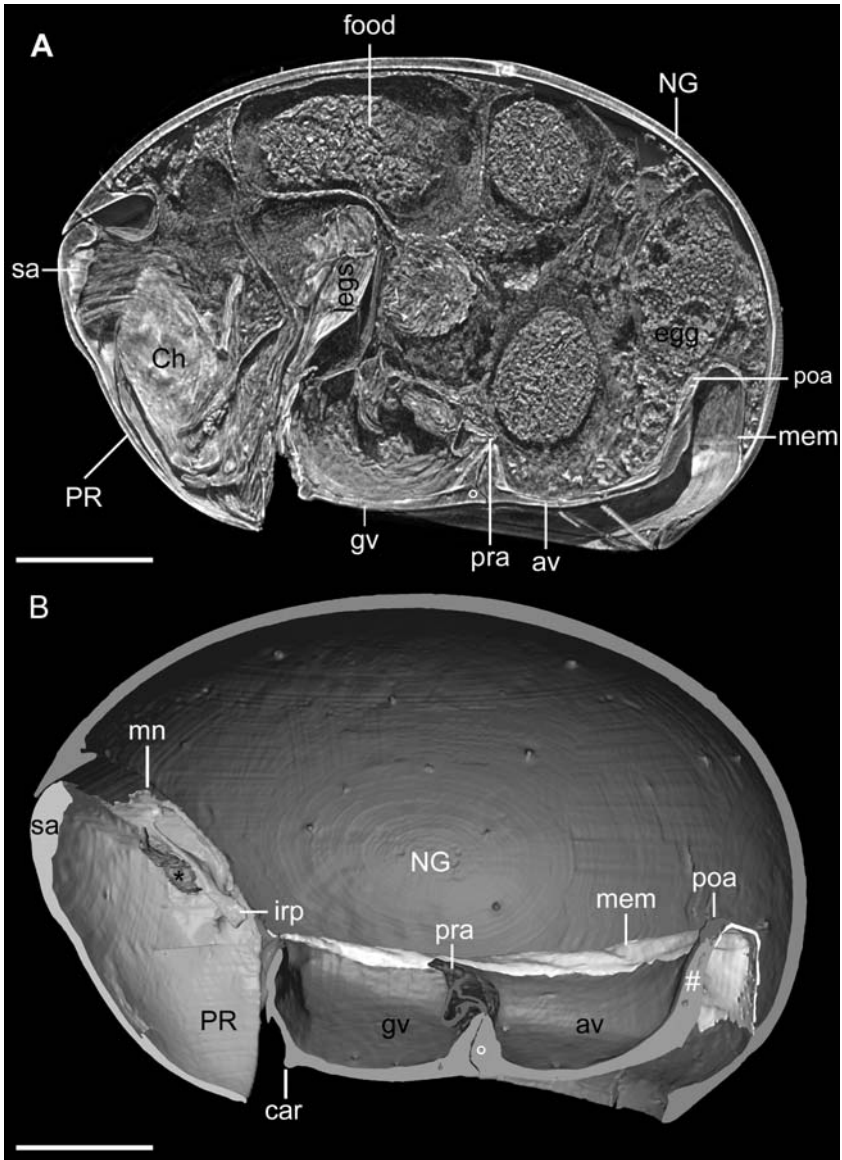


Fig. 2 *Phthiracarus longulus*, nearly encapsulated animal. A: Virtual sagittal section of a rendition of synchrotron X-ray microtomography data (scale bar: 100 μm); B: Virtual sagittal section of 3D-model of synchrotron X-ray microtomography data (scale bar: 100 μm). ap: anal plate; av: anal valve; car: carina; Ch: chelicera; food: food bolus; gp: genital plate; gv: genital valve; irp: inferior retractor process; mem: anogenital membrane; mn: manubrium; NG: notogaster; PR: prodorsum; pra: preanal apodeme; poa: postanal apodeme; sa: sagittal apodeme. Asterisk indicates the bothridium, degree indicates the anterior anal lock and pound indicates posterior anal lock.

Notogaster

The notogaster (*NG*) is hardened and quite thick (Fig. 2). Except anteriorly, the U-shaped ventral margin is more or less plain (Figs. 1A, E, 2), but at each anteroventral corner is a tooth (*d*) that articulates with the ventral plates, and that extends internally into a ridge (Fig. 1C). There is no terminal notogastral fissure (Fig. 1A). The border is provided with a tectum throughout, separated into two main parts, on either side of the corner tooth. The anterior tectum accommodates the prodorsum when encapsulated (Figs. 2B, 4A) and consists of the lateral anterior tectum (Fig. 1B; *TLA*), which encompasses the tectonotal notch (*tn*, Fig. 1A) and smoothly transitions into the pronotal tectum (*TPN*) at a point dorsally of the tectonotal notch. Posterior to the tooth the tectum (Fig. 4B) protects the articulation with the collective ventral plates. A scale receptacle (*sr*) inside the tectonotal notch is present (Figs. 1B, 3D).

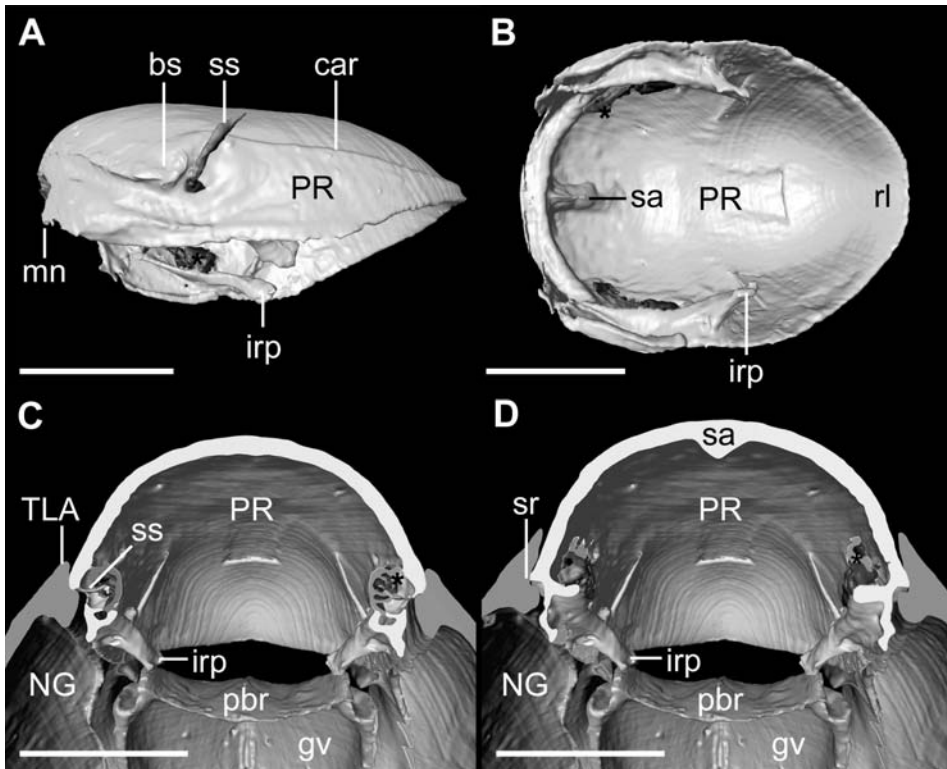


Fig. 3 *Phthiracarus longulus*, nearly encapsulated animal. Renderings of 3D-model of synchrotron X-ray microtomography data. A: Lateral view of the prodorsum (scale bar: 100 μ m); B: Ventral view of the prodorsum (scale bar: 100 μ m); C: Virtual frontal section in the region of the opening of the bothridium (scale bar: 100 μ m); D: Virtual frontal section in the region of the scale receptacle (scale bar: 100 μ m); bs: bothridial scale; car: carina; gv: genital valve; irp: inferior retractor process; mn: manubrium; NG: notogaster; pbr: phragmatal bridge; PR: prodorsum; rl: rostral limb; sa: sagittal apodeme; sr: scale receptacle; ss: sensillus; TLA: lateral anterior tectum. Asterisk (*) indicates the bothridium.

Podosoma

The coxisternum, forming the ventral center of the podosoma, encompasses the coxisternal umbilicus, a large area of membrane capable of compensating for the change of coxisternal form during ptychoid movement. Three articulations, or furrows, are present (not shown; compare Sanders & Norton 2004): the abjugal line (marking the intersection of podosomal membrane and the epiprosoma), the sejugal line (marking the intersection of hysterosoma and proterosoma) and the disjugal line (marking the intersection of podosomal membrane and opisthosoma). The areas of muscle insertion located in the membranous part of the podosoma do not seem to differ in any way from the rest of the podosomal membrane (Fig. 4B).

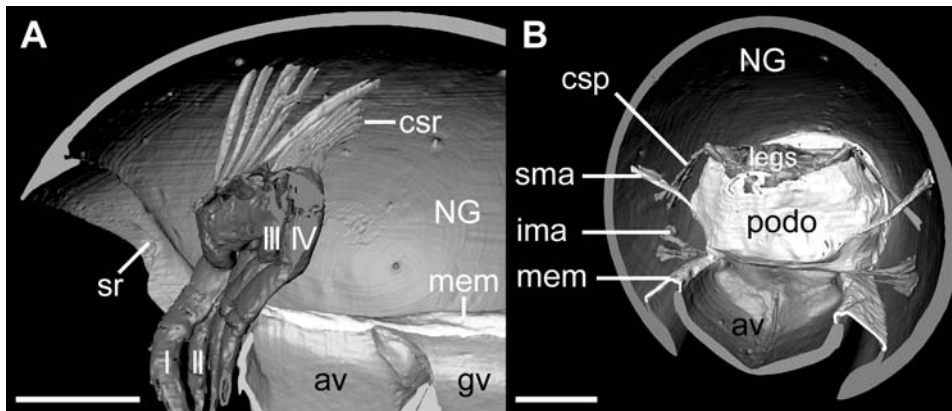


Fig. 4 *Phthiracarus longulus*, nearly encapsulated animal. DVP. Renderings of 3D-model of segmented synchrotron X-ray microtomography data. A: Virtual sagittal section showing the coxisternal retractor (csr) and its origin and insertion (scale bar: 100 μ m); B: Virtual cross section showing the inferior (ima) and superior (sma) membrane adjusters and the newly discovered coxisternal protractor (csp; scale bar: 100 μ m); I–IV: walking legs 1–4; av: anal valve; csp: coxisternal protractor; csr: coxisternal retractor; gv: genital valve; ima: inferior membrane adjuster; mem: anogenital membrane; NG: notogaster; podo: podosomal membrane; sma: superior membrane adjuster; sr: scale receptacle.

Subcapitulum

The capitular apodeme is developed as a large triangular, flat process with margins reinforced by a lemniscus (Figs. 6A, 7C). The mentum projects posteriorly in a shape similar to that of the capitular apodeme (Figs. 6A, 7C). The taenidiophore is located laterally between the base of the capitular apodeme and the projection of the mentum (Fig. 6A).

3.2 Muscular elements

Dorsoventral muscles of the prosoma (DVP)

The coxisternal retractor (csr) of *Phthiracarus longulus* consists of about 20 to 30 muscle fibres, originating dorsally on the notogaster and inserting on apodeme 2 and apodemal shelves 3 and 4 of the epimeres (Fig. 4A). The newly discovered coxisternal protractor (csp)

originates lateral on the notogaster and inserts directly onto the lateral margin of the sejugal apodeme (Fig. 4B). It consists of about 3 muscle fibres and is in encapsulated state directed dorsoposteriorly. The inferior and the superior podosomal membrane adjustors (*ima* and *sma*, respectively) both originate laterally on the notogaster and insert on the podosomal membrane (Fig. 4B).

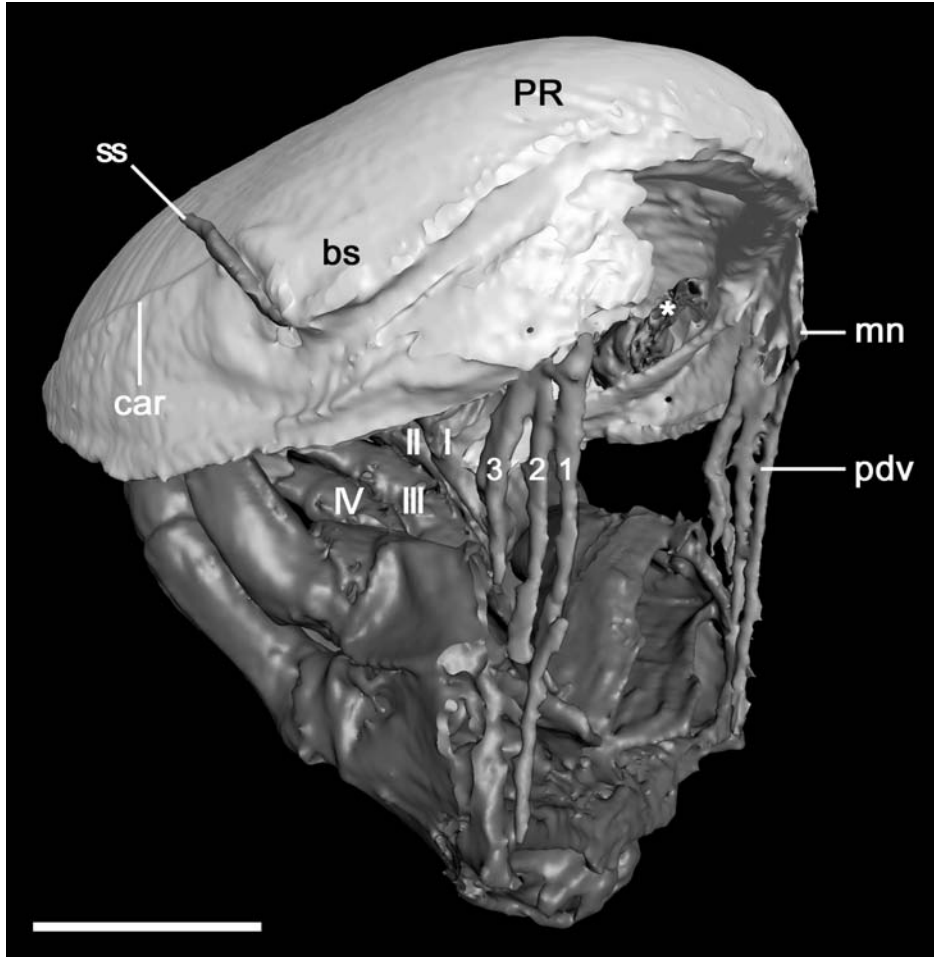


Fig. 5 *Phthiracarus longulus*, nearly encapsulated animal. Renderings of 3D-model of segmented synchrotron X-ray microtomography data of the prodorsum and podosoma, showing the prodorsal dorsoventral (DVP) muscle system (pdv1, pdv2 and pdv3), lateral view (scale bar: 50 μ m). I-IV: walking legs 1-4; bs: bothridial scale; car: carina (dorsal and ventral); irp: inferior retractor process; mn: manubrium; pdv1-3: prodorsal dorsoventral muscle 1-3; PR: prodorsum. Asterisk indicates the bothridium..

As the name implies, the inferior podosomal membrane adjustor (consisting of two muscle bands with 8 muscle fibres each) is situated more ventrally than the superior podosomal membrane adjustor (consisting of 2 muscle fibres) is. The *ima* inserts on the podosomal membrane via tendons, whilst the *sma* inserts directly. The prodorsal dorsoventral muscle (*pdv*) comprises three portions (Fig. 5; *pdv1*, *pdv2*, *pdv3*). *Pdv1* (two muscle fibres) and *pdv2* (one muscle fibre) originate on the exobothridial field and insert on the lateral margin of apodemes 1 and 2, respectively. *Pdv3* consists of only one muscle fibre; it originates ventrally on the manubrium and inserts on the sejugal apodeme.

Endosternal division of the prosoma (EDP)

The anterior and posterior dorsal endosternal muscles (*ade* and *pde*, respectively) each consists of at least two muscle fibres (Fig. 6B). Both muscles insert on the endosternum, but the *ade* originates on the tip of the manubrium, whilst the long, thin *pde* originates dorsolaterally on the notogaster at about its midlength. The subcapitulum endosternal retractor (*ser*) and the taenidiophore endosternal retractor (*ter*) both consist of two muscle fibres and have the endosternum as a common origin (Fig. 6A). The *ser* inserts on the mentum of the subcapitulum and the *ter* inserts on the tip of the taenidiophore (whether via a tendon or not was not determined).

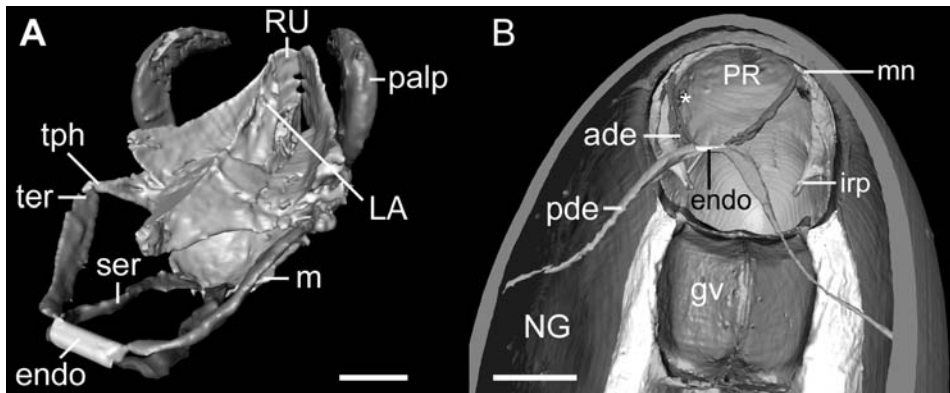


Fig. 6 *Phthiracarus longulus*, nearly encapsulated animal. EDP. Renderings of 3D-model of segmented synchrotron X-ray microtomography data. A: Subcapitulum (*ser*) and taenidiophore endosternal retractor (*ter*), dorsolateral view (scale bar: 50 μ m); B: Anterior (*ade*) and posterior dorsal endosternal muscle (*pde*), dorsal view of virtual frontal section (scale bar; 100 μ m); *ade*: anterior dorsal endosternal muscle; *av*: anal valve; *endo*: endosternum (in this form not visible in original data, but for reasons of clearness reconstructed this way); *gv*: genital valve; *irp*: inferior retractor process; *LA*: labrum; *m*: mentum of subcapitulum; *mem*: anogenital membrane; *NG*: notogaster; *palp*: palpus; *pde*: posterior dorsal endosternal muscle; *PR*: prodorsum; *RU*: rutellum; *ser*: subcapitulum endosternal retractor; *ter*: taenidiophore endosternal retractor; *tph*: taenidiophore. Asterisk (*) indicates the bothridium.

Longitudinal division of the prosoma (LDP)

The inferior prodorsal retractor (*ipr*) consists of about 20–25 muscle fibres (Fig. 7A). It originates dorsolaterally on the notogaster (at about the same level as the coxisternal retractor) and inserts via tendons on the inferior retractor process and the intercalary wall induration of the prodorsum. The prodorsum lateral adjustor (*pla*) comprises two muscle bands with two muscle fibres each (Fig. 7B). The origin is dorsal on the first quarter of the notogaster. The narrow insertion is via a tendon on the short manubrium. The subcapitular retractor (*scr*) also consists of two muscle bands with two muscle fibres (Fig. 7C).

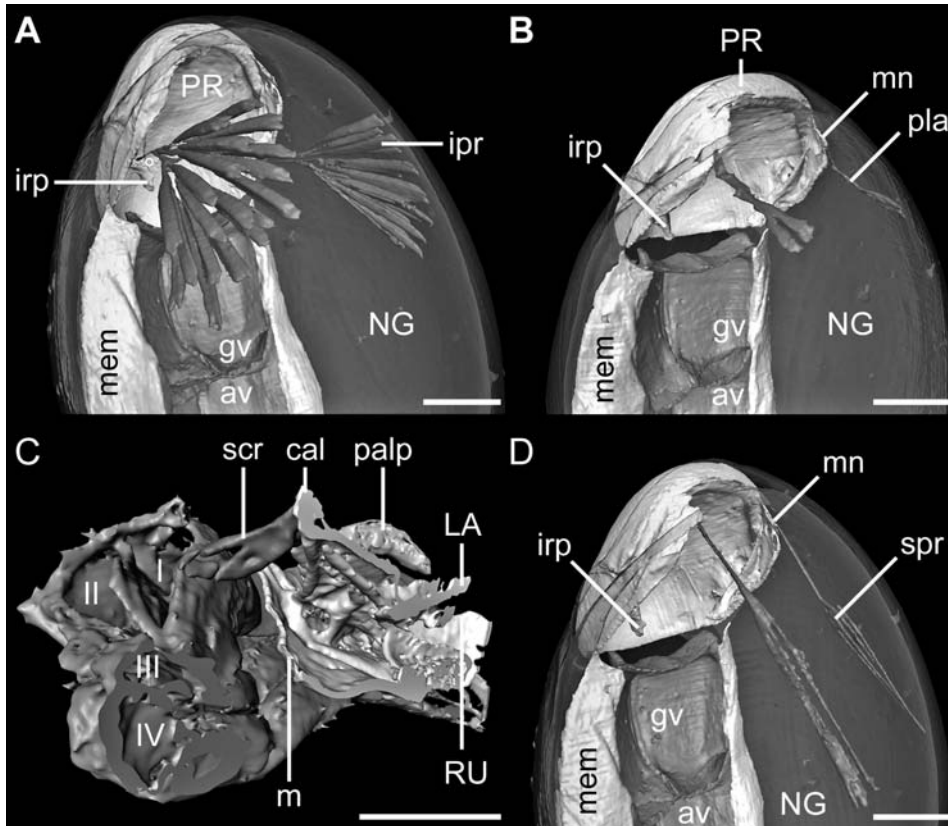


Fig. 7 *Phthiracarus longulus*, nearly encapsulated animal. LDP. Renderings of 3D-model of segmented synchrotron X-ray microtomography data. A: Dorsolateral view of anterior half with transparent notogaster, showing both sets of inferior prodorsal retractors (*ipr*, scale bar: 50 μ m); B: Same, showing prodorsum lateral adjustors (*pla*, scale bar: 50 μ m); C: Subcapitular retractor (*scr*), posterolateral view of virtual sagittal section of the reconstructed 3D-model of the legs and subcapitulum (scale bar: 100 μ m); D: Same as in A showing superior prodorsal retractors (*spr*, scale bar: 50 μ m). I–IV: walking legs 1–4; av: anal valve; cal: lemniscus of the capitular apodeme; gv: genital valve; ipr: inferior prodorsal retractor; irp: inferior retractor process; LA: labrum; m: mentum of subcapitulum; mem: anogenital membrane; mn: manubrium; NG: notogaster; palp: pedipalp; pla: prodorsum lateral adjustor; PR: prodorsum; RU: rutellum; spr: superior prodorsal retractor.

It originates on the first and second apodeme of the coxisternum and inserts directly on the anchoral process of the subcapitular apodeme. The superior prodorsal retractor (*spr*) originates as 2–4 muscle fibres dorsally on the notogaster at about half its length and inserts via a single tendon on the manubrium (Fig. 7D).

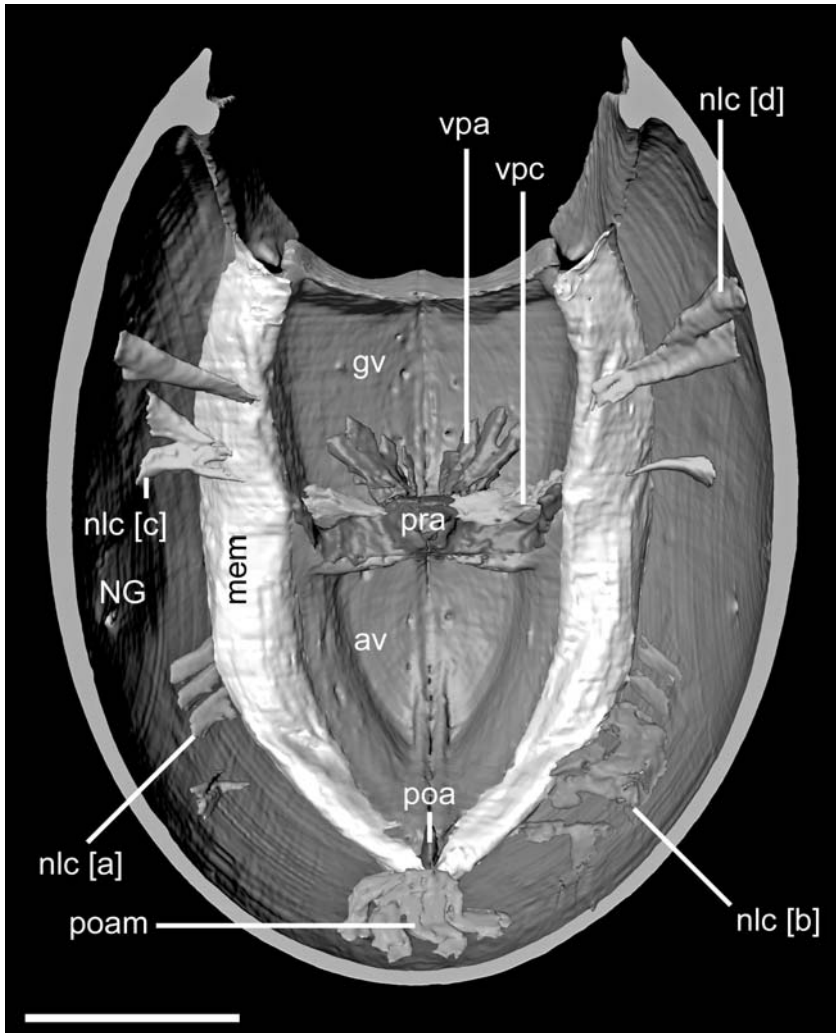


Fig. 8 *Phthiracarus longulus*, nearly encapsulated animal. OCS. Renderings of 3D-model of segmented synchrotron X-ray microtomography data, dorsal view of virtual frontal section (scale bar: 100 μm). av: anal valve; gv: genital valve; mem: anogenital membrane; NG: notogaster; nlc [a]: portion a of notogaster lateral compressor; nlc [b]: portion b of notogaster lateral compressor; poa: postanal apodeme; poam: postanal muscle; pra: preanal apodeme; vpa: ventral plate adductor; vpc: ventral plate compressor..

Opisthosomal compressor system (OCS)

The ventral plate adductor (*vpa*) and the ventral plate compressor (*vpc*) both originate on the preanal apodeme (Fig. 8). The ventral plate adductor runs diagonally towards its more anterior insertion on the genital valves and consists of at least 12 muscle fibres, probably subdivided into six muscle bands with two muscle fibres each. The ventral plate compressor is directed laterally and inserts entirely on the genital valves and consists of five muscle bands with an unknown number of muscle fibres. The notogaster lateral compressor (*nlc*) originates on the ventral curvature of the notogaster and inserts on the anogenital membrane; it is probably divided into four portions (compare discussion): portion a (three muscle bands with two muscle fibres each) and b (at least five muscle fibres) are restricted to the last third of the animal, at the level of the anal valves (Fig. 8; *nlc [a]*, *nlc [b]*). Portions c (two muscle bands) and d (two muscle bands with a total of about three muscle fibres) are located in the first half of the animal (Fig. 8; *nlc [c]*, *nlc [d]*).

Additional muscles

The cheliceral retractor (*chr*) originates on the exobothridial field and the sagittal apodeme (not shown). It inserts directly onto the posterior surface of the basal cheliceral segment. The trochanteral abductor (*tab*) originates on the endosternum and inserts on the inner surface of the leg trochanter (not shown). The cheliceral retractor and the trochanteral abductor have not been studied in detail because their role in the ptychoid mechanism is only indirect. The postanal muscle (*poam*; also known as the ‘holoventral levator’, Sanders & Norton 2004), originates terminally on the notogaster and inserts directly on the postanal apodeme; it consists of 10–15 muscle fibres (Fig. 8).

4. Discussion

A significant functional aspect of ptychoidy relates to how the animal accommodates large changes in internal volume and hemocoel pressure that must accompany the closing and opening of the body, and a related issue is how legs that attach to a coxisternum surrounded by extensive soft cuticle are sufficiently supported (Sanders & Norton 2004). Mites of the two superfamilies of Ptyctima – Phthiracaroida and Euphthiracaroida – have many similarities, but the external differences are significant and probably affect how haemocoel pressure is controlled, as well as other ptychoid functions. However, muscles systems have until now not been studied in detail for the Phthiracaroida. Below, we compare the morphological adaptations to ptychoidy between the Phthiracaroida (*Phthiracarus longulus*) and the Euphthiracaroida (*Euphthiracarus cooki*, Sanders & Norton, 2004; and *Rhysotritia ardua* Koch, 1841 and *Oribotritia banksi* Oudemans, 1916, Schmelzle et al. 2008, 2009) and also inside the Phthiracaroida (*Phthiracarus nitens* Nicolet, 1855, in: Wauthy 1984).

4.1 Comparison of exoskeleton

Prodorsum

The inner texture of the prodorsum of *Phthiracarus longulus* is uniform (Fig. 3B) as it is in *Euphthiracarus cooki* and *Rhysotritia ardua*, but it is rough-textured in *Oribotritia banksi*. The rostrrophragma is well differentiated in all four species. The manubrium of *P. longulus*

(Figs. 2B, 3A) and *O. banksi* is relatively shorter than the elongated manubrium of *E. cooki* and *R. ardua*. Also, in *P. longulus* it looks more delicate than in the euphthiracaroid species. The inferior retractor process of *P. longulus* (Figs. 2B, 3) is longer than in the euphthiracaroid species, but the angle at which it is directed is similar in all species. Except for *O. banksi* all species possess a sagittal apodeme (Fig. 3B, D). The bothridial scale covers the bothridium and base of the sensillus from above in all species except for *E. cooki*, although in *P. longulus* it is shifted slightly posterior (Figs 3A, 5). In the encapsulated state the very short sensillus of *P. longulus* lies in a ridge between the prodorsum and the notogaster (Fig. 1B), whereas it becomes pinched between prodorsum and notogaster in *O. banksi* and *R. ardua*; it stands free in *E. cooki* because its origin is dorsal to the bothridial scale. The internal system of chambers and short tracheae around the bothridium (not described here in detail) differs from that of euphthiracaroid mites but probably has a similar respiratory function (Figs 3C, D, 5; Grandjean 1967, Norton et al. 1997)

Opisthosomal venter

The opisthosomal venter of *Phthiracarus longulus*, and phthiracaroid mites in general, essentially differs from that of euphthiracaroid mites. Unlike the latter, there are no hardened plicature plates in phthiracaroid mites; instead in its place is the broad and pliable U-shaped anogenital membrane (Figs 2, 8). Unlike the rather simple, elongated ventral plates of euphthiracaroid mites, those of *P. longulus* are rather boat-shaped with a flat lateral margin (Figs 1A, 2, 8). In the encapsulated state the surrounding anogenital membrane is safely stored inside the notogaster (Figs 2, 8). The structure of the anterior and posterior anal lock of *P. longulus* (Fig. 1A, D) is similar to that of *Hoplophthiracarus* sp. (van der Hammen 1989), although both, right-fitting and left-fitting, locks have been found to be uniformly distributed in *P. longulus* (and also in: Wauthy 1984, about *Phthiracarus nitens*; Parry 1979, about the genus *Phthiracarus* Perty 1841). The state of right-fitting or left-fitting anterior locks thus is a matter of intraspecific variation and not, like van der Hammen (1989) stated, a specific character with taxonomical value.

Notogaster

The U-shaped ventral margin of the notogaster perfectly matches that of the ventral plates, ensuring a tight connection during ptychosis. The presence of a broad marginal tectum (Fig. 4B) covering the articulation ensures that no membrane (stored inside the notogaster) is exposed to possible attack by predators (Figs 1E, 2, 8). Except for some derived members of Synichotritiidae (e.g. Norton & Lions 1992), euphthiracaroid mites lack a marginal tectum along the ventral edge of the notogaster. The scale receptacle (Fig. 3D) present inside the tectonotal notch resembles those of *E. cooki* and *R. ardua*, but the problem of a pinched sensillus (in *R. ardua* and *O. banksi*) is solved in *P. longulus* by having a ridge along which the resting sensillus can lie during encapsulation (Figs 1B, 4A). *Oribotritia banksi* completely lacks a scale receptacle; instead, the bothridial scale rests on the tectonotal notch during encapsulation. Both *P. longulus* and *O. banksi* lack a terminal notogastral fissure (Fig. 1A), which is an adaptation present in *E. cooki* and *R. ardua*. This fissure probably allows slightly more flexing in the rather rigid cuticle during lateral compression events, which are not part of the ptychoid process in *P. longulus*. The tooth at the anteroventral corner of the notogastral

margin in *P. longulus* (Fig. 1C) is also present in *E. cooki*, but not in *O. banksi* or *R. ardua*. In contrast to *E. cooki* this tooth is prolonged internally as a ridge in *P. longulus* and forms an articulation for the ventral plates. The tectonotal notch separates the anterior notogastral tectum into two parts (pronotal and lateral anterior tecta) in euphthiracaroid species, but not in *P. longulus* (Fig. 1A, B).

Podosoma and subcapitulum

The principal morphology of muscular insertion points on these structures is similar among studied phthiracaroid and euphthiracaroid species.

4.2 Comparison of musculature

Dorsoventral muscles of the prosoma (DVP)

The coxisternal retractor of *P. longulus* consists of 20–30 fibres (Fig. 4A), which is an intermediate number between that of Oribotritiidae (*O. banksi* with 80 muscle fibres) and Euphthiracaridae (*R. ardua* with 17 muscle fibres, *E. cooki* with 12 muscle fibres). Since *P. longulus* (540 µm total length) is intermediate in size between *E. cooki* (300 µm) and *R. ardua* (900 µm), this contradicts the general correlation we suggested earlier (Schmelzle et al. 2009) that the number of *csr* muscle fibres increases with body size within the Ptyctima. The correlation still holds within the Euphthiracaroida, so perhaps there is a slight difference between these groups in the relationship of muscle fibres to body size; more data are needed for confirmation. The coxisternal protractor (*csp*) originates anteriorly to the superior membrane adjustor and inserts directly onto the lateral margin of the sejugal apodeme (Fig. 4B). In the encapsulated state its dorsoposteriorly directed course suggests a role as protractor for the coxisternum during reopening of the animal. We assume a change of its working direction when switching to the active state (when the legs and coxisternum are protracted). Then the *csp* should be directed anterioventrally and probably assumes a role as an auxiliary and adjusting retractor for the coxisternum. None of the studied euphthiracaroid mites show any evidence of this muscle (Schmelzle et al. 2008, 2009). The inferior membrane adjustors are quite similar among the species. Whilst *P. longulus* has two muscle bands with eight muscle fibres (Fig. 4B), *O. banksi* has two muscle bands with ten muscle fibres and *R. ardua* also has two muscle bands with nine muscle fibres (unknown for *E. cooki*). Regarding the superior membrane adjustors, *P. longulus* with two single muscle fibres (Fig. 4B) resembles *E. cooki* (3–4 muscle fibres), but differs strongly from *O. banksi* (nine muscle fibres) and *R. ardua* (two muscle bands with 1–3 fibres each). Regarding its origin and insertion there is no essential difference noticeable amongst these species. Portions 1 and 2 of the prodorsal dorsoventral muscle do not differ among *P. longulus* (Fig. 5), *O. banksi* and *R. ardua*, but the third portion (*pdv3*) of *P. longulus* (Fig. 5) shows only one muscle fibre, while the other species have two.

Endosternal division of the prosoma (EDP)

The numbers of muscle fibres in the 4 muscles of the EDP are the same in *P. longulus*, *O. banksi* and *R. ardua*. The only difference among the studied species is that the taenidiophore endosternal retractor of *E. cooki* has only one muscle fibre (two in other

species; Fig. 6A). The anterior dorsal endosternal muscle seems to be relatively longer in *P. longulus* (Fig. 6B) than in *O. banksi* and *R. ardua*; its insertion is more similar to *O. banksi* (a similar small area of insertion probably because of the relatively short manubrium) than to *R. ardua* (a large manubrium). The taenidiophore endosternal retractor seems to either insert directly or via a very short tendon ($< 1 \mu\text{m}$) on the taenidiophore in *P. longulus* (Fig. 6A), but via a prominent tendon in all of the studied euphthiracaroid mites.

Longitudinal division of the prosoma (LDP)

The number of muscle fibres (mf) of the inferior prodorsal retractors correlates roughly with body size: *E. cooki* (13 mf, 300 μm body length); *P. longulus* (20–25 mf, 540 μm body length; Fig. 7A); *R. ardua* (28–32 mf, 900 μm body length); *O. banksi* (90–100 mf, 1800 μm body length). In all species studied they insert via tendons onto both the inferior retractor process and the intercalary wall induration of the prodorsum. The prodorsum lateral adjustor of *P. longulus* (Fig. 7B) is similar to that of *O. banksi* regarding number of muscle bands (two), muscle fibres (two), and its insertion on the manubrium via tendons. The *pla* of *R. ardua* has two muscle bands with a maximum of five muscle fibres and inserts broadly and directly on the manubrium. The subcapitular retractor seems identical in *P. longulus* (Fig. 7C), *O. banksi* and *R. ardua*, originating on both apodemes 1 and 2; in contrast it originates only on apodeme 1 in *E. cooki*. The superior prodorsal retractor appears to insert onto the basal part of the manubrium via a tendon in *P. longulus* (Fig. 7D), *O. banksi* and *R. ardua*, but directly in *E. cooki*; it consists of 2–4, 4, 4 and 3 muscle fibres, respectively.

Opisthosomal compressor system (OCS)

Because of the great variation in the associated cuticular plates, the terminology of muscles in this system has varied. Herein we use a more generalised terminology, proposed previously (Schmelzle et al. 2009; cf. Tab. 2). The ventral plate adductor of *P. longulus* consists of at least twelve muscle fibres, probably subdivided into two muscle bands with six muscle fibres each; it originates on the preanal apodeme and runs anteriorly to insert on the genital valve (Fig. 8). Compared to the *vpa* of *E. cooki* and *R. ardua* (*O. banksi* lacks the *vpa*) the number of muscle fibres is noticeably smaller, but the area of insertion is more restricted (only the posterior half of the genital valve). The insertion of the ventral plate compressor of *P. longulus* (five muscle bands with an unknown number of muscle fibres) also is limited to the genital valve, probably due to the broad extension of the preanal apodeme (Fig. 8). In *E. cooki* (five muscle bands with an unknown number of muscle fibres), *O. banksi* (25 muscle fibres) and *R. ardua* (10–20 muscle fibres) the *vpc* inserts on both the genital and anal valves of the ventral plates. It appears, that Wauthy (1984) combined in his ‘anterior median muscles’ (*MMA*; in his figure 2B) our muscles *vpa* and *vpc*, but differentiated the tendons (*tam* and *tpm*, respectively; his figure 1C). However, in the text he wrote that the origin of the *MMA* is dorsally on the notogaster. We believe this to be a confusion with the ‘lateral rectal muscle’ of Heethoff & Norton (2009; *lrm*). The notogaster lateral compressor of *P. longulus* has a gap between an anterior and a posterior part (the anal region; Fig. 8), whereas in euphthiracaroid species it runs continuously along nearly the complete length of the ventral plates. Accordingly the number of muscle bands and fibres is very different. In *P. longulus* the *nlc* has probably four portions. Portion a (Fig. 8; *nlc [a]*) is clearly visible, whilst portion b is hard to detect. The reconstruction therefore could only be done for the right side of the animal.

Portion c and d of the *nlc* are difficult to distinguish from the genital papillae retractors (not shown), because they overlap with the *nlc* on nearly their whole length and their origin laterally on the notogaster and the direction they run to (median) are essentially the same. In contrast to Wauthy's research on *P. nitens* (1984) we found the genital papillae retractors (his *pga*, *pgm* and *pgp*) to originate laterally on the notogaster and not on the genital valves (cf. Fig. 2B of Wauthy 1984). Wauthy (1984) also described four portions of the *nlc* (his MF_1 , MF_2 , MF_3 , and MF_4). His MF_4 thereby corresponds to our portions a and b of the *nlc*, his MF_3 to our portion c and the MF_2 to portion d of the *nlc*. We believe his MF_1 to be our *ima*, which inserts on the podosomal membrane, close to but not on the anogenital membrane. It yet is not fully understood if portions c and d really are portions of the *nlc* (as in Wauthy 1984) with insertion on the anogenital membrane or if they are portions of the genital papillae retractor (which would mean that Wauthy 1984 was wrong). Unfortunately, the spatial resolution of our data meets its limit in this case.

This makes it difficult to compare the results with the studied euphthiracaroid mites. In *P. longulus* the *nlc* has at least three muscle bands with two muscle fibres each (portion a) and a separate second portion (b) with about five muscle fibres. Also there are two additional portions (c, d) with two muscle bands with an unknown number of muscle fibres and two muscle bands with a total of about three muscle fibres, respectively. In contrast, in *E. cooki* the *nlc* has 21 muscle bands with an unknown number of muscle fibres, in *O. banksi* it has 30–34 muscle bands with 2–6 muscle fibres and in *R. ardua* it has 25 muscle bands with 3–6 muscle fibres. In the euphthiracaroid species the notogaster lateral compressor originates ventrally on the notogaster and inserts on the medial edge of the ventral plates, whilst in *P. longulus* it originates laterally on the notogaster and inserts on the anogenital membrane.

Additional muscles

The cheliceral retractor originates on both the exobothridial field and the sagittal apodeme of the prodorsum of *P. longulus*. The same is true of *R. ardua* and *E. cooki*, but in *O. banksi* there is no sagittal apodeme. The trochanteral abductor of *P. longulus* is well developed and appears to be in a single frontal plane, unlike in the euphthiracaroid species studied. The postanal muscle seems similar in all species. It consists of 10–15 muscle fibres in *P. longulus* (Fig. 8), eight muscle bands with 4–5 fibres each in *O. banksi*, and two muscle bands with 10–20 fibres each in *R. ardua*. Only in *O. banksi* it inserts through tendons onto the postanal apodeme. Our *poam* probably corresponds with the 'posterior median muscles' of Wauthy (1984; *MMP*). The number of muscle fibres drawn in his Fig. 2B (four muscle fibres) for *Phthiracarus nitens* appears in comparison to our findings in *P. longulus* to be very low.

5. Conclusions

In this study we have shown that phthiracaroid and euphthiracaroid mites clearly differ in a number of characters that relate to functional aspects of ptychoidy. The most prominent differences are in the morphology of the ventral plates, the presence or absence of plicature plates and a posterior notogastral tectum, the number of muscle bands and fibres (e.g. the postanal muscle), the origin/insertion of the notogaster lateral compressor and the newly discovered coxisternal protractor muscle. However, the location of the taeniophore and its connection to the subcapitulum as well as the shape of the capitular apodeme support the common origin of both groups.

While the morphological differences are clear, their functional importance remains to be elucidated in the future.

6. Acknowledgements

We thank Wojciech Niedbała for helpful information. We thank Karl-Heinz Hellmer for the critical-point drying and taking the SEM micrographs. We thank Paavo Bergmann, Michael Laumann and Peter Cloetens for their help with experiment SC-2127 at the ESRF in Grenoble and the European Synchrotron Radiation Facility for the allocated beam time.

7. References

- Akimov, I. A. & A. V. Yastrebtsov (1991): Skeletal-Muscular System of Oribatid Mites (Acariformes: Oribatida). – *Zoologische Jahrbücher für Anatomie und Ontogenie der Tiere* **121**: 359–379.
- Alberti, G., R. A. Norton & J. Kasbohm (2001): Fine structure and mineralisation of cuticle in Euarthropoda and Lohmannioidea (Acari: Oribatida). – In: Halliday, R. B., D. E. Walter, H. C. Proctor, R. A. Norton & M. J. Colloff (eds): *Acarology: Proceedings of the 10th International Congress*. – CSIRO Publishing, Melbourne: 230–241.
- Balogh, J. & P. Balogh (1992): The oribatid mites genera of the world, Vol. 1. – Hungarian National Museum Press, Budapest: 263 pp.
- Betz, O., U. Wegst, D. Weide, M. Heethoff, L. Helfen, W. K. Lee & P. Cloetens (2007): Imaging applications of synchrotron x-ray micro-tomography in biological morphology and biomaterial science. I. General aspects of the technique and its advantages in the analysis of arthropod structure. – *Journal of Microscopy* **22**: 51–71.
- Grandjean, F. (1934): Observations sur les Oribates (6e série). – *Bulletin du Muséum national d'Histoire naturelle* **6**: 353–360.
- Grandjean, F. (1954): Essai de classification des Oribates. – *Bulletin de la Société Zoologique de France* **78**: 421–446.
- Grandjean, F. (1967): Nouvelles observations sur les Oribates (5e série). – *Acarologia* **9**: 242–272.
- Grandjean, F. (1969): Considérations sur le classement des Oribates leur division en 6 groupes majeurs. – *Acarologia* **11**: 127–153.
- Hammen, L. van der (1989): *Glossary of Acarological Terminology*. – SPB Academic Publishing by Publishers, The Hague: 576 pp.
- Heethoff, M. & R. A. Norton (2009): Role of musculature during defecation in a particle-feeding arachnid, *Archezogetes longisetosus* (Acari, Oribatida). – *Journal of Morphology* **270**: 1–13.
- Heethoff, M., M. Laumann & P. Bergmann (2007): Adding to the reproductive biology of the parthenogenetic oribatid mite *Archezogetes longisetosus* (Acari, Oribatida, Trhypochthoniidae). – *Turkish Journal of Zoology* **31**: 151–159.
- Heethoff, M., L. Helfen & P. Cloetens (2008): Non-invasive 3D-visualization of the internal organization of microarthropods using synchrotron X-ray-tomography with sub-micron resolution. – *JOVE* **15**: doi:10.3791/737
- Hoebel-Mävers, M. (1967): Funktionsanatomische Untersuchungen am Verdauungstrakt der Hornmilben (Oribatei). – Dissertation, Universität Braunschweig: 45 pp.
- Märkel, K. (1964): Die Euphthiracaridae Jacot, 1930, und ihre Gattungen (Acari: Oribatei). – *Zoologische Verhandelingen, Leiden* **67**: 4–78.
- Niedbała, W. (2008): Ptyctimous Mites (Acari: Oribatida) of Poland. – *Fauna Poloniae, Polish Academy of Sciences, Warszawa*: 242 pp.

- Norton, R. A. (1984): Monophyletic groups in the Enarthronota (Sarcoptiformes). – In: Griffiths, D. A. & C. E. Bowman (eds): *Acarology VI*, vol. I. – Ellis Horwood, Chichester: 233–240.
- Norton, R. A. (1994): Evolutionary aspects of oribatid mite life histories and consequences for the origin of the Astigmata. – In: Houck, M. (ed): *Mites. Ecological and evolutionary analyses of life-history patterns*. – Chapman and Hall, New York: 99–135.
- Norton, R. A. (2001): Systematic relationships of Nothrolahmanniidae, and the evolutionary plasticity of body form in Enarthronota (Acari: Oribatida). – In: Halliday, R. B., D. E. Walter, H. C. Proctor, R. A. Norton & M. J. Colloff (eds): *Acarology: Proceedings of the 10th International Congress*. – CSIRO Publishing, Melbourne: 58–75.
- Norton, R. A. & V. Behan-Pelletier (1991): Calcium carbonate and calcium oxalate as cuticular hardening agents in oribatid mites (Acari: Oribatida). – *Canadian Journal of Zoology* **69**: 1504–1511.
- Norton R. A. & J. C. Lions (1992): North American Synichotritiidae (Acari: Oribatida) 1. *Apotritia walkeri* n. g., n. sp., from California. – *Acarologia* **33**: 285–301.
- Rasputnig, G. (2006): Chemical alarm and defence in the oribatid mite *Collohmanna gigantea* (Acari: Oribatida). – *Experimental and Applied Acarology* **39**: 177–194.
- Sanders, F. H. & R. A. Norton (2004): Anatomy and function of the ptychoid defensive mechanism in the mite *Euphthiracarus cooki* (Acari: Oribatida). – *Journal of Morphology* **259**: 119–154.
- Saporito, R. A., M. A. Donnelly, R. A. Norton, H. M. Garraffo, T. F. Spande & J. W. Daly (2007): Oribatid mites as a major dietary source for alkaloids in poison frogs. – *Proceedings of the National Academy of Sciences* **104**: 8885–8890.
- Schmelzle, S., L. Helfen, R. A. Norton & M. Heethoff (2008): The ptychoid defensive mechanism in Euphthiracaroida (Acari: Oribatida): A comparison of exoskeletal elements. – *Soil Organisms* **80** (2): 227–241.
- Schmelzle, S., L. Helfen, R. A. Norton & M. Heethoff (2009): The ptychoid defensive mechanism in Euphthiracaroida (Acari: Oribatida): A comparison of muscular elements with functional considerations. – *Arthropod Structure and Development* **38** (6): 461–472, doi:10.1016/j.asd.2009.07.001
- Shimano, S., T. Sakata, Y. Mizutani, Y. Kuwahara & J. I. Aoki (2002): Geranial: The alarm pheromone in the nymphal stage of the oribatid mite, *Nothrus palustris*. – *Journal of Chemical Ecology* **28**: 1831–1837.
- Walker, N. A. (1965): Euphthiracaridae of California Sequoia litter, with a reclassification of the families and genera of the world. – *Fort Hayes Studies, Science Series No 3*, 1–155.
- Wauthy, G. (1984): Observations on the ano-genital region of adult *Phthiracarus nitens* (Oribatida: Mixonomata). – In: Griffiths, D. A. & C. E. Bowman (eds): *Acarology VI*. – Horwood, Chichester, Vol. 1: 268–275.
- Wauthy, G., M. Leponce, N. Banaï, G. Sylin & J. C. Lions (1998): The backward jump of a box moss mite. – *Proceedings of the Royal Society – Biological Sciences* **265**: 2235–2242.
- Yastrebtsov, A. V. (1991): Peculiarities of the muscular system and skeletal parts of the oribatid mite *Oribotritia* sp. (Oribatida, Ptyctima). – *Revue d'Entomologie de l'URSS*. **70**: 495–499 (in Russian).

Publication 4

**A morphological comparison of two closely related ptychoid oribatid mite species:
Phthiracarus longulus and *P. globosus* (Acari: Oribatida: Phthiracaroidea).**

Schmelzle, S., Norton, R.A., Heethoff, M.

Published in Soil Organisms 84 (2), pp. 431–443.

Submitted	Accepted	Published
2 February 2012	26 March 2012	2012

Authors' contribution:

- Schmelzle, Sebastian: Specimen collection and fixation, specimen preparation, data acquisition, data processing, data analysis, image processing, manuscript writing and preparation
- Norton, Roy A.: Specimen collection and fixation, general support and discussion, revision of manuscript
- Heethoff, Michael: Supervision, data acquisition, general support and discussion, revision of manuscript

Methods used:

- Synchrotron X-ray microtomography (SR μ CT)
- Scanning Electron Microscopy (SEM)

A morphological comparison of two closely related ptychoid oribatid mite species: *Phthiracarus longulus* and *P. globosus* (Acari: Oribatida: Phthiracaroidea)

Sebastian Schmelzle^{1*}, Roy A. Norton² and Michael Heethoff¹

¹ Universität Tübingen, Institut für Evolution und Ökologie, Abteilung Evolutionsbiologie der Invertebraten, Auf der Morgenstelle 28E, 72076 Tübingen, Germany

² State University of New York, College of Environmental Science and Forestry, 1 Forestry Drive, Syracuse NY 13210, USA

* Corresponding author: Sebastian Schmelzle (e-mail: schmelzle@oribatida.com)

Abstract

We studied exoskeletal and muscular adaptations to ptychoidity in the oribatid mite *Phthiracarus globosus* (Phthiracaridae, Phthiracaroidea) using synchrotron X-ray microtomography, and compared the results to *Phthiracarus longulus*, a closely related mite that we investigated earlier. As expected, both species show high similarity in most of the characters investigated, but there were also clear differences: the sensillus groove is more prominent and the bothridial scale is more angular in *P. globosus* than in *P. longulus*. The coxisternal retractor first found in *P. longulus* was also found in *P. globosus* and therefore could be a synapomorphy for the genus. The number of muscle fibres of the anterior dorsal endosternal muscle (ade), inferior prodorsal retractor (ipr), ventral plate adductor (vpa) and the notogaster lateral compressor (nlc) found in *P. globosus* is double or even triple that found in *P. longulus*. Our results suggest that muscle morphology might provide a phylogenetically informative set of characters for oribatid mite systematics, when more data are available.

Keywords: Synchrotron X-ray microtomography, SR- μ CT, Ptychoidity, Phthiracaridae, Box mite, Predator defence

1. Introduction

Ptychoidity is the most complex morphological defensive mechanism in oribatid mites. It enables the mite to retract its legs and coxisternum into the idiosoma and encapsulate itself by deflecting the prodorsum ventrad as a seal (Sanders & Norton 2004). Ptychoidity appears to have independently evolved in three groups of the Oribatida: the Mesoplophoridae, Protoplophoridae and Ptyctima (Euptyctima in Weigmann 2006). All species of Ptyctima, consisting of the two superfamilies Phthiracaroidea and Euphthiracaroidea, are ptychoid as adults. The functional details of ptychoidity are best known for Euphthiracaroidea, with three species having been studied: *Euphthiracarus cooki* (Euphthiracaridae; Sanders & Norton 2004), *Rhysotritia ardua*, (Euphthiracaridae; Schmelzle et al. 2008, 2009) and *Oribotritia*

banksi (Oribotritiidae; Schmelzle et al. 2008, 2009). Similar information is available for only a single species of Phthiracaroida: *Phthiracarus longulus* (C. L. Koch, 1841; Phthiracaridae; Schmelzle et al. 2010). These studies have shown clear differences between Euphthiracaroida and Phthiracaroida, such as a different organization of the ventral plates and their associated musculature (Schmelzle et al. 2010), and also noticeable differences within Euphthiracaroida, which can be found in the fusion of the ventral plates and qualitative and quantitative muscle morphology (Euphthiracaridae and Oribotritiidae; Schmelzle et al. 2008, 2009). These findings suggest that muscle morphology might provide phylogenetically informative data for the Ptyctima, but closely related species must be investigated to determine the generality of similarities and homologies at a phylogenetically small scale. Hence, we investigated a second species of Phthiracaridae, *P. globosus* (C. L. Koch, 1841). We used synchrotron X-ray microtomography to show that the two closely related species are characterised by clear differences concerning exoskeletal and muscular characters that relate to ptychoidy.

2. Materials and Methods

Specimens: *Phthiracarus globosus* (synonyms: *P. globus* Parry, 1979; *P. gl.* Kamill, 1981; *Hoplophora globosa* Koch, 1841) is a Holarctic species of the family Phthiracaridae that is common and abundant in temperate forest litter (Niedbala 2002, Weigmann 2006). Adults for our studies (mean total length of 495 μm , $n = 3$, $sd = 12.1$) were collected from accumulated decaying needles and cone scales of introduced Norway spruce (*Picea abies*) in LaFayette, Onondaga Co., NY, USA.

Sample preparation: Specimens were killed and fixed in 1% glutaraldehyde for 60 h and stored in 70% ethanol. For the final preparation, specimens were dehydrated in an increasing ethanol series with steps of 70, 80, 90, 95 and 100%, with three changes at each step and 10 min between changes. After storage in fresh 100% ethanol they were critical-point dried in CO_2 (CPD 020, Balzers).

Scanning electron microscopy: Critical-point dried specimens were either glued onto a T-section-like metal foil or directly onto a stub and then sputter-coated with a 20 nm thick layer of gold or a gold-palladium mixture, respectively. Micrographs were taken on a Zeiss Evo LS10 scanning electron microscope at 10 keV and a Cambridge Stereoscan 250 Mk2 scanning electron microscope at 20 keV.

Synchrotron X-ray microtomography: Critical-point dried animals were fixed by the notogaster to the tip of a plastic pin (1.2 cm long; 3.0 mm diameter) using instant adhesive. Radiographs were taken at the European Synchrotron Radiation Facility (ESRF) in Grenoble at beamline ID19 with a beam energy of 20.5 keV and at a sample–detector distance of 20 mm. A cooled 14-bit CCD-camera with a resolution of 2048 x 2048 pixels and an effective pixel size of 0.7 μm per pixel was used (a detailed description of the method is given in Betz et al. 2007, Heethoff & Cloetens 2008, Heethoff et al. 2008). The data were visualized with the programs VGStudio MAX 1.2.1 (Volume Graphics, Heidelberg, Germany) and three-dimensional modeling of cuticular elements was conducted with amira™ 4.0.1 (Mercury Computer Systems Inc., Chelmsford, MA). Muscle fibres were counted using the original phase contrast microtomography data. Different portions of muscles are called muscle bands and subdivisions of muscle bands are called muscle fibres (Sanders & Norton 2004).

Tab. 1 Abbreviations, origin and insertion of the muscular elements associated with ptychoidy in *Phthiracarus globosus* and *P. longulus*.

Muscle	Abbr.	Origin	Insertion
Dorsoventral muscles of the prosoma			
coxisternal protractor	csp	notogaster, lateral	sejugal apodeme
coxisternal retractor	csr	notogaster, dorsal	apodeme 2 of the epimeres, apodemal shelves 3 and 4
inferior podosomal membrane adjustor	ima	anterior half of notogaster, ventrolateral	podosomal membrane
prodorsal dorsoventral muscle 1	pdv1	exobothridial field	lateral margin of apodemes 1
prodorsal dorsoventral muscle 2	pdv2	exobothridial field	lateral margin of apodemes 2
prodorsal dorsoventral muscle 3	pdv3	manubrial sclerite	sejugal apodeme
superior podosomal membrane adjustor	sma	notogaster, lateral	podosomal membrane
Endosternal division of the prosoma			
anterior dorsal endosternal muscle	ade	manubrial sclerite	endosternum
posterior dorsal endosternal muscle	pde	notogaster, dorsolateral	endosternum
subcapitulum endosternal retractor	ser	endosternum	mentum of subcapitulum
taenidiophore endosternal retractor	ter	endosternum	taenidiophore
Longitudinal division of the prosoma			
inferior prodorsal retractor	ipr	notogaster, dorsolateral	inferior retractor process, intercalary wall induration
prodorsum lateral adjustor	pla	notogaster, dorsolateral	manubrial sclerite
subcapitular retractor	scr	apodeme 1, 2 of the epimeres 1	anchoral process of subcapitular apodeme
superior prodorsal retractor	spr	notogaster, dorsal	basis of manubrial sclerite
Opisthosomal compressor system			
notogaster lateral compressor	nlc	notogaster, ventral curvature	anogenital membrane
ventral plate adductor	vpa	preanal apodeme	genital valve
ventral plate compressor	vpc	preanal apodeme	lateral edge of genital valve
Additional muscles			
postanal muscle	poam	terminal at posterior end of notogaster	postanal apodeme

3. Results and Discussion

Exoskeletal elements: *Phthiracarus globosus* is more spherical than *P. longulus*. This affects the notogaster, the prodorsum and the ventral plates, which are all broader and shorter than those of *P. longulus* (Figs 1–3). The interior and outer surfaces of the prodorsum of both species are homogeneously textured (Fig. 1). The sagittal apodeme is more prominent in *P. longulus* than in *P. globosus* (Figs 2b; 3b, c). The bothridial scale, covering the bothridium (Fig. 3a) is more rounded in *P. longulus* than in *P. globosus*. Phthiracarid mites do not possess a true manubrium like that of Euphthiracaroida, i. e. an elongated posteroventral apodemal process of the prodorsum serving as an attachment structure for the origin and insertion of prodorsal retractors and adjustors (Sanders & Norton 2004, Schmelzle et al. 2008, 2009), despite our previous statement to that effect (Schmelzle et al. 2010). Instead, in both *Phthiracarus* species a manubrium-like sclerotized field lies within the articulating membrane adjacent to the posteroventral corner of the prodorsum (Fig. 3a, c, e) acting as functional manubrium: for this we use the term ‘manubrial sclerite’ (ms). The notogaster of *P. globosus* is more spherical and its cuticle is thicker (12–18 μm ; Fig. 3d) than that of *P. longulus* (8–14 μm). Its anterior margin is separated into the lateral anterior tectum and the pronotal tectum by the tectonotal notch (Fig. 1a, b). Both allow for a tight connection of prodorsum and notogaster. The tectonotal notch exhibits a prominent sensillus groove (Fig. 3d) offering the sensillus (Fig. 1a, b) a place to rest and a scale receptacle (Fig. 3d) harbouring the bothridial scale whilst the animal is encapsulated. The sensillus groove is more pronounced in *P. globosus* than in *P. longulus*. This leads to a more defined position and less squeezing of the sensillus (Figs 1b, 3f) during encapsulation. At the ventral margin of the notogaster a medial ridge-like indentation is present (Fig. 1c) and also more pronounced in *P. globosus* than in *P. longulus*. This allows for a tight connection of ventral plates and notogaster in which the indentation (Fig. 1c) and the notch between the anal valves act according to the lock-and-key principle.

Thus, both phthiracarid species share the organisation of the ventral plates into distinct anal and genital valves, and also the manubrial sclerite. In these, they differ from most Euphthiracaroida, which have a ‘true’ manubrium (a solid, cuticular process of the prodorsum) and elongated, bomb-bay like ventral plates, which may be fused in a variety of ways (Sanders & Norton 2004, Schmelzle et al. 2008). Of the exoskeletal elements that relate to ptychoidy, the two phthiracarid species differ in the shape of the bothridial scale, the size of the sagittal apodeme and the depth of the sensillus groove.

Muscular elements: In the following sections muscles will be addressed by their abbreviations only (cf. Tab. 1). The csp (dorsoventral muscles of the prosoma; Fig. 4b), originating laterally on the notogaster and inserting on the sejugal apodeme of the epimeres, can be found in both phthiracarid species but is not known in Euphthiracaroida. The csp therefore might be a synapomorphic character for the genus *Phthiracarus* or even the Phthiracaroida. Within the endosternal division of the prosoma the ade is the only muscle showing a noticeable difference between species: that of *P. longulus* consists of 2 muscle fibers while that of *P. globosus* consists of 5–6 muscle fibers (Fig. 5a). It originates at the endosternum and inserts on the manubrial sclerite in both species. The ipr originates dorsolaterally on the notogaster and inserts on the inferior retractor process and the intercalary wall induration of the prodorsum of both species, but the ipr of *P. globosus* (Fig. 6a) consists of almost twice the amount of muscle fibers seen in *P. longulus* (35–40 and 20–25 muscle fibers, respectively). The same is true for the spr: it consists of 4 muscle bands with 2 muscle fibers each in *P. globosus*

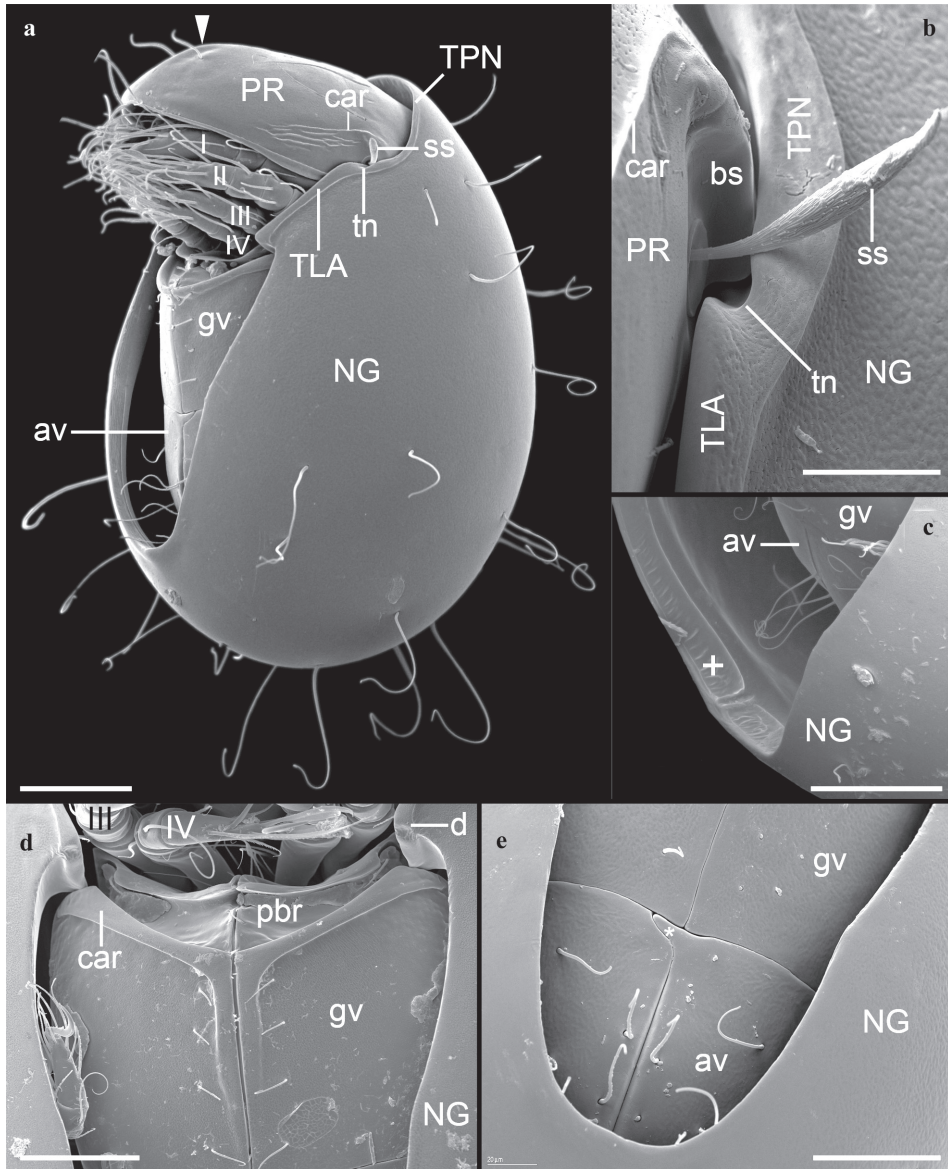


Fig. 1 *Phthiracarus globosus*. Scanning electron micrographs. **a**: Lateroventral overview of half encapsulated specimen (the withdrawn position of the ventral plates and the curled ends of notogastral setae are considered fixation artefacts; scale bar: 100 μ m). **b**: Detail of the bothridial scale, the sensillus and the lateral anterior tectum (scale bar: 25 μ m). **c**: Detail of the simple U-shaped ventral margin of the notogaster (scale bar: 100 μ m). **d**: Detail of the articulation of the ventral plates and notogaster, the phragmatal bridge and ventral tooth (scale bar: 100 μ m). **e**: Detail of the anterior anal lock (scale bar: 50 μ m). Asterisk indicates the anterior lock of the anal plates, plus-symbol indicates the U-shaped plain lateral margin of the notogaster with a medial ridge-like indentation, arrowhead indicates the prodorsal ledge. (For abbreviations see in legend of Fig. 2).

(Fig. 6d) in comparison to 2–4 muscle fibers in *P. longulus*, even though both species are similar in size (495 μm and 540 μm , respectively). In both species, the spr originates dorsally on the notogaster and inserts on the basis of the manubrial sclerite. The nlc of *P. globosus* consists of 15–18 muscle bands with 1 or 2 muscle fibers each (Fig. 7a), whereas that of *P. longulus* consists of 3 muscle bands with 2 muscle fibers each and an additional portion of at least 5 muscle fibers. The nlc originates laterally on the notogaster and its insertion is restricted to the last third of the anogenital membrane (Fig. 7a). This corrects our previous statement about this muscle; portions ‘nlc [c]’ and ‘nlc [d]’ of Schmelzle et al. (2010) are in fact the retractors of the genital papillae (gpr), as already suspected by the authors. The vpa of *P. globosus* (Fig. 7b, c) has nearly twice the number of muscle fibers than that of *P. longulus* (10 muscle bands with 2–3 muscle fibers each and at least 12 muscle fibers, respectively; Fig. 7b, c), but in both species it originates on the preanal apodeme and inserts on the genital valve. The poam (originating terminally on the posterior end of the notogaster and inserting on the postanal apodeme) consists of 4–6 muscle bands with about 3–4 muscle fibers in *P. globosus* (Fig. 7d), compared to probably 4 muscle bands with a total of 10–15 muscle fibers in *P. longulus* (in contrast to Schmelzle et al. 2010), but the borders between the muscle bands seem to be less clear than in *P. globosus*.

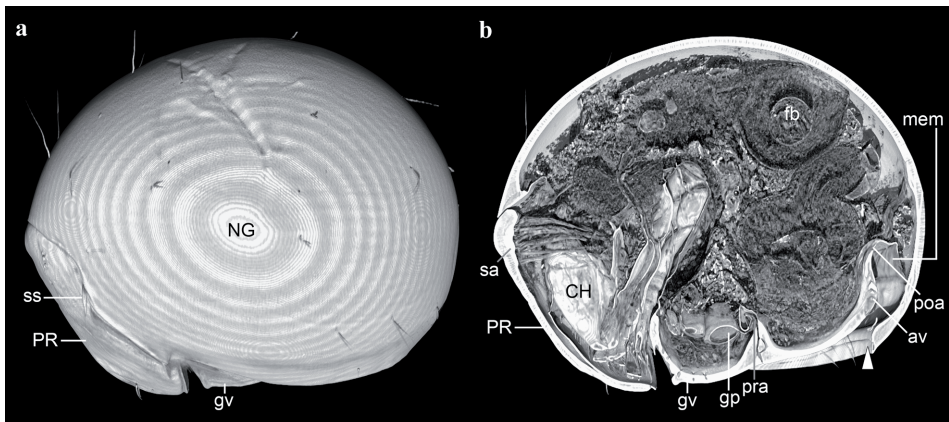


Fig. 2 *Phthiracarus globosus*, nearly encapsulated animal, lateral view. **a**: Overview of the animal (rendition of synchrotron X-ray microtomography data). **b**: Overview of a virtual sagittal section of a volume rendering of synchrotron X-ray microtomography data. Symbols: arrowhead indicates the U-shaped plain lateral margin of the notogaster.

Abbreviations: I–IV - walking legs 1–4, av - anal valve, bs - bothridial scale, car - carina, Ch - chelicera, csp - coxisternal protractor, csr - coxisternal retractor, d - ventral tooth of lateral anterior tectum, endo - endosternum, fb - food bolus, gp - genital papilla, gv - genital valve, ima - inferior membrane adjustor, irp - inferior retractor process, m - mentum of subcapitulum, mem - anogenital membrane, ms - manubrial sclerite, NG - notogaster, pbr - phragmatal bridge, pde - posterior dorsal endosternal muscle, ph - pharynx, PR - prodorsum, pra - preanal apodeme, poa - postanal apodeme, rl - rostral limb, RU - rutellum, sma - superior membrane adjustor, sa - sagittal apodeme, ser - subcapitulum endosternal retractor, sg - sensillus groove, sr - scale receptacle, ss - sensillus, ter - taenidiophore endosternal retractor, TLA - lateral anterior tectum, tn - tectonotal notch, tph - taenidiophore, TPN - pronotal tectum.

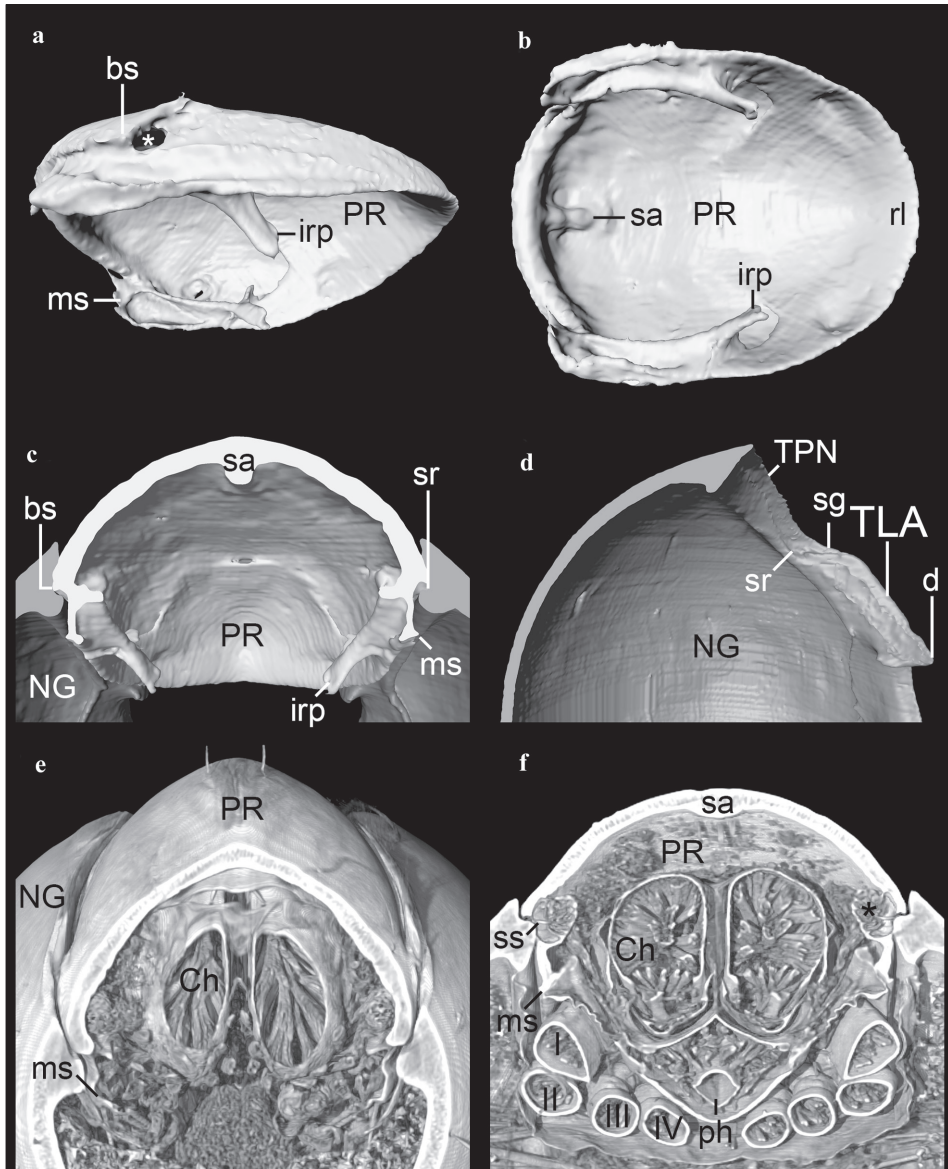
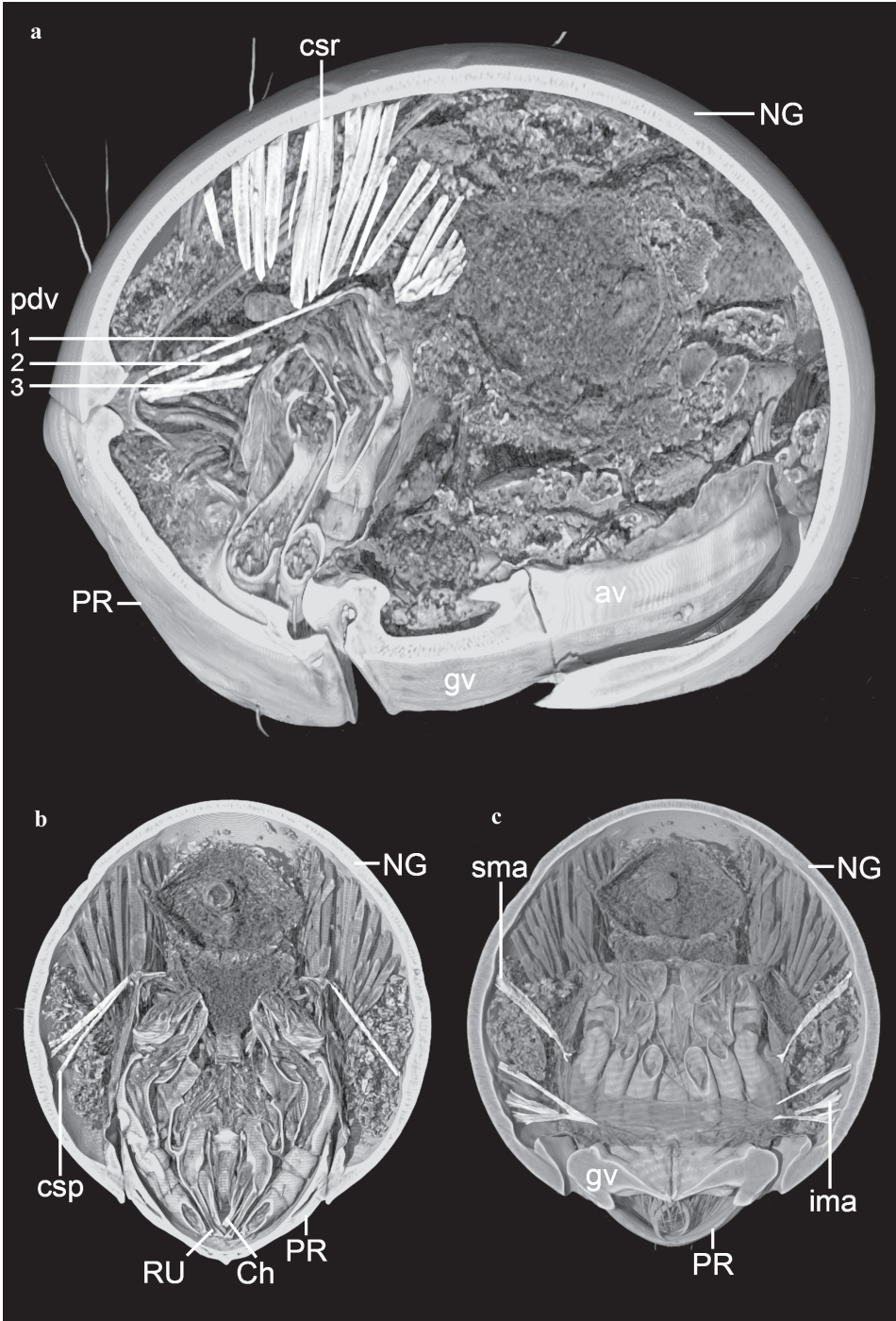


Fig. 3 *Phthiracarus globosus*, nearly encapsulated animal. Renderings of 3D-model (a–d) and volume rendering (e, f) of synchrotron X-ray microtomography data; c–f showing a dorsal view. **a:** Lateroventral view of the prodorsum. **b:** Ventral view of the prodorsum. **c:** Virtual frontal section in the region of the bothridial scale and its scale receptacle. **d:** Lateral view of virtual sagittal section showing the tectonotal notch with its scale receptacle and the sensillus groove. **e:** Virtual frontal section in the region of the manubrial sclerite. **f:** Virtual frontal section in the region of the opening of the bothridium. Asterisk in A and F indicates the location of the bothridium. (For abbreviations see in legend of Fig. 2)



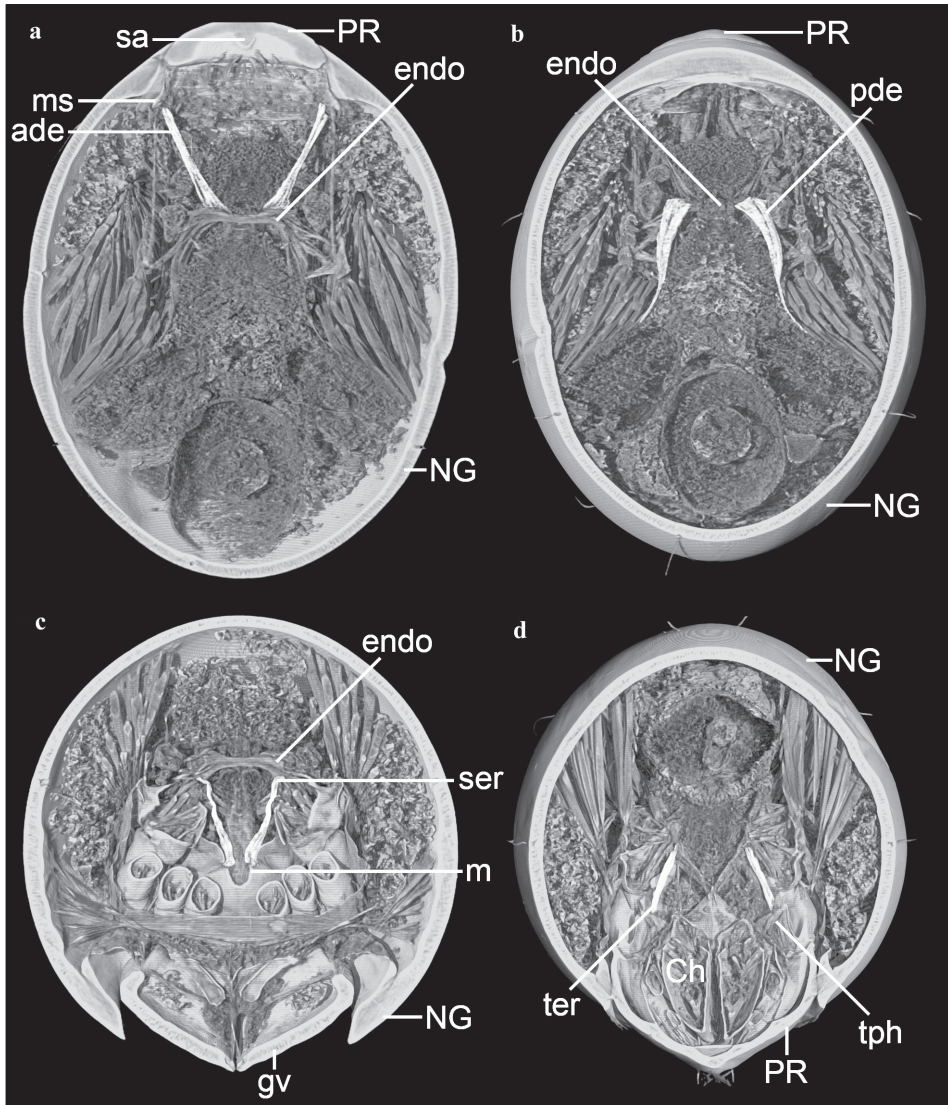


Fig. 5 *Phthiracarus globosus*, nearly encapsulated animal. Endosternal division of the prosoma. Volume renderings of synchrotron X-ray microtomography data. **a**: Dorsal view of virtual frontal section showing the anterior dorsal endosternal muscle (ade). **b**: Dorsal view of virtual frontal section showing the posterior dorsal endosternal muscle (pde). **c**: Virtual cross section showing the subcapitulum endosternal retractors (ser), posterior view. **d**: Virtual cross section showing the taeniophore endosternal retractors (ter), posterior view.

Fig. 4 (page 438) *Phthiracarus globosus*, nearly encapsulated animal. Dorsoventral muscles of the prosoma. Volume renderings of synchrotron X-ray microtomography data. **a**: Virtual sagittal section showing the coxisternal retractor (csr) and the prodorsal dorsoventral muscles 1–3 (pdv1–3) from lateral. **b**: Virtual cross section showing the coxisternal protractor (csp), posterior view. **c**: Virtual cross section showing the inferior (ima) and superior (sma) membrane adjustor, posterior view. (For all abbreviations see in legend of Fig. 2)

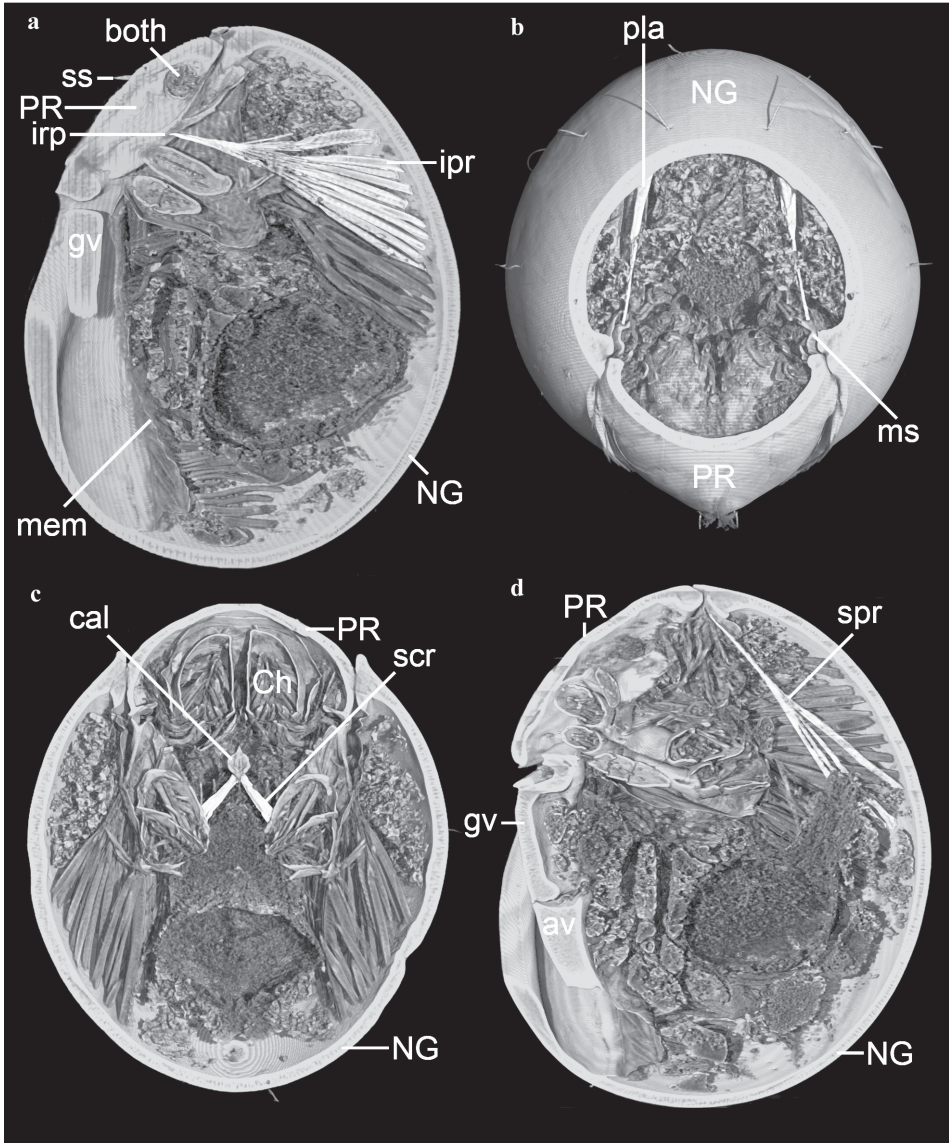


Fig. 6 *Phthiracarus globosus*, nearly encapsulated animal. Longitudinal division of the prosoma. Volume renderings of synchrotron X-ray microtomography data. **a**: Virtual sagittal section showing the inferior prodorsal retractors (ipr), lateral view. **b**: Anterior view of virtual cross section showing the prodorsum lateral adjustors (pla). **c**: Anterior view of virtual cross section showing the subcapitular retractor (scr). **d**: Virtual sagittal section showing the superior prodorsal retractors (spr), lateral view.

Abbr.: av - anal valve, both - bothridium, cal - lemniscus of the capitular apodeme, Ch - chelicera, gv - genital valve, ipr - inferior prodorsal retractor, irp - inferior retractor process, mem - anogenital membrane, ms - manubrial sclerite, NG - notogaster, pla - prodorsum lateral adjustor, PR - prodorsum, spr - superior prodorsal retractor, ss - sensillus.

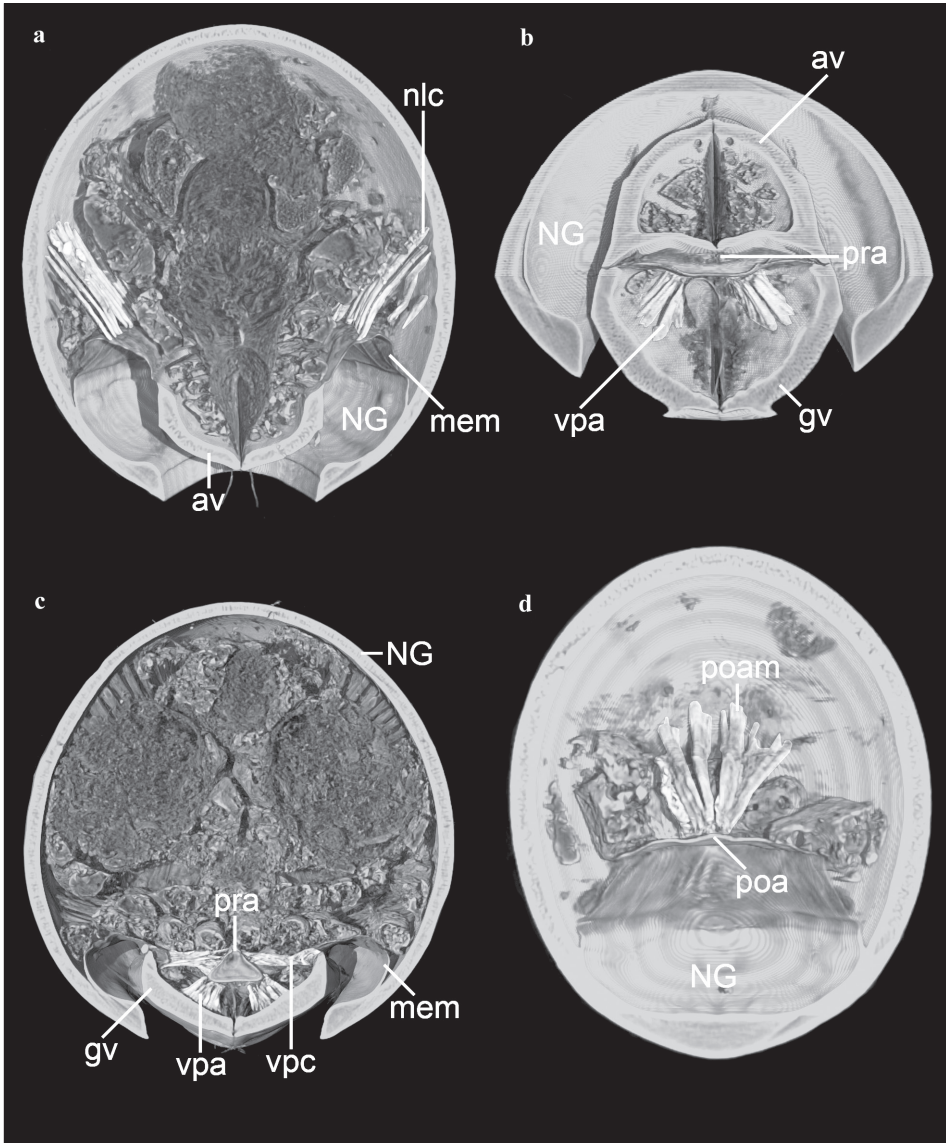


Fig. 7 *Phthiracarus globosus*, nearly encapsulated animal. Opisthosomal compressor system. Volume renderings of segmented synchrotron X-ray microtomography data. **a:** Anterior view on virtual cross section showing the notogaster lateral compressor (nlc). **b:** Combination of virtual cross and frontal section, anterodorsal view showing the ventral plate adductors (vpa). **c:** Virtual cross section showing the ventral plate adductors (vpa) and ventral plate compressors (vpc), viewing from anterior. **d:** Anterior view of virtual cross section showing the postanal muscle (poam).

Abbr.: av - anal valve, gv - genital valve, mem - anogenital membrane, NG - notogaster, nlc - notogaster lateral compressor, poa - postanal apodeme, poam - postanal muscle, pra - preanal apodeme, vpa - ventral plate adductor, vpc - ventral plate compressor.

4. Conclusions

Even though *Phthiracarus longulus* and *P. globosus* show a strong similarity, they clearly differ in some exoskeletal and muscular characters. The csp is present in *P. longulus* and *P. globosus* but so far in no euphthiracaroid mite. Further investigations of other genera (e.g. *Steganacarus*) and outgroups are necessary to possibly confirm the csp as a group synapomorphy of Phthiracaroida. The number of bands/fibers observed for several muscles in *P. globosus* does not correlate with the size of the two species. In fact, the smaller *P. globosus* features double to triple the number of bands/fibers as were seen in *P. longulus* (ade, ipr, hva and nlc). We see no obvious reason for the difference, but suspect that the muscle volume might be more or less equal in the two species and just be distributed differently.

Most of the characters found in both species show a strong similarity and differences can only be found in the quality or quantity of certain, homologous characters (e.g. the depth of the sensillus groove and the number of muscle fibres of the ipr, respectively). By contrast, differences between the Phthiracaroida and the Euphthiracaroida are at a larger scale, i. e., the presence or absence of complete features (e.g. the manubrium, the organisation of the ventral plates and the csp). Thus, informative signals of large phylogenetic scale can be found mainly in the presence or absence of characters, while those of small scale are found mostly in the quality or quantity of certain homologous features.

5. Acknowledgements

We thank Karl-Heinz Hellmer for the critical-point drying and Karl-Heinz Hellmer and Monika Meinert for taking the SEM micrographs. We thank Paavo Bergmann, Michael Laumann, Lukas Helfen and Peter Cloetens for their help with experiment SC-2127 at the ESRF in Grenoble and the European Synchrotron Radiation Facility for the allocated beam time. We thank the PRO ACAROLOGIA BASILIENSIS for funding the project.

6. References

- Betz, O., U. Wegst, D. Weide, M. Heethoff, L. Helfen, W. K. Lee & P. Cloetens (2007): Imaging applications of synchrotron x-ray micro-tomography in biological morphology and biomaterial science. I. General aspects of the technique and its advantages in the analysis of arthropod structure. – *Journal of Microscopy* **22**: 51–71.
- Heethoff, M. & P. Cloetens (2008): A comparison of synchrotron X-ray phase contrast tomography and holotomography for non-invasive investigations of the internal anatomy of mites. – *Soil Organisms* **80** (2): 205–215.
- Heethoff, M., L. Helfen & P. Cloetens (2008): Non-invasive 3D-visualization of the internal organization of microarthropods using synchrotron X-ray-tomography with sub-micron resolution. – *Journal of Visualized Experiments* **15**: e737, DOI: 10.3791/737.
- Niedbala, W. (2002): Ptyctimous mites (Acari, Oribatida) of the Nearctic Region. – *Monographs of the Upper Silesian Museum, Bytom* **4**: 1–261.
- Sanders, F. H. & R. A. Norton (2004): Anatomy and function of the ptychoid defensive mechanism in the mite *Euphthiracarus cooki* (Acari: Oribatida). – *Journal of Morphology* **259**: 119–154.
- Schmelzle, S., L. Helfen, R. A. Norton & M. Heethoff (2008): The ptychoid defensive mechanism in Euphthiracaroida (Acari: Oribatida): A comparison of exoskeletal elements. – *Soil Organisms* **80** (2): 227–241.
- Schmelzle, S., L. Helfen, R. A. Norton & M. Heethoff (2009): The ptychoid defensive mechanism in Euphthiracaroida (Acari: Oribatida): A comparison of muscular elements with functional considerations. – *Arthropod Structure and Development* **38** (6): 461–472.

-
- Schmelzle, S., L. Helfen, R. A. Norton & M. Heethoff (2010): The ptychoid defensive mechanism in *Phthiracarus longulus* (Acari, Oribatida, Phthiracaroidae): Exoskeletal and muscular elements. – *Soil Organisms* **82** (2): 253–273.
- Weigmann, G. (2006): Hornmilben (Oribatida). – Goecke & Evers, Keltern: 520 pp.

Accepted 26 March 2012

Publication 5

**Mechanics of the ptychoid defense mechanism in Ptyctima (Acari, Oribatida):
one problem, two solutions.**

Schmelzle, S., Norton, R.A., Heethoff, M.

Published in *Zoologischer Anzeiger – A Journal of Comparative Zoology* 254, pp. 27–40.

Submitted	Accepted	Published
8 April 2014	17 September 2014	2015

Authors' contribution:

- Schmelzle, Sebastian: Specimen preparation, data acquisition, data processing, data analysis, image processing, manuscript writing and preparation
- Norton, Roy A.: Specimen collection and fixation, general support and discussion, revision of manuscript
- Heethoff, Michael: Supervision, data acquisition, general support and discussion, revision of manuscript

Methods used:

- Synchrotron X-ray microtomography (SR μ CT)
- Scanning Electron Microscopy (SEM)
- High-speed videography



Mechanics of the ptychoid defense mechanism in Ptyctima (Acari, Oribatida): One problem, two solutions

Sebastian Schmelzle^{a,*}, Roy A. Norton^b, Michael Heethoff^{a,*}

^a Technische Universität Darmstadt, Fachbereich Biologie, Fachgebiet Zoologie, Ökologische Netzwerke, Schnittspahnstr. 3, 64287 Darmstadt, Germany

^b State University of New York, College of Environmental Science and Forestry, 1 Forestry Drive, Syracuse, NY 13210, USA

ARTICLE INFO

Article history:

Received 8 April 2014

Received in revised form

17 September 2014

Accepted 17 September 2014

Corresponding Editor: P. Michalik.

Keywords:

Functional morphology

Ptychoidy

Phthiracaroida

Phthiracaridae

Phthiracarus longulus

Euphthiracaroida

Euphthiracaridae

Acrotritia ardua

Rhysotritia ardua

Synchrotron X-ray microtomography

ABSTRACT

The most complex mechanical defense of oribatid mites is ptychoidy, in which the animals can retract their legs and gnathosoma into the idiosoma and encapsulate by deflecting the prodorsum. Since Acari lack most antagonistic musculature, extension of appendages is facilitated through hemolymph pressure that in mites mostly is generated by dorso-ventral compression of the opisthosoma. The hardened notogaster of box mites requires a different system of pressure generation that is also able to accommodate huge hemolymph movement accompanying ptychoidy. We compared the functional morphology of ptychoidy in one model species from each of the two ptyctime superfamilies, Euphthiracaroida and Phthiracaroida, using synchrotron X-ray microtomography and high-speed videography. We show that the two groups evolved very different functional modes of hydrostatic pressure control. While euphthiracaroids employ a lateral compression of the notogaster using all muscles of the opisthosomal compressor system, phthiracaroids employ a dorsoventral compression generated by only the notogaster lateral compressor and additionally the postanal muscle; these retract the temporarily unified ventral plates into the idiosoma, revealing the *poam* as an integral part of the opisthosomal compressor system in this group. The primitive mode of operation for generating hemolymph pressure in the Ptyctima probably was lateral compression, as molecular studies indicate that Phthiracaroida evolved within Euphthiracaroida. In this hypothesis, dorsoventral compression evolved secondarily in phthiracaroid mites, but whether the immediate ancestors of Ptyctima used lateral or dorsoventral compression remains to be determined.

© 2014 Elsevier GmbH. All rights reserved.

1. Introduction

1.1. General

Oribatid mites are a speciose (9000 described species; Schatz, 2002) and old group of Devonian, Silurian or even Precambrian origin (Schaefer et al., 2010, and references therein). Reaching high densities of up to 400,000 individuals/m², they represent an important part of soil decomposer systems, and should also be a significant resource for soil predators (Heethoff et al., 2009). Their feeding mode (particle feeding; Norton, 2007; Heethoff and Norton, 2009a,b) and use of relatively low quality food are unusual for che-licerates and have been considered constraints that resulted – for most species – in comparatively slow movement, low reproductive

potential and prolonged generation time (Norton, 1994; Sanders and Norton, 2004; Heethoff et al., 2007).

To achieve the long adult life necessary for reproduction, oribatid mites evolved various defensive strategies including mechanical, chemical and behavioral mechanisms. Chemical defense is based on the secretion of allomones from a pair of opisthonotal exocrine glands, and can be effective even against larger predators like rove beetles (Heethoff et al., 2011; Heethoff and Rasputnig, 2012; Heethoff, 2012). Mechanical defensive mechanisms include elongated setae that in some cases can also be erected (Norton, 2001), and cuticular hardening by sclerotization or additionally biomineralization using calcium carbonate, calcium oxalate or calcium phosphate (Norton and Behan-Pelletier, 1991a,b; Alberti et al., 2001). Behavioral defenses often go along with either chemical and/or mechanical mechanisms, e.g. flight behavior upon perception of alarm-pheromones, thanatosis ('playing dead') in combination with a turtle like "retraction" of the legs within protective cavities or under overhanging tecta (Schmid, 1988; Norton, 2001, 2007) or the ability to jump (Krisper, 1990; Wauthy et al., 1998).

* Corresponding authors. Phone: +49 61511675415; fax: +49 61511675412.

E-mail addresses: sebastianschmelzle@gmail.com, schmelzle@bio.tu-darmstadt.de (S. Schmelzle), michael@heethoff.de (M. Heethoff).

Table 1
Glossary of terms.

Term	Definition
Ptychoidy	The mechanism/body form/ability to encapsulate
Ptychosis	The process of changing between states/the process 'enabled' by the ptychoid body form
Emptychosis	The process of encapsulation
Ecptychosis	The process of extension/re-opening
Extended	The state of being extended/open. 'Active' mode of operation, i.e. walking, feeding, etc.
Encapsulated	The state of being encapsulated/closed. 'Inactive' mode of operation

The most complex mechanical defensive mechanism is ptychoidy (Sanders and Norton, 2004), in which the animals can effectively deflate the rather soft podosoma, retract their legs and gnathosoma into the idiosoma and encapsulate themselves (Fig. 1). This seems always to be combined with biomineralization (Pachl et al., 2012) and can in some species also be combined with chemical defense by secretion of repellents (e.g. chrysomelidial as shown for the euphthiracaroid mite genus *Oribotritia*; Raspotnig et al., 2008; Raspotnig, 2010) and rarely – as a mechanical and behavioral addition – also an escape-jump (Wauthy et al., 1998).

Ptychoidy probably evolved three times independently: one time each in the Ptyctima, the Mesoplophoridae and the Protoplophoridae (Grandjean, 1932, 1969; Norton, 1984, 2001; Sanders and Norton, 2004; Pachl et al., 2012). The Ptyctima consist of the two ptychoid superfamilies Euphthiracaroida (comprising the families Euphthiracaridae, Oribotritiidae and Synichotritiidae) and Phthiracaroida (comprising only one family, the Phthiracaridae) (Fig. 2). Ptychoidy is enabled through a system of exoskeletal and muscular elements and has four different systems of muscles that are actively involved in emptychosis, the process of encapsulation (Sanders and Norton, 2004; cf. Table 1). It seems to be highly effective: rove beetles of the genus *Stenus* are not able to crack the cuticle of *Euphthiracarus cribrarius* (Berlese, 1904) (own unpublished observations). Interestingly, ptychoidy is ineffective against

Euconus pubicollis (Müller and Kunze, 1822), a rove beetle of the sub-family Scydmaeninae, who given a choice of heavily protected oribatid mites prefers species of the family Phthiracaridae to others (Jałoszyński and Olszanowski, 2013).

So far the morphology associated with ptychoidy has been well studied within Euphthiracaroida and Phthiracaroida (Sanders and Norton, 2004; Schmelzle et al., 2008, 2009, 2010, 2012), but the mechanics behind it have been studied only by Sanders and Norton (2004) for *Euphthiracarus cooki* (Norton, Sanders and Minor, 2003). Like Acari in general, both groups lack most antagonistic musculature (except e.g. in the claws and chelicerae; Heethoff and Koerner, 2007; Heethoff and Norton, 2009b), such that movements of appendages, e.g. the straightening of a flexed leg segment, require a hydraulic system. This system becomes especially important in ptychoidy, as ecptychosis is also achieved through hydraulic pressure. This process of reopening requires forced displacement of the relatively large volumes of fluid needed to re-inflate the podosoma and protrude the legs and gnathosoma. In species of Euphthiracaroida, this hydraulic action seems to be facilitated by only one active system, the so-called opisthosomal compressor system (OCS; Sanders and Norton, 2004; Fig. 3). This muscle system exists in species of the other superfamily, Phthiracaroida, as well (Schmelzle et al., 2010, 2012), but the morphology of the ventral plates (cf. Schmelzle et al., 2008, 2010) and at least one of the muscles of the OCS suggest a different mode of operation that also involves the postanal muscle (*poam*), so far not included in the OCS.

Another morphological peculiarity is the coxisternal protractor (*csp*) so far found only within the genus *Phthiracarus* (Schmelzle et al., 2010, 2012) but none of the euphthiracaroid species. Its position indicates a direct involvement and a unique mode of operation in ptychoidy.

To investigate and compare these subjects in both ptyctime superfamilies, we used synchrotron X-ray microtomography and high-speed videography. Before proceeding and going into detail, it is necessary to summarize and compare some morphological details of the two superfamilies.

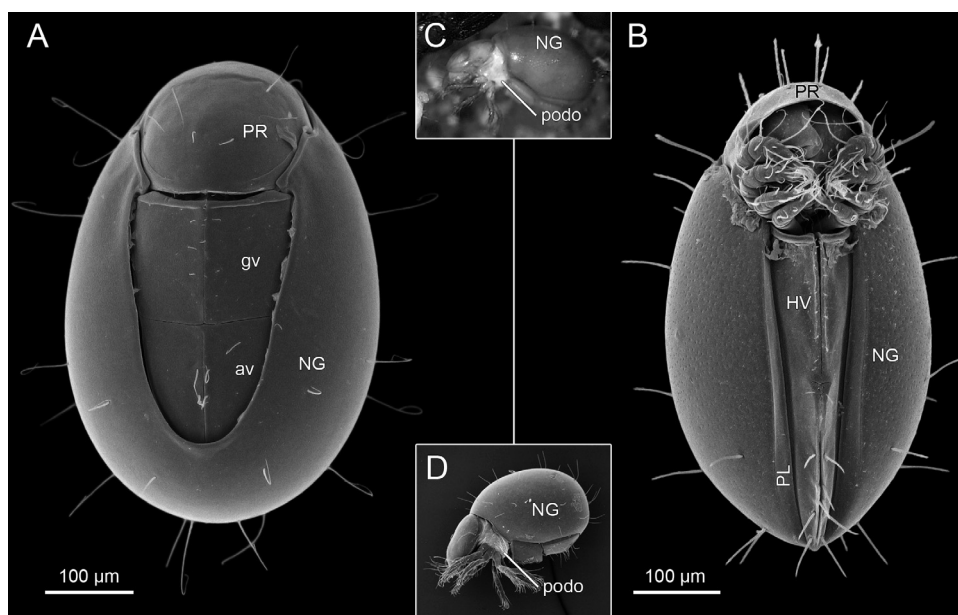


Fig. 1. Scanning electron micrographs of (A) phthiracaroid species *Phthiracarus longulus* in encapsulated state and (B) euphthiracaroid species *Acrotitia ardua* in partially encapsulated state, ventral view. Lateral view of phthiracaroid species (C) *Hoplophthiracarus* sp. (light microscopic image) and (D) *Phthiracarus* sp. (scanning electron micrograph). (C–D) In the extended state the soft podosomal membrane (highlighted) connecting the notogaster, coxisternum, gnathosoma and prodorsum is visible. av, anal valves; gv, genital valves; HV, holovenal plates; NG, notogaster; PL, plicature plates; podo, podosomal membrane; PR, Prodorsum. Source of (D): Marilyn Clayton, Natural Resources Canada, Canadian Forest Service, 2013.

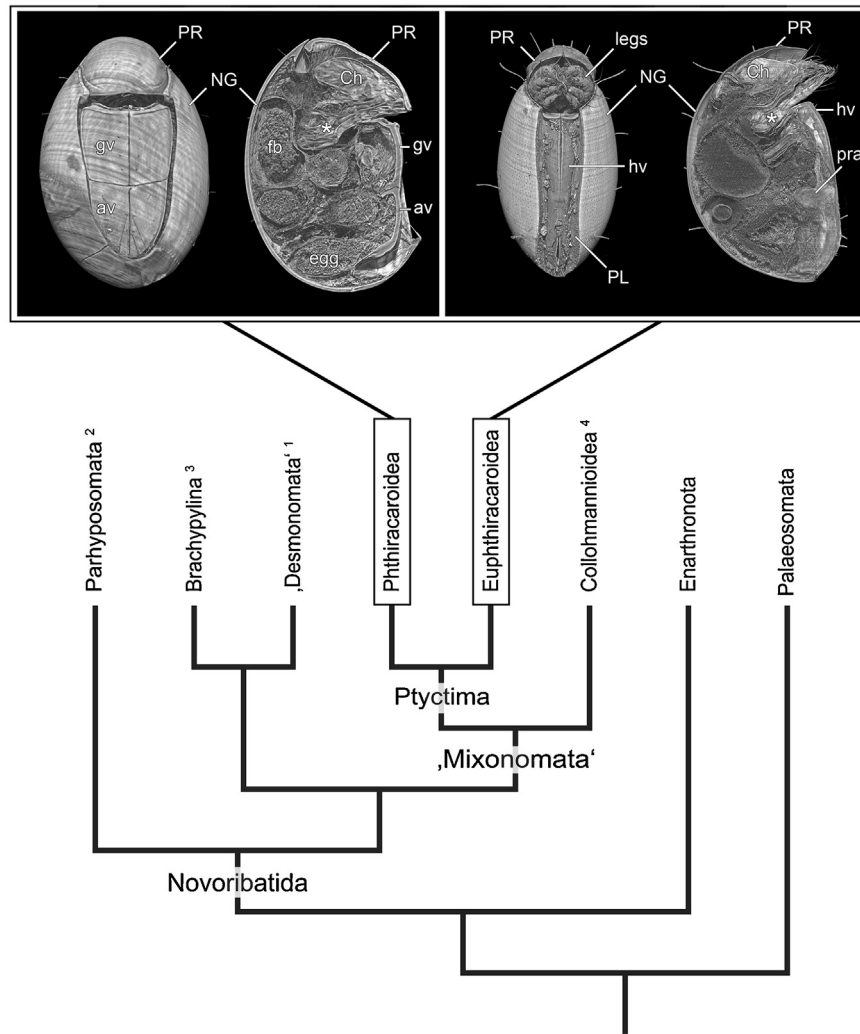


Fig. 2. Phylogeny of selected groups of Oribatida (modified after Heethoff et al., 2009) showing the position of the Ptyctima and indicating the position of species/groups discussed in Section 4.6. Top images show voxel renderings of encapsulated *Phthiracarus longulus* (left) and partially encapsulated *Acrotrititia ardua* (right) as overview (left) and sagittal section (right), respectively. ¹ *Archezogetes longisetosus*, *Hermannia gibba*, *Nothrus palustris*; ² *Parhyposomatus* sp.; ³ Brachypylina; ⁴ Collohmanniidae; av, anal venter; Ch, chelicera; fb, food bolus; gv, genital venter; hv, holoventral plates; NG, notogaster; PL, plicature plates; PR, prodorsum. Asterisk indicates the position of the walking legs I–IV within the idiosoma.

1.2. Morphological background (based on the findings of Sanders and Norton, 2004; Schmelzle et al., 2008, 2009, 2010, 2012)

So far, the morphology of ptychoydy has been studied in three of the four families of Ptyctima, but only for a few species. These include Phthiracaridae (Schmelzle et al., 2010, 2012 for *Phthiracarus longulus* (Koch, 1841) and *Phthiracarus globosus* (Koch, 1841), respectively), Euphthiracaridae (Sanders and Norton, 2004 for *E. cooki*; Schmelzle et al., 2008, 2009 for *Acrotrititia (Rhysotritia) ardua* (Koch, 1841)) and Oribotritiidae (Schmelzle et al., 2008, 2009 for *Oribotritia banksi* (Oudemans, 1916)). Only Synichotritiidae remains unexamined. The terms phthiracaroid and euphthiracaroid species/mites will be used below when referring to traits that are found in the respective studied species, but it is perhaps too early to be generalizing about superfamily traits.

The phthiracaroid and euphthiracaroid species clearly differ in some externally visual key features (Fig. 1). The ventral plates of, for example, *P. longulus* consist of two pairs of valves arranged in tandem; the posterior valves comprise fused anal and adanal plates (anal venter, av), while the anterior valves comprise fused genital and agenital plates (genital venter, gv). The plates are laterally and posteriorly embedded in the soft anogenital membrane that

connects them to the notogaster, and anteriorly they connect to the coxisternum via the soft podosomal membrane. In the encapsulated state the ventral plates tightly align with the notogaster and create a smooth connection. At the same time the soft anogenital membrane is hidden inside the encapsulated animal and therefore not accessible to predators.

The essential plates comprising the anal and genital venter are the same in Euphthiracaroida, but they are elongated and variously fused according to family and genus. In most Euphthiracaridae (e.g. *A. ardua*) they are fused to form a single pair of valves, the so-called holoventral plates (HV; Fig. 1). In contrast to the valves of Phthiracaridae, they are not embedded in voluminous soft membrane but are tightly articulated and rather framed by the so-called plicature plates, probably formed by sclerotization or mineralization of the formerly surrounding soft membrane. The plicature plates in turn articulate with the notogaster. In cross section the ventral (holoventral plates in Euphthiracaridae) and plicature plates combined have an M-like shape (Fig. 3F).

According to Sanders and Norton (2004) based on their study of *E. cooki* the OCS in Euphthiracaridae consists of three paired groups of muscles, also present in phthiracaroid species. The (i) notogaster lateral compressor (*nlc*) spans the complete length of

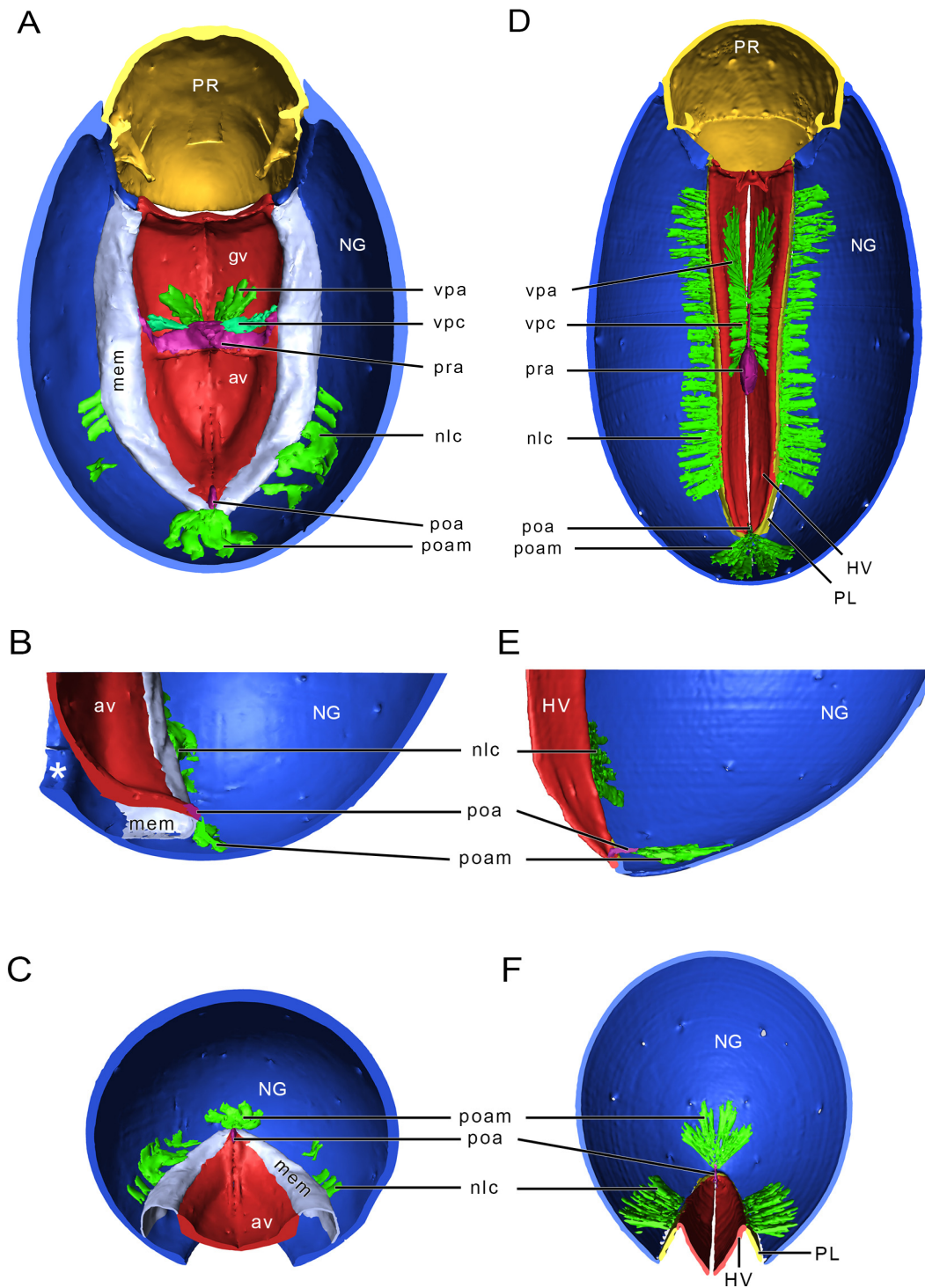


Fig. 3. Virtual sections of 3D-models of reconstructed Synchrotron X-ray microtomography data for the phthiracaroid species *Phthiracarus longulus* (A–C) and the euphthiracaroid species *Acrotritia ardua* (D–F) showing the muscles of the Opisthosomal Compressor System (OCS; in green). (A), (D) Horizontal sections, dorsal view. (B), (E) Sagittal sections, lateral view of the posterior body region (anterior to top). (C), (F) Cross sections, anterior view of the posterior body region (dorsal to top). In blue: notogaster; in red: ventral plates (*P. longulus*: anal and genital valves; *A. ardua*: holoventral plates); in gray: anogenital membrane. av, anal valves; gv, genital valves; HV, holoventral plates; mem, anogenital membrane; NG, notogaster; nlc, notogaster lateral compressor; poa, postanal apodeme; poam, postanal muscle; PL, plicature plates; PR, prodorsum; pra, preanal apodeme; vpa, ventral plate adductor; vpc, ventral plate compressor. The asterisk indicates the tectum surrounding the notogastral gap acting as a hard limit for the depression of the ventral plates. To activate interactive 3D content embedded in this article, please click on the figure. Further options, e.g. different views, are available in the viewer. Interactive 3D content of *Acrotritia ardua* shows exoskeletal elements and the muscles of the opisthosomal compressor system (OCS); interactive 3D content of *Phthiracarus longulus* shows exoskeletal elements, the muscles of the opisthosomal compressor system (OCS), and the coxisternal protractor (*csp*). (For interpretation of the references to color in this figure legend, the reader is referred to the web version of this article.)

the ventral plates, originating laterally on the notogaster and inserting along the junction of plicature and holovertral plates. The (ii) ventral plate compressor (*vpc*; called holovertral compressor (*hvc*) in Sanders and Norton, 2004) and (iii) ventral plate adductor (*vpa*; called holovertral adductor (*hva*) in Sanders and Norton, 2004) both originate on the preanal apodeme (located at the connection point of anal and genital venter; *pra*; Fig. 3A and D) and respectively insert on the lateral edge of the holovertral plates and the genital region of the holovertral plates (Fig. 3D–F; cf. Schmelzle et al., 2009). The postanal muscle (*poam*) is also associated with the ventral plates. It originates at the posterior end of the notogaster and inserts on the postanal apodeme (located at the posterior end of the ventral plates; *poa*; Fig. 3).

In phthiracaroid species the *nlc* is restricted to the posterior third and originates ventrolaterally on the notogaster, but in contrast to euphthiracaroid species it inserts on the anogenital membrane (Fig. 3A–C). The origin and insertion of the *poam*, *vpa* and *vpc* are the same in both groups.

The coxisternal protractor (*csp*) is so far found in only phthiracarid species and is present in each one examined (*P. longulus* and *P. globosus*). It originates laterally on the notogaster and inserts on the sejugal apodeme of the coxisternum (Fig. 4, encapsulated series).

2. Material and methods

2.1. Specimens

Phthiracarus longulus (Koch) (cf. Schmelzle et al., 2010) was chosen to represent Phthiracaridae, which in its broad sense is the only family in Phthiracaroida. *Acrotritia ardua* (Koch) (= *Rhysotritia ardua* (Koch)) (cf. Schmelzle et al., 2008, 2009) represents Euphthiracaridae, one of three families comprising the superfamily Euphthiracaroida. Both are common and abundant in temperate forest litter: *P. longulus* is a Holarctic species and *A. ardua* is distributed nearly worldwide. Adults for our studies (*P. longulus*: length about 540 μm ; *A. ardua*: length about 900 μm) were collected from accumulated decaying needles and cone scales of introduced Norway spruce (*Picea abies*) in LaFayette, Onondaga Co., NY, USA.

2.2. Sample preparation

Specimens for morphological analysis were killed and fixed in 1% glutaraldehyde for 60 h and stored in 70% ethanol. For the final preparation, specimens were dehydrated in an increasing ethanol series with steps of 70, 80, 90, 95 and 100%, with three changes at each step and 10 min at each change. After storage in fresh 100% ethanol they were critical point dried in CO_2 (CPD 020, Balzers).

2.3. Scanning electron microscopy

Critical point dried specimens were glued directly onto a stub and then sputter-coated with a 20 nm thick layer of gold-palladium. Micrographs were taken on a Cambridge Stereoscan 250 Mk² scanning electron microscope at 20 keV.

2.4. Synchrotron X-ray microtomography

Critical point dried animals were fixed by the notogaster to the tip of a plastic pin (1.2 cm long; 3.0 mm diameter) using instant adhesive. For each specimen, 1500 radiographs were recorded at the European Synchrotron Radiation Facility (ESRF) in Grenoble using beamline ID19 with beam energy of 20.5 keV and using a sample-detector distance of 20 mm. A cooled 14-bit CCD-camera with a resolution of 2048 \times 2048 pixel and an effective pixel size

of 0.7 μm per pixel was used (a detailed description of the method is given in Betz et al., 2007; Heethoff and Cloetens, 2008; Heethoff et al., 2008). The data were visualized with the program VGStudio MAX 1.2.1 (Volume Graphics, Heidelberg, Germany) and three-dimensional modeling of muscles and cuticular elements was conducted with amiraTM 4.0.1 (Mercury Computer Systems Inc., Chelmsford, MA, USA). Muscle fibers were counted using the original tomographic data or, if that was not possible, by the number of split ends in the resulting 3D model. Different portions of muscles are called muscle bands and subdivisions of muscle bands are called muscle fibers (Sanders and Norton, 2004). Original data of *A. ardua* and *P. longulus* is deposited in Morph-D-Base (S. Schmelzle_20140917-M-3.1 and S. Schmelzle_20140917-M-4.1, respectively).

2.5. High-speed videography

Mites were attached to a flattened tip of an insect pin using instant adhesive or water. Artificial stimuli, such as wind or touching with a fine insect needle to setae, were applied to provoke encapsulation of the mites. High-speed recordings were performed with a Photron Fastcam SA3 at different frame rates and analyzed using tpsDig[®] 2.16 (by F. James Rohlf 2010, <http://life.bio.sunysb.edu/morph/soft-dataacq.html>).

2.6. Functional analyses

Encapsulated and extended conditions were simulated *in silico* for both ptychoid species (based on one SR- μCT dataset of one specimen each) in amiraTM through rotation and translation of the prosomal and ventral plate surface (only for phthiracaroid species) based on the high-speed footage. The coordinates (*x*, *y*, *z*) of muscle origin and insertion of the *poam* were measured once in both situations. The length and spatial organization were calculated in a Cartesian coordinate system, where the X-axis corresponded to the medial – lateral axis, the Y-axis corresponded to the anterior – posterior axis and the Z-axis corresponded to the ventral – dorsal axis. Based on *in silico* simulations the ‘real’ operating angle was measured one time and the maximum theoretical operating angle of the ventral plates during entychosis was measured four times (to minimize measuring errors due to the use of the approximate center of the broad origin of the *poam* as measuring point; cf. Fig. 5). Also, at the same time the calculations of the *poam* were verified.

The volume was calculated for both species by using the approximate formula of an ellipsoid, having measured (a) the length, (b) the width and (c) the height. The volume change by lateral compression of the notogaster in *A. ardua* was calculated by changing the values of the half axes of the ellipsoid. The retraction of the ventral plates inside the notogaster of *P. longulus* was determined by (a) the calculation of a three sided pyramid and (b) the area of an image of the ventral plates (in square pixels; measured with ImageJ 1.46). The volume for both was calculated by using the generalized pyramid formula, where *h* is the measured dorsal displacement of the ventral plates. Based on the measurement of the maximum theoretical operating angle we also calculated the maximum dorsal displacement of the ventral plates and the resulting volume change.

Additionally we made a ‘whole body’ 3D model of *P. longulus* by segmenting the complete, encapsulated animal as one material (cuticle, organs, etc. combined) in contrast to segmenting the cuticular elements (notogaster) only (filling the space where the ventral plates would be in natural state as well) and then measuring the volume of the resulting 3D model with amiraTM 4.0.1 (Mercury Computer Systems Inc., Chelmsford, MA, USA). To account for the volume loss caused by the dorsal displacement of the ventral plates, we afterwards segmented the “empty” space left behind (the space between the ventral plates in the virtual natural state and the virtual retracted state). Additionally, we segmented one of two fecal

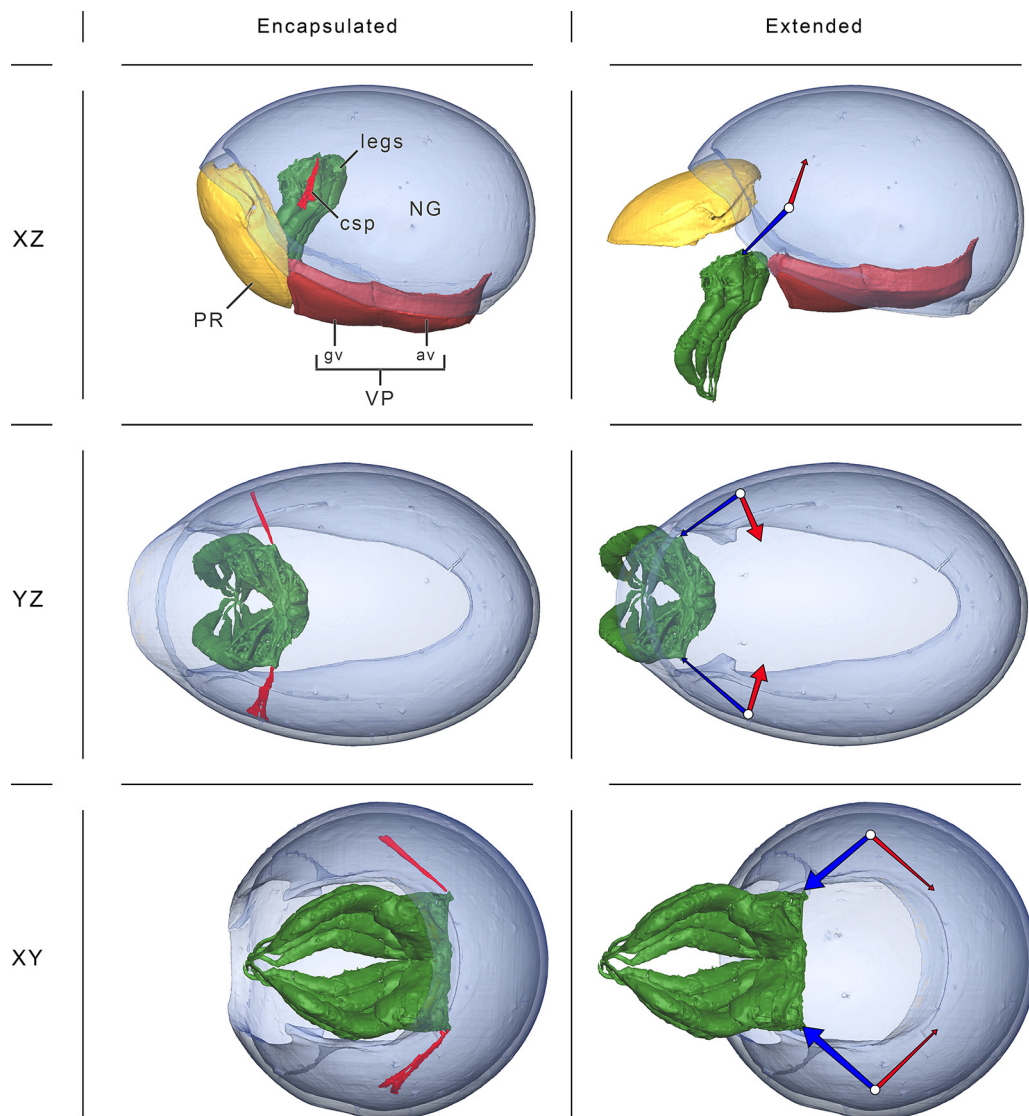


Fig. 4. Illustration showing the state (position and orientation) of the coxisternal protractor (*csp*) in the three major axes, in both encapsulated and extended states in a 3D model of the phthiracaroid species *Phthiracarus longulus*. The notogaster is shown transparent. The position of ventral plates (encapsulated series) and the position of prodorsum, legs and ventral plates (extended series) are simulated *in silico* to show the presumed 'natural state'. For better visibility of the *csp* the prodorsum and ventral plates are not shown in the YZ and XY orientation. Encapsulated series: the *csp* is shown in the state it was segmented, originating laterally on the notogaster and inserting on the sejugal apodeme of the coxisternum. Extended series: The origin (white circle) of the *csp* and its positions in encapsulated (red arrow) and simulated extended state (blue arrow) are shown to illustrate a change of orientation and thus a change in function during ptychosis. The shape of the arrow indicates the point of insertion lying below (small arrowhead) or above (large arrowhead) the plane comprising the origin of the *csp*. av, anal venter; *csp*, coxisternal protractor; gv, genital venter; legs, walking legs I–IV; NG, notogaster; PR, prodorsum; VP, ventral plates; XZ, lateral view; YZ, dorsal view; XY, frontal view. (For interpretation of the references to color in this figure legend, the reader is referred to the web version of this article.)

pellets, one of the five present eggs and the food bolus found in the ventriculus.

2.7. Terminology

Throughout the manuscript, we apply the terminology suggested in Schmelzle et al. (2009) to the muscles of the opisthosomal compressor system. The issue of functional muscle terminology is addressed in detail in the discussion.

3. Results

3.1. Pressure build-up

High-speed recordings of ptychosis in *A. ardua* showed a change in the overall width of the notogaster as well as the

width of the space between the notogastral edges, *i.e.* of the gap holding the ventral plates (Fig. 6; cf. Supplementary material, *Acrotritia.ardua.entropychosis.mp4*). During ecptychosis the notogaster shows a lateral compression as well as a narrowing of the notogastral gap and during entropychosis there is decompression and a widening of the notogastral gap (Fig. 6). High-speed recordings of ptychosis in several mites of the genus *Phthiracarus* showed no sign of a deformation of the notogaster during entropychosis or ecptychosis (Fig. 7; cf. Supplementary material, *Phthiracarus.sp.ecptychosis.mp4*). However, their ventral plates – functionally united into one ventral plate by virtue of complex junctures (as described in detail by Wauthy, 1984) – are retracted into the idiosoma at their posterior point during ecptychosis and are protruded up to the point of maximum alignment with the protecting tectum surrounding the notogastral gap (Fig. 3B) during entropychosis; this creates a temporarily unified opisthosoma that

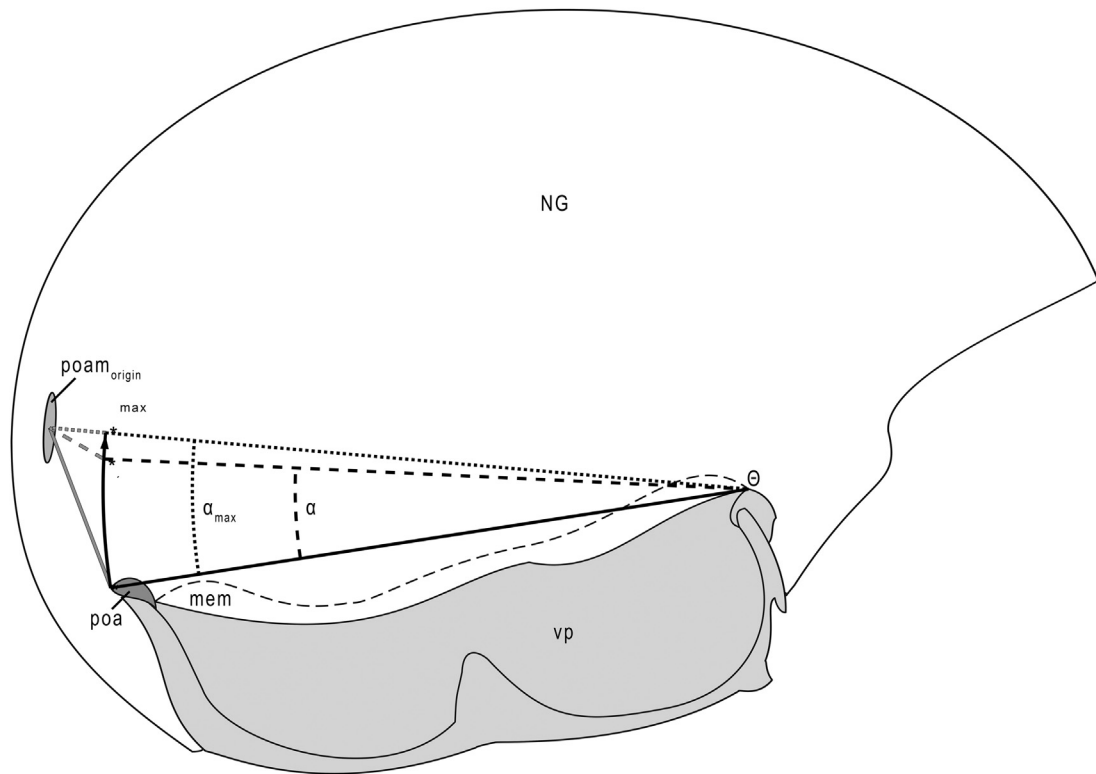


Fig. 5. Schematic illustration of operating angle α (as found in the fixed specimen) and the maximum operating angle α_{\max} of the phthiracaroid species *Phthiracarus longulus* (lateral view of opisthosoma, anterior to right). The operating angle α is enclosed by the baseline (the virtual line connecting the fulcrum Θ and the origin of the postanal muscle (*poam*) on the postanal apodeme) positioned as it would be in the encapsulated state (solid black line) and the baseline as found in the fixed animal (dashed black line), where the ventral plates are to a certain degree retracted into the idiosoma. The solid and dashed gray lines indicate the positioning of the *poam* in these two states, respectively, originating on the terminal end of the notogaster (*poam*_{origin}) and inserting on the preanal apodeme (* and *, respectively). For the calculation of the angles the circular origin of the *poam* has been reduced to its midpoint. The maximum operating angle α_{\max} is enclosed by the baseline positioned as it would be in the encapsulated state (solid black line) and the maximum virtual baseline (dotted black line) constituting a straight line with the *poam* (dotted gray line); inserting on the preanal apodeme at *^{max}). Because of its direction the *poam* has at that point no more influence on the retraction of the ventral plates into the idiosoma. *: point of insertion of the *poam* on the ventral plates in encapsulated state; *: point of insertion of the *poam* on the ventral plates as found in the fixed animal; *^{max}: point of insertion of the *poam* on the ventral plates in the state of maximum retraction of the ventral plates into the idiosoma. mem: anogenital membrane; NG: notogaster; poa: postanal apodeme (dark gray); *poam*_{origin}: origin of the postanal muscle on the notogaster (medium gray); vp: ventral plates (light gray).

constitutes a hard-limit for fluids (the maximal opisthosomal volume). At the same time the anterior part of the ventral plates keeps its position, acting as a fulcrum for this rocking motion.

Motions observable in the high-speed recordings during the chronological concurrence of eptychosis and entpychosis suggest that hemolymph pressure is increased/decreased by opisthosomal compression in the form of lateral compression/depression of the notogaster in *A. ardua* and the retraction/protraction of the ventral plates into and out of the space defined by the notogaster (opisthosoma) in *P. longulus*.

Hence, a simultaneous contraction of all the muscles of the OCS in *A. ardua* leads to a transmission of the force via the preanal apodeme (acting as a kingpost) onto the notogaster, leading to a tighter folding of the M-shaped ventral cross-section, a narrowing of the notogastral gap and hence a lateral compression of the notogaster (Fig. 8). Compression of the *poam* at the same time appears not to contribute directly to pressure generation; at most it stabilizes the ventral plates, since at its point of insertion the ventral plates are more or less firmly connected to the notogaster via the plicature plates.

In *P. longulus* on the other hand, the simultaneous contraction of the *nlc* and the *poam* applies their force to the anogenital membrane, which then transmits it to the united ventral plates. This causes the plates to retract into the idiosoma at their posterior end (Figs. 7 and 9), depicting a circular path around a fulcrum at the anterior connection of the ventral plates and notogaster (dashed circle; Fig. 10A). At that time the contraction of the *vpc* and *vpa*

probably ensures that the genital valves remain closed; clearly the two muscles are not related to the retraction of the ventral plates and therefore do not contribute directly to the build-up of pressure.

So, the pressure build-up in euphthiracaroid species is facilitated by contraction of three muscles of the OCS (*nlc*, *vpa* and *vpc*) leading to a lateral compression of the notogaster. By contrast, in phthiracaroid species it is facilitated through the contraction of one muscle of the OCS (the notogaster lateral compressor *nlc*; Fig. 9) and additionally the *poam* leading to a retraction of the ventral plates inside the opisthosoma around a fulcrum at the anterior connection of the ventral plates and notogaster (Figs. Fig. 3 and 10B).

3.2. Functional analyses of the postanal muscle (*poam*; cf. Table 2)

Since the *poam* is important for building the pressure in phthiracaroid mites, we simulated its dynamic during ptychosis. The mean length of the muscle in *P. longulus* changes from 104 μm in the encapsulated state (ventral plates maximally protruded and

Table 2

Parameters of the postanal muscle (*poam*) in two species of ptychoid oribatid mites. The brackets indicate the relative change from encapsulated to extended state and vice versa.

State		<i>Phthiracarus longulus</i>	<i>Acrotritia ardua</i>
Encapsulated	Length (μm)	104 (100%) (173%)	65 (100%)
Extended	Length (μm)	60 (58%) (100%)	65 (100%)

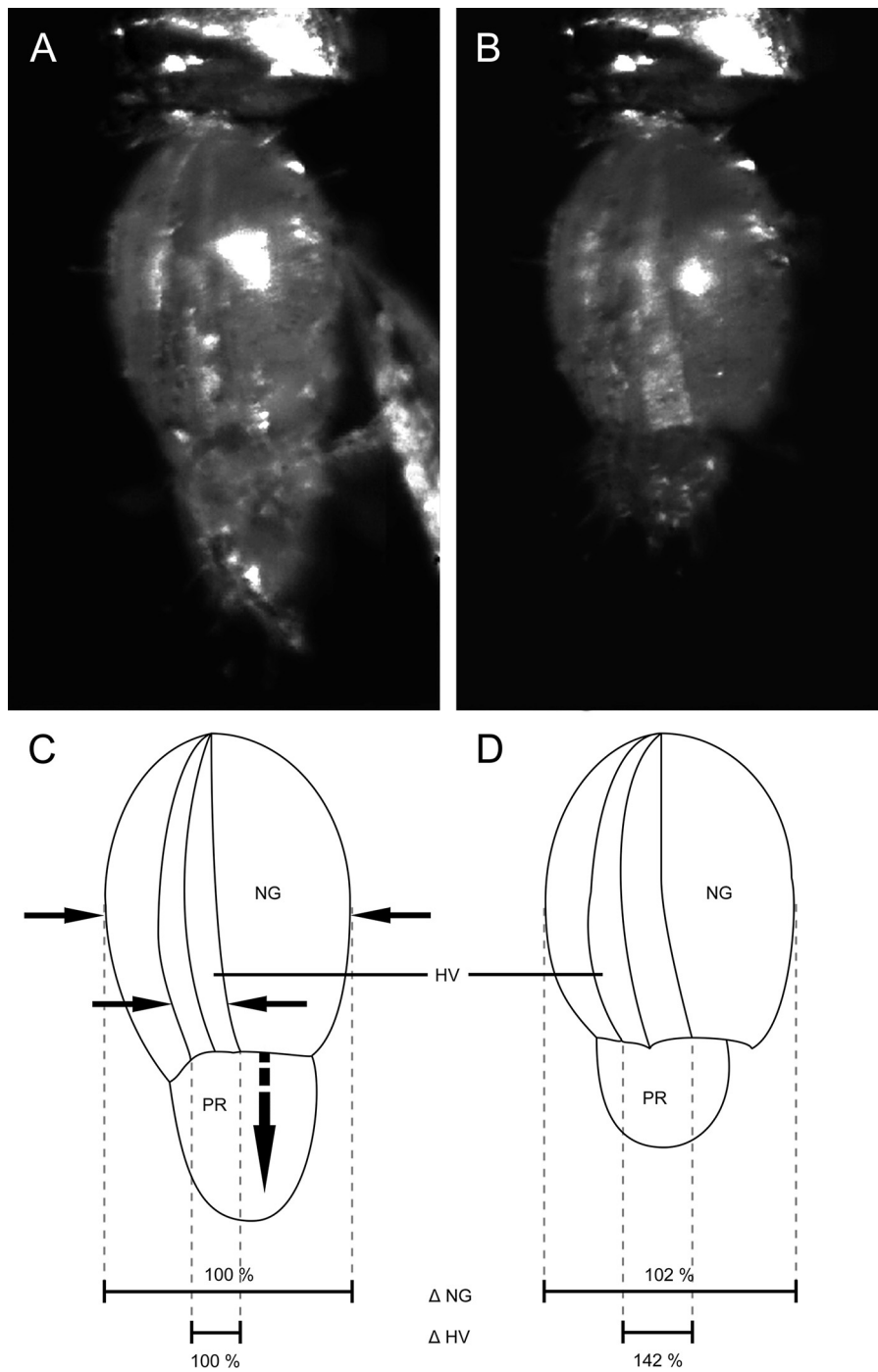


Fig. 6. *Acrotitia ardua* (Euphthiracaridae), ventrolateral view, anterior to bottom. All images show the orientation as recorded. (A), (B) Freeze frames of high-speed recording (recorded for about 4 s at 250 frames per second) of the beginning (A) and the end (B) of encapsulation (enptychosis) (cf. Supplementary material, *Acrotitia ardua*.enptychosis.mp4). (C), (D) Schematic illustration of (A) and (B) showing the lateral compression with relative width of the ventral plate gap (ΔHV) and lateral width of the animal (ΔNG). HV, holoventral plates; NG, notogaster; PR, prodorsum.

aligned with the notogaster) to 60 μm in the extended state (ventral plates retracted inside the opisthosoma). This corresponds approximately to a contraction of 40%. Since euphthiracaroid mites do not retract their ventral plates into the idiosoma, the length of the *poam* in extended and encapsulated conditions remains mostly unchanged (65 μm).

3.3. Volume change (cf. Table 3)

During enptychosis not only the change of the state of the exoskeletal elements, but presumably also the compression

(e.g. the caeca and the ventriculus) and re-stowage of the organs creates additional space for the legs and the gnathosoma inside the notogaster. Therefore we presume the encapsulated animal to be in a state of 'maximum compression'. Theoretical volume changes were calculated based on the assumption that the encapsulated animal thus is an enclosed system and that the change of the state of the exoskeletal elements alone is responsible for the volume changes and therefore also the pressure changes within the ptychoid animals (Figs. 6 and 10; see also Supplemental material, Fig. 11).

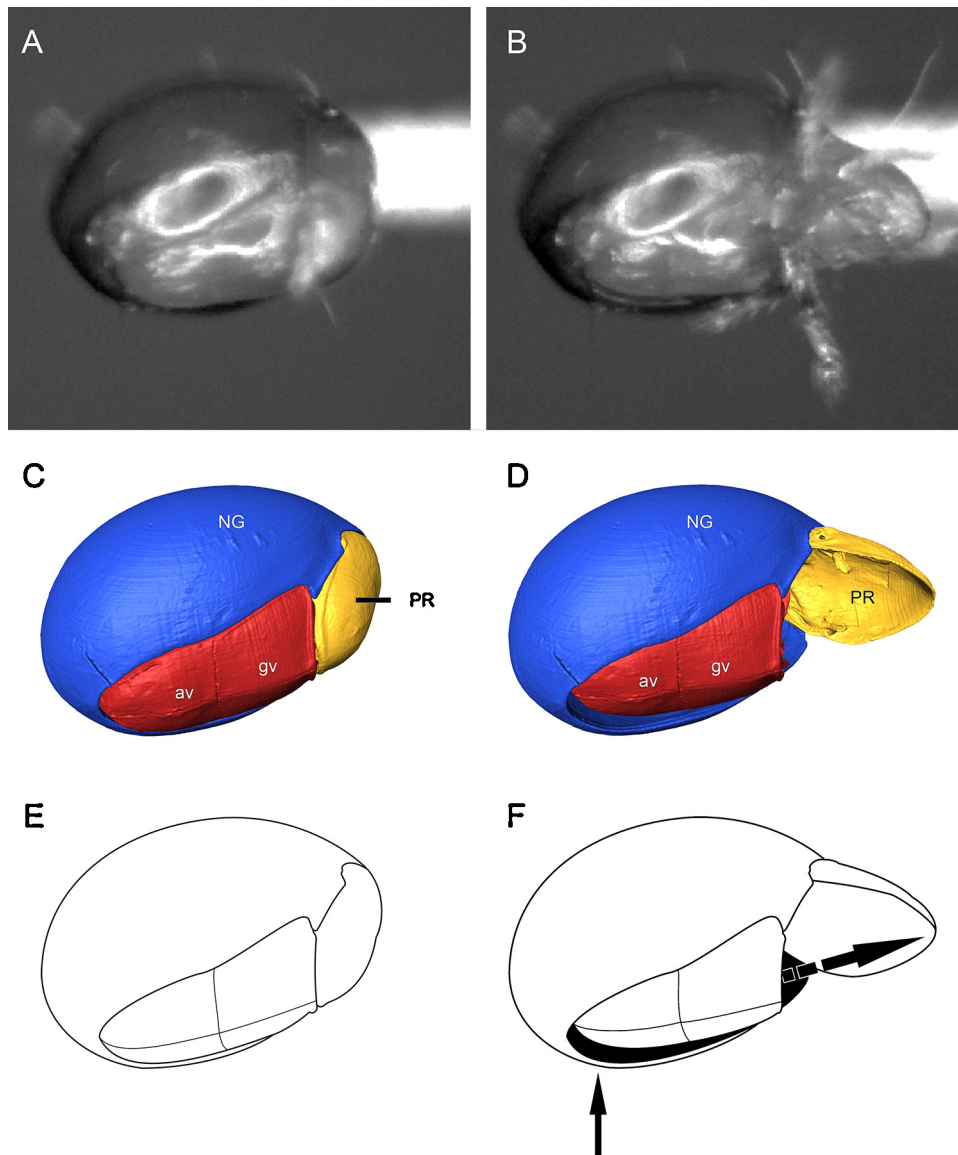


Fig. 7. *Phthiracarus* sp. (Phthiracaridae), ventrolateral view, anterior to right. All images show the orientation as recorded. (A), (B) Freeze frames of high-speed recording of the beginning (A) and end (B) of the reopening of the animal (ecptychosis) (cf. Supplementary material, *Phthiracarus.sp.ecptychosis.mp4*). (C), (D) *In silico* simulation of 3D models of both stages based on high-speed recording (recorded for about 0.75 s at 250 frames per second). (E), (F) Schematic illustration of the retraction of the ventral plate and the opening of the prodorsum. Solid arrow indicates the ventral plate retraction and dashed arrows the resulting opening of the prodorsum. av, anal valves; gv, genital valves; NG, notogaster; PR, Prodorsum.

The measured operating angle after the intake of the ventral plates is 10.6° in *P. longulus*, which corresponds to a retraction of the posterior end of the ventral plates into the idiosoma (Fig. 5) of about $57\ \mu\text{m}$. The mean volume of the encapsulated animal changes to 98.6% of the original volume. The volume measured in the 'whole body' 3D model of *P. longulus* changes to 96.8% of the original volume due to the retraction of the ventral plates inside the notogaster of about $57\ \mu\text{m}$. The mean maximum theoretical operating angle of 15.3° ($n=4$; $\sigma=0.29$) in *P. longulus* leads to the intake of the ventral plates of $81\ \mu\text{m}$, thus leading to a theoretical maximum volume change of 2.0% (based on the calculated model) and 4.6% (based on the 'whole body' model) instead of 1.4%. In *A. ardua* the lateral compression of the notogaster reduces the volume to 97.7% of the original (uncompressed) volume. In euphthiracaroid mites, the posterior-most point of the ventral plates is connected to the notogaster by a narrow, hardened conjunction, rather than a broad, soft

(membranous) only there is no intake of the plates and no operating angle could be determined.

The 3D model of one egg of *P. longulus* has a volume of about 3% of the body volume of an adult female, a fecal pellet about 0.7% and a food bolus about 1.8%. Considering that the studied animal carried five eggs, two fecal pellets and one food bolus, the total volume of the 'disposables' was about 18% of the body volume.

3.4. The role of the coxisternal protractor (*csp*) during ptychosis in Phthiracaridae

In extended state, the orientation of the *csp* is, due to its origin (laterally on the notogaster) and insertion (on the sejugal apodeme of the coxisternum), ventrad, anteriad and mediad (Fig. 4, extended series). However, during emptychosis the legs are retracted into the

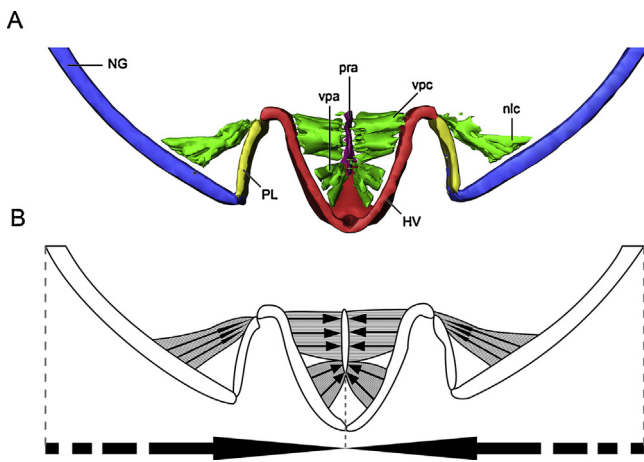


Fig. 8. Euphthiracaridae. (A) Virtual cross section in the ventral region of the 3D-model of reconstructed Synchrotron X-ray microtomography data of *Acrotrititia ardua* in encapsulated state. (B) Schematic illustration of force transmission during ecptychosis showing the build-up of hemolymph pressure through lateral compression of the entire notogaster. Solid arrows indicate force vectors of the muscles and dashed arrows underneath show the resulting overall force. HV, holovenal plates; NG, notogaster; nlc, notogaster lateral compressor; PL, plicature plates; pra, preanal apodeme; vpa, ventral plate adductor; vpc, ventral plate compressor. Some muscles are shown approaching but not attaching to sclerites (e.g. at *); this is an artifact based on the method of phase contrast tomography exhibiting a black outline of the different structures in the original data.

idiosoma and therefore the insertion of the *csp* on the coxisternum is shifted inwards, which leads to a dorsad, posteriad and mediad orientation (Fig. 4, encapsulated series).

3.5. Further observations

When triggering emptychosis by different stimuli through the course of the experiments we observed a hesitation of mites of both

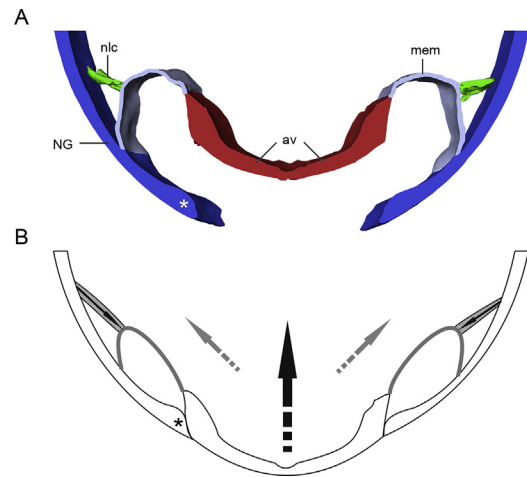


Fig. 9. Phthiracaridae. (A) Virtual cross section in the ventral region of the 3D-model of reconstructed Synchrotron X-ray microtomography data of *Phthiracarus longulus* in encapsulated state. (B) Schematic illustration of force transmission during ecptychosis showing the build-up of hemolymph pressure through intake of the ventral plates into the idiosoma. The illustration was adapted to show the natural state of the ventral plates enclosed by the notogaster in the encapsulated state. Solid arrows indicate force vectors of the muscles and dashed arrows the resulting overall force. av, anal valves; mem, anogenital membrane; nlc, notogaster lateral compressor; NG, notogaster. The asterisk indicates the tectum surrounding the notogastral gap, acting as a hard limit for the depression of the ventral plates in (B), but freely projecting in (A).

groups to encapsulate completely. Only after emphatic application of mechanical stimuli was encapsulation completed.

4. Discussion

4.1. Pressure build-up

Phthiracaroid species create hemolymph pressure differently than do euphthiracaroid species. Euphthiracaroid species produce

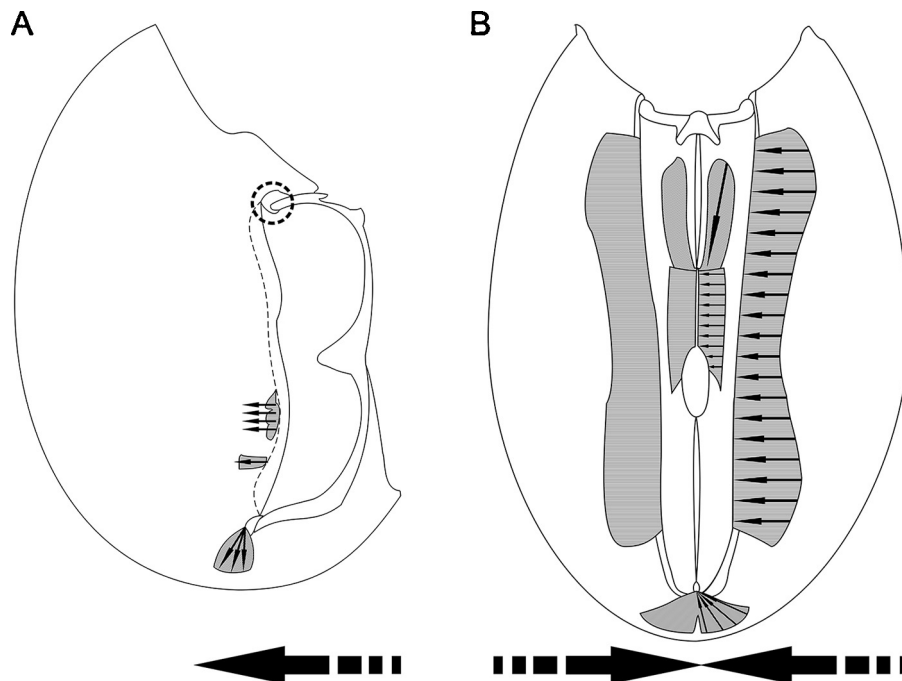


Fig. 10. Schematic illustration of force transmission in the opisthosoma (anterior to top) during ecptychosis in *Ptyctima*. (A) Phthiracaridae, lateral view; dotted circle indicates the fulcrum of the ventral plates. (B) Euphthiracaridae, ventral view; force vectors shown only for the right side. Solid arrows indicate force vectors of the muscles and dashed arrows underneath the resulting overall force.

Table 3

Volume calculations (rounded) and operating angles (α , α_{\max}) of the ventral plates of the ptychoid oribatid mites *Phthiracarus longulus* and *Acrotrititia ardua*. The volume (V) of *P. longulus* in encapsulated and extended states was calculated using two different methods (a and b; see Section 2 for detailed description) and also was segmented and measured as ‘whole body’ 3D model (3D). Also, where applicable, the maximum volume change was calculated based on the maximum theoretical working angle and the resulting maximum intake of the ventral plates.

	<i>P. longulus</i> (a)	<i>P. longulus</i> (b)	<i>P. longulus</i> (\bar{x})	<i>P. longulus</i> (3D)	<i>A. ardua</i>
V (encapsulated) [mm ³]	0.03874	0.03874	0.03874	0.03682	0.17564
V (extended) [mm ³]	0.03823	0.03816	0.03820	0.03563	0.17196
$\Delta(V)$	0.00051	0.00057	0.00054	0.00119	0.00367
$\Delta(V_{\text{ex/enc}})$	98.7%	98.5%	98.6%	96.8%	97.7%
α	10.6°	10.6°	10.6°	–	–
α_{\max} (mean)	15.275°	15.275°	15.275°	–	–
$\Delta(\alpha/\alpha_{\max})$	69.39%	69.39%	69.39%	–	–
V(max) [mm ³]	0.03802	0.03793	0.03798	0.03514 (est.)	–
$\Delta(V_{\text{max/enc}})$	98.1%	97.9%	98.0%	95.4% (est.)	–

pressure through lateral compression of the notogaster, using the ventral plates as a hinge and transmitting medially directed muscle forces via a kingpost, the preanal apodeme (cf. *E. cooki* in Sanders and Norton, 2004; *A. ardua* and *O. banksi* in Schmelzle et al., 2008, 2009). As Norton (2007) suspected, Phthiracaroid species create hemolymph pressure by retracting the posterior end of the ventral plates into the idiosoma (cf. *P. longulus* in Schmelzle et al., 2010; *P. globosus* in Schmelzle et al., 2012); this is enabled by a voluminous membrane articulating with the notogaster posteriorly and laterally, while anterolaterally a narrow, tight connection acts as a fulcrum for this rocking motion. The same is probably true for the entire superfamilies that these two families represent, Euphthiracaroida (probably also its families Oribotritiidae and – solely based on their external morphology – Synichotritiidae) and Phthiracaroida (cf. Norton and Lions, 1992; Lions and Norton, 1998; Sanders and Norton, 2004; Schmelzle et al., 2008, 2009, 2010, 2012).

These two different modes of pressure build-up within the Ptyctima could also explain why *E. pubicollis* given a choice of only heavily sclerotized mites prefer Phthiracaridae to the others (Jałoszyński and Olszanowski, 2013). After completely covering the animals with digestive fluid (possibly killing or anesthetizing the mites so that the muscles relax), *E. pubicollis* turns the phthiracarid mites on their dorsal side and then trying to pry open the prodorsum with their mandibles usually whilst pressing down on the ventral plates (Jałoszyński and Olszanowski, 2013), thereby increasing hydrostatic pressure within the animals which leads to an increase of pressure on the prodorsum until it opens and in doing so clears the way for access to vulnerable soft membrane of the mites. Also given as a choice were species of Euphthiracaridae, but in contrast to Phthiracaridae they were more or less neglected. It is possibly easier to push in the ventral plates into the idiosoma (with no hardened cuticle supporting the ventral plates from their dorsal side but only embedded in soft membrane) and to open the prodorsum than to compress the whole mineralized notogaster of Euphthiracaridae with enough force up to the point of sufficient internal pressure for the prodorsum to snap open.

The first detailed study about the functional morphology of ptychoidy was conducted on *E. cooki* (Sanders and Norton, 2004) and the newly created terminology regarding elements involved in ptychoidy was based on the peculiarity of elements found in euphthiracaroid species. However, in contrast to Euphthiracaroida there is no lateral compression of the notogaster in Phthiracaroida, which leads to several misleading terms, e.g. the “notogaster lateral compressor (nlc)” (cf. Schmelzle et al., 2009).

Another issue is the postanal muscle (*poam*), which in both superfamilies originates terminally on the notogaster and inserts on the postanal apodeme (not as Wauthy, 1984, wrote on the anogenital membrane). This muscle was not considered part of the opisthosomal compressor system by Sanders and Norton in a study

regarding *E. cooki* (2004); rather, it presumably has a passive role in that group, acting as a stabilizing band holding back the ventral plates. But in phthiracaroid species it gains functional importance for the build-up of hemolymph pressure by retracting the ventral plates, and must be considered an important part of the OCS.

4.2. Functional analyses of postanal muscle (*poam*) (cf. Table 2)

Since the *poam* assumes a different role in the two ptychoid groups, the calculation of its dynamic (change in length between extended and encapsulated state; Heethoff and Norton, 2009a) elucidates its function. In *P. longulus* the length shows an explicit dynamic between the extended and encapsulated condition (of about 60% of its original length), whereas in the euphthiracaroid mite *A. ardua* the dynamic is negligible. In *A. ardua* as in *E. cooki* (Sanders and Norton, 2004) and *O. banksi* (Schmelzle et al., 2009) the *poam* provides suspension (by isometric contraction) and thus stabilizes the ventral plates to withstand the hemolymph pressure created by lateral compression of the notogaster. The *poam* of *A. ardua* is mainly directed dorsad, because the hemolymph pressure is directed outwards (ventrad) and the efficiency of the *poam* acting as a band (and transmitting the force onto the notogaster) is highest when directed exactly in the axis of the force induced by the hemolymph pressure on the ventral plates, namely the dorsoventral axis. In phthiracaroid species the function of the *poam* is to aid in retraction of the ventral plates, not their suspension and stabilization. The ventral plates are retracted into the idiosoma and thereby they are anterolaterally connected to the notogaster. This connection serves as a fulcrum for the rocking motion of the ventral plates. The distinctly posterior and dorsal direction of the *poam* probably relates to the circular path that the ventral plates follow around their anterior fulcrum, allowing it to pull with constantly high force at all times of the sequence.

4.3. Volume change (cf. Table 3)

For phthiracaroid mites the purely theoretical volume (based on the formula of an ellipsoid) and the measured volume of the ‘whole body’ 3D model differ by only about 5%, so the formulae constitute a reasonable approximation of the volume of an encapsulated ptychoid mite and we assume that the same is true for euphthiracaroid mites. The theoretical relative volume change during ptychosis based on the calculations shows no clear difference between the euphthiracaroid mite *A. ardua* and the phthiracaroid species *P. longulus*. However, the measured volume change in the ‘whole body’ 3D model of *P. longulus* is about twice that of the corresponding calculated volume change.

The relative volume change of about 2–3.5% seems to be effective for ptychoidy in both groups. Phthiracaroid species also have additional leeway (about 0.5% based on calculations and about 1.4% based on the ‘whole body’ model) regarding the higher maximum

operating angle α_{\max} of the ventral plates, at which point the force vector of the *nlc* also could have leveled with the ventral plates; it would have no more pull and therefore should not be able to lead to a further intake of the ventral plates by contraction. Nonetheless, the dimensions of the volume change and the resulting pressure change due to the intake of the ventral plates seems quite low, in contrast to our expectations.

In the active, extended state the animals need a relatively high hemolymph pressure to keep the membranous cuticle of the podosoma inflated (acting as a stable basis for the coxisternum that is surrounded only by membrane and not connected to hardened cuticle) and also to act as antagonists to flexor and retractor muscles during the movement of the legs and gnathosoma. The internal pressure created during emptychysis by retraction of the podosoma and gnathosoma into the idiosoma is supposedly very high, so that a volume and resulting pressure change of only about 3% due to the intake of the ventral plates is sufficient for emptychysis. This in turn means that in the encapsulated state the animals have to counter a high pressure on the prodorsum, which is mainly achieved by the contraction of the huge inferior prodorsal retractor (*ipr*) inserting on the inferior retractor process of the prodorsum and may also be aided by the coxisternal retractor (*csr*) inserting on the coxisternum, the 'base plate' of the legs. Furthermore, the connection consisting of the bothridial scale on the prodorsum and the scale receptacle on the notogaster (cf. Sanders and Norton, 2004; Schmelzle et al., 2008, 2009, 2010, 2012) provides a mechanism that aids in countering the pressure on the prodorsum by firmly interlocking prodorsum and notogaster. Presumably, this leads to a lower amount of muscle force needed to keep the prodorsum shut, thereby allowing the muscles to 'relax' a little and in the process save energy and increase the maximum possible time of encapsulation.

In both models of *P. longulus* (mathematical and 'whole body' 3D model) the anogenital and podosomal membranes are mathematically not taken into account due to (i) their extremely dynamic behavior (folding and inflation based on pressure and muscle tension) and (ii) the lack of a dataset allowing for the reconstruction and exact measurement of the inflated volume. The cavity formed by the inflated membrane certainly plays a major role by being the main recipient of the displaced hemolymph (shifting from the opisthosoma to the prosoma) (cf. Fig. 3 and Fig. 9). Hypothetically accounting for the inflated membrane undergoing a considerable volume change during ptychosis and the rather small volume change caused by the opisthosomal compression, chances are that the overall change in volume and therefore pressure is in reality zero. That would result in a more or less constant pressure level on the displaced fluid, peaking at the onset of en- and emptychysis but being more or less instantaneously 'absorbed' by the membrane and the process of emptychysis itself.

It remains unclear how ptychoid animals manage the volume increase associated with feeding and egg development, and the decrease during defecation and oviposition. The change can be considerable: in our measured individual, the total volume of such 'disposables' (about 18% of the total body volume) exceeded the volume change due to the intake of the ventral plates by a factor of 6. A food bolus, in contrast to fecal pellets and eggs, seems to be spongy and therefore compressible. The food residues in the fecal pellets are already highly condensed and the eggs are mostly composed of fluids. Hence, both are expected to be relatively incompressible. Reduction in hemolymph quantity seems to be a suitable way to compensate for the intake of food, but the rebuilding of hemolymph to compensate for defecation and especially oviposition would seem too slow to be effective. Possibly the compensation for increasing or decreasing disposable contents etc. is only regulated by the magnitude of opisthosomal compression, but a 'fluxional' system, in which the animals strictly control input and

output to maintain a more or less constant pressure level, seems to be more likely. The same is probably true for individuals with no gut/oviduct contents, like young females or non-feeding males that are still able to maintain the ptychoid defensive mechanism. Also, considering that the number of eggs found in non-ptychoid mite species (which also hemolymph pressure as antagonistic force), such as *Archezogetes longisetosus* Aoki (Trhypochthoniidae) with egg contents as high as 30 (Heethoff et al., 2007), the number of eggs found in *P. longulus* (5) is comparatively small. Besides their low activity and rate of resource accumulation the number of eggs in ptychoid species might be intentionally kept low so as to not jeopardize the functionality of the ptychoid defensive mechanism.

4.4. The role of the coxisternal protractor (*csp*) during ptychosis in Phthiracaridae

The orientation of the *csp* in the extended state clearly suggests a role as retractor for the legs during emptychysis. However, its orientation in the encapsulated state (dorsad, posteriad and mediad, with the first two being opposite to the orientation in the extended state), so that a contraction of the *csp* during emptychysis might add force as well as give a direction to the hemolymph movement. So the change in orientation of the *csp* during ptychosis leads to a bi-functional role as (i) protractor as well as (ii) retractor of the legs.

4.5. Further observations

As noted, mites hesitated to encapsulate completely after application of artificial stimuli. Possibly this is due to the stimuli being identified by the mites as insufficient because of e.g. the absence of chemical cues and/or the unnatural nature of the mechanical cue. Also, the final movements needed to complete encapsulation might be very strenuous, so the cost-value-ratio might lead to a 'wait-and-see' tactic, in which the animals encapsulate completely only if the stimulus is strong enough and/or sufficiently persistent. Furthermore, an incomplete encapsulation enables the animals to use their strong claws to firmly attach to the substrate (cf. Heethoff and Koerner, 2007, for *A. longisetosus*), which in some cases might be a better choice than to let go entirely. For example, the highly effective predator *E. pubicollis* turns the mite on its dorsal side and then presses on the ventral plates to create the hydrostatic pressure needed to get access to soft membrane (Jałoszyński and Olszanowski, 2013). If the mite retains the ability to attach to the substrate (with the ventral plates facing the substrate) it may give an advantage when confronted with such an attack.

4.6. Structural and functional homologies in non-ptychoid mites and their phylogenetic implications

Since two very different modes of opisthosomal compression are exhibited by Ptyctima, two different scenarios for the evolution of ptychoidy in this group are possible: either (i) lateral compression (as in Euphthiracaroidea) was ancestral, with dorsoventral compression (as in Phthiracaroidea) being derived from it; or (ii) dorsoventral compression was ancestral and lateral compression was derived from such an ancestor. In either case, the muscles associated with generation of hemolymph pressure must have reoriented during the evolution of Ptyctima. To choose between scenarios requires knowledge of the relationships between the two superfamilies of Ptyctima, i.e. if they are monophyletic sister groups or if one of them is paraphyletic (and if so, which), and also an understanding of the compression mode in their close non-ptychoid relatives.

Non-ptychoid mites often achieve pressure build-up by direct muscular dorsoventral compression of the hysterosoma, such as

by contraction of “dorsoventral muscles” of *Archezogozetes longisetosus* (Aoki, 1965) (*dvm* in Heethoff and Norton, 2009b; cf. Fig. 2¹), the “dorsolateral muscles” of *Parhyppochthonius* sp. (Akimov and Yastrebtsov, 1991; Sanders and Norton, 2004; cf. Fig. 2²) and the ‘curtain-like series’ linking notogaster and ventral plate as described for brachypylinae mites by Grandjean, 1959 (cf. Fig. 2³). According to Sanders and Norton (2004) the *nlc* found in *E. cooki* is probably a “derivative of these evolutionarily plastic dorsolateral muscles”. Other examples are the dorsoventral muscles of *Hermannia gibba* (Koch, 1839) (Akimov and Yastrebtsov, 1991; cf. Fig. 2¹) and the “dorsal compressor muscles” and “ventral compressor muscles” of *Nothrus palustris* (Koch, 1840) (Akimov and Yastrebtsov, 1989; cf. Fig. 2¹). Hoebel-Mävers (1967) (referring to *Nothrus palustris*) stated that the ventral plates could be distinguished from the notogaster only by a simple fold between them, so a shift in origin of muscles would not be evolutionarily difficult.

So, we can hypothesize that muscle insertion on the notogaster and the adanal plates may go back in time to a common ancestral muscle (or series) inserting on the hysterosoma. That in turn would mean that the *nlc* might be homologous with the outer anal muscles (*oam*) and dorsoventral muscles (*dvm*) of *A. longisetosus* (cf. Heethoff and Norton, 2009b). Considering this, the primitive mode of operation for the build-up of hemolymph pressure in Oribatida most likely was due to dorsoventral compression of the opisthosoma and that, in turn, means that the dorsoventral compression mode in phthiracaroid species (the intake of the ventral plates) would seem logically ancestral. However, molecular studies (Pachl et al., 2012) indicate Phthiracaridae evolved within Euphthiracaroida and therefore the dorsoventral orientation of the opisthosomal compression must represent a functional reversal and the mode of lateral compression would be plesiomorphic within the Ptyctima.

Lateral compression seems to have been ancestral within Ptyctima, but is it an apomorphy of the group or did it evolve prior to the appearance of Ptyctima? Little has been written about the origin of Ptyctima, but the only family that has been supported (explicitly or implicitly) as its sister group based on morphological traits is the non-ptychoid family Collohmanniidae (Štorkán, 1925; Grandjean, 1966, 1967; Norton, 2006; cf. Fig. 2⁴). Molecular data are equivocal on this topic (Dabert et al., 2010; Pachl et al., 2012).

Among other characters, species of Collohmanniidae possess a preanal apodeme unlike that of any Oribatida outside Euphthiracaroida (Norton, 2006). The musculature associated with this apodeme is also similar, enabling Collohmanniidae species to create hemolymph pressure through lateral compression of the notogaster, as in Euphthiracaroida. This would mean that lateral compression predated Ptyctima, and could have been preadaptive, i.e. facilitating the evolution of ptychoidity.

Answers to the questions of why a reversal from lateral back to dorsoventral compression would happen and if there is an advantage of the phthiracaroid structure and function remain unclear.

5. Conclusions

We have shown that mechanisms of pressure build-up in examples from two families of the Ptyctima, Phthiracaridae and Euphthiracaridae, are essentially different. Both families rely on more or less the same muscle systems, though with partially different functions. For example, the *poam* has a more important role in the process of ecptychosis in Phthiracaridae due to its function as a retractor of the ventral plates, and therefore should be considered as a part of the OCS. All this is probably true for the entire superfamilies that these two families represent. The ancestral mode of opisthosomal compression in Ptyctima seems to be lateral compression of the notogaster, based on molecular evidence

(Pachl et al., 2012) that Phthiracaroida evolved within Euphthiracaroida, and on the striking similarities of the latter with the closely related Collohmanniidae (Norton, 2006).

When contracting, the *csp* – so far only found in the genus *Phthiracarus* – acts as protractor as well as a retractor for the legs.

Acknowledgements

We thank Marilyn Clayton, the Natural Resources Canada, the Canadian Forest Service and the Government of Canada for permission to use one of their scanning electron microscope images. We thank Karl-Heinz Hellmer for the critical point drying and for taking the SEM micrographs. We thank the European Synchrotron Radiation Facility in Grenoble for supporting this project through allocation of beam time (user experiment SC-2127), and thank Peter Cloetens, Lukas Helfen, Paavo Bergmann and Michael Laumann for their help during the experiment.

Appendix A. Supplementary data

Supplementary data associated with this article can be found, in the online version, at <http://dx.doi.org/10.1016/j.jcz.2014.09.002>.

References

- Akimov, I.A., Yastrebtsov, A.V., 1989. The muscular system and skeleton elements of an oribatid mite *Nothrus palustris*. Zool. Z. 68, 57–67 (in Russian).
- Akimov, I.A., Yastrebtsov, A.V., 1991. Skeletal-muscular system of oribatid mites (Acariformes: Oribatida). Zool. Jahrb. Abt. allg. Zool. Physiol. Tiere 121, 359–379.
- Alberti, G., Norton, R.A., Kasbohm, J., 2001. Fine structure and mineralization of cuticle in *Enarthronota* and *Lohmannioidea* (Acari: Oribatida). In: Halliday, R.B., Walter, D.E., Proctor, H.C., Norton, R.A., Colloff, M.J. (Eds.), Proceedings of the 10th International Congress of Acarology. CSIRO Publishing, Melbourne, pp. 230–241.
- Betz, O., Wegst, U., Weide, D., Heethoff, M., Helfen, L., Lee, W.-K., Cloetens, P., 2007. Imaging applications of synchrotron X-ray phase-contrast microtomography in biological morphology and biomaterials science. I. General aspects of the technique and its advantages in the analysis of millimetre-sized arthropod structure. J. Microsc. 227 (1), 51–71.
- Dabert, M., Witalinski, W., Kazmierski, A., Olszanowski, Z., Dabert, J., 2010. Molecular phylogeny of acariform mites (Acari: arachnida): Strong conflict between phylogenetic signal and long-branch attraction artifacts. Mol. Phylogenet. Evol. 56, 222–241.
- Grandjean, F., 1932. La famille des Protoplophoridae. Bull. Soc. Zool. France 57, 10–36.
- Grandjean, F., 1959. Observations sur les Oribates (39e série). Bull. Mus. nat. d'Hist. nat. (2e sér.) 31, 248–255.
- Grandjean, F., 1966. Collohmanna gigantea Selln (Oribate). Première partie. Acarologia 8, 328–357.
- Grandjean, F., 1967. Nouvelles observations sur les Oribates (5e série). Acarologia 9, 242–272.
- Grandjean, F., 1969. Considerations sur le classement des oribates: leur division en 6 groupes majeurs. Acarologia 11, 127–153.
- Heethoff, M., 2012. Regeneration of complex defensive oil-gland secretions and its importance for chemical defense in an oribatid mite. J. Chem. Ecol. 38, 1116–1123.
- Heethoff, M., Koerner, L., 2007. Small but powerful—the oribatid mite *Archezogozetes longisetosus* Aoki (Acari, Oribatida) produces disproportionately high forces. J. Exp. Biol. 210, 3036–3042.
- Heethoff, M., Cloetens, P., 2008. A comparison of synchrotron X-ray phase contrast tomography and holotomography for non-invasive investigations of the internal anatomy of mites. Soil Organ. 80, 205–215.
- Heethoff, M., Norton, R.A., 2009a. A new use of synchrotron X-ray microtomography (SR- μ CT): three-dimensional biomechanical modeling of chelicerate mouthparts and calculation of theoretical bite forces. Invert. Biol. 128, 332–339.
- Heethoff, M., Norton, R.A., 2009b. Role of musculature during defecation in a particle-feeding arachnid, *Archezogozetes longisetosus* (Acari, Oribatida). J. Morphol. 270, 1–13.
- Heethoff, M., Rasputnig, G., 2012. Expanding the ‘enemy-free space’ for oribatid mites: evidence for chemical defense of juvenile *Archezogozetes longisetosus* against the rove beetle *Stenus junco*. Exp. Appl. Acarol. 56, 93–97.
- Heethoff, M., Laumann, M., Bergmann, P., 2007. Adding to the reproductive biology of the parthenogenetic oribatid mite *Archezogozetes longisetosus* (Acari, Oribatida Trhypochthoniidae). Turk. J. Zool. 31, 151–159.
- Heethoff, M., Helfen, L., Cloetens, P., 2008. Non-invasive 3D-visualization of the internal organization of microarthropods using synchrotron X-ray-tomography with sub-micron resolution. J. Vis. Exp. 15, e737.

- Heethoff, M., Norton, R.A., Scheu, S., Maraun, M., 2009. Parthenogenesis in oribatid mites (Acari, Oribatida): evolution without sex. In: Schön, J., Martens, K., van Dijk, P. (Eds.), *Lost Sex*. Springer, Dordrecht, pp. 241–257.
- Heethoff, M., Koerner, L., Norton, R.A., Rasputnig, G., 2011. Tasty but protected—first evidence of chemical defense in oribatid mites. *J. Chem. Ecol.* 37, 1037–1043.
- Hoebel-Mävers, M., 1967. Funktionsanatomische Untersuchungen am Verdauungstrakt der Hornmilben (Oribatei). (Dissertation Universität Braunschweig), pp. 45.
- Jałoszyński, P., Olszanowski, Z., 2013. Specialized feeding of *Euconnus pubicollis* (Coleoptera: Staphylinidae: Scydmaeninae) on oribatid mites: Prey preferences and hunting behavior. *Eur. J. Entomol.* 110 (2), 339–353.
- Krisper, G., 1990. The jump of the mite-genus *Zetorches* (Acarida Oribatida). *Zool. Jahrb., Abt. Anat. Ont. Tiere* 120, 289–312.
- Lions, J.-C., Norton, R.A., 1998. North American Synchotritiidae (Acari: Oribatida) 2. *Synchotritia spinulosa* and *S. caroli*. *Acarologia* 39, 265–284.
- Norton, R.A., 1984. Monophyletic groups in the Enarthronota (Sarcoptiformes). In: Griffiths, D.A., Bowman, C.E. (Eds.), *Acarology VI*, vol. 1. Ellis Horwood Publ, Chichester, UK, pp. 233–240.
- Norton, R.A., 1994. Evolutionary aspects of oribatid mite life histories and consequences for the origin of the Astigmata. In: Houck, M. (Ed.), *Mites. Ecological and Evolutionary Analyses of Life-history Patterns*. Chapman and Hall, New York, NY, pp. 99–135.
- Norton, R.A., 2001. Systematic relationships of Nothrolahmanniidae and the evolutionary plasticity of body form in Enarthronota (Acari: Oribatida). In: Halliday, R.B., Walter, D.E., Proctor, H.C., Norton, R.A., Colloff, M.J. (Eds.), *Acarology: Proceedings of the 10th International Congress*. CSIRO Publishing, Melbourne, pp. 58–75.
- Norton, R.A., 2006. First record of *Collohmanna* (*C. schusteri* n. sp.) and *Hermannia* (*H. sellnicki* n. sp.) from Baltic amber, with notes on Sellnick's genera of fossil oribatid mites (Acari: Oribatida). *Acarologia* 46, 111–125.
- Norton, R.A., 2007. Holistic acarology and ultimate causes—examples from oribatid mites. In: Morales-Malacara, J.B., Behan-Pelletier, V.M., Ueckermann, E., Pérez, T.M., Estrada-Nenegas, E.G., Badii, M. (Eds.), *Acarology XI: Proceedings of the International Congress*. Sociedad Latinoamericana de Acarología. Universidad Nacional Autónoma México, México, pp. 3–20.
- Norton, R.A., Behan-Pelletier, V.M., 1991a. Calcium carbonate and calcium oxalate as hardening agents in oribatid mites (Acari: Oribatida). *Can. J. Zool.* 69, 1504–1511.
- Norton, R.A., Behan-Pelletier, V.M., 1991b. Epicuticular calcification in Phyllozetes (Acari: Oribatida). In: Dusbábek, F., Bukva, V. (Eds.), *Modern Acarology*, vol. 2. SPB Academic Publishing Bv./Academia, The Hague/Prague, pp. 323–324.
- Norton, R.A., Lions, J.-C., 1992. North American Synchotritiidae (Acari: Oribatida) 1. *Apotritia walkeri* n. g., n. sp., from California. *Acarologia* 33, 285–301.
- Pachl, P., Domes, K., Schulz, G., Norton, R.A., Scheu, S., Schaefer, I., Maraun, M., 2012. Convergent evolution of defense mechanisms in oribatid mites (Acari Oribatida) shows no “ghosts of predation past”. *Mol. Phylogenet. Evol.* 65, 412–420.
- Rasputnig, G., 2010. Oil gland secretions in Oribatida (Acari). In: Sabelis, M.W., Bruin, J. (Eds.), *Trends in Acarology*. Springer, Dordrecht, pp. 235–239.
- Rasputnig, G., Kaiser, R., Stabentheiner, E., Leis, H.-J., 2008. Chrysolomelidial in the opisthonal glands of the oribatid mite, *Oribotritia berleseii*. *J. Chem. Ecol.* 34, 1081–1088.
- Sanders, F.H., Norton, R.A., 2004. Anatomy and function of the ptychoid defensive mechanism in the mite *Euphthiracarus cooki* (Acari: Oribatida). *J. Morphol.* 259, 119–154.
- Schaefer, I., Norton, R.A., Scheu, S., Maraun, M., 2010. Arthropod colonization of land-Linking molecules and fossils in oribatid mites (Acari Oribatida). *Mol. Phylogenet. Evol.* 57, 113–121.
- Schatz, H., 2002. Die Oribatidenliteratur und die beschriebenen Oribatidenarten (1758–2001)–Eine Analyse. *Abh. Ber. Naturkunde. Görlitz* 74 (1), 37–45.
- Schmelzle, S., Helfen, L., Norton, R.A., Heethoff, M., 2008. The ptychoid defensive mechanism in Euphthiracaroidea (Acari: Oribatida): A comparison of exoskeletal elements. *Soil Organ.* 80 (2), 227–241.
- Schmelzle, S., Helfen, L., Norton, R.A., Heethoff, M., 2009. The ptychoid defensive mechanism in Euphthiracaroidea (Acari: Oribatida): A comparison of muscular elements with functional considerations. *Arthrop. Struct. Dev.* 38 (6), 461–472, <http://dx.doi.org/10.1016/j.asd.2009.07.001>.
- Schmelzle, S., Helfen, L., Norton, R.A., Heethoff, M., 2010. The ptychoid defensive mechanism in *Phthiracarus longulus* (Acari: Oribatida): exoskeletal and muscular elements. *Soil Organ.* 82 (2), 253–273.
- Schmelzle, S., Norton, R.A., Heethoff, M., 2012. A morphological comparison of two closely related ptychoid oribatid mite species: *Phthiracarus longulus* and *P. globosus* (Acari: Oribatida: Phthiracaroidea). *Soil Organ.* 84 (2), 431–443.
- Schmid, R., 1988. Morphological Adaptations in a Predator-Prey-System: Scydmaenidae and Armoured Mites. *Zool. Jahrb., Abt. Syst. Ökol. Geogr. Tiere* 115, 207–228.
- Štorkán, J., 1925. Přispěvky ku známostem o českých Oribatidech (Acarina). *Publ. Fac. Sci. l'Univ. Charles* 42, 1–40 (in Czech).
- Wauthy, G., 1984. Observations on the ano-genital region of adult *Phthiracarus nitens* (Oribatida: Mixonomata). In: Griffiths, D.A., Bowman, C.E. (Eds.), *Acarology IV*, vol. 1. Ellis Horwood Publ, Chichester, UK, pp. 268–275.
- Wauthy, G., Leponce, M., Banaï, N., Sylin, G., Lions, J.-C., 1998. The backward jump of a box moss mite. *Proc. R. Soc. Ser. B-Biol. Sci.* 265, 2235–2242.

ACKNOWLEDGEMENTS

I am greatly indebted to a lot of people for making this thesis possible by supporting and encouraging me both professionally and personally, for their help, know-how, fruitful discussion, constructive criticism, and ideas, but also for socializing and distraction. Thank you all so much!

I would especially like to thank:

My Mum, Claudia Eichele-Schmelzle, for always being there, encouraging and supporting me all these years, for her endless patience and love.

My Dad, Paul Alfred Schmelzle, for always believing in me, supporting and promoting me, for his advice and his love.

The rest of my family for their support over all the years, especially my granddad Erwin Eichele and my aunt Ursula Eichele-Datcu as well as Ursula Störzbach.

Hannes Hornbacher for his friendship and his support. And for dragging me to the theatre... ^^ Thanks for always being there for me!

Oliver Betz and Daniela Weide for introducing me to SRμCT, VGStudio MAX, and Amira; Oliver Betz for his help, support, and for providing a place in his department and, accepting me as PhD student; Daniela Weide for discussion and for being a pleasant office mate.

Michael Heethoff, without whom this project would have never been possible. Thank you for your patience, discussion, constructive criticism, ideas, motivation, help, and for supporting and promoting me all these years and for introducing me to the life beneath our feet, especially of course the Oribatida. I am very grateful and forever indebted to you!

Roy A. Norton for his incredible work and tremendous amount of help over the years.

Michael Laumann, Paavo Bergmann and Jan Prochel for their support, discussion, ideas and help. And for making our workgroup a second home.

All other members of the workgroup Evolutionary Biology of Invertebrates, especially Julius Braun, Christian Schmitt and Marius Kluck as well as Lars Koerner, Jan Woyzichovski, Heiner Goetz, Gerwin Gold, Ferdinand Kluge and Franz Langer. A workgroup to remember!

The 'Ars bene agendi', 'Tübingen Anglo-Irish Theatre Group', 'Provisional Players' and 'Zweitagsfliege' and all the people involved in the BrechtBau theatre productions, especially Moritz Keller, James Kelsey Nelson and Oliver Schröder. Good times!

'2nd floor productions' for being an incredible home, especially Silvester Plank, Nina Widmaier and Christian Widmer.

Katja Wehner-Gehring for proof reading and helpful comments on this thesis.

Christopher Kaiser-Bunbury for helpful comments on the layout.

Lukas Helfen for his tremendous help with data acquisition and reconstruction as well as helpful comments on the papers.

Karl-Heinz Hellmer for critical point drying, his brilliant SEM pictures, and his enormous patience in doing so.

Klaus Eisler and Monika Meinert for their help.

Anna Luise Cohrs for making things possible and her help on—what felt like millions of—form pages.

Anne Jürgens-Hellmer for her support and pleasant talks in the workgroup hallways.

I would like to thank the PRO ACAROLOGIA BASILIENSIS for partial funding of my PhD, especially Reinhard Gerecke for encouraging me to apply and for his help in doing so, and the Bundesministerium für Bildung und Forschung for funding the ASTOR project and in doing so indirectly funding the last chapter of my PhD.

Elsevier for giving my papers a suitable home, their new rights management system, which makes things so much easier, and for giving me the rights to publish my papers in this thesis.

Soil Organisms for giving my papers a suitable home, for being open access and for giving me the rights to publish my papers in this thesis.

Anonymous reviewers for their comments on the papers.

My examiners for a rather pleasant defense, namely Michael Heethoff, Oliver Betz, Nils Anthes and Karl-Heinz Köhler.

Both, the ESRF, Grenoble, and the ANKA, Karlsruhe, for beam time and the ESRF for a cantina which is beyond competition. And of course thanks to all of the crew on site making our beam times successful, especially Peter Cloetens, Thomas van de Kamp and Tomy dos Santos Rolo as well as Patrik Vagovic and Angelica Cecilia.

Nico Blüthgen and the members of his workgroup for providing a homely new working environment in Darmstadt and for proof listening to my defense talk, constructively criticizing and encouraging me.

All the friends not yet listed for supporting me over the years, talks and distraction from work through socializing, especially Steffen Maier, Björn Kasper, Daniel Nowack as well as many, many more.

And finally, thanks to all the people who over all those years forwarded job opportunities to me and of course to all the people who hired me.

